

General Disclaimer

One or more of the Following Statements may affect this Document

- This document has been reproduced from the best copy furnished by the organizational source. It is being released in the interest of making available as much information as possible.
- This document may contain data, which exceeds the sheet parameters. It was furnished in this condition by the organizational source and is the best copy available.
- This document may contain tone-on-tone or color graphs, charts and/or pictures, which have been reproduced in black and white.
- This document is paginated as submitted by the original source.
- Portions of this document are not fully legible due to the historical nature of some of the material. However, it is the best reproduction available from the original submission.

(NASA-CR-144185) THERMAL SUPPORT FOR SCALE
SUPPORT Final Report (Lockheed Missiles and
Space Co.) 352 p HC \$10.50 CSCL 22B

N76-19219

Unclas
G3/18 18486

Lockheed

HUNTSVILLE RESEARCH & ENGINEERING CENTER

LOCKHEED MISSILES & SPACE COMPANY, INC.
A SUBSIDIARY OF LOCKHEED AIRCRAFT CORPORATION

HUNTSVILLE, ALABAMA



Lockheed

Missiles & Space Company, Inc.

HUNTSVILLE RESEARCH & ENGINEERING CENTER

Cummings Research Park
4800 Bradford Drive,
Huntsville, Alabama

**THERMAL SUPPORT FOR SPACE
SUPPORT**

FINAL REPORT

January 1976

Contract NAS8-25569

Prepared for National Aeronautics and Space Administration
Marshall Space Flight Center, Alabama 35812

by

William G. Dean

APPROVED:

B. Hobson Shirley
B. Hobson Shirley, Supervisor
Engineering Sciences Section

George D. Perry
for J.S. Farrior
Resident Director

FOREWORD

This final report presents the results of work performed by personnel of the Lockheed-Huntsville Research & Engineering Center for the Astronautics Laboratory of NASA-Marshall Space Flight Center under Contract NAS8-25569, "Thermal Support for Space Shuttle." This work was conducted in three phases.

The NASA Contracting Officer's Representative (COR) for Phase I of this contract was Mr. R. R. Fisher, S&E-EP-44. The period of performance for this phase was from February to September of 1970. The COR for Phase II and Phase III of this work was Dr. K. E. McCoy, S&E-EP-44. The period of performance for Phase II was from February 1971 through June 1973. The period of performance for Phase III was from June 1973 through January 1976.

The Lockheed-Huntsville Project Engineer for this contract was Mr. William G. Dean.

CONTENTS

Section		Page
	FOREWORD	ii
1	INTRODUCTION AND SUMMARY	1
2	TECHNICAL DISCUSSION	3
3	CONCLUSION AND APPRECIATION	4
	REFERENCES	5

Appendixes

- A - N Documentation Produced Under Contract NAS8-25569,
Phase III

Section 1 INTRODUCTION AND SUMMARY

The primary purpose of this contract was to provide thermal support in the design of the Thermal Protection System (TPS) for the Space Shuttle vehicle. The work conducted covered a wide range of problems. However, these can be grouped generally into three phases:

Phase I: Analyses in support of MSFC "Point Design" Shuttle configuration:

- Generation of temperature boundaries of the Space Shuttle "point design."
- Leading edge and noscap TPS material investigation.

Phase II: Support of three TPS test facilities as follows:

- MSFC 36 x 36-Inch Panel Radiant Lamp Test Facility
- MSFC Structural/Thermal Test Facility (STTF), and
- MSFC Hot-Gas O₂/H₂ Burner Test Facility.

Phase III: The following tasks were performed during Phase III:

- Hot Gas Facility (HGF) Support
- Guarded Tank Support
- Shuttle External Tank (ET) Thermal Design Handbook Support
- 20-Inch LH₂ Tank Test Support
- Radiant Tests of BX-250 Foam Panels Support
- External Tank (ET) Thermal Protection System (TPS) Development Support
- 70-Inch LH₂ Tank Test Support

- MTF/MPTA Flame Bucket Heating Rate Analysis
- Task to Summarize and Document all Test Data of BX-250 Foam
- SSME Seal Leaks/Vent Duct Heating Problem Analysis
- MSFC Hot-Gas Test Facility Modifications Study
- AEDC Foam Test Support Task
- Langley BX-250 and CPR-42/Arc-Jet Test Support Task
- Langley CPR-421 Foam Tests in Mach 10 Tunnel Support
- Independent Assessment of Candidate TPS Materials (for ET)
- Hot Gas Facility (HGF) Testing of Candidate TPS Materials (Planning)
- Independent Continuing Review of ET Contractor's TPS Development Efforts
- Review of ET Contractors Document (on analysis methods for predicting CPR-421 performance from data)
- Protuberance Heating Review (as related to ET contractor's instrumentation "island" problem)
- AEDC SRB/TPS Materials Test Support Task
- MSFC Hot Gas Facility Modification/Fabrication Task, and
- AEDC Tunnel C Tests of CPR-421 Foam Using 36-Inch Curved Panel Support.

References 1 and 2 summarize the work done on the first two phases. These were designated as "interim final reports," since the contract was still in progress at the time of their publication.

Approximately 40 documents were published under Phases I and II of this contract, which were discussed in the interim reports. This report documents the work covered during Phase III.

Section 2
TECHNICAL DISCUSSION

Since the tasks completed under this contract were documented as they were accomplished, the method used for this final report is to present copies of the various technical reports published. These are presented as appendixes in the back of this report.

Any question regarding any of this work may be directed to the Lockheed-Huntsville Project Engineer.

Section 3

CONCLUSION AND APPRECIATION

Lockheed-Huntsville takes this opportunity and means to express its appreciation for the privilege of performing this contract for NASA-MSFC. Throughout this contract, we at Lockheed-Huntsville have always experienced excellent working relationships and cooperation from all NASA employees involved. It is felt that this has made it possible for much valuable technical work to be accomplished.

REFERENCES

1. Dean, W.G., "Thermal Support for Space Shuttle -- Interim Final Report," LMSC-HREC D225916, Lockheed Missiles & Space Company, Huntsville, Ala., June 1972.
2. Dean, W.G., "Thermal Support for Space Shuttle -- Second Interim Final Report," LMSC-HREC TR D306662, Lockheed Missiles & Space Company, Huntsville, Ala., June 1975.

Appendixes A through N

DOCUMENTATION PRODUCED UNDER CONTRACT NAS8-25569,
PHASE III

Appendix A

Dean, W. G., and Z. S. Karu, "Determination of Thermal Conductivity of CPR-421 Insulation from Boiloff Rate and Temperature Data from 20-Inch LH₂ Tank," LMSC-HREC TN D390295, Lockheed Missiles & Space Company, Huntsville, Ala., July 1974.

TECHNICAL NOTE

LOCKHEED

Huntsville Research & Engineering Center

Contract NAS8-25569 **Date** July 1974 **Doc.** LMSC-HREC TN D390295

Title: DETERMINATION OF THERMAL CONDUCTIVITY OF CPR-421 INSULATION FROM BOILOFF RATE AND TEMPERATURE DATA FROM 20-INCH LH₂ TANK

FOREWORD

This report presents the results of a data analysis task performed by personnel of the Lockheed-Huntsville Research & Engineering Center under Contract NAS8-25569. The NASA Contracting Officer's Representative (COR) for this study is Dr. Kenneth E. McCoy, EP-44.

INTRODUCTION AND SUMMARY

The LH₂ boiloff rates from the 20-inch LH₂ tank and the temperatures at different depths in the CPR-421 material were available from several tests. These tests were run by the NASA-MSFC Test Division. From the boiloff data, the heat transfer rate was obtained. The thermal conductivity evaluated for the material was plotted against its mean temperature and a straight-line "least squares" fit of the points was obtained. The resulting curve compared favorably with the Upjohn Company thermal conductivity curve for CPR-421 material which was obtained from NASA-MSFC.

TECHNICAL DISCUSSION

Figure 1 is a sketch of the 20-inch LH₂ tank lined on the outside with CPR-421 material. The tank was filled to a certain level with LH₂. It was allowed to stand for sufficient time in an ambient environment for the thermocouples, embedded at premeasured depths in the foam, to reach steady state values. The LH₂ boiloff and the temperature data for all the tests were available and some of the typical data are presented in Table 1.

The heat transfer rate through the tank is calculated as follows:

$$\dot{q} = \frac{\dot{m} h_{fg}}{A}, \frac{\text{Btu}}{\text{ft}^2 \cdot \text{hr}}$$

where

\dot{m} = LH₂ boiloff rate, lbm/hr

h_{fg} = heat of vaporization of LH₂, Btu/lbm

A = wetted area of tank, ft²
(obtained from an LH₂ level sensor)

With the heat transfer rate, \dot{q} , known the thermal conductivity is obtained from

$$\dot{q} = \frac{K}{\Delta x} (T_H - T_C), \frac{\text{Btu}}{\text{ft}^2 \cdot \text{hr}}$$

where

K = thermal conductivity of foam, Btu-in/hr-ft²-°F

Δx = thickness of foam in.

T_H, T_C = temperatures across thickness Δx of foam, °F

The thermal conductivity thus evaluated is tabulated in Table 1 with the average temperature. The average value taken is that between T_H and T_C .

RESULTS AND CONCLUSIONS

A plot (Fig. 2) of the thermal conductivity of the CPR-421 material was made against the mean temperature of the material. A straight line "least

squares" fit of the points was used. As Fig. 2 shows, these data compare reasonably with a similar Upjohn Company curve obtained from NASA-MSFC. However, these latest data give a higher conductivity than the Upjohn values. This is possibly because the latest data contain some effects of penetration heat leaks from such items as fill and drain lines, vent pipes, etc. These heat leaks would tend to raise the heat leak into the tank and LH_2 boiloff rates, thus indicating a higher apparent CPR-421 conductivity.

Zain Karu
Zain Karu
Heat Protection Systems

W. G. Dean
W. G. Dean, Project Engineer
Space Shuttle Thermal Support Study

Juan K. Lovin
Juan K. Lovin, Supervisor
Thermodynamics & Structures Section

Attach: (1) Table 1
(2) Figures 1 and 2

Table 1
20-INCH LH₂ TANK TEST DATA AND THERMAL CONDUCTIVITY
OF CPR-421 MATERIAL

Test Number	Time (sec)	L _{H2} Boiloff (lbm/hr)	Wetted Height, in Cyl. Portion (in.)	ΔX (in.)	T _H (°F)	T _C (°F)	T _{average} (°F)	K Btu-in (hr-ft ² -°F)
274-024	7,614	6.21	34.69	5/16	49.6	-31.6	9.0	.236
				9/16	49.4	-120.6	-35.6	.203
				3/4	50.1	-183.2	-66.5	.198
				1.0	50.5	-423	-186.3	.130
				11/16	-31.6	↓	-227.	.108
				7/16	-120.6	↓	-271.	.089
				1/4	-183.2	↓	-303.	.064
				5/16	53.8	-26.7	13.6	.230
				9/16	53.8	-113.6	-29.9	.199
	8,480	5.72	32.65	3/4	55.1	-175.8	-60.4	.192
				1.0	54.3	-423	-184.4	.124
				11/16	-26.7	↓	-225.	.103
				7/16	-113.6	↓	-268.	.084
				1/4	-175.8	↓	-299.	.060
274-025	3,433	7.58	47.03	5/16	50.	-26.2	11.9	.241
				9/16	52.	-114.2	-31.1	.199
				3/4	51.6	-177.1	-62.8	.192
				1.0	51.3	-423.	-185.9	.124
				1 1/16	-26.2	↓	-225.	.102
				7/16	-114.2	↓	-268.	.083
				1/4	-177.1	↓	-300.	.060
	18,114	865	41.57	5/16	60.1	-19.0	20.6	.293
				9/16	64.2	-110.7	-23.3	.238
				3/4	63.0	-175.5	-56.3	.233
				1.0	65.0	-423	-179.	.152
				11/16	-19.0	↓	-221.	.126
				7/16	-110.7	↓	-267.	.104
				1/4	-175.5	↓	-299.	.075
274-026	4,185	6.07	41.00	5/16	43.5	-38.6	2.3	.230
				9/16	41.9	-126.0	-42.1	.176
				3/4	43.3	-188.6	-72.6	.170
				1.0	43.3	-423	-189.6	.113
				11/16	-38.6	↓	-231.	.094
				7/16	-126.0	↓	-275.	.077
				1/4	-188.6	↓	-305.	.056
	9,001	5.13	30.52	5/16	54.2	-26.6	13.8	.216
				9/16	54.6	-113.9	-29.7	.187
				3/4	54.9	-174.7	-59.9	.183
				1.0	52.0	-423	-185.5	.118
				11/16	-26.6	↓	-225	.097
				7/16	-113.9	↓	-269	.079
				1/4	-174.7	↓	-299	.056
274-027	4,367	7.85	47.68	5/16	68.1	-17.8	25.2	.219
				9/16	67.3	-108.4	-20.6	.192
				3/4	67.8	-171.1	-51.7	.189
				1.0	68.6	-423	-177.2	.122
				11/16	-17.8	↓	-221	.102
				7/16	-108.4	↓	-266	.084

Table 1 (Concluded)
 20-INCH LH₂ TANK TEST DATA AND THERMAL CONDUCTIVITY
 OF GPR-421 MATERIAL,

Test Number	Time (sec)	LH ₂ Boiloff (lbm/hr)	Wetted Height, in Cyl. Portion (in.)	Δ (in.)	T _H (°F)	T _C (°F)	T _{average} (°F)	$\frac{K}{\text{hr-ft}^2\text{-}^\circ\text{F}}$
	15,018	6.21	37.03	1/4	-171.1	-423.	-297	.060
				5/16	69.8	-17.4	26.2	.209
				9/16	69.3	-109.2	-20.0	.184
				3/4	70.0	-172.8	-51.4	.180
				1.0	69.9	-423.	-176.6	.119
				11/16	-17.4	↓	-220	.099
				7/16	-109.2	↓	-266	.081
				1/4	-172.8	↓	-298	.058

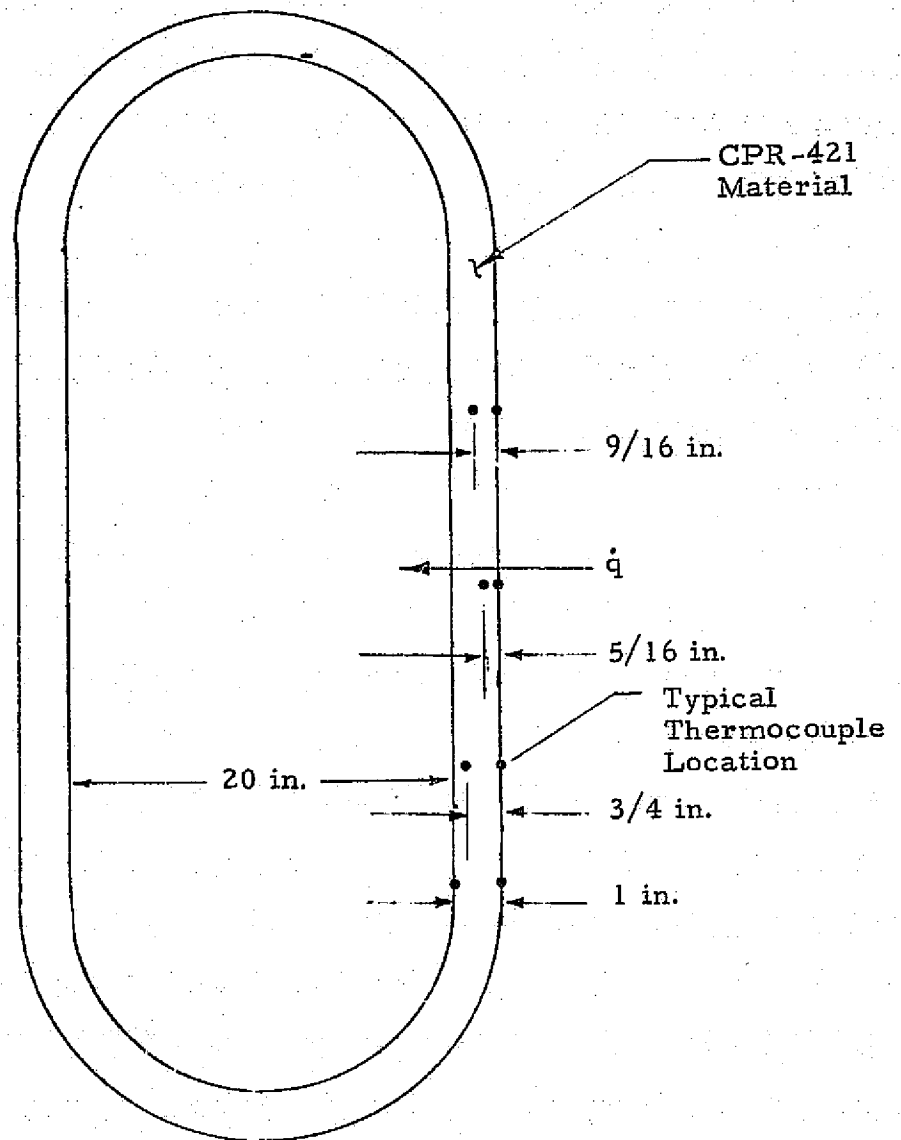


Fig. 1 - Cross-Sectional Sketch of 20-Inch LH_2 Tank Showing CPR-421 Material Insulation

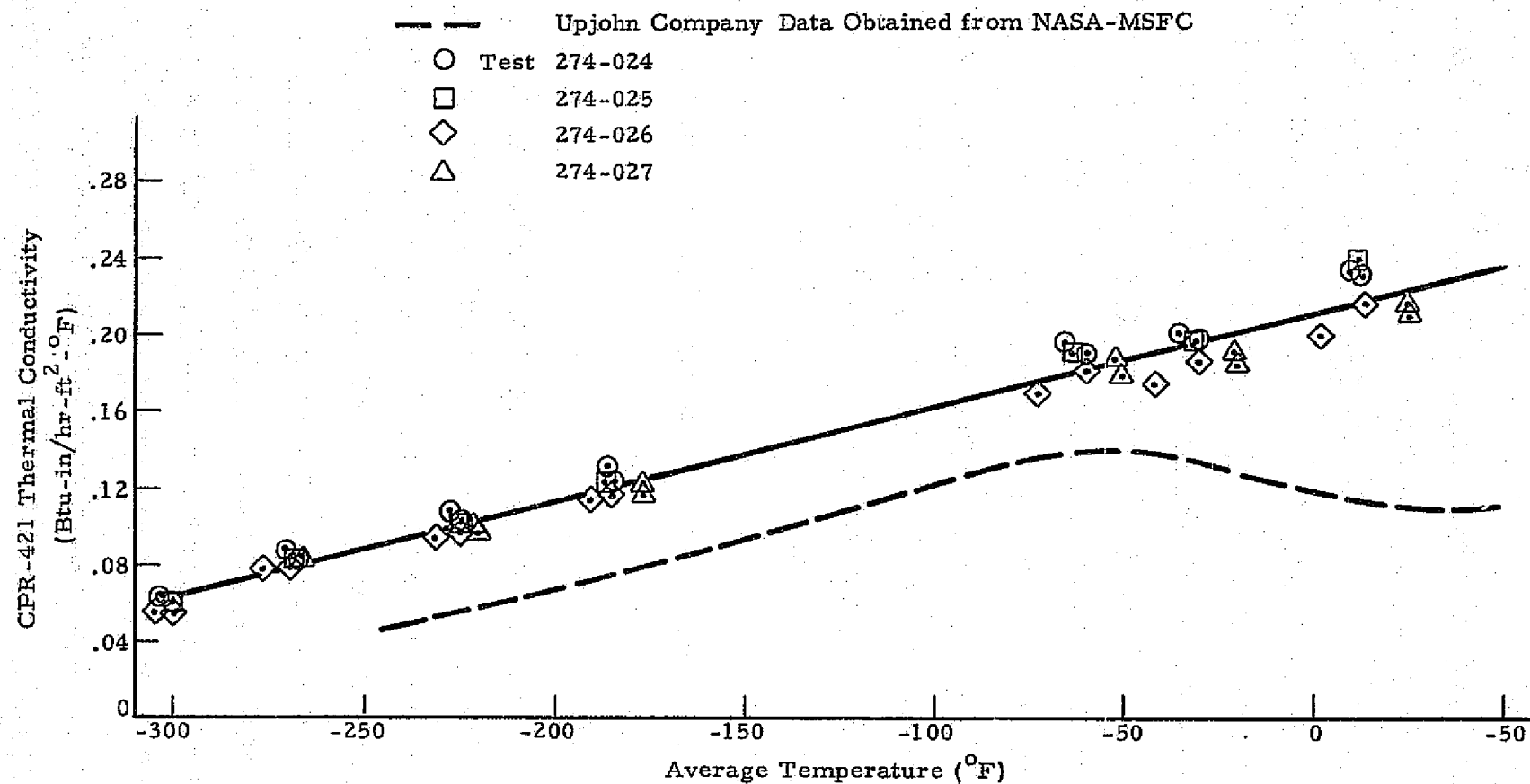


Fig. 2 - CPR-421 Material Thermal Conductivity vs Average Temperature Compared with Uphohn Data from NASA-MSFC

Appendix B

Dean, W. G., "Results and Analysis of BX-250 Foam Tests at MSFC,"
LMSG-HREC TN D390268, Lockheed Missiles & Space Company,
Huntsville, Ala., July 1974.

TECHNICAL NOTE

LOCKHEED

Huntsville Research & Engineering Center

Contract NAS8-25569

Date July 1974

Doc. LMSC-HREC TN D390268

Title: RESULTS AND ANALYSIS OF BX-250 FOAM TESTS AT MSFC

FOREWORD

This report was written by personnel at the Lockheed-Huntsville Research & Engineering Center under Contract NAS8-25569. The NASA-MSFC Contracting Officer's Representative (COR) for this study is Dr. Kenneth E. McCoy, S&E-ASTN-PTC. This report documents tests conducted on BX-250 foam by MSFC in their facilities. Mr. Chuck Verschoore and Mr. Stan Chamberlain were the MSFC test project engineers responsible for the tests.

1.0 INTRODUCTION

A number of panel tests of candidate thermal protection system (TPS) materials for the Space Shuttle External Tank (ET) have been run in the MSFC Hot Gas Facility (HGF). The results of these tests have now been correlated and analyzed. This report describes the Hot Gas Facility and summarizes and analyzes the BX-250 foam test results. Also, results from the MSFC Radiant Heater Facility BX-250 foam tests are presented and discussed.

There is no ground test facility in which all the parameters affecting the TPS performance can be simulated completely. It is therefore necessary to look at the degree of simulation achieved and determine the effect this may have on predicted flight performance. A discussion of this problem is also presented herein.

2.0 DISCUSSION

2.1 MSFC HOT GAS FACILITY DESCRIPTION

The NASA-MSFC Hot Gas Facility (HGF) consists of a combustion chamber, throat section, expansion nozzle, test section and diffuser. The combustion chamber burns either hydrogen and oxygen or hydrogen and air, at chamber pressures from approximately 65 to 150 psia and oxidizer-to-fuel (O/F) ratios of 13 to 20. The Mach number at the nozzle exit plane is approximately 4. Materials may be tested in the facility as panels in the nozzle sidewalls and diffuser centerbody, or as a leading edge mounted on the front of the centerbody. The tests discussed herein were run as panels in the nozzle sidewalls. Figure 1 shows a sketch of the HGF.

Figures 2 and 3 show the calculated flowfield parameters (Mach number, temperature, pressure, density and velocity) along the nozzle boundary layer edge as a function of distance from the throat. This is for a typical test condition, 80 psia chamber pressure, and O/F = 14, burning GOX/H₂. Additional information on the HGF heating rates, pressures, shear, and chemical species is given in discussion of extrapolation of the HGF results to flight conditions (Section 4.0).

2.2 SUMMARY OF TESTS CONDUCTED AND RESULTS OBTAINED

Table 1 presents a summary of the HGF testing of the candidate ET TPS materials. The test numbers shown are for materials tests only. A number of calibration tests were also run which are not shown here. The O/F ratios shown are mass ratio values. The TPS panels tested were run in the third nozzle section on the side and top locations as shown in Fig. 1. The panel sizes were 12 x 17 inches with the 12-inch direction aligned with the flow. Most of the panel material thicknesses were 0.75 inches. Heating rates and pressures were measured during calibration runs using a calibration panel as shown in Fig. 4. The calibration panel contained eight calorimeters and eight pressure taps. The heating rates presented in Table 1 are averaged

over the four values down the panel centerline. The pressures are averaged from all eight locations. Two types of recession rates are presented: (1) based on measured post-test thickness values, and averaged along the panel centerline, and (2) based on weight-loss data. The recession rates are calculated using the total recession and dividing by the total run time. No instantaneous recession rates as a function of time during the tests were measured. Various comments are given in Table 1 for added information where needed. It is noted that some test numbers are missing in Table 1. Some of these missing tests were aborts, others were calibration runs. No data were obtained in some cases for various reasons such as instrumentation loss, etc. These cases are so indicated in Table 1 by ND (no data).

An attempt was made to measure temperature within the foam as a function of time. Difficulty was encountered in getting good temperature data due to conduction in the thermocouple wires, large thermal capacitance of the wires compared to the foam, and installation problems. Therefore these data are not presented herein. Perhaps these data could be salvaged with more analysis and presented later.

Most of the panels tested are BX-250 foam since this is the primary Shuttle ET-LH₂ tank TPS material. Color movies of the panels were made during the tests on many runs. (These are available for the side panels only since the camera is mounted on the nozzle side directly across from the panel.) These movies are available from Mr. Stan Chamberlain, NASA-MSFC Test Division.

Figures 5 and 6 show post-test photographs of typical BX-250 foam panels. Post-test photos are available for most of the panels from Dr. Ken McCoy, NASA-MSFC Engineering Analysis Division.

Table 2 presents a description and the nominal density values of the various materials tests. Table 3 presents actual density values for several BX-250 "trim" panels. These were measured from plugs cut from the panels after the tests.

2.3 ANALYSIS OF RESULTS

The BX-250 foam is presently the primary Space Shuttle external LH_2 tank thermal protection system material. Therefore, correlations of the BX-250 data from the HGF tests were made. Two specific correlation methods were used. The first was a recession rate versus heating rate method, the second was through the use of computer routines developed during the course of this study.

2.3.1 Data Correlation Using Recession Rate vs Heating Rate Method

Figures 7 and 8 show the results of the surface recession rate versus heating rate correlation. Figure 7 is based on data from measured material thickness changes from before and after testing. Figure 8 is based on weight loss data from weight before and after tests. The straight lines of Figs. 7 and 8 are "least-squares" fits of the data. All recession rate data are based on average rates, that is, the total recession is divided by the total run time. All heating rates are "cold-wall" values based on a wall temperature of $70^\circ F$.

Figure 9 presents a refinement of the recession data of Fig. 7. As the foam surface recedes, a "depression" is left in the nozzle wall where the foam specimen is mounted. (The foam is, of course, initially flush with the nozzle wall plane at the beginning of each test.) This depression causes a thickening of the boundary at this location, hence a reduction in heating rate. In order to take this effect into account the calibration panel was mounted at several recessed depths, and calibration runs were made. From these calibration run data a curve of recession depth versus measured heating rate was made. This curve was then used to make corrections on all the heating rates as presented in Fig. 7, which was based on flush-mounted measured heating rate values. A least squares fit was then made of the adjusted data and compared to the unadjusted data. Figure 9 shows this comparison. The adjusted results give about a 10 to 15% increase in recession rate at a given heating rate.

As seen from the curves of Figs. 7, 8 and 9, the recession rate versus heating rate type correlation worked well and should be useful in predicting flight vehicle foam thickness requirements.

2.3.2 Data Correlations Using Computer Routines

The first computer method used for correlation purposes was to develop a program which performed a heat balance at the foam surface. The program accounts for surface recession, heat conduction into the foam, convective heating to the surface, and heat radiated away from the surface. The surface recession rates are calculated using an Arrhenius equation of the form

$$\dot{m} = Ae^{-B/T}$$

where

- \dot{m} = mass loss rate
- A, B = correlation constants
- e = natural log base
- T = surface temperature

The constants A and B are usually determined from experimental data. This is done by plotting recession rate as a function of $1/T$ on semi-log paper. The value of A is then obtained from the intercept of the plot and B is the slope. However, in this case the surface temperature, T, was not measured. Therefore the constants A and B were determined by trial and error to match the calculated surface recession rate using calculated surface temperatures from the computer program. The resulting values which matched the measured recession during several of the early tests were: $A = 8.16 \text{ lbm/sec}$, and $B = 9000^\circ\text{R}$. In addition to these constants there is also a term, H, called "heat of reaction" for the foam. The value used for this term was 4000 Btu/lb .

Figure 10 shows the surface recession versus time as calculated by the program compared to the total measured recession at the end of the run (no recession versus time values were measured during the tests). This curve is for test No. 36, in the HGF at a heating of $3.75 \text{ Btu/ft}^2\text{-sec}$. The

thermal properties density, specific heat, and thermal conductivity used in this analysis are given in Tables 4, 5 and 6, respectively.

This program was also used to calculate temperature-time histories throughout the foam thickness. The results were compared to measured values from thermocouples. The agreement was generally not good. This is attributed to the highly transient nature of the problem and difficulty in obtaining good experimental data because of the use of large thermocouple wires, use of high density potting compound to hold the thermocouple plugs in place, and difficulty in getting accurate thermocouple "bead" locations.

Figure 11 shows another comparison of HGF data and the computer program results. The three calculated points are at heating rates of 1.0, 2.0, and 4.0 Btu/ft²-sec. The agreement is reasonably good, but to obtain this agreement the constants A, B and H had to be revised from those used in matching the earlier tests such as No. 36 shown on Fig. 10. The revised values of these constants are $A = .816 \text{ lbm/ft}^2\text{-sec}$, $B = 12,000^\circ\text{R}$, and $H = 0.0 \text{ Btu/lb}$. It is therefore felt that additional work is needed in definition of the best values of these constants before application of the type model to a flight vehicle design.

2.3.3 Additional Correlations

In addition to this simple computer model, it is recommended that three other methods of analysis should be tried. These are to: (1) use the Lockheed "WOTA" ablation analysis program, Ref. 1; (2) the NASA-Houston "STAB II" ablation program, Ref. 2; and (3) a transient, one-dimensional routine using the \dot{R} versus \dot{q} curve approach with the corrected data of Fig. 9. Results of these effort can then be compared and a selection of the best method made for application to the flight vehicle design.

2.3.4 Comparison of HGF Data with Data from Other Sources

Figure 12 shows a comparison of the HGF data with some preliminary data obtained from NASA-Langley in their Arc Jet Facility. These Langley data must still be considered preliminary at the present time since they are unpublished and were obtained by phone. The BX-250 foam for these tests was made by MSFC and shipped to Langley for testing. It had a nominal density of approximately 2.3 lb/ft^3 . However, the agreement is seen to be reasonably good. The Langley data were taken at a pressure of 0.01 to 0.1 atm. Figure 12 also shows a curve fit equation for recession rate versus heating rate as determined by Langley for their data. The equation of the dotted line curve is $\dot{R} = 5.0 \times 10^{-4} \times (\dot{q})^2$. This curve is also seen to agree well with the MSFC HGF data.

To obtain the "recession threshold" heating rate the HGF data can be extrapolated back to the zero recession point. This gives a heating rate of approximately $0.75 \text{ Btu/ft}^2\text{-sec}$, below which there is no recession. The Langley data agree with this in that their lowest heating data point of $0.6 \text{ Btu/ft}^2 \text{ sec}$ did not yield any recession. (This threshold value was later confirmed in a series of BX-250 foam tests using the MSFC "Guarded Tank" in the radiant test facility.)

3.0 MSFC RADIANT HEATER/VACUUM TANK TESTS OF BX-250 FOAM

3.1 Introduction

Due to the fact that the MSFC Hot Gas Facility tests were conducted at pressures which were below those expected at the time of peak heating, and in an atmosphere which was not air, it was decided that additional tests were needed to determine the effect of these parameters. Because of this a number of tests were planned and carried out in the MSFC Radiant Heater Panel Test Facility. The following sections give a brief discussion of these tests and the results. It is planned that a more detailed documentation of these tests will be published later.

3.2 Objectives

The following are the objectives of this series of tests:

- Determine effect of presence of H₂O vapor on recession rate of BX-250 foam.
- Determine BX-250 recession rate under radiant heat input in an inert atmosphere.
- Determine BX-250 recession rate under radiant heat input in an air environment.
- Determine BX-250 recession rates at radiant heat inputs similar to HGF tests and at similar and varying oxygen partial pressures.
- Determine the effect of pressure on recession rate in an air environment.
- Determine the effect of shear on BX-250 recession.

3.3 Test Article Description

The test articles for these tests were 12 x 17-inch panels of 3/4-inch BX-250 foam on 1/8-inch aluminum back plates. The panels were identical to those used in the HGF tests.

3.4 Test Facility

These tests were performed in the MSFC 15-foot top-loading vacuum chamber in the S-I dynamic test stand, Building 4557. The foam panels were suspended above the radiant lamp assembly. The radiant heater facility consists of watercoded reflectors and tubular quartz lamps. It has an opening size of approximately 24 x 28 inches.

3.5 Instrumentation and Data

Instrumentation consisted of thermocouples 1/8, 1/4 and 3/8 inches below the foam surface and on the aluminum back-plate. The thermocouple

layout is identical to the HGF tests. Thermocouple locations were verified by X-ray. Heat flux was monitored by a single calorimeter placed next to the panel at the midpoint of the long (17 inches) side. This side heat flux was correlated with that at the center of the panel using a calibration panel with a calorimeter in its center. The centerline heat flux was then determined from the side heat flux measured during the foam panel tests.

The recessions were measured by weighing the panel before and after each test and by establishing the height of the surface relative to a fixed reference before and after each test. The height measurements were made to the closest 1/64 inch. Weights were measured with an accuracy of ± 0.1 gram.

Still color photographs were made of the panel after each test. The tests were monitored in real time on television and a video tape was made for later review

3.6 Results

Figure 13 presents a summary of the results of these tests in the form of recession rate versus heating rate. These results are based on measured recession rates, as opposed to weight loss data. The heating rates are based on pretest calibration rather than post-test calibration data. The post-test calibration data also give a good correlation but results in a slightly higher recession/heating rate curve.

Because some of the heat-flux calibration data encountered repeatability problems, these results must still be considered preliminary at present. However, this problem is not expected to significantly change the conclusions drawn from the data.

In Fig. 13 the radiant test data are compared to the Langley and MSFC HGF data which were obtained on a convective heating environment to show the effects of shear on recession.

3.7 Conclusions

From observations and analyses of these results the following conclusions can be drawn:

- There is no apparent effect of pressure or gas content (O_2, H_2O) on BX-250 foam recession in the ranges tested.
- There is a significant effect of shear on BX-250 recession rate.
- The recession rate of BX-250 in a radiant environment correlates well with heating rate.

4.0 PROBLEMS ASSOCIATED WITH APPLICATION OF BX-250 GROUND TEST DATA TO SPACE SHUTTLE ET DESIGN

After making tests and reducing and correlating the data, the next step is to determine how to use the data in the flight vehicle TPS design. There is no ground test facility where all the parameters affecting the TPS performance can be simulated completely. It is therefore necessary to look at the degree of simulation achieved and determine the effect this may have on predicted flight performance. The simulation parameters to be considered are:

- Heating Rate
- Aerodynamic Shear
- Enthalpy
- Oxygen Content
- Pressure

Although each of these parameters are interrelated, an attempt is made to discuss each of the parameters discussed individually in the following sections.

4.1 Heating Rate

At the present time it appears that the BX-250 foam performance or recession rate is governed primarily by the applied heating rate and the best method of correlation and application to flight design is through the recession rate versus heating rate.

The cold-wall heating rate, \dot{q} , levels being achieved in the Hot Gas Facility vary from approximately 0.6 to 4.4 Btu/ft²-sec. For the ET/LH₂ tank flight conditions, Rockwell International predicts values from 0.0 to about 4.6 Btu/ft²-sec (see Ref. 3). This is for body location No. 7420 on the forward end of the ET/LH₂ tank, at an assumed wall temperature of 460°R. For the ET/LOX tank at body location No. 7010 the heating rate ranges from 0.0 to 4.3 Btu/ft²-sec at a 460°R wall temperature. (These values are for the "3A nominal" trajectory.)

No problem is expected in applying the ground test data to ET/LOX/LH₂ tank TPS design insofar as heating rate variations are concerned. This is because of: (1) a good correlation of recession rate versus heating rate was obtained (see Fig. 7), and (2) the heating rates expected in flight are in the same range as those where the ground test data were taken. This application to flight can be handled through use of a computer routine with a variable heating rate input capability. Another point to be considered here is the fact that most of the area of the ET, except for the aft dome, has a heating rate level for most of the flight time which is below the "recession threshold" heating rate level of 0.75 Btu/ft²-sec. In other words most of the ET area is expected to have very little or no recession during flight.

Application of the data to the ET aft dome, however, presents a different problem from that of the rest of the tank since the heating rates there are considerably higher and almost purely radiative rather than convective. Most of the radiant facility data were taken at a rate below the expected flight level of

approximately 7 Btu/ft²-sec (see Fig. 13). The MSFC "guarded tank" was tested at a heating rate of 6.0 Btu/ft²-sec, however these data must still be considered preliminary at present. Also these data were taken at a "high" pressure of 1 atm. Because of this situation, the aft dome application problem remains unsolved until more data are taken at the appropriate heating rates, and pressures.

4.2 Aerodynamic Shear

The shear levels being experienced in the HGF tests at an oxygen-to-fuel ratio (O/F) of 12 are calculated to be 0.16 to 0.67 lbf/ft² while the typical predicted flight levels for the ET per Rockwell are 0 to 1.9 lbf/ft². Initially this situation presented a challenge because: (1) the simulation is on the low (unconservative) side, and (2) because it was felt that the foam materials were quite "shear-sensitive."

However, after observation of the data from numerous tests, it seems that this problem may not be as serious as first thought. It now appears that there is a low shear level which is sufficient to keep the "char" removed. Once this level is exceeded, then the higher shear levels do not really change the material performance until they become high enough to remove the "virgin" material. These higher levels are apparently higher than those to be experienced in flight. Therefore, the material recession may not increase with shear in the range between initiation of char removal and virgin material removal. Langley personnel have also expressed this as their interpretation of their foam test data. This means that the HGF and Langley data can then be extrapolated to flight without having identical shear levels.

Another aspect of the shear problem is that of what happens in a shock impingement area. The first part of the problem is to determine what the shear level is for the flight case and the second part is to try to simulate this in a ground test. The best practical solution to this seems to be to test the foam in the HGF in the region where a shock strikes the wall on the dome lid

or on the centerbody. This should also be supported by a study of how well the HGF shock angle, strength, velocity gradient, etc., simulate the flight values.

4.3 Enthalpy

The term "enthalpy" as used in ablative materials test work refers to the total (or recovery) value in the freestream (or boundary layer edge) as opposed to the static value. In the HGF for an $O/F = 12$, the total enthalpy is approximately 3900 Btu/lb. In flight the value varies from 0 to about 300 Btu/lb at the time of maximum heating and then to about 12,000 Btu/lb at 500 seconds. Ablative material performance is affected by the enthalpy level in two ways. The first is through the convective heating blockage in the boundary layer. As the ablator decomposes, it gives off gases which enter the boundary layer and form a layer of "cool," insulating gas at the surface. The higher the boundary layer edge enthalpy (or temperature) becomes, the more effective this "cooling" mechanism becomes. If the HGF enthalpy is much higher than the flight value, the result would be to get more effectiveness in the ground tests than will be experienced in flight. This is undesirable because it is in the unconservative direction. If the HGF enthalpy is lower than the flight value the results will be conservative. An effort was made to attack this problem analytically. An estimate was made of this difference in effectiveness. It was concluded that there was probably not a large difference.

The second way that enthalpy effects the foam performance is through the recovery temperature. The temperature drop across the boundary layer from the recovery temperature to the wall temperature is in effect the "driving potential" to force the heat into the surface. Therefore, it is possible to have varying surface temperatures at a constant heating rate if the recovery temperature is varying. Intuitively, it would seem that the higher the wall (or surface) temperature the higher the recession rate, even at a constant heating rate. However, this is not obvious from observation of the data.

4.4 Oxygen Content

The HGF can simulate various oxygen content environments because it can be run using either air or gaseous oxygen as the oxidizer. Also each oxidizer can be run at various O/F ratios. Running with oxygen at an O/F of 13 produces an oxygen content at the sample test area of about 36%. With air the O₂ content is near zero. In flight the value is near 20%. O₂ content affects the performance of an ablating material through chemical reactions which involves the use of oxygen. Generally, in the higher temperature ablators, which form a carbon char layer, the surface gets hot enough to oxidize or burn at a rapid rate and oxygen content is a very critical parameter. However, with the foam materials it is felt that the surface will probably never get hot enough for this oxidization mechanism to become significant. Rather, since the charring material is so fragile, it is felt that it will be kept swept away by the aerodynamic shear before reaching a high temperature.

Oxygen content may also effect the "burning rate" of the virgin material and it has been shown by Thermogravimetric Analysis (TGA) data that oxygen does affect the reaction rate of the foam in a static gas environment. This is observed by running samples in air and in argon. However, the reaction rates are essentially the same in air and argon up to about 850°F after which the air data show the sample reacting much faster than the argon data. If it can be shown that in a shearing environment the material surface is being removed before it reaches 850°F then the oxygen content in ground tests versus flight will become insignificant. It is presently felt that the most of the materials is removed before reaching 850°F.

4.5 Pressures

Pressure affects material performance in two ways. The first is through the heating rate and shear. The higher the pressures, the higher the shear and heating rate will be. This part of the effect can be handled as discussed above under "heating rates," and "aerodynamic shear." In the second part of the problem, increased pressures affect material response through providing more

available oxygen to the surface for reactions. In this respect it affects performance in a way similar to oxygen content. Physically this is a combined effect of the two parameters which is the oxygen partial pressure or the product of percent oxygen content and "total" pressure.

The HGF pressures are about .04 to 0.1 psia at the locations presently being used for test. The flight values range from 14.7 psi to 0. At the location of maximum heating on the ET LOX tank (point 7010) the pressure is approximately 1.8 psi at the time of maximum heating. At 500 seconds, which is near the time of the second heating spike, the pressure is essentially zero.

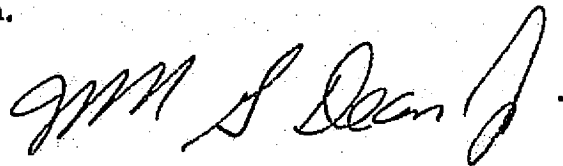
Presently it appears from the data that there is no significant pressure effect on the foam performance in the range of pressures of interest. This statement is made for two reasons: (1) in the radiant heating test results the pressure was varied by a factor of 20 times with no apparent effect on recession at a constant heating rate, and (2) the data correlate well as recession versus heating rate which would not be expected from a "pressure sensitive" material. (This opinion is also shared by Langley personnel who conducted the tests for MSFC.)

5.0 Conclusions

As a result of analyses, data comparison, and testing of BX-250 foam at MSFC the following conclusions are drawn:

- The data correlates well in the form of recession rate versus heating rate.
- The results of the Langley Arc Jet and the MSFC Hot Gas Test Facility test agree well.
- The radiant tests showed that shear definitely affects the foam recession rate.

- There is apparently no pressure, O_2 , or H_2O content effect on foam recession rate in the ranges of interest.
- There are no insurmountable problems in extrapolation/application of the ground test data to flight vehicle design.



W. G. Dean, Project Engineer
Space Shuttle Thermal Support Contract

Approved:



Juan K. Lovin, Supervisor
Thermodynamics & Structures Section

Attach: (1) References
(2) Tables 1 through 7
(3) Figs. 1 through 13

REFERENCES

1. Dean, W. G., "A User's Manual 'WOTA' - NASA/Lockheed-Huntsville Working Tool Ablation Program," LMSC-HREC A712574, Lockheed Missiles & Space Company, Huntsville, Ala., November 1965.
2. Curry, D. M., "An Analysis of a Charring Ablation Thermal Protection System," NASA TN D-3150, December 1965.
3. "Space Shuttle Flight and Ground System Specification Induced Environment Design Requirements," Vol. X, JSC 07700, Appendix 10, Johnson Space Center, Houston, Texas, October 1973.

Table 1
SUMMARY OF HGF PANEL TESTING

Test No.	Cham. Pres. (psia)	O/F Ratio	Propellant	Run Time (sec)	Material		Average Heating Rate over Panel (Btu/r ² -sec)		Average Static Pressure over Panel (psia)		Measured Recession Rate (Average) (10 ⁻³ sec/in)		Recession Rate Based on Weight Loss (10 ⁻³ in/sec)	
					Side	Top	Side	Top	Side	Top	Side	Top	Side	Top
21	80	13.0	GOX/H ₂	300	Calib. Panel	Cork	3.75	1.91	.075	.032	ND	ND	ND	ND
24	100	15.0	Air/H ₂	85	BX-250 Trim 1	BX-250 Trim 2	1.54	0.65	.05	.055	—	—	2.24	.59
30 ¹	100	15.0	Air/H ₂	302	BX-250 Trim 1	BX-250 Trim 2	1.54	0.65	.05	.055	1.1	Nil	1.03	.395
31	80	13.0	GOX/H ₂	305	Calib. Panel	BX-249	3.75	1.91	.075	.032	CP	1.20	CP	2.10
33	110	13.0	GOX/H ₂	55	Calib. Panel	SLA 561	5.39	2.9	.086	.07	CP	Nil	CP	.11
34	80	13.0	GOX/H ₂	24	BX-250 Trim 4	CPR 421	3.75	1.91	.075	.032	8.3	0.6	9.5 ²	5.74
35	110	13.0	GOX/H ₂	41	Silicone Sponge Ablator	BX-250 Trim 3	5.3	2.9	.086	.07	Nil ³	4.3	2.7	6.47
36	80	13.0	GOX/H ₂	68	DC Silicone Ablator	BX-250 Trim-Coated	3.75	1.91	.075	.032	Nil	9.38 ⁴	.016	18.1
37	107	13.0	GOX/H ₂	37	High Density Foam	Calib. Panel	5.39	2.9	.086	.07	.086	CP	—	CP
43	80	14.0	GOX/H ₂	44.8	BX-250 C.R.	G.E. Silicone Foam	3.25	1.65	.075	.032	—	—	3.93	.13
44	80	14.0	GOX/H ₂	48.4	BX-250 Trim MI No. 2	BX-250 Trim MI No. 1	3.25	1.65	.075	.032	—	2.9	6.95	5.15
45	110	14	GOX/H ₂	33.6	BX-250 Trim 5	BX-250 Trim Coated 2	4.4	2.40	—	—	9.6	4.45	7.8	8.0
46	80	14	GOX/H ₂	44	BX-250 Trim WI-1	Calib. Panel Recessed	3.25	1.65	—	—	5.0	CP	6.8	CP
47	110	14	GOX/H ₂	122	SLA-561-5	Avco 480-1U	4.4	2.40	—	—	Nil	Nil	.37	.058
73	80	20	GOX/H ₂	100	BX-250 Trim 8	BX-250 Trim 9	2.4	1.15	—	—	2.6	0.9	—	—
79	100	15	Air/H ₂	150	BX-250 Trim 11	BX-250 Trim 12	1.6	1.15	—	—	1.8	(Swelled)	2.0	1.1
80	150	15	Air/H ₂	100	BX-250 Trim 14	BX-250 Trim 10	2.3	1.44	—	—	3.2	0.7	3.3	1.7
81	63	14.2	GOX/H ₂	100	BX-250 Trim 15	BX-250 Trim 13	2.52	0.97	—	—	3.8	1.3	4.05	2.35
82	63	14.2	GOX/H ₂	30	BX-250 Trim 16	BX-250 Trim 17	2.52	0.97	—	—	4.3	0.3	6.0	2.48

1. The same panels were used in Test 30 as in Test 24. They were first run 85 seconds in Test 24, then an additional 300 seconds in Test 30.
2. Thermocouple plugs were lost, causing high weight loss.
3. Some surface irregularities and charring of surface occurred but no overall change in panel thickness was noted.
4. Flow broke down, causing high pressure transient at shutdown. This caused abnormally high recession rate.

Notes: ND = no data; CP = calibration panel; CR = control rise

Table 2

NOMINAL DENSITY VALUES FOR VARIOUS MATERIALS
WHICH WERE TESTED IN HOT GAS FACILITY

Material	Nominal Density lb/ft ³
BX-250 Foam	2.0
BX-249 Pour Foam	2.0
BX-250 High Density Foam	5.0*
GE Silicone Sponge	20.0
Dow Corning Silicone Ablator	55.0
Cork	30.0
SLA-561-S	15.0
CPR-421	4.0
AVCO 480-1u	16.0

*Approximate value.

Table 3

MEASURED DENSITY VALUES FROM BX-250 FOAM PANELS
TESTED IN HOT GAS FACILITY (POST-TEST MEASURE-
MENTS. CHAR REMOVED BEFORE MEASUREMENT
OF DENSITY)

Panel from Test Number	Measured Density** (lb/ft ³)	
44 (Top)	2.36	<u>±</u> 0.14
44 (Side)	2.16	<u>±</u> 0.21
45	2.55	<u>±</u> 0.16
72*	2.84	<u>±</u> 0.16
73	2.39	<u>±</u> 0.24
80	2.23	<u>±</u> 0.17

* Panel appeared to be made in three "layers;" ∴ density not applicable

** Tolerance on density due to weight and measurement inaccuracy

Table 4

**BX-250 FOAM DENSITY VERSUS TEMPERATURE
USED IN COMPUTER MODEL ANALYSES**

Temperature (°R)	Density (lb/ft ³)
0	2.0
550	2.0
675	1.0
1293	0.5

Table 5

**BX-250 FOAM SPECIFIC HEAT VERSUS TEMPERATURE
USED IN COMPUTER MODEL ANALYSES**

Temperature (°R)	Specific Heat (Btu/lb-°R)
0	0.3
642	1.2
760	1.0

Table 6

**BX-250 THERMAL CONDUCTIVITY VERSUS TEMPERATURE
USED IN COMPUTER MODEL ANALYSES**

Temperature (°R)	Thermal Conductivity (Btu/ft-sec-°R)
0	23×10^{-8}
110	46×10^{-8}
160	115×10^{-8}
260	22×10^{-7}
360	32×10^{-7}
460	42×10^{-7}
1060	53×10^{-7}

Table 7
SUMMARY OF PLANNED RADIANT HEATER/VACUUM
FACILITY BX-250 FOAM PANEL TESTS

Test No.	Environment Gas % Weight	Chamber Total Pressure (psia)	Heat Flux (Btu/ft ² -sec)	Planned Run Time (sec)	Purpose
1	40% O ₂ /60% H ₂ O	0.03	1.65	150	Duplicate HGF tests without shear. Establish baseline for later comparison.
2		0.05	2.5	75	
3		0.08	3.25	50	
4		0.095	4.25	60	
5	Dry Air	0.03	1.65	150	Duplicate Tests 1, 2, and 3, 4 in air environment.
6		0.05	2.5	75	
7		0.08	3.25	50	
8		0.095	4.25	50	
9	Dry Air	0.3	1.65	150	Recession rates at pressures 10 x HGF test pressures.
10		0.5	2.5	75	
11		0.8	3.25	50	
12		0.95	4.25	50	
13	Dry Air	0.6	1.65	150	Recession rates at pressures 20 x HGF test pressures.
14		1.0	2.5	75	
15		1.6	3.25	50	
16		1.9	4.25	50	
17	Dry Air	1.2	1.65	150	Recession rates at 40 times HGF test pressure.
18		2.0	2.5	75	
19		3.2	3.25	50	
20	O ₂ /N ₂ = 40/60	0.03	1.65	150	Duplicate Tests 1, 2 and 3 with no H ₂ O vapor to study water vapor effects
21		0.05	2.5	75	
22		0.08	3.25	50	
23		0.095	4.25	50	
24		0.03	1.65	150	Duplicate Tests 1, 2, and 3 in inert atmosphere.
25		0.05	2.5	75	
26		0.08	3.25	50	

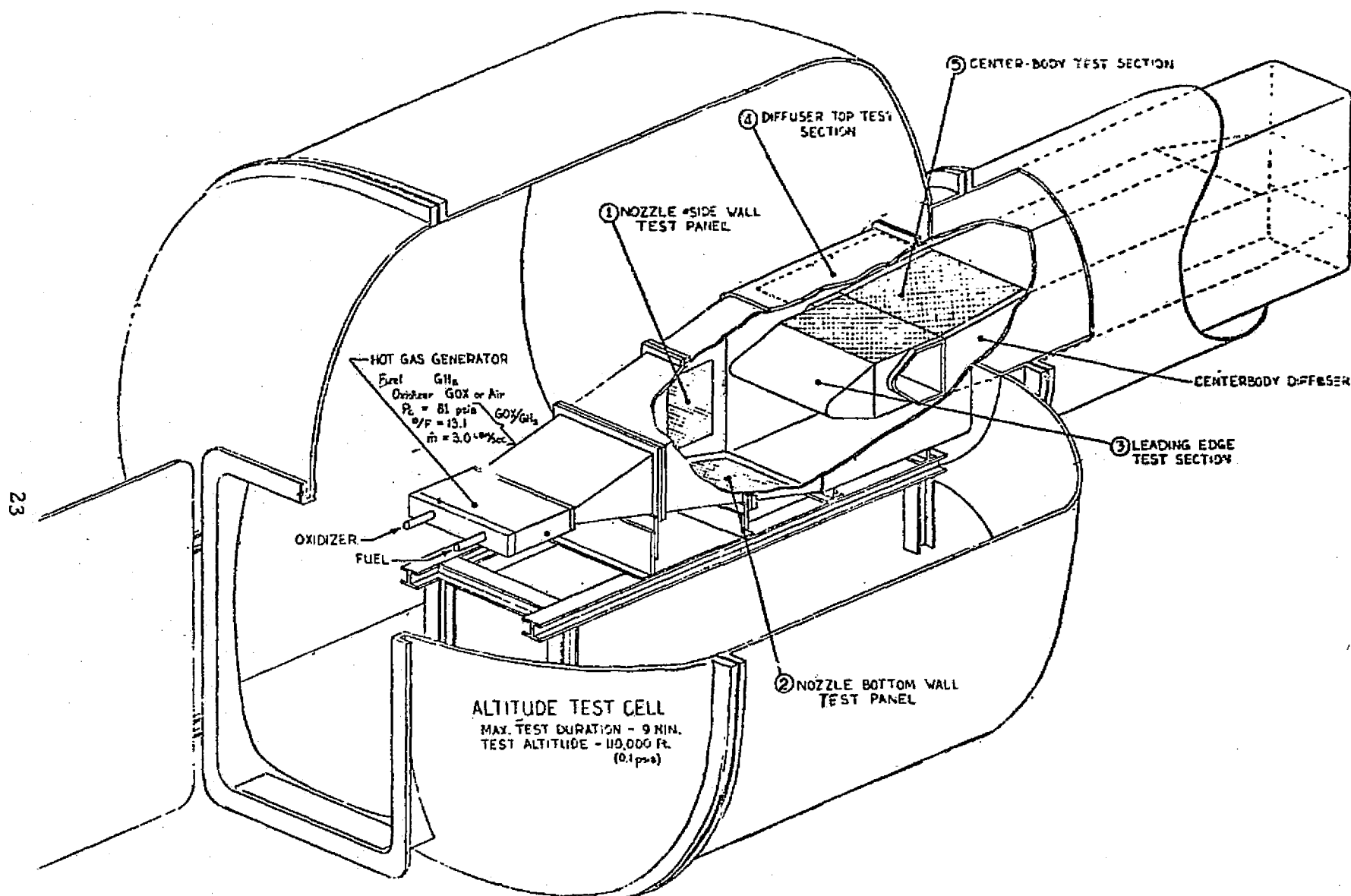


Fig. 1 - NASA-MSFC Hot-Gas Test Facility (Figure obtained from NASA)

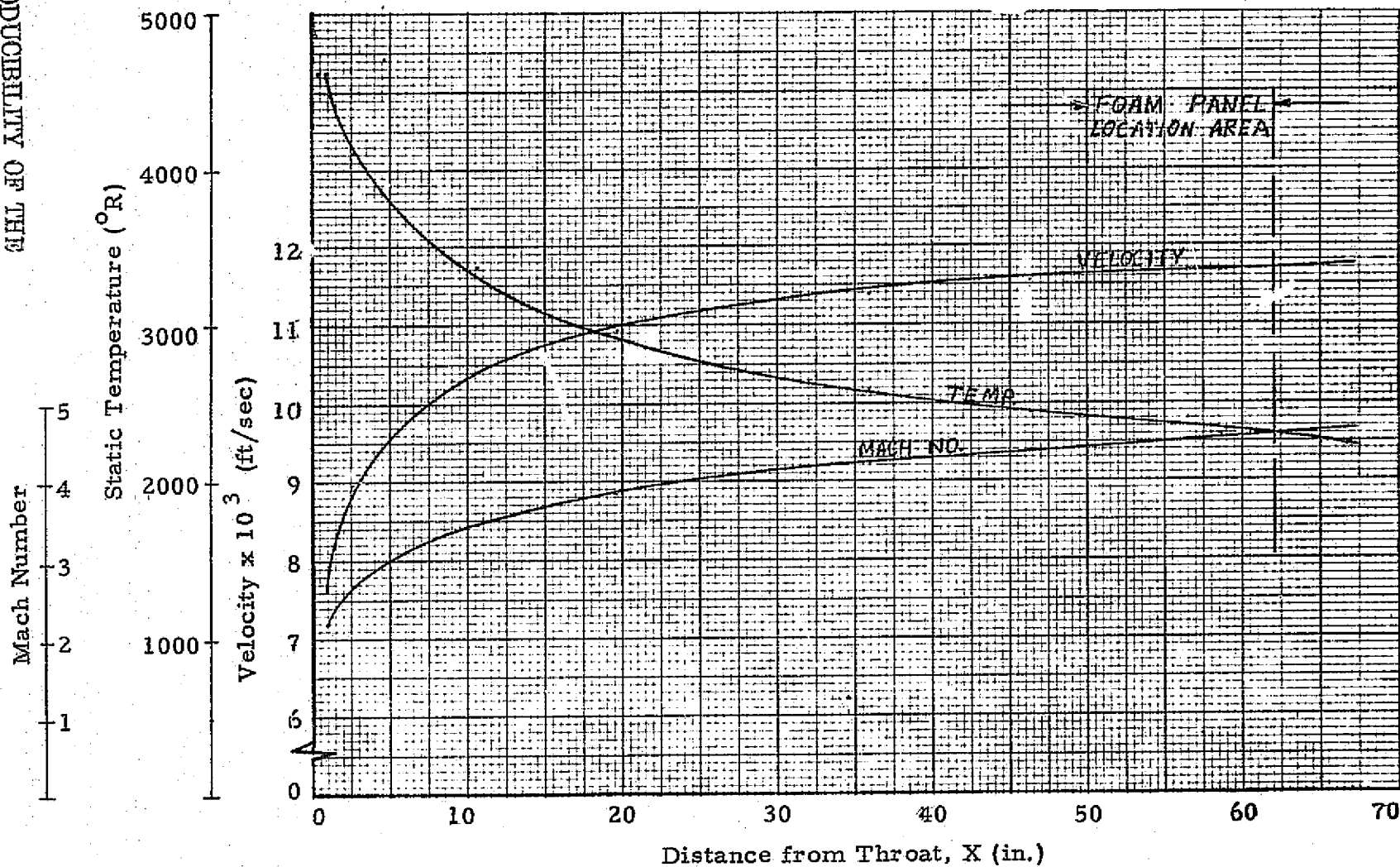


Fig. 2 - Flowfield Conditions Along the Edge of the Boundary Layer in the Hot Gas Facility for $\text{O/F} = 14$ (GOX/H_2), $P_c = 80$ psi

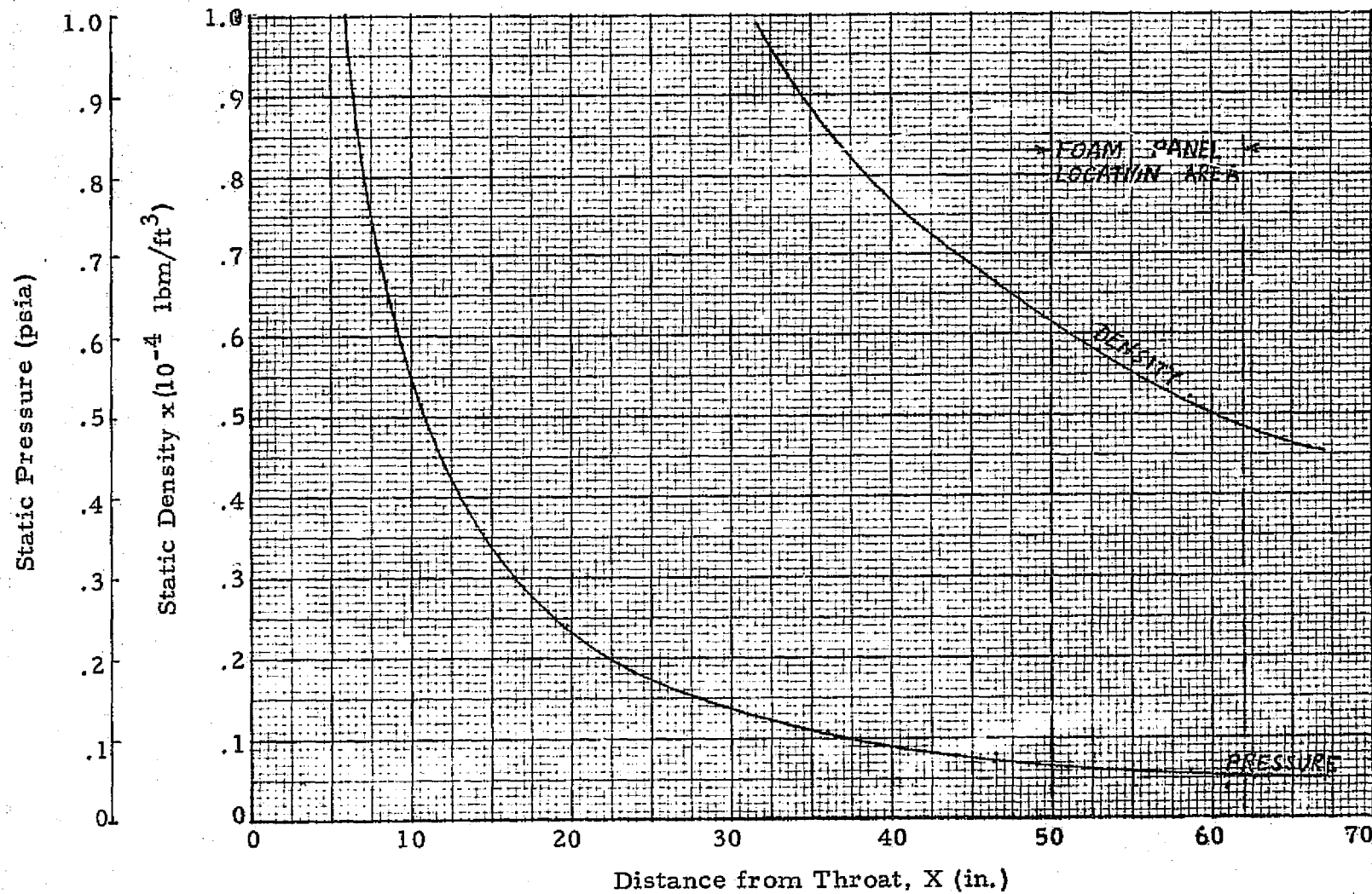
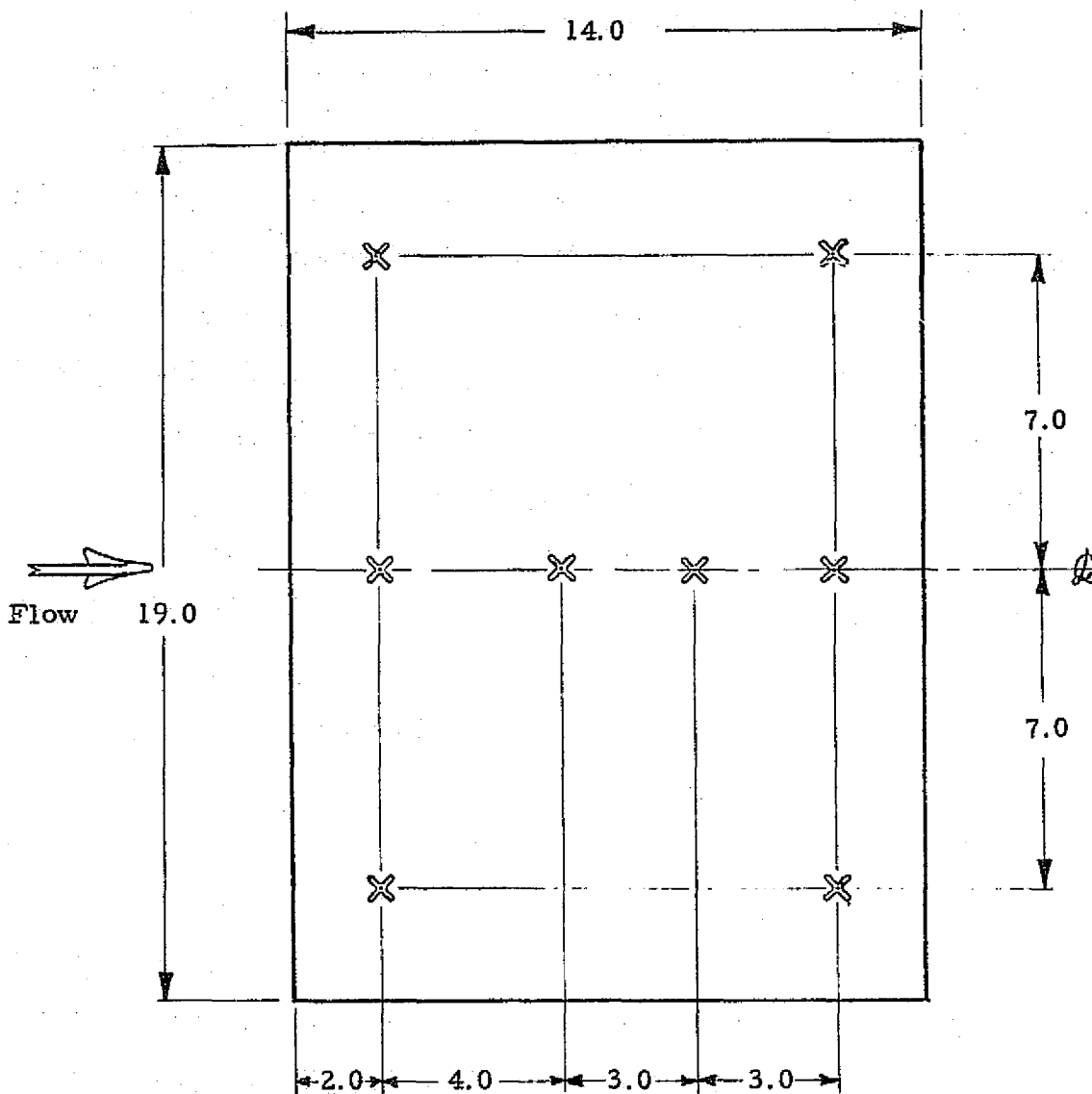


Fig. 3 - Flowfield Conditions Along the Edge of the Boundary Layer in the Hot Gas Facility for O/F = 14 (GOX/H₂), P_c = 80 psi




Note:  Calorimeter and pressure tap locations (Pressure and heating rates are measured at each location.)

Fig. 4 - Hot-Gas Test Facility Calibration Panel Showing Pressure Tap and Calorimeter Locations

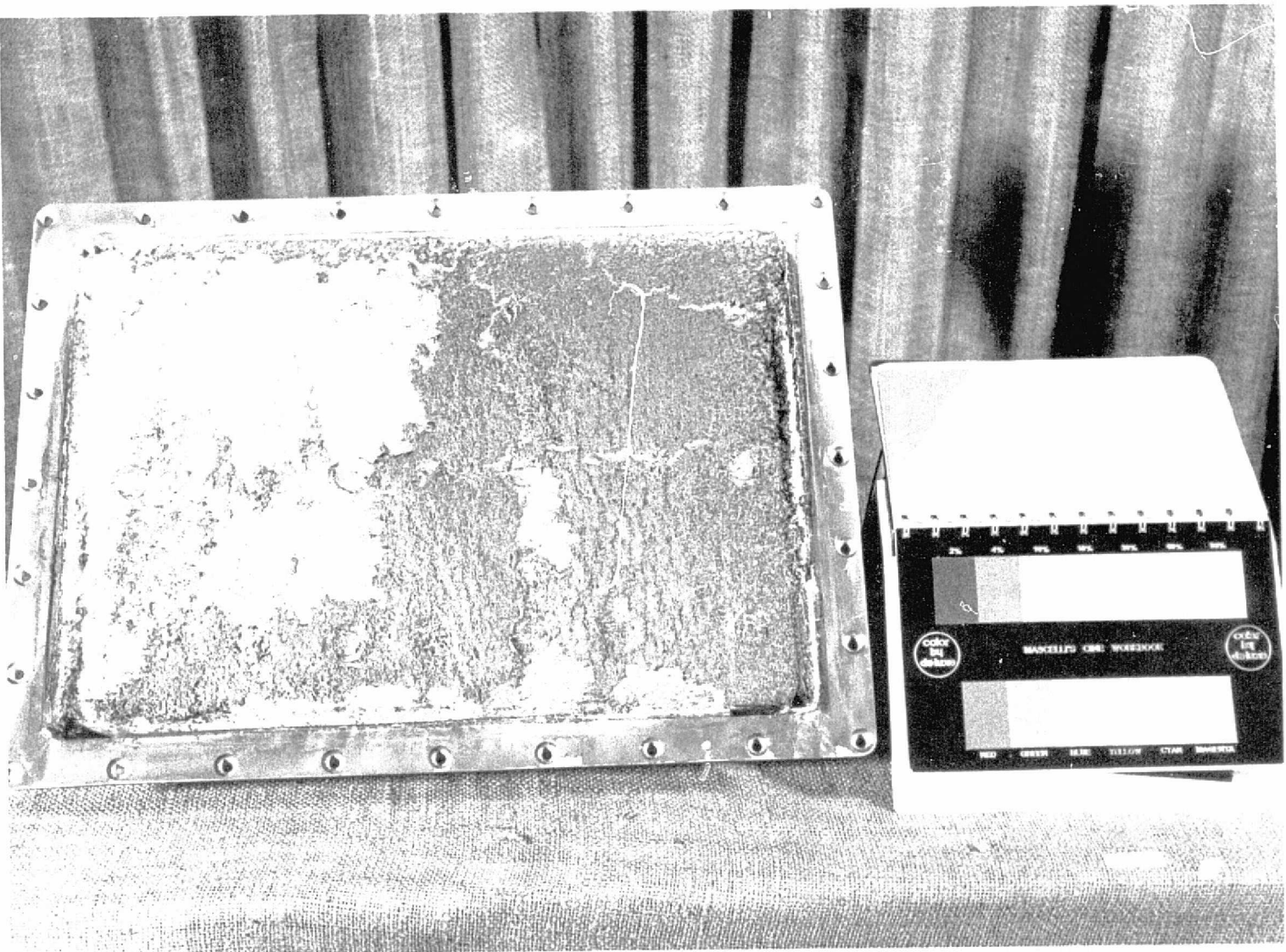


Fig. 5 - Typical Post-Test Photographs of BX-250 Foam Panels Tested in MSFC Hot Gas Test Facility (Panel shown is for Test No. 45, sidewall location)

LMSC-HREC TN D390268

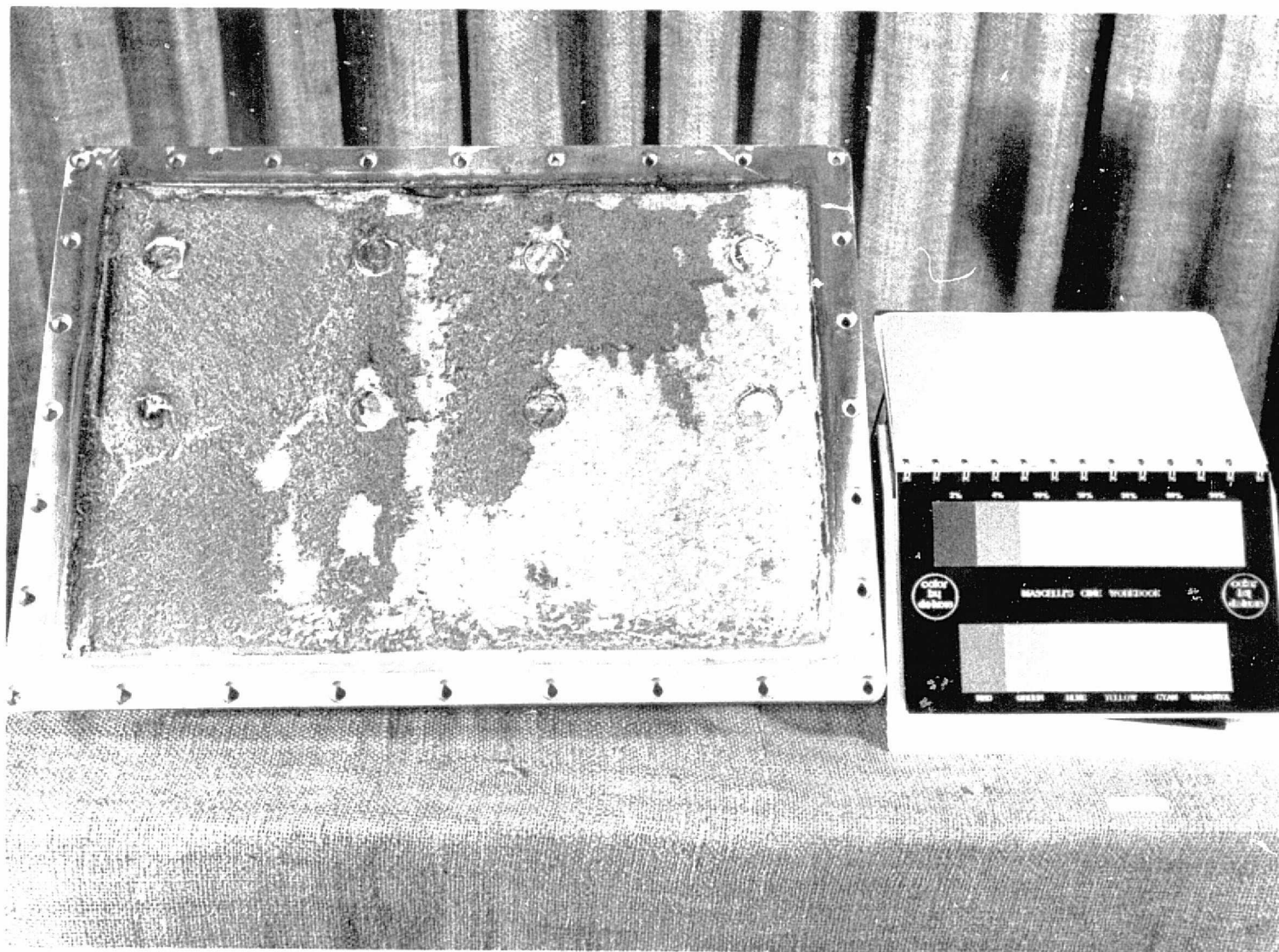


Fig. 6 - Typical Post-Test Photograph of BX-250 Foam Panels Tested in MSFC Hot Gas Test Facility (Panel shown is from Test No. 44, sidewall location)

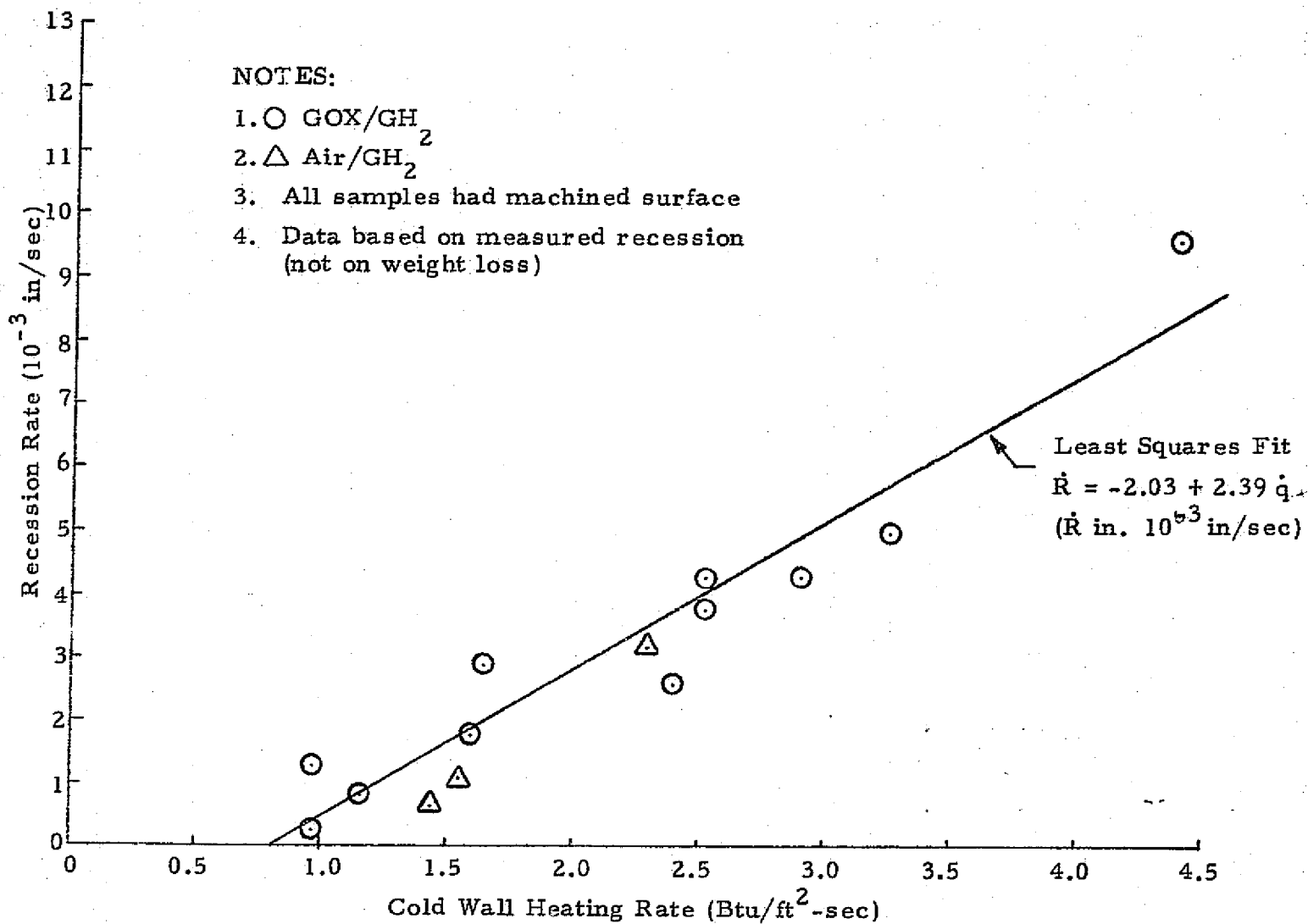


Fig. 7 - Recession Rate vs Heating Rate for MSFC Hot Gas Facility Tests of BX-250 Foam

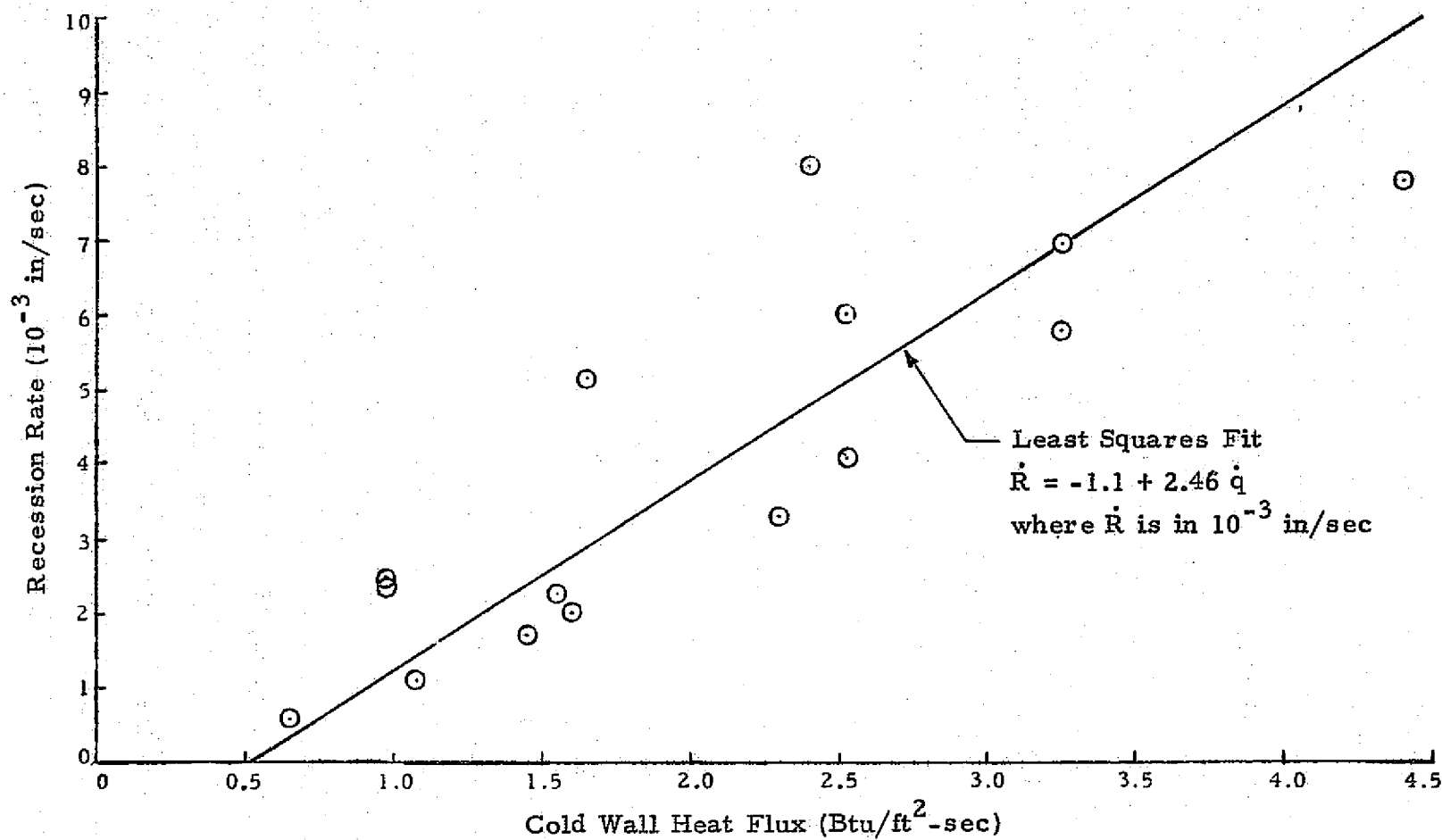


Fig. 8 - Recession Rate vs Heating Rate as Obtained from Weight-Loss Data

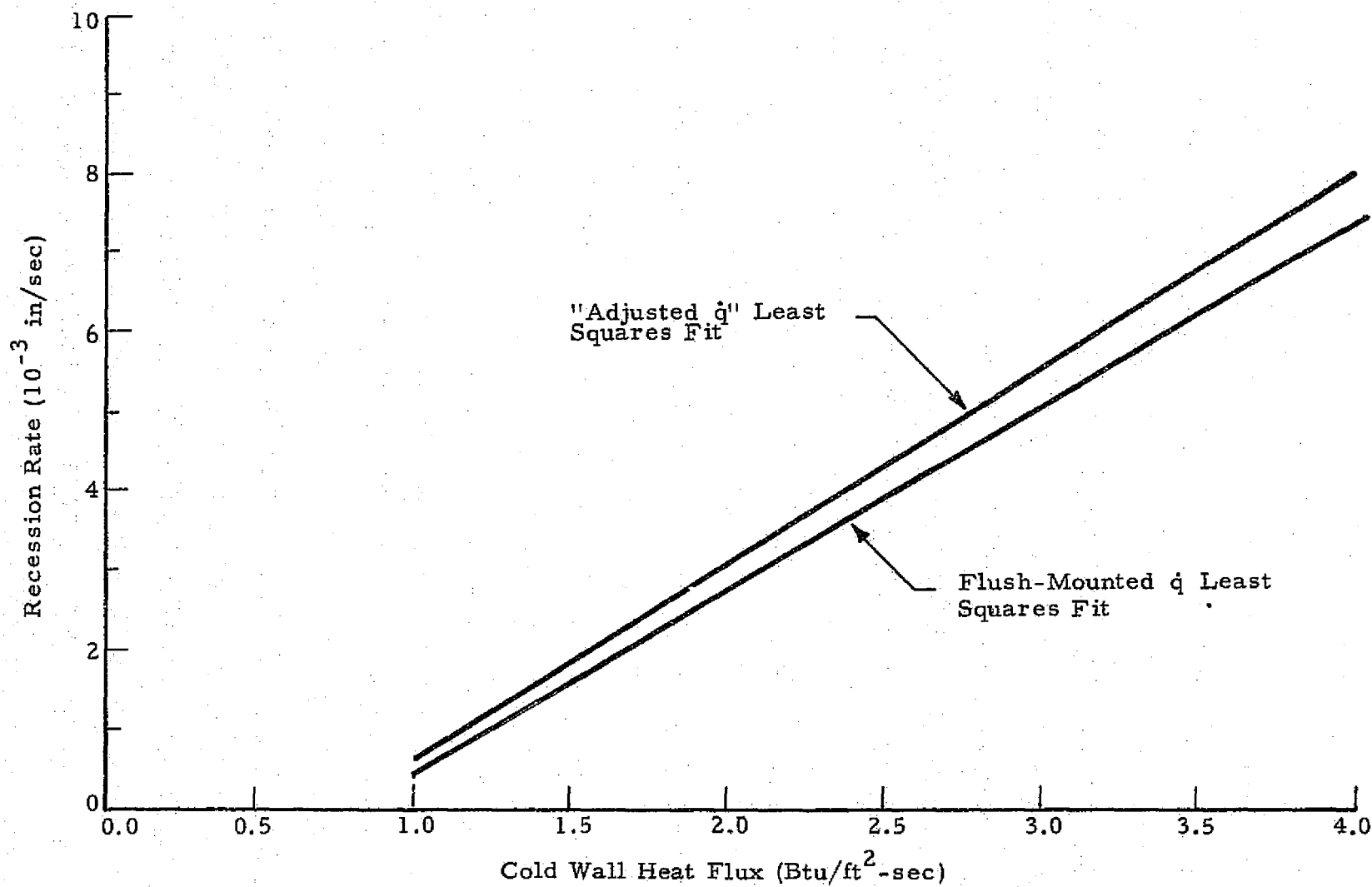


Fig. 9 - Comparison of Data with and Without Adjustments for Reduction in Heating Due to Panels Not Being Flush with the Nozzle Surface

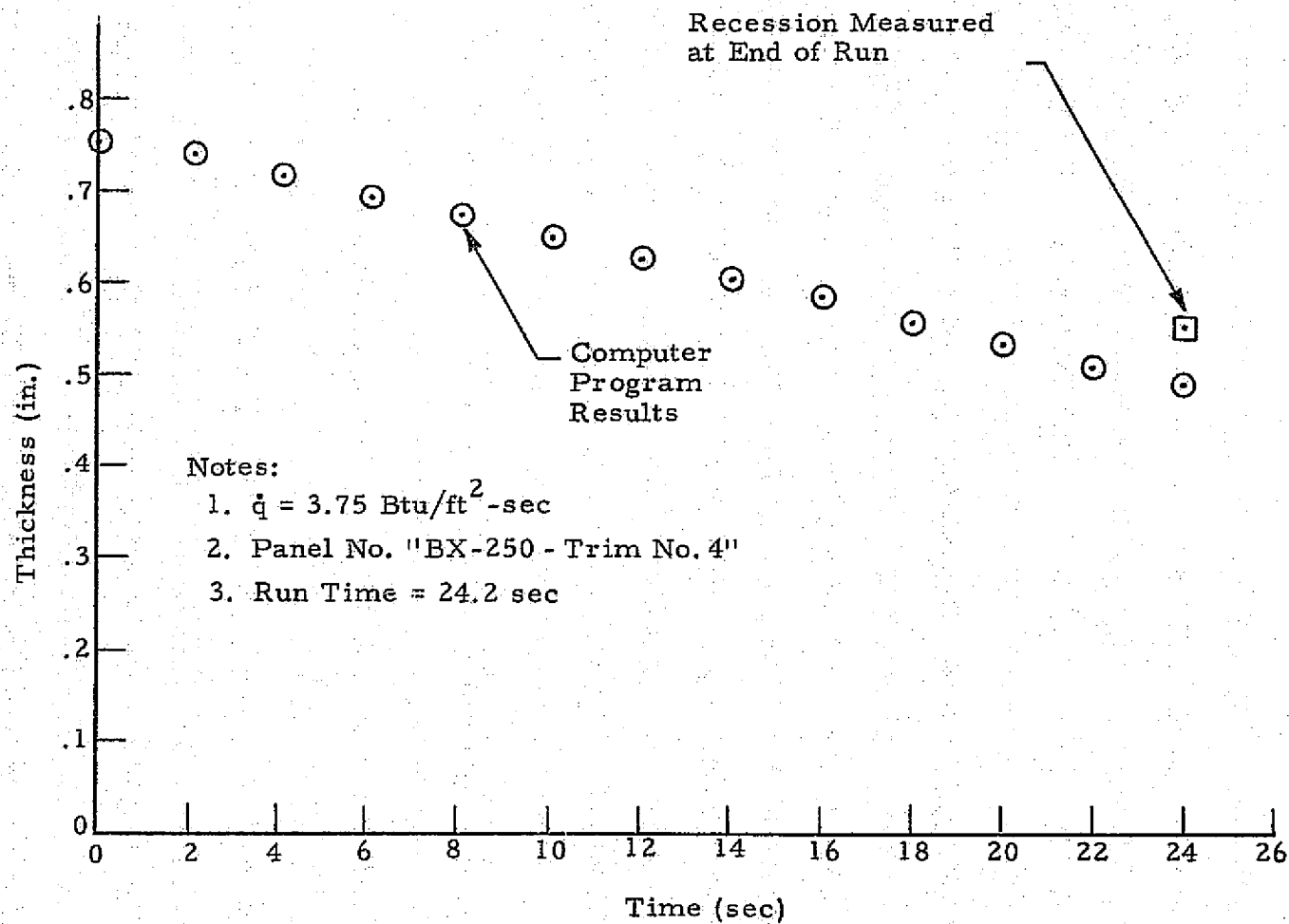


Fig. 10 - Comparison of Thickness vs Time from Test No. 34 with Computer Program Results

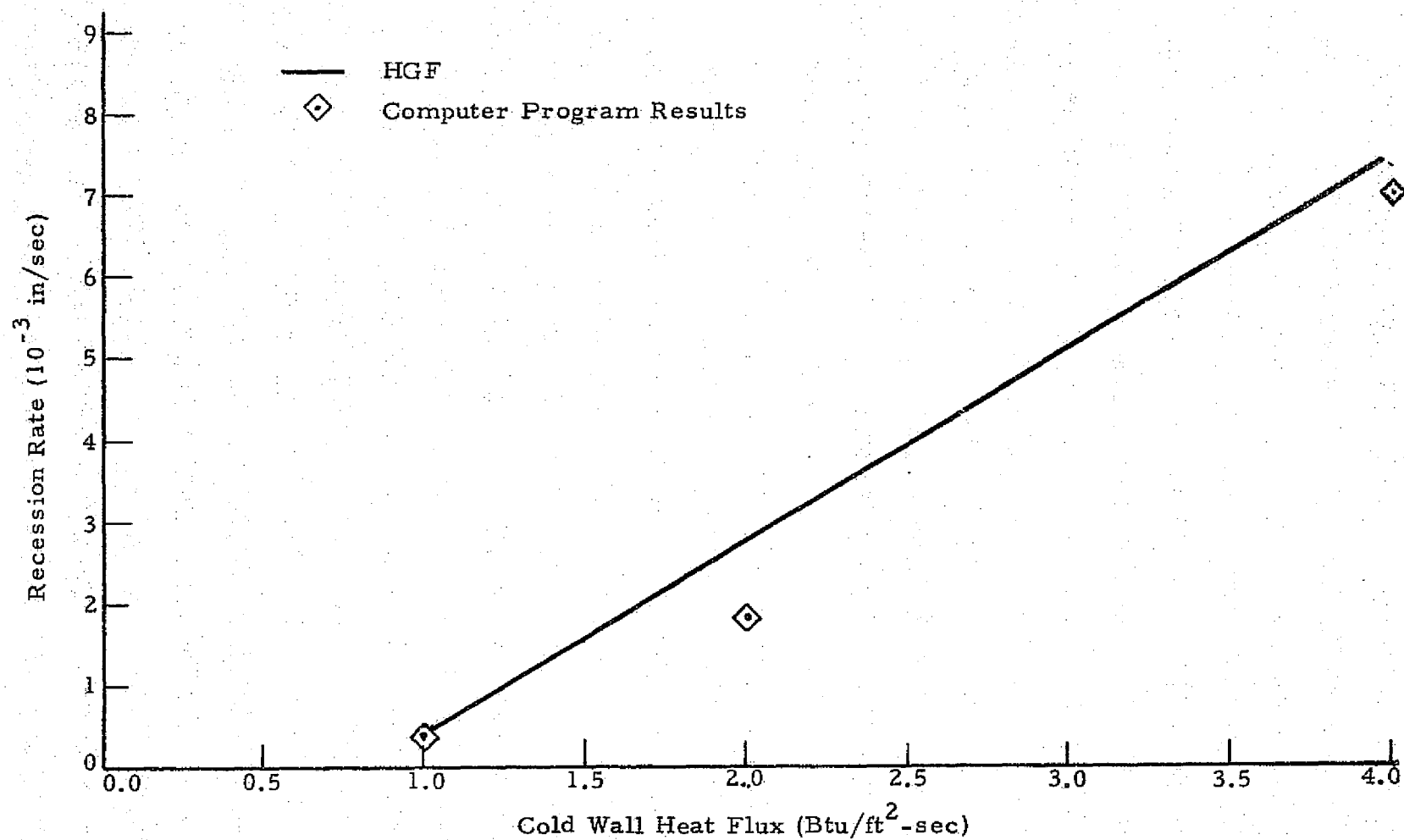


Fig. 11 - Comparison of Computer Program Results with Hot Gas Facility Tests

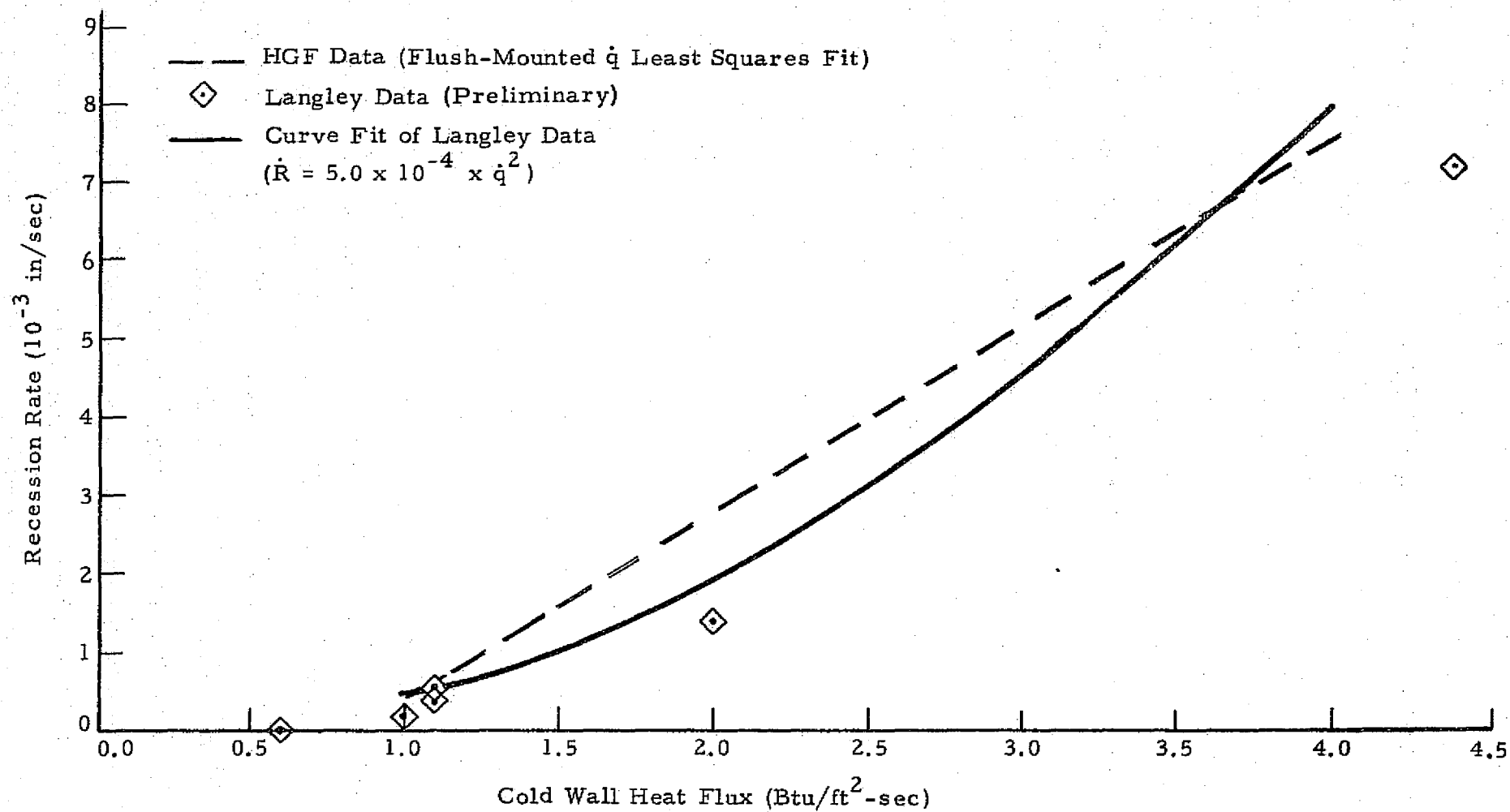


Fig. 12 - Comparison of Hot Gas Facility Data with Langley Arc Jet Data

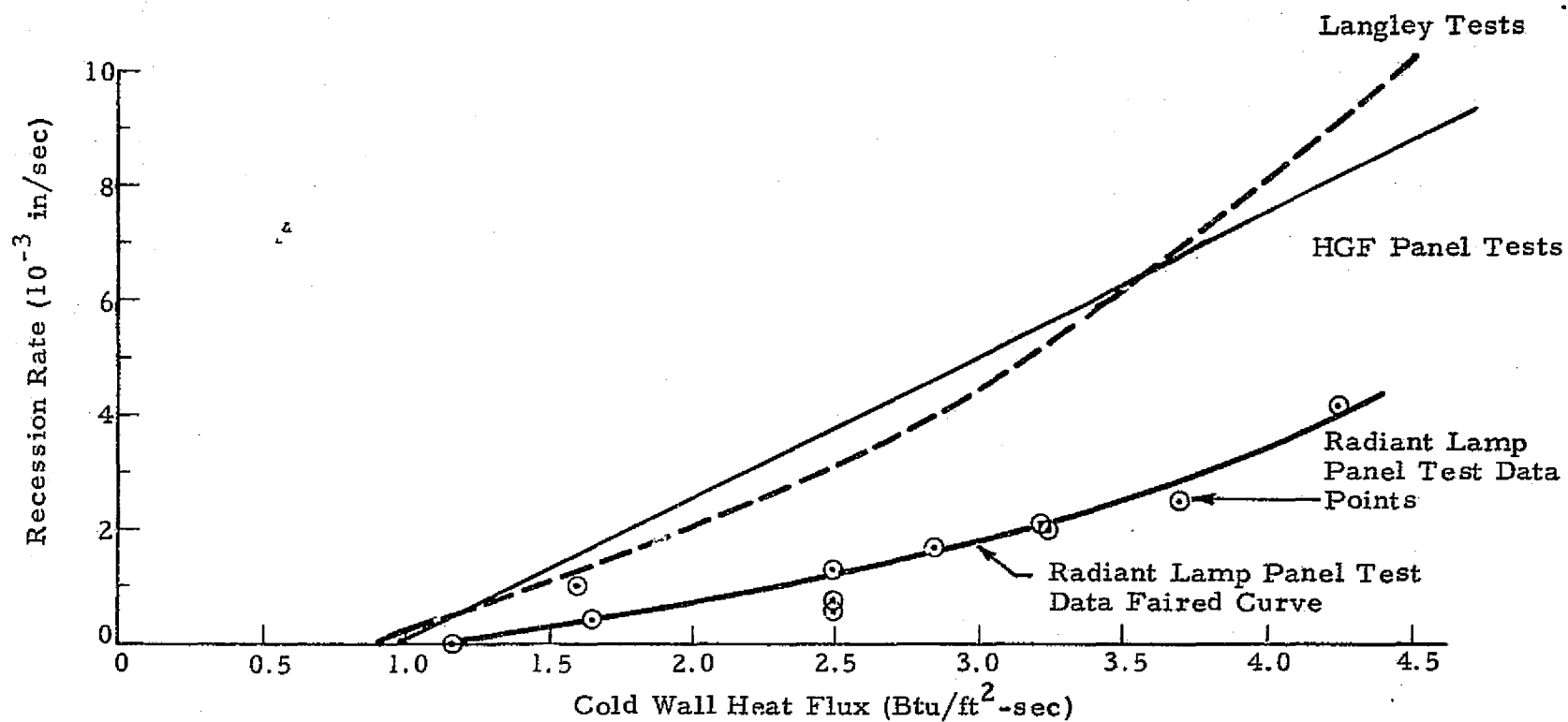


Fig. 13 - Recession Rate vs Heat Flux for BX-250 Foam in MSFC Radiant Panel Tests Facility Compared to Langley Arc Jet and MSFC Hot Gas Facility Data

Appendix C

Dean, W.G., "Discussion of the Degree of Simulation of Critical Parameters in Hot Gas Facility Foam Ablation Tests and Application Results to Flight Conditions on the Space Shuttle External Tank," LMSC-HREC TN D306905, Lockheed Missiles & Space Company, Huntsville, Ala., October 1973.

TECHNICAL NOTE

Appendix C

LOCKHEED

Huntsville Research & Engineering Center

Contract NAS8-25569

Date Oct. 1973

Doc. LMSC-HREC TN D306905

Title: DISCUSSION OF THE DEGREE OF SIMULATION OF CRITICAL PARAMETERS IN HOT GAS FACILITY FOAM ABLATION TESTS AND APPLICATION OF RESULTS TO FLIGHT CONDITIONS ON THE SPACE SHUTTLE EXTERNAL TANK

FOREWORD

This report presents the results of work performed by the Lockheed-Huntsville Research & Engineering Center under Contract NAS8-25569. The NASA-MSFC Contracting Officer's Representative (COR) for this study is Dr. Kenneth E. McCoy, S&E-ASTN-PTC.

INTRODUCTION

The NASA-MSFC Hot Gas Facility (HGF) consists of a combustion chamber, throat section, expansion nozzle, test section and diffuser. The combustion chamber burns either hydrogen and oxygen or hydrogen and air, at chamber pressures from approximately 65 psia to 110 psia and oxidizer-to-fuel (O/F) ratios of 13 to 20. The Mach number in the test section is approximately 4. Materials may be tested in the facility as panels in the nozzle sidewalls and diffuser centerbody, or as a leading edge mounted on the front of the centerbody. The tests discussed herein were run as panels in the nozzle sidewalls. Figure 1 shows a sketch of the HGF.

A number of panel tests of candidate thermal protection system (TPS) materials for the Space Shuttle External Tank (ET) have been run in the facility. The results of these tests are now being correlated in conjunction with a computer program to develop a means of predicting foam performance on the ET during flight. As in any ground test facility, not all the parameters affecting the TPS performance can be simulated completely. It is therefore necessary to look at the degree of simulation achieved and determine the effect this may have on predicted flight performance. The parameters to be considered are:

- Heating Rate
- Aerodynamic Shear

- Enthalpy
- Oxygen Content
- Pressure

DISCUSSION

Each of the parameters is now discussed individually in the following sections. (An appendix is provided at the end to explain how the values quoted in the discussion were obtained).

Heating Rate: The cold-wall heating rate, \dot{q} , levels being achieved in the Hot Gas Facility vary from approximately 0.6 to 4.4 Btu/ft²-sec. For the ET flight conditions, Rockwell predicts values from 0.0 to about 3.5 Btu/ft²-sec (Ref. 1)* (NASA-MSFC predicts values considerably higher than these.) However, regardless of which values are selected for design, the effect of time-varying \dot{q} can be taken into account properly by the computer program being developed. The Hot Gas Facility test levels are close enough to the flight levels to provide "safe" interpolation.

Aerodynamic Shear: The shear levels being experienced in the Hot Gas Facility tests at an oxygen-to-fuel ratio (O/F) of 12 are calculated to be 0.16 to 0.65 lbf/ft² while the predicted flight levels for the ET per Rockwell are 0 to 1.9 lbf/ft². This situation presents a challenge because: (1) the simulation is on the low (unconservative) side, and (2) because it is felt that the foam materials are quite "shear-sensitive." There is no known way to accurately calculate the shear effect in the computer analyses without the use of experimental data. It is therefore desirable to run additional tests at the same heating rate as in the Hot Gas Facility, but at varying shear levels. Some qualitative idea of the shear sensitivity could be obtained by running a zero-shear test in a radiant heating facility.

* 1. "Space Shuttle Program External Tank Project Induced Environment," Vol. II, SP-ET-00 02.1, Marshall Space Flight Center, Ala., March 1973.

Another aspect of the shear problem is that of what happens in a shock impingement area. The first part of the problem is to determine what the shear level is for the flight case and the second part is to try to simulate this in a ground test. The best practical solution to this seems to be to test the foam in the HGF in the region where a shock strikes the wall on the dome lid or on the centerbody. This should also be supported by a study of how well the HGF shock angle, strength, velocity gradient, etc., simulate the flight values.

Enthalpy: The term "enthalpy" as used in materials test work refers to the total or recovery value in the freestream (or boundary layer edge) as opposed to the static value. In the HGF for an $O/F = 12$, the enthalpy is approximately 3900 Btu/lb. In flight the value varies from 0 to about 600 Btu/lb at the time of max heating and about 13,000 Btu/lb at 500 seconds. Ablative material performance is affected by the enthalpy level through the convective heating blockage in the boundary layer. As the ablator decomposes, it gives off gases which enter the boundary layer and form a layer of "cool," insulating gas at the surface. The higher the boundary layer edge enthalpy (or temperature) becomes, the more effective this "cooling" mechanism becomes. If the HGF enthalpy is much higher than the flight value, the result would be to get more effectiveness in the ground tests than will be experienced in flight. This is undesirable because it is in the unconservative direction. If the HGF enthalpy is lower than the flight value the results will be conservative. This problem can be attacked analytically and an estimate made of this difference in effectiveness. This additional effect can then be corrected for the computer analysis. This should also be backed up by additional tests at additional enthalpy levels, perhaps in other facilities. Also the radiant lamp tests mentioned earlier should be of assistance in this problem.

Oxygen Content: The Hot Gas Facility can simulate various oxygen content environments because it can be run using either air or gaseous oxygen as the oxidizer. Also each oxidizer can be run at various O/F ratios. Running with oxygen at an O/F of 13 produces an oxygen content at the sample test area of

about 36%. With air the O_2 content is near zero. (In flight the value is near 20%). O_2 content affects the performance of an ablating material through chemical reactions which involves the use of oxygen. Generally in the higher temperature ablators, which form a carbon char layer, the surface gets hot enough to oxidize or burn at a rapid rate and oxygen content is a very critical parameter. However, with the foam materials it is felt that the surface will probably never get hot enough for this oxidization mechanism to become significant. Rather, since the charring material is so fragile, it is felt that it will be kept swept away by the aerodynamic shear before reaching a high temperature. (It is noted that this is still a hypothesis at the present time, and more study is needed for verification of the surface temperature).

It has been shown by Thermogravimetric Analysis (TGA) data that oxygen does affect the reaction rate of the foam in a static gas environment. This is observed by running samples in air and argon. However, the reaction rates are essentially the same in air and argon up to about 850°F after which the air data show the sample reacting much faster than the argon data. If it can be shown that in a shearing environment the material surface is being removed before it reaches 850°F then the oxygen content in ground tests versus flight will become insignificant.

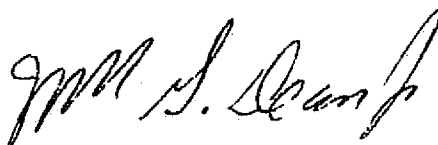
Pressure: Pressure affects material performance in two ways. The first is through the heating rate and shear. The higher the pressures are, the higher the shear and heating rate will be. This part of the effect can be handled as discussed above under "heating rates," and "aerodynamic shear." In the second part of the problem, increased pressures affect material response through providing more available oxygen to the surface for reactions. In this respect it affects performance in a way similar to oxygen content. Physically this is a combined effect of the two parameters which is the oxygen partial pressure or the product of percent oxygen content and "total" pressure.

The Hot Gas Facility pressures are about 0.04 to 0.1 psia at the locations presently being used for tests. The flight values range from 14.7 to 0. At the point of maximum heating on the ET sidewall the pressure is approximately 5.5

psi at the time of maximum heating. At 500 seconds, which is near the time of the second heating spike, the pressure is only about .006 psia. Therefore, when applying the HGF results to the flight case, corrections must be made for pressure variation. The normal method of correlating ablation performance data with pressure is to show recession rate as a function of temperature with an oxygen partial pressure term to the 0.4 or 0.5 power. This can be done with our existing computer program. However, this type correlation has been developed with data from materials which operate at much higher surface temperatures where the surface is rapidly oxidizing. Therefore, such an approach will be used with caution when being applied to the foam materials until more data become available.

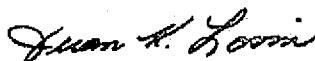
One approach to improving the simulation of oxygen partial pressure in the Hot Gas Facility is to run at additional O/F ratios. This varies the O₂ concentration and partial pressure. This will provide more data points to check the "0.4 to 0.5 power" form of correlation.

Also, radiant lamp tests are being run at various pressures to study the oxygen partial pressure effect.



W. G. Dean, Project Engineer
Space Shuttle Thermal Support Contract

Approved:



Juan K. Lovin, Supervisor
Thermodynamics & Structures Section

Attach: (1) Figure 1
(2) Appendix
(3) Addendum I

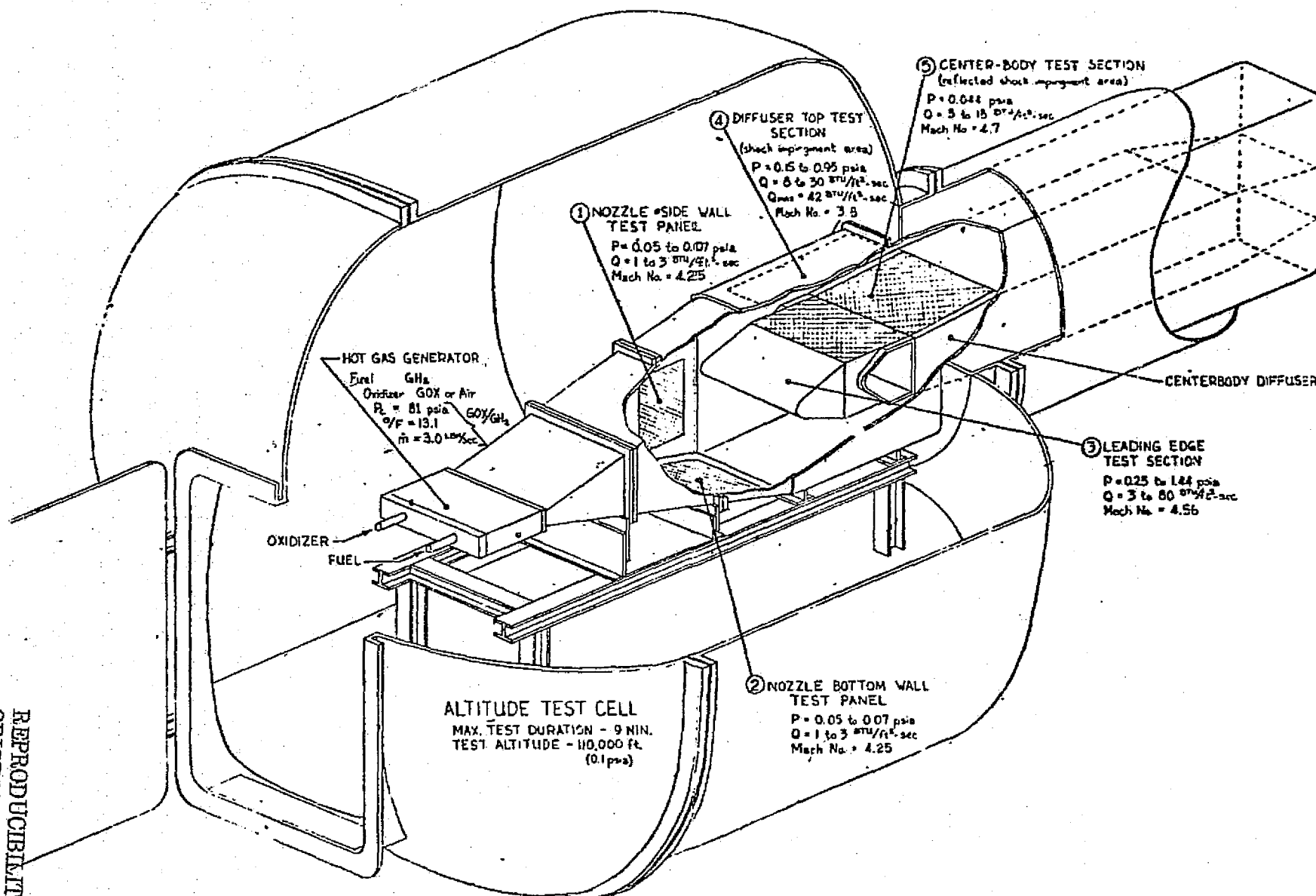


Fig. 1 - NASA-MSFC Hot-Gas Test Facility (Figure obtained from NASA)

Appendix

This appendix is provided to explain how the values quoted in the main writeup discussion were obtained.

Heating Rates: The heating rates quoted in the writeup were taken from the measured data in the Hot Gas Facility (HGF). The 0.6 value is for air/hydrogen at a chamber pressure of 100 psia. The 4.4 value is for oxygen/hydrogen at a chamber pressure of 110 psia. These are average values over the surface of the panels.

Shear Stress Calculation Method: The shear stress was calculated from the following relation.

$$\tau_w = C_f \frac{1}{2} \rho_e V_e^2 \frac{1}{gc}$$

where

τ_w = shear stress at the wall, lbf/ft²

C_f = skin friction coefficient

$\rho_e V_e$ = density-velocity at boundary layer edge,
lbm/ft³, ft/sec

gc = dimensional conversion factor, 32.2
ft-lbm/lbf-sec²

The skin-friction coefficient, C_f , is calculated using Reynolds analogy which states that heat and momentum are transferred through the boundary layer by analogous processes. Mathematically,

$$S_t = C_f/2 \tag{A.1}$$

where

St = Stanton Number = $h_c / \rho_e V_e C_p$

h_c = heat transfer coefficient, Btu/ft²-sec-°R

C_p = specific heat, Btu/lbm-°R

Therefore

$$C_f = 2 St = 2 h_c / \rho_e V_e C_p$$

The heat-transfer coefficient is determined from the heating rate (measured or calculated) as follows: (In this case HGF measured values were used).

$$\begin{aligned} \dot{q} &= h_c (T_{aw} - T_w) \\ \text{or } h_c &= \frac{\dot{q}}{T_{aw} - T_w} \end{aligned} \quad (A.2)$$

where

$$\dot{q} = \text{heating rate, Btu/ft}^2\text{-sec}$$

$$T_{aw} = \text{adiabatic wall temperature, } ^\circ\text{R}$$

$$T_w = \text{wall temperature, } ^\circ\text{R}$$

so

$$C_f = \frac{2 \dot{q}}{(T_{aw} - T_w) \rho_e V_e C_p}$$

since

$$C_p T_{aw} = H_{aw}, \text{ adiabatic wall enthalpy, Btu/lbm}$$

$$C_p T_w = H_w, \text{ wall enthalpy, Btu/lbm}$$

$$C_f = \frac{2 \dot{q}}{(H_{aw} - H_w) \rho_e V_e}$$

and

$$\tau_w = \frac{2 \dot{q}}{(H_{aw} - H_w) \rho_e V_e} \left[\frac{1}{2} \rho_e V_e^2 \right] \left[\frac{1}{gc} \right]$$

$$\tau_w = \frac{\dot{q} V_e}{(H_{aw} - H_w) gc}$$

The preceding derivations for a Prandtl number, Pr , of unity. For non-unity Prandtl number gases, a "modified" Reynolds analogy is used where $(Pr_e)^{-2/3}$ is used as follows:

$$\tau_w = \frac{\dot{q} V_e Pr_e^{-2/3}}{(H_{aw} - H_w)gc} \quad (A.3)$$

For the values stated in the writeup the "modified" method was used and τ_w calculated as follows:

$$\begin{aligned} \dot{q} &= \text{measured value in HGF, } 4.4 \text{ Btu/ft}^2\text{-sec} \\ V_e &= \text{velocity from Lockheed Method-of-Characteristics program, Ref. A-1. } (V_e = 12,000 \text{ ft/sec at the third nozzle section.}) \end{aligned}$$

The values of H_{aw} , H_w are taken from a Lockheed PLIMP program (Ref. A-2) run. (These are real-gas equilibrium values.)

$$\begin{aligned} H_{aw} &= 3480 \text{ Btu/lbm (assuming a recovery factor of .89)} \\ H_w &= 210 \text{ Btu/lbm} \\ Pr^{-2/3} &= .6722^{-2/3} = 1.3, \text{ } Pr \text{ is obtained from Svehla, Ref. A-3. (Real-gas, equilibrium value at our pressure and temperature)} \\ \tau_w &= \frac{4.4 \times 12,000 \times 1.3}{(3480 - 210)(32.2)} = .65 \text{ lbf/ft}^2 \end{aligned}$$

These values are for an O/F of 12, burning oxygen/hydrogen, at a chamber pressure of 80 psi.

For an air run with a $P_c = 142$ psia, O/F = 20 the shear calculation is as follows at the third nozzle section:

$$\begin{aligned} \tau_w &= \frac{\dot{q} V_e Pr_e^{-2/3}}{(H_{aw} - H_w)(gc)} \\ \dot{q} &= 0.6 \text{ Btu/ft}^2\text{-sec} \end{aligned}$$

$$V_e = 7845 \text{ ft/sec}$$

$$H_{aw} = 1340 \text{ Btu/lb}$$

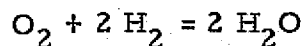
$$H_w = 222 \text{ Btu/lb}$$

$$Pr = .74 \text{ (approximate)}$$

from which $\tau_w = .16 \text{ lbf/ft}^2$.

Oxygen Content: O_2 content can be estimated as follows:

For a stoichiometric condition the following chemical equation applies:



Using molecular weights to convert this to weights:

$$2 (16) + 2 (2 \times 1) = 2 (2 \times 1 + 16)$$

$$32 \text{ lb oxygen} + 4 \text{ lb hydrogen} = 36 \text{ lb } H_2O$$

that is: for every 1 lb of hydrogen burned, 8 lbs of oxygen are required.

Assume we are running at an oxygen to fuel weight ratio, O/F , of 13. Then for each 1 lb of H_2 we use 8 lbs of O_2 and 5 lbs "excess" O_2 , producing 9 lbs of H_2O and 5 lbs of "free" O_2 . The ratio of free oxygen in the flow is then $5/14$, or 35.6%.

The computer programs used at Lockheed use a more sophisticated method taking into account real gas effects (dissociation and ionization). Chemical equilibrium is assumed at each temperature. The methods are contained in the "CEC" program, Ref. A-4. Results of this program for a $P_c = 80 \text{ psi}$, $O/F = 12$ oxygen/hydrogen are as follows:

① Species	② Mole Fraction	③ Molecular Weight	④ ② x ③	⑤ Mass Fraction = ④/Molecular Wt., Mixture*
H	.0293	1.0	0.029	0
O	.0394	16.0	0.63	0.0334, (3.0%)
HO ₂	.0001	33.0	0	0
OH	.123	17.0	2.09	0.111, (11.0%)
H ₂	.055	2.0	0.11	0
O ₂	.168	32.0	5.34	0.287, (28.7%)
H ₂ O	.585	18.0	10.50	<u>0.56,</u> <u>(56.0%)</u>
Total				0.991 (99.0%)

For the air/hydrogen case it can easily be shown that there is no free O₂. This is because for stoichiometric conditions the O/F is near 40. We are running the HGF at O/F of about 15 with air. This means that we are very fuel (H₂) rich and all available O₂ is completely used up.

The air/hydrogen stoichiometric O/F condition of 40 can be shown approximately as follows: As shown earlier we need 8 lbs of O₂ for each 1 lb of H₂. Also, in air we have about 4 lbs of N₂ for every 1 lb of O₂. Therefore, for each 1 lb of H₂ we have 8 lbs of O₂ and 32 lbs of N₂ for a total of 40 lbs of air for every 1 lb of H₂.

Pressures: The pressures quoted in the writeup for the HGF are measured values averaged over the panel area. The low value of 0.04 psia is for the air runs on the top panel, the high value of 0.1 psia is for an oxygen run on the side panel. The flight values quoted are from North American/Rockwell (Ref. A-5).

* The molecular weight of the mixture is 18.78.

REFERENCES

- A-1. Prozan, R. J., "Development of a Method-of-Characteristics Solution for the Supersonic Flow of an Ideal, Frozen or Equilibrium Reacting Gas/Mixture, LMSC-HREC D162220-III, Lockheed Missiles & Space Company, Huntsville, Ala., May 1970.
- A-2. Wojciechowski, C. J., and M. M. Penny, "Development of High Altitude Plume Impingement Analysis for Calculating Heating Rates, Forces and Moments," LMSC-HREC D162867-I, Lockheed Missiles & Space Company, Huntsville, Ala., March 1971.
- A-3. Svehla, R. A., "Thermodynamic and Transport Properties for the Hydrogen-Oxygen System," NASA SP-3011 (1964).
- A-4. Zeleznik, F. J., and S. Gordon, "A General IBM 704 or 7094 Computer Program for Computation of Chemical Equilibrium Compositions, Rocket Performance and Chapman-Jouguet Detonations," NASA TN D-1454, October 1962.
- A-5. "Space Shuttle Program External Tank Project Induced Environment," Vol. II, SP-ET-00 02.1, Marshall Space Flight Center, Ala., March 1973.

Addendum I

Equation A-3 should read:

$$\tau_w = \frac{\dot{q} V_e \text{Pr}_e^{2/3}}{(H_{aw} - H_w) g_c}$$

rather than:

$$\tau_w = \frac{\dot{q} V_e \text{Pr}_e^{-2/3}}{(H_{aw} - H_w) g_c}$$

This yields a corrected value of

$$\tau_w = 0.39 \text{ lbf/ft}^2$$

rather than

$$\tau_w = 0.65 \text{ lbf/ft}^2$$

for the oxygen/hydrogen, O/F = 12 case, and

$$\tau_w = 0.11 \text{ lbf/ft}^2$$

rather than

$$\tau_w = 0.16 \text{ lbf/ft}^2$$

for the air/hydrogen, O/F = 20 case.

Appendix D

Dean, W. G., and R. O. Hedden, "SSME Flame Bucket Heating on the F-1 Test Stand," LMSC-HREC D390451, Lockheed Missiles & Space Company, Huntsville, Ala., November 1974.

TECHNICAL NOTE

Appendix D

LOCKHEED

Huntsville Research & Engineering Center

Contract NAS8-25569 Date Nov. 1974 Doc. LMSC-HREC TN D390451

Title: SSME FLAME BUCKET HEATING ON THE F-1 TEST STAND

FOREWORD

This report presents the results of heating rate analyses performed by personnel of the Lockheed-Huntsville Research & Engineering Center under Contract NAS8-25569. The NASA Contracting Officer's Representative (COR) for this study is Dr. Kenneth E. McCoy, EP-44.

INTRODUCTION AND SUMMARY

Analytical studies to predict the heating rates for sea level testing of the SSME using the F-1 water-cooled test stands at North American Rockwell and the NASA Mississippi Test Facility have been conducted. The purpose of the studies was to determine if the water flow rate was sufficient to keep the flame bucket cooled for sustained SSME testing. Since the heating rates for the F-1 were unknown from previous tests, analyses for both the SSME and F-1 were performed for comparison and are presented herein.

TECHNICAL DISCUSSION

Heating rate analyses for the SSME and F-1 were performed to determine if the F-1 test facilities were adequate for SSME testing. The exhaust plume flow fields were predicted using the GASL mixing program (Refs. 1 and 2) assuming equilibrium chemistry to obtain the fluid properties along the flame bucket upstream of the shock.

A small computer program using the techniques presented in Ref. 3 was developed to obtain the fluid properties downstream of the shock. Shock angles at various locations along the flame bucket were calculated using the weak shock solution for attached shocks. At any location where shock angle solutions could not be obtained a parallel shock was assumed.

For the attached shock, the flow properties directly behind the shock were used as the local flow conditions. However, additional calculations are necessary to obtain the local flow conditions behind the parallel shock. After passing the flow through the parallel shock, the turning angle was calculated. Either a compression or an expansion was then used to calculate the local flow conditions.

The local flow conditions were used in the Multiple Pressure Gradient Program (Ref. 4) to obtain the heating rates. The program is based on the Blasius flat plate heating method modified to use Eckerts' reference enthalpy solution for evaluation of the boundary layer properties. The method is further modified to use an equivalent characteristic running length obtained by integrating the variable flow properties along the boundary layer edge from the plate leading edge to each particular location.

RESULTS AND CONCLUSIONS

Comparisons were made between the SSME and F-1 calculated heating rates along the flame bucket and pressures throughout the exhaust plumes. Figures 1 and 2 present the flame bucket heating rates for the SSME and F-1, respectively. Using Figs. 1 and 2, it was determined that the total heat load for the F-1 is approximately 60% greater than for the SSME; however, the maximum heating rate for the SSME is approximately 60% higher than for the F-1. It was concluded that the same amount of coolant used in the F-1 testing would be more than adequate for the SSME, but it would be necessary to change the coolant injection hole patterns to compensate for the high heat flux area of the SSME plume.

Figures 3 and 4 present the pitot pressures along the flame bucket, while Figs. 5 and 6 show the pitot pressures along the plume centerlines as a function of distance from the exhaust planes for the SSME and F-1, respectively. From these data it was determined that the maximum static pressures encountered would be 58.4 psia for the F-1 and 80.8 psia for the SSME at a distance of approximately 57 ft from the nozzle exit planes for a 3 deg cant angle. Also shown on Fig. 5 is a comparison of the pitot pressures presented in Ref. 5 and those calculated using the program presented in Refs. 1 and 2. Based on the maximum static pressures along the flame bucket, existing facilities pressures were determined to be adequate.

R.O. Hedden

R.O. Hedden
Heat Protection Systems Group

Wm G. Dean

William G. Dean, Project Engineer
Space Shuttle Thermal Support Contract

Approved:

Juan K. Lovin

Juan K. Lovin, Supervisor
Thermodynamics & Structures Section

Attach: (1) References
(2) Figs. 1 through 6

REFERENCES

1. Edelman, R., and O. Fortune, "Mixing and Combustion in the Exhaust Plumes of Rocket Engines Burning RP1 and Liquid Oxygen," Technical Report No. 631, General Applied Sciences Laboratories, Inc., Westbury, N. Y., November 1966.
2. Audeh, B. J., "Equilibrium Shear Layer Program," TM 54/20-169, LMSC-HREC A784899, Lockheed Missiles & Space Company, Huntsville, Ala., December 1967.
3. Ames Research Staff, "Equations, Tables, and Charts for Compressible Flow," Report 1135, National Advisory Committee for Aeronautics, 1953.
4. Blackledge, M. L., and C. J. Wojciechowski, "Real Gas Multiple Pressure Gradient Heating Rate Program," LMSC-HREC A783781, Lockheed Missiles & Space Company, Huntsville, Ala., May 1967.
5. S&E-AERO-AT/Thermal Environment Branch, "Orbiter SSME Cluster Plume Impingement on MTF S-IC Facility Flame Deflector," S&E-AERO AT-73-18, National Aeronautics and Space Administration, Marshall Space Flight Center, May 1973.

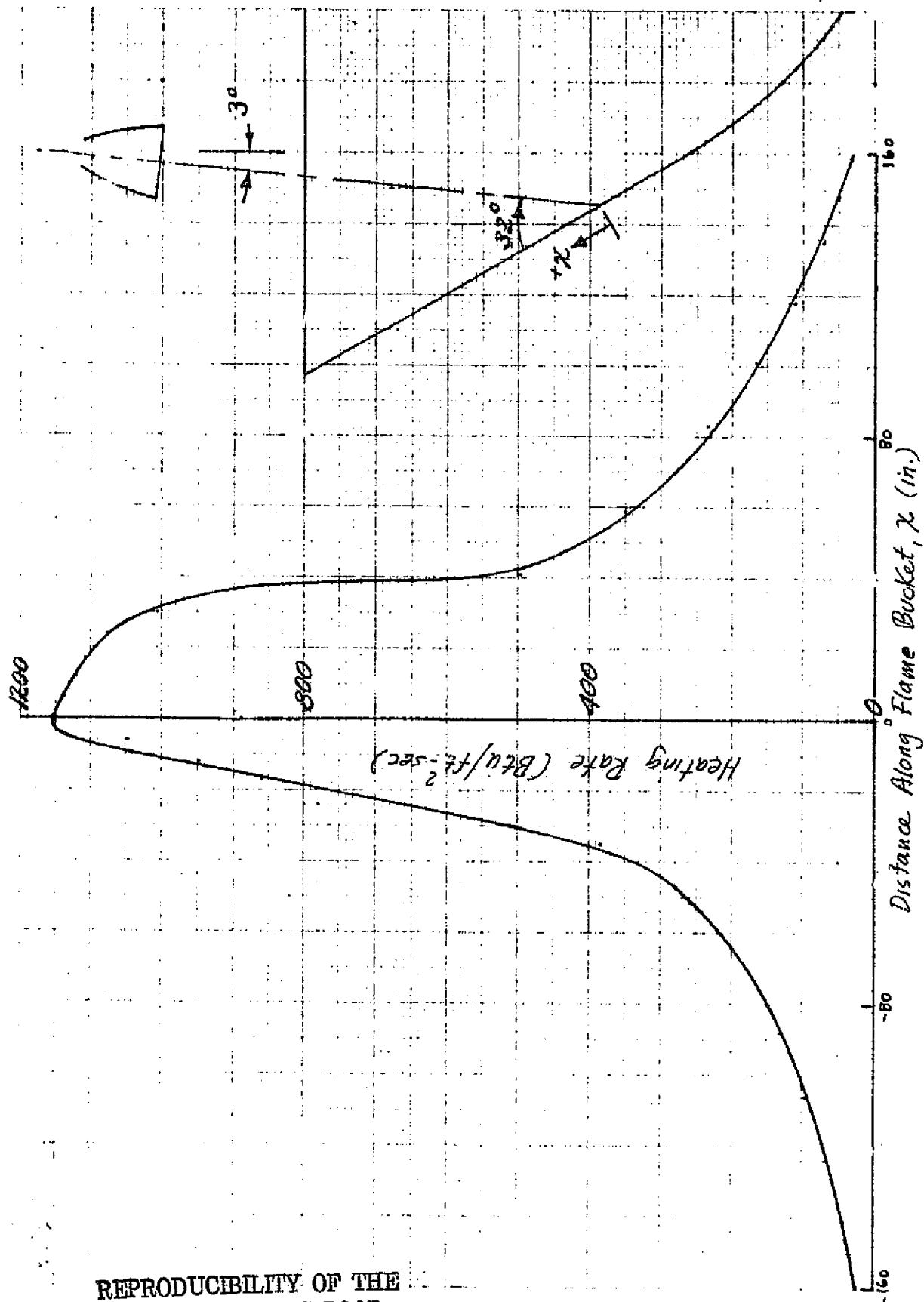


Fig. 1 - SSME Flame Bucket Heating

REPRODUCIBILITY OF THE
ORIGINAL PAGE IS POOR

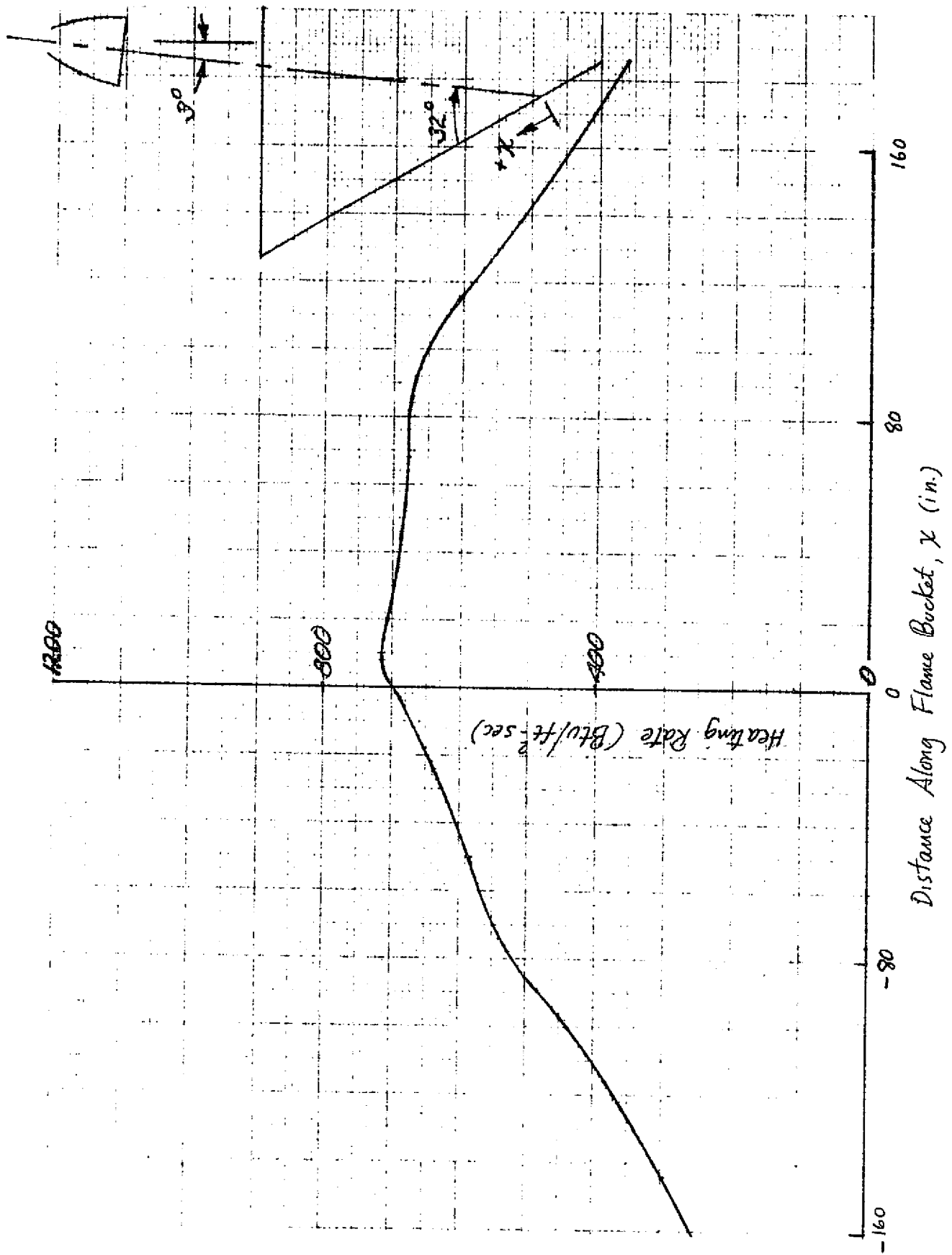


Fig. 2 - F-1 Flame Bucket Heating

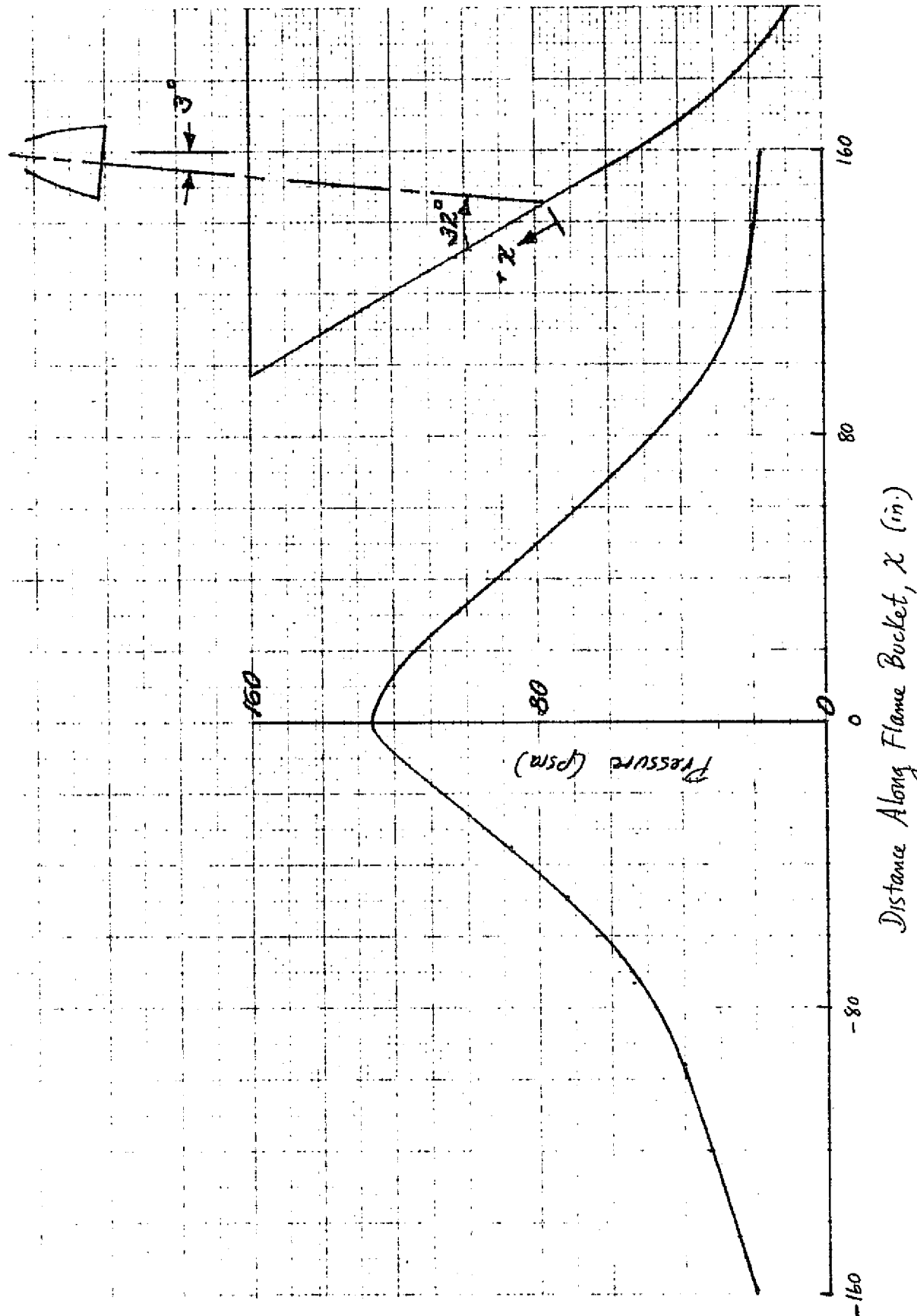


Fig. 3 - SSME Flame Bucket Pitot Pressure

REPRODUCIBILITY OF THE
ORIGINAL PAGE IS POOR

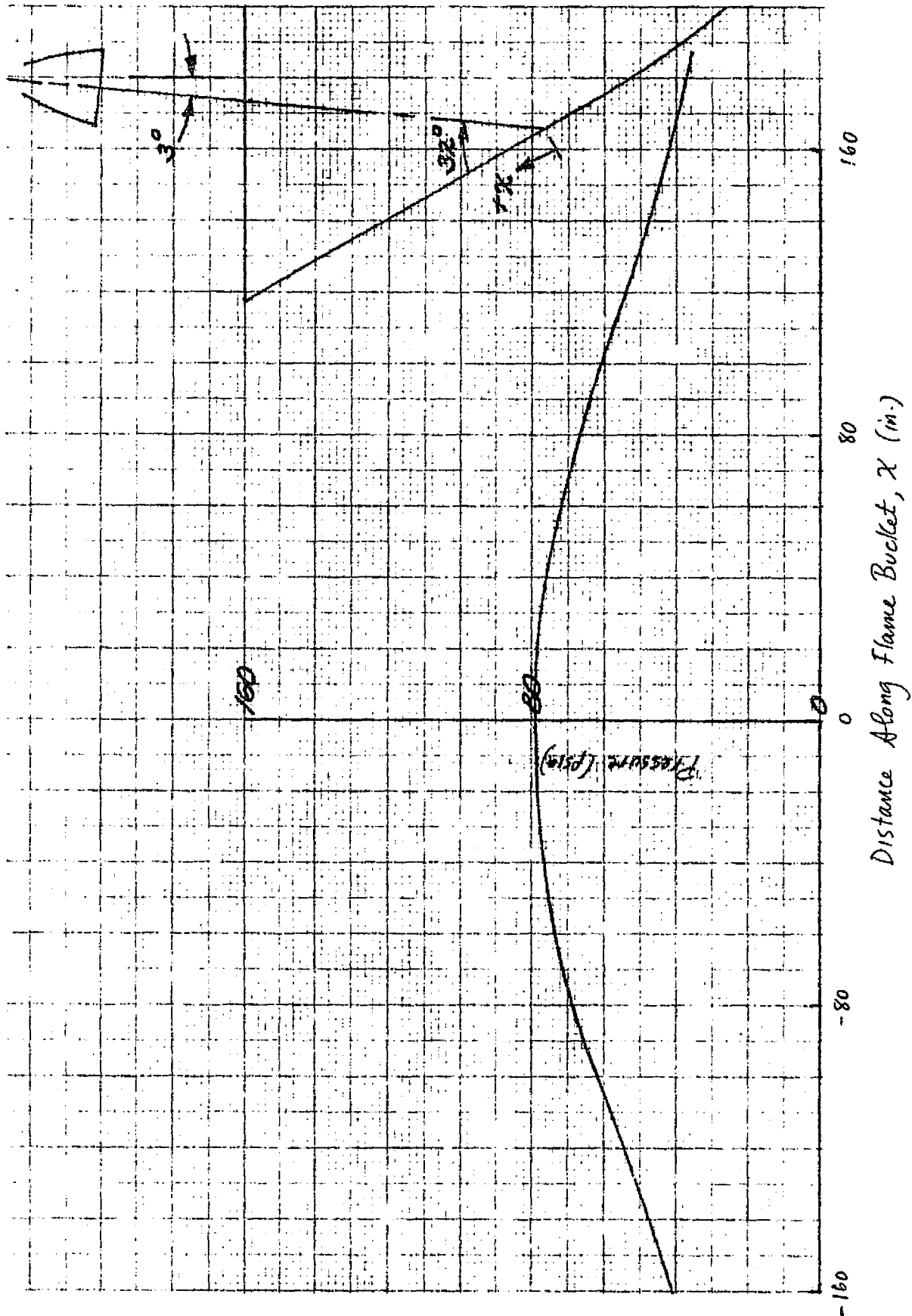


Fig. 4 - F-1 Flame Bucket Pitot Pressure

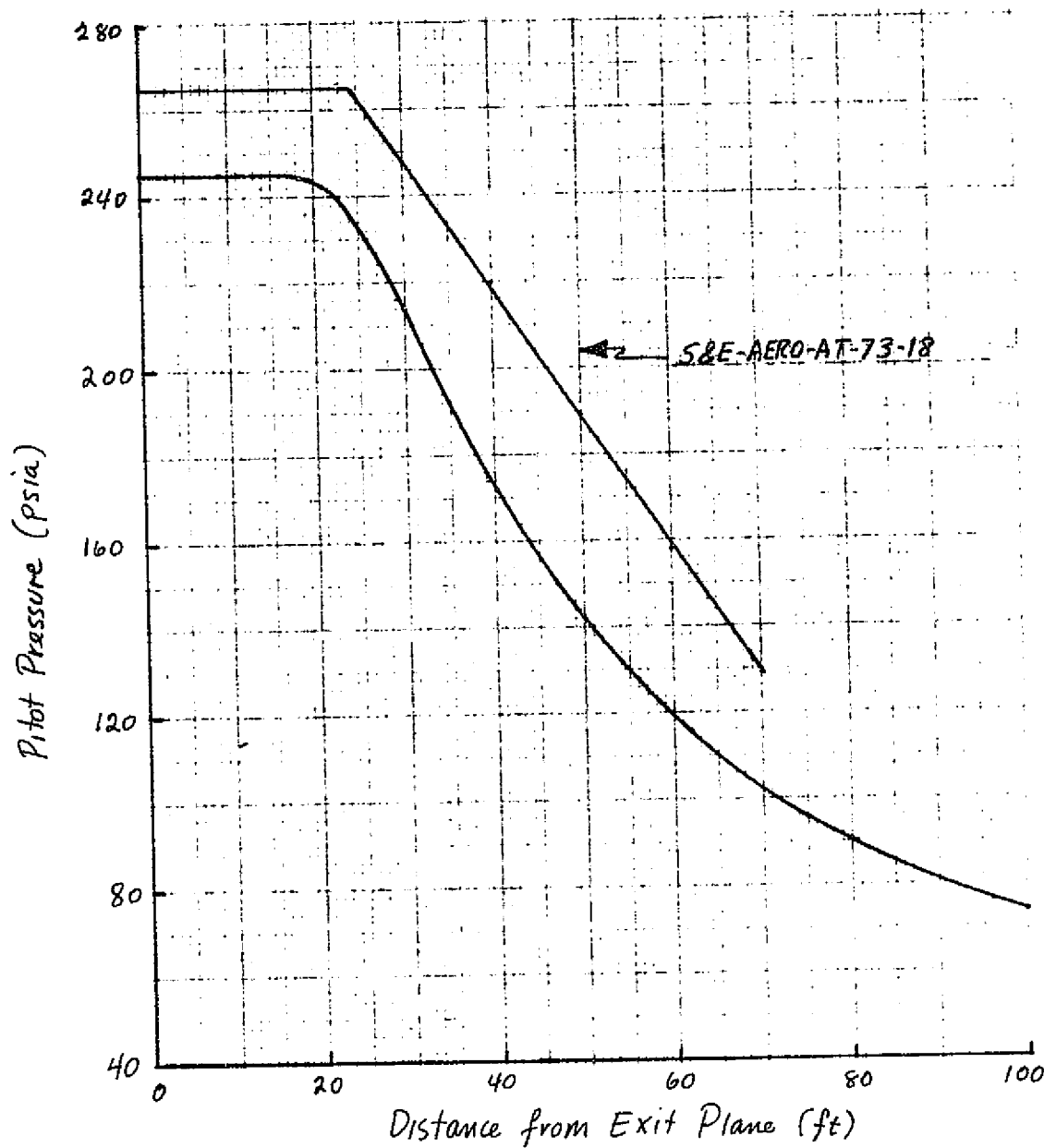


Fig. 5 - SSME Plume Pitot Pressure Along Exhaust Plume Centerline

REPRODUCIBILITY OF THE
ORIGINAL PAGE IS POOR

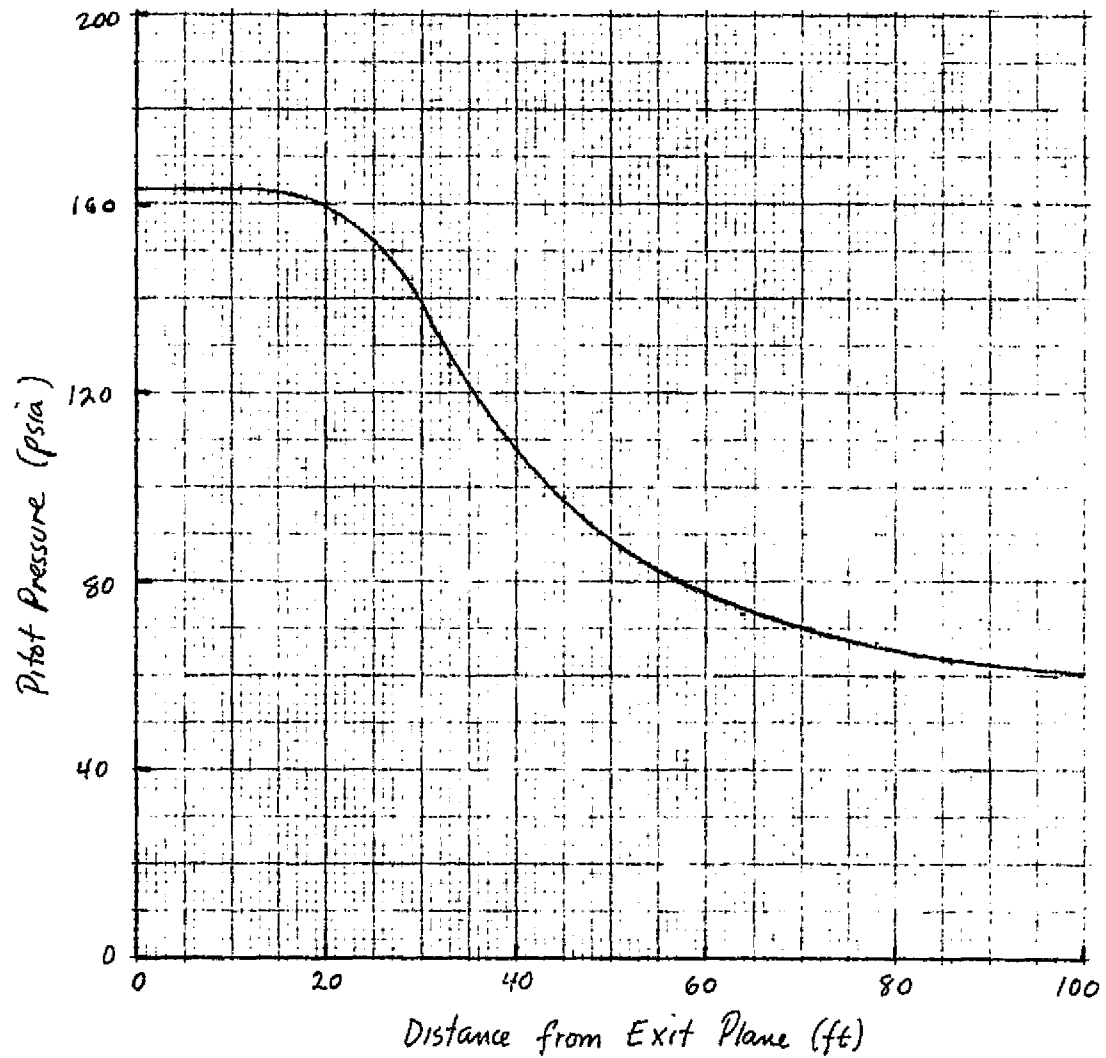


Fig. 6 - F-1 Plume Pitot Pressure Along Exhaust Plume Centerline

Appendix E

Karu, Z. S., "Determination of Thermal Conductivity of BX-250 Foam Insulation from Boiloff Rate and Foam Temperature Data from 20-Inch LH₂ Tank," LMSC-HREC TN D306939, Lockheed Missiles & Space Company, Inc., Huntsville, Ala., November 1973.

LOCKHEED

Huntsville Research & Engineering Center

Contract NAS8-25569 **Date** November 1973 **Doc.** LMSC-HREC TN D306939

Title: DETERMINATION OF THERMAL CONDUCTIVITY OF BX 250 FOAM
INSULATION FROM BOILOFF RATE AND FOAM TEMPERATURE
DATA FROM 20-INCH LH_2 TANK

FOREWORD

This report presents the results of a data analysis task performed by personnel of the Lockheed-Huntsville Research & Engineering Center under Contract NAS8-25569. The NASA Contracting Officer's Representative (COR) for this study is Dr. Kenneth E. McCoy, S&E-ASTN-PTC.

INTRODUCTION AND SUMMARY

The LH_2 boiloff rates from the 20-inch LH_2 tank and the temperatures at different depths in the BX 250 foam, lined on the outside along with a thin ablative insulation, were available from several tests. These tests were run by the MSFC-NASA Test Division. From the boiloff data, the heat transfer rate was obtained. Because the ablative insulation did not cover the entire tank, but just the cylindrical part, a corrected heat transfer rate through the cylindrical portion was obtained knowing the rate through the BX 250 foam on the hemispherical part of the tank. The thermal conductivity evaluated for the foam was plotted against its mean temperature and a straight-line "least squares" fit of the points was obtained. The resulting curve compared favorably with the Rockwell International thermal conductivity curve for BX 250 foam which was obtained from NASA-MSFC.

TECHNICAL DISCUSSION

Figure 1 is a sketch of the 20-inch LH_2 tank lined on the cylindrical part with an ablative insulation and BX 250 spray foam and with BX 250 foam only on the hemispherical segments. Various tests were performed on the tank with ablative materials such as cork, high density foam, Raybestos (silicone sponge rubber) SLA-561 and SS-41. Tests were also run with BX 250 alone. With each insulation the tank was filled to a certain level with LH_2 . It was allowed to stand

for sufficient time in room condition environment for the thermocouples, embedded at premeasured depths in the foam, to reach steady state values. The LH_2 boiloff and the temperature data for all the tests were available and some of the typical data are presented in Table 1.

The heat transfer rate through the tank is calculated as follows:

$$\dot{q} = \frac{\dot{m} h_{fg}}{A}, \frac{\text{Btu}}{\text{ft}^2 \cdot \text{hr}}$$

where

\dot{m} = LH_2 boiloff rate, lbm/hr

h_{fg} = heat of vaporization of LH_2 , Btu/lbm

A = wetted area of tank, ft^2
(obtained from an LH_2 level sensor)

Since, for most of the tests, the cylindrical part of the tank is lined with an ablator and foam and the hemispherical segments with the foam alone, the heating rate \dot{q} , as calculated above, is not the same through the two sections of the tank. In order to obtain the actual heat transfer rate \dot{q}_1 (see Fig. 1) through the ablative and foam layers, it is necessary to know the heat transfer rate \dot{q}_2 through just the foam layer on the bottom hemispherical segment. Fortunately, \dot{q}_2 can be obtained from one of the tests performed with the tank having an identical thickness of BX 250 foam all around it with no ablator.

That is:

$$\dot{q}_2 = \frac{\dot{m}_f h_{fg}}{A_f}, \frac{\text{Btu}}{\text{ft}^2 \cdot \text{hr}}$$

where

\dot{m}_f = boil-off rate in BX 250 foam tank, lbm/hr.

A_f = wetted area in BX 250 foam tank, ft^2 .

Therefore, the true heat transfer rate through ablator-foam insulation, \dot{q}_1 , is obtained from the following heat balance:

$$\dot{q} A = \dot{q}_1 A_1 + \dot{q}_2 A_2$$

where

A_1 = wetted area in the cylindrical tank portion, ft^2

A_2 = hemispherical tank segment area, ft^2

$$A = A_1 + A_2$$

With the true value of the heat transfer rate, \dot{q}_1 , through the ablator and foam layers, the thermal conductivity is obtained from

$$\dot{q}_1 = \frac{K}{\Delta x} (T_H - T_c), \frac{\text{Btu}}{\text{ft}^2 \cdot \text{hr}}$$

where

K = thermal conductivity of foam, $\text{Btu-in/hr-ft}^2 \cdot ^\circ\text{F}$

Δx = thickness of foam in.

T_H, T_c = temperatures across thickness Δx of foam, $^\circ\text{F}$

The thermal conductivity thus evaluated is tabulated in Table 1 with the mean temperature.

RESULTS AND CONCLUSIONS

A plot (Fig. 2) of the thermal conductivity of the BX 250 spray foam was made against the mean temperature of the foam. A straight line "least squares" fit of the points was used. As Fig. 2 shows, this characteristic compares fairly well with a similar Rockwell International curve obtained from NASA-MSFC.

Zain Karu
Zain Karu

Heat Protection Systems

W. G. Dean
W. G. Dean, Project Engineer
Space Shuttle Thermal Support Study

Juan K. Lovin

Juan K. Lovin, Supervisor
Thermodynamics & Structures Section

Attach: (1) Table 1
(2) Figures 1 and 2

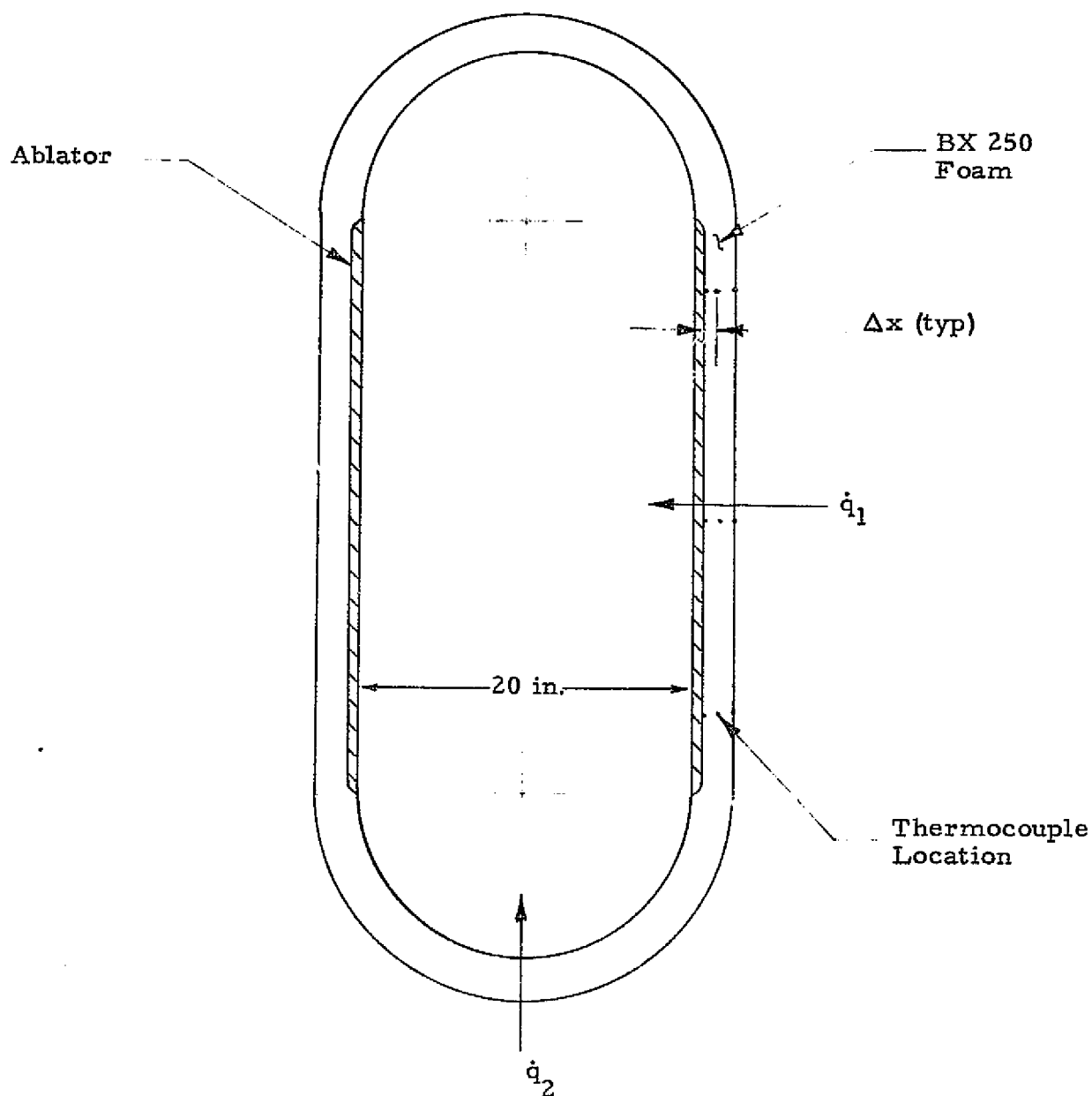


Fig. 1 - Cross-Sectional Sketch of 20-Inch LH₂ Tank Showing The Ablator and Foam Insulation

REPRODUCIBILITY OF THE
ORIGINAL PAGE IS AS

- ⊙ Cork/BX 250
- BX 250/High Density Foam
- ◇ Raybestos/BX 250
- ▽ SLA-561/BX 250
- ▽ SS-41/BX 250
- ⊙ BX 250

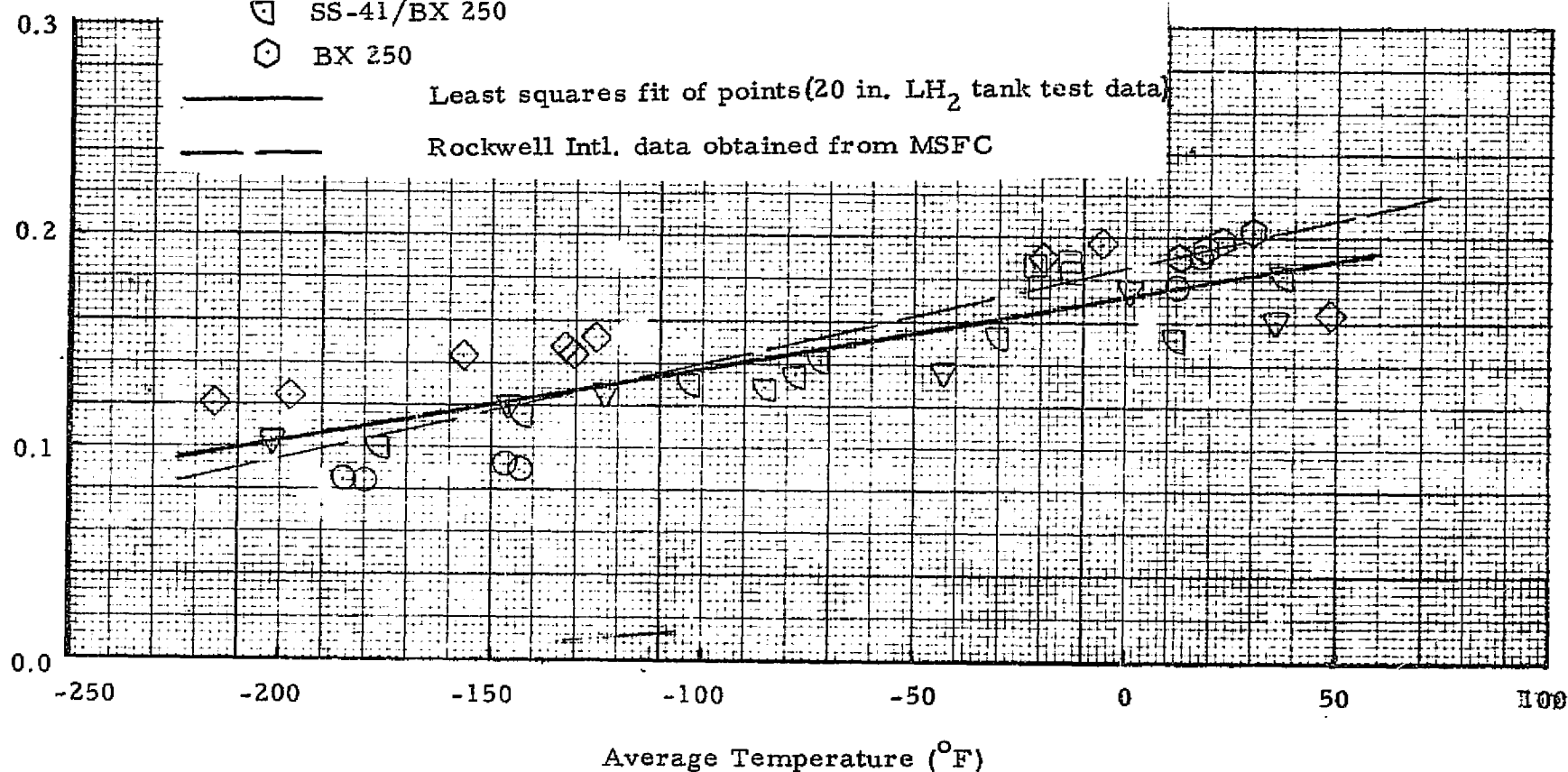


Fig. 2 - BX 250 Foam Thermal Conductivity vs Average Temperature Compared with Rockwell International Data from NASA-MSFC

Table 1
20-INCH LH₂ TANK TEST DATA AND THERMAL CONDUCTIVITY
OF BX 250 FOAM

Tank Insulation	Test/Fill No.	LH ₂ Boiloff (lbm/hr)	Wetted Height in Cyl. Portion (in.)	ΔX (in.)	T_H (°F)	T_c (°F)	T_{mean} (°F)	K Btu-in (hr-ft ² ·°F)
BX 250	005/1	6.05	43.8	11/32	65.6	-20.8	22.4	.198
				10/32	68.4	- 8.2	30.1	.203
	006/1	5.52	42.55	11/32	54.9	-29.5	12.7	.189
				10/32	56.6	-18.1	19.3	.194
Cork/BX 250	003/2	5.48	42.0	9/32	52.1	-16.8	17.7	.190
					49.3	-25.1	12.1	.176
				3/4	52.1	-338.9	-143.1	.089
					42.4	-336.4	-147.0	.092
BX 250/High Density Foam	004/1	6.62	42.0	15/32	-17.1	-343.4	-180.3	.084
					-25.5	-345.5	-185.5	.085
	007/1	4.8	42.0	11/32	14.5	-57.5	-57.5	.186
				10/32	19.2	-45.8	-13.3	.188
BX 250/High Density Foam	008/3	4.7	42.0	11/32	16.5	-57.7	-20.6	.176
				10/32	19.4	-54.2	-12.9	.184
Raybestos/BX 250	013/1	7.58	42.0	3/8	-109.8	-321.4	-215.6	.121
				1/2	-59.7	-335.7	-197.7	.124
				3/4	22.5	-336.0	-156.8	.143
				7/8	70.6	-321.4	-125.4	.152
				7/8	71.0	-335.7	-132.4	.147
				7/8	74.4	-336.	-130.8	.145
				1/2	70.6	-109.8	-19.6	.189
				3/8	71.0	-59.7	-5.7	.195
				1/8	74.4	22.5	48.5	.164
BX 250/SLA-561	016/4	7.2	42.0	5/32	-153.3	-250.4	-201.9	.103
				5/16	-62.3	-229.6	-146.0	.120
				1/2	4.3	-251.2	-123.5	.126
				15/32	67.0	-153.3	-43.2	.137
				11/32	64.1	-62.3	0.9	.175
				5/32	66.8	4.3	35.6	.161
BX 250/54-41	019.4	6.15	43.82	3/16	-128.7	-224.5	-176.6	.100
				7/16	-45.9	-239.3	-142.6	.115
				9/16	6.4	-212.7	-103.2	.131
				19/32	68.8	-128.7	-30.0	.153
				11/32	69.2	-45.9	11.7	.152
				7/32	67.6	6.4	37.0	.182
				25/32	68.8	-224.5	-77.9	.135
				25/32	69.6	-239.3	-85.1	.129
				25/32	67.6	-212.7	-72.6	.142

Appendix F

Dean, W. G., "Average Recession Rate vs Heating Rate of BX-250 Foam Panels in the NASA-MSFC Radiant Lamp Test Facility," LMSC-HREC TN D390468, Lockheed Missiles & Space Company, Huntsville, Ala., December 1974.

LOCKHEED**Huntsville Research & Engineering Center****Contract** NAS8-25569**Date** Dec. 1974**Doc.** LMSC-HREC TN D390468**Title:** AVERAGE RECESSION RATE VERSUS HEATING RATE OF BX-250 FOAM PANELS
IN THE NASA - MSFC RADIANT LAMP TEST FACILITY

FOREWORD

This report presents the results of a data analysis task performed by personnel of the Lockheed-Huntsville Research & Engineering Center under Contract NAS8-25569. The NASA Contracting Officer's Representative (COR) for this study is Dr. Kenneth E. McCoy, EP-44.

INTRODUCTION AND SUMMARY

The average recession, the heating rate and the duration of test for the 12x17 in. BX-250 foam panels tested in the radiant lamp facility were available for several tests. These tests were run by the NASA-MSFC Test Division. The recession rate of the foam was calculated and plotted against the heating rates at the center of the panel. The resulting curve, when compared with similar characteristics obtained from the NASA-MSFC Hot Gas Facility and the Langley Arc Jet Facility, indicated much smaller recession rates. This is true because there is no shear on the foam in the radiant lamp tests.

TECHNICAL DISCUSSION

Figure 1 is a schematic of the calibration panel with a heat flux sensor located in the middle of the panel. Another heat flux sensor was mounted next to the panel and readings on these two sensors were obtained simultaneously for a desired range of heating rates. During the actual foam tests, the outer sensor served as a reference for obtaining the desired heating rate in the middle of the panel.

The average recession of the BX-250 foam, the pre-calibration and post-calibration heating rates on the panel center and the duration of each test performed in the radiant lamp facility were available for about 16 tests. Table 1 lists this data and also the average recession rate which is obtained as follows:

$$\text{Recession Rate, in./sec} = \frac{\text{Average Recession, in.}}{\text{Duration of Test, sec.}}$$

Figures 2 and 3 show plots of the recession rate versus foam center pre- and post-calibration heat fluxes respectively. Similar characteristics obtained from tests performed on panels in the Hot Gas Facility and the Langley Arc Jet

Facility are also shown. The radiant lamp test numbers are indicated near their corresponding data points in the figures. However, it should be noted that points for tests 36, 37 and 38 are not plotted. It is believed that the data are bad for these three tests as the heat flux sensors were replaced after test 38.

RESULTS AND CONCLUSIONS

It is seen from Figs. 2 and 3 that the average recession rates of the BX-250 foam in the radiant lamp tests are much smaller than the rates obtained in the other two facilities. This is due to the absence of shear forces on the panel in the static radiant lamp tests.

Zain S. Karu

Zain S. Karu
Heat Protection Systems Group

W. G. Dean

W. G. Dean, Project Engineer
Space Shuttle Thermal Support Contract

Approved:

Juan K. Lovin

Juan K. Lovin, Supervisor
Thermodynamics & Structures Section

Attach: (1) Table 1
(2) Figs. 1 through 3

Table 1

Test No.	Panel	\dot{Q} , Reference (Btu/ft ² -sec)	Pre-Cal. \dot{Q} , Center (Btu/ft ² -sec)	Post-Cal. \dot{Q} , Center (Btu/ft ² -sec)	BX-250 Foam Average Recession (in.)	Test Duration (sec)	Average Recession Rate (in./sec)
P-009-18	C	1.13	2.50	2.43	.058	75	.000774
19	D	1.46	3.25	3.25	.099	50	.00198
20	J	1.14	2.50	2.64	.044	75	.00059
21	G	1.40	Not available	3.36	.156	50	.00175
22	H	.735	1.65	1.80	.062	150	.00041
23	E	1.08	2.50	2.65	.068	84	.00081
31	K	.46	1.164	1.164	.010	150	.00007
32	L	1.14	2.50	2.604	.102	79	.00129
33	M	1.78	3.70	3.75	.124	50	.00248
34	N	.905	1.60	1.80	.146	147	.00099
35	O	1.41	2.85	2.83	.129	75	.00172
36	P	1.76	*	*	.181	53	.00342
37	Q	.805	*	*	.115	148	.00078
38	R	1.41	*	*	.263	76	.00346
39	S	1.41	3.216	3.216	.107	51	.00210
40	T	1.76	4.25	3.994	.224	54	.00415

* Bad data; not used

REPRODUCIBILITY OF THE
ORIGINAL PAGE IS POOR

LMSC-HREC TN D390468

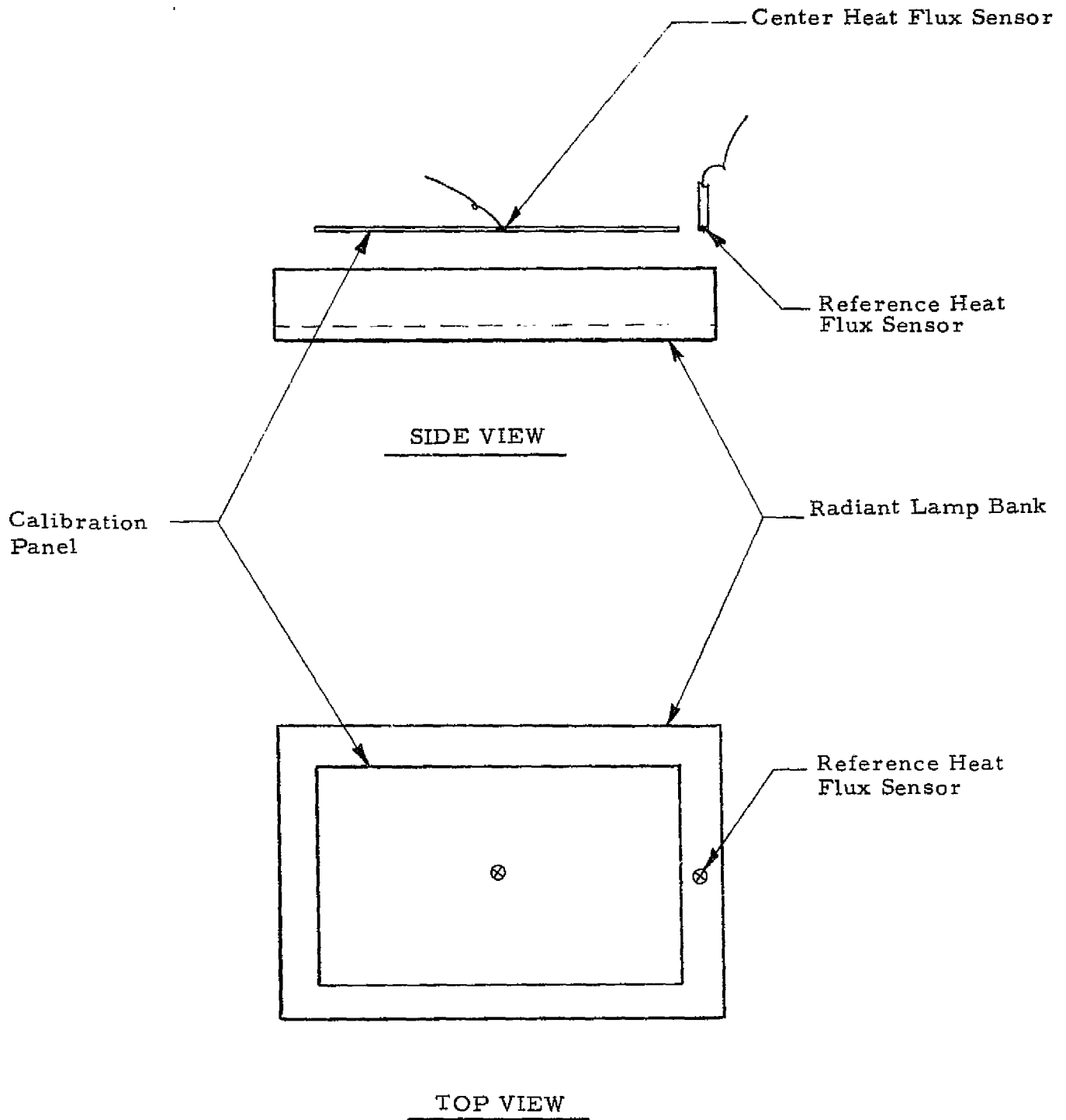


Fig. 1 - Sketch of the Radiant Lamp Test Calibration Panel Set Up Showing the Reference and Center Heat Flux Sensors

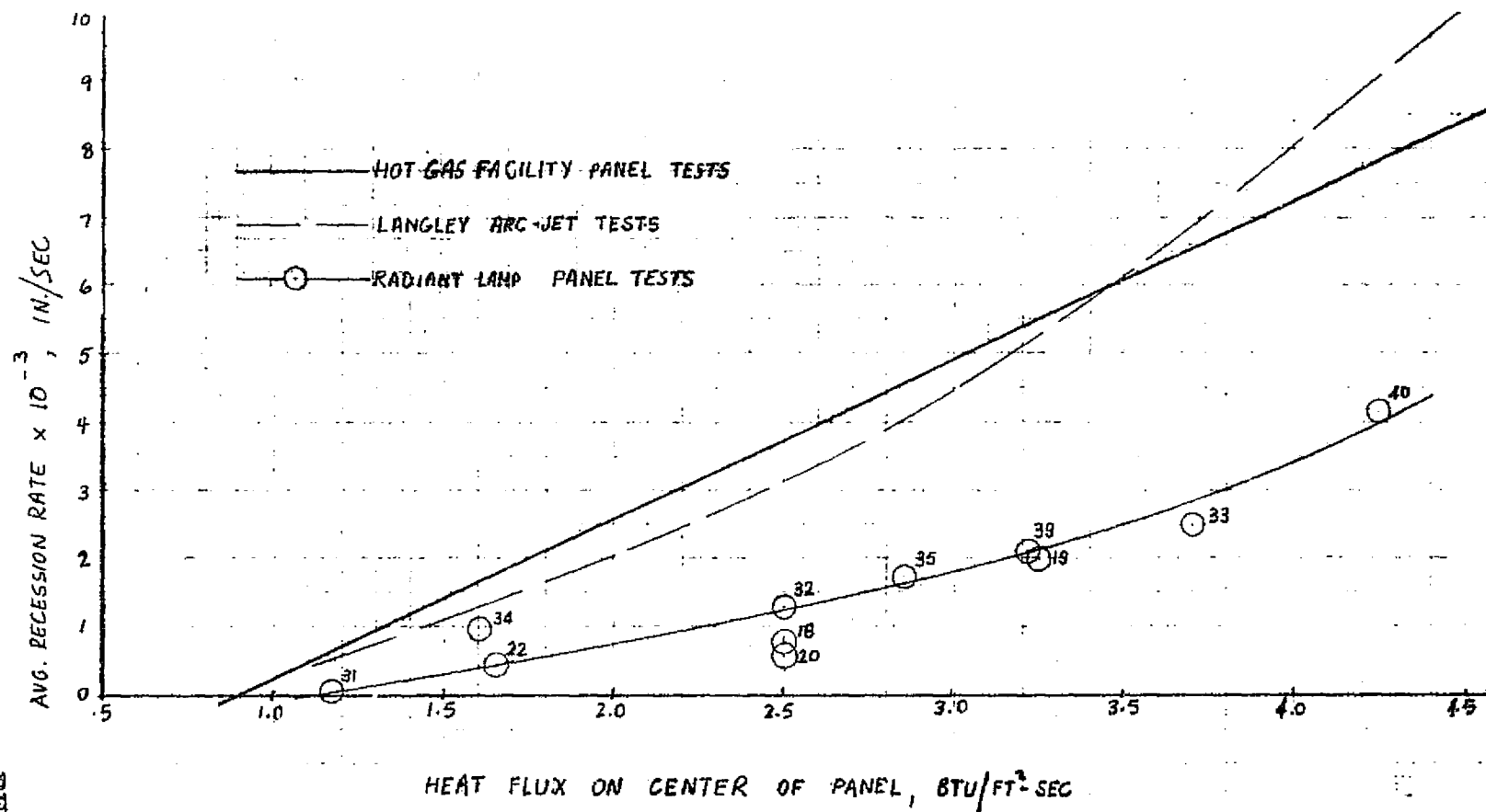


Fig. 2 - Average Recession Rate vs Pre-Calibrated Heating Rate in the Center of BX-250 Foam Panel

REPRODUCIBILITY OF THE
ORIGINAL PAGE IS POOR

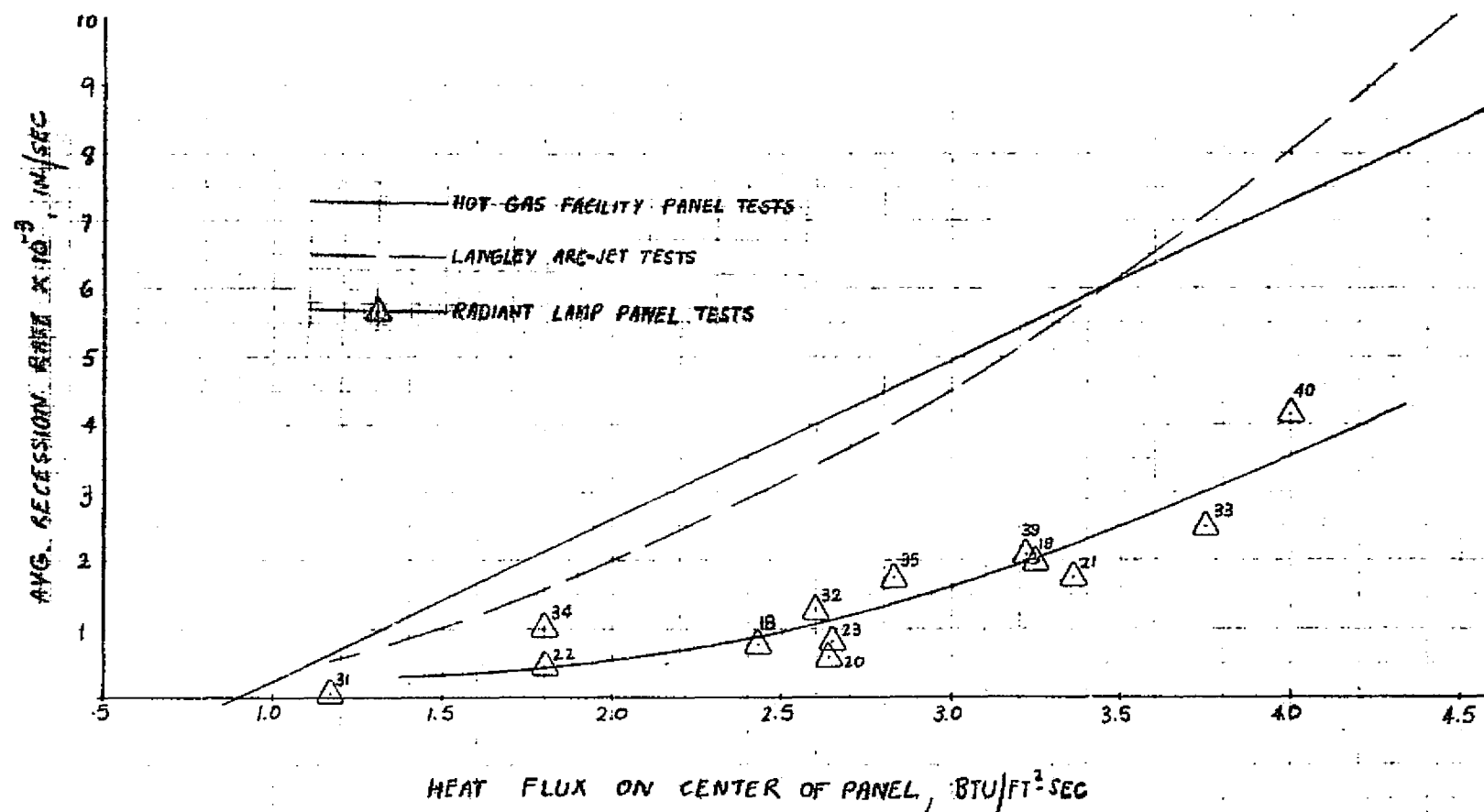


Fig. 3 - Average Recession Rate vs Post-Calibrated Heating Rate in the Center of BX-250 Foam Panel

Appendix G

Dean, W. G., "Results of Tests of CPR-421 Foam in the Langley Mach 10 Continuous Flow Hypersonic Wind Tunnel," LMSC-HREC TN D390678, Lockheed Missiles & Space Company, Huntsville, Ala., February 1975.

Lockheed

Missiles & Space Company, Inc.

HUNTSVILLE RESEARCH & ENGINEERING CENTER

Cummings Research Park
4800 Bradford Drive,
Huntsville, Alabama

RESULTS OF TESTS OF CPR-421
FOAM IN THE LANGLEY MACH 10
CONTINUOUS FLOW HYPERSONIC
WIND TUNNEL

February 1975

Contract NAS8-25569

Prepared for National Aeronautics and Space Administration
Marshall Space Flight Center, Alabama 35812

by
W. G. Dean

APPROVED:

Juan K. Lovin
Juan K. Lovin, Supervisor
Thermodynamics & Structure Section

FOREWORD

This report documents the results of a test program conducted by NASA-Langley Research Center in support of the NASA-MSFC development of the Space Shuttle External Tank. The tests were conducted by NASA-Langley and were planned and monitored by NASA-MSFC with support from Lockheed-Huntsville. CPR-421 foam samples were supplied by the Martin Marietta Corporation, Michoud Operations, contractor for the External Tank.

The Lockheed-Huntsville support was conducted under Contract NAS8-25569, "Space Shuttle Thermal Support." The NASA-MSFC contracting Officer's Representative for this contract is Dr. Kenneth E. McCoy, EP44.

SUMMARY

A series of tests of the CPR-421 foam material was run in the Langley Continuous Flow Hypersonic Tunnel (CFHT) facility at a Mach number of 10. The material specimens were mounted on the flap of a flat plate/wedge-type model. Tunnel conditions were held constant and the local heating rate and pressure to the foam surface were varied by changing the flap deflection angle. The boundary layer was tripped to turbulent flow using trip strips.

This report describes these tests and the foam performance results. There was a large amount of scatter in the data. The foam performed better in the CFHT than in the Langley Arc Jet Facility tests, but it still developed streaks in its surface.

CONTENTS

Section	Page
FOREWORD	ii
SUMMARY	iii
NOMENCLATURE	vii
1 INTRODUCTION	1
2 TECHNICAL DISCUSSION	2
2.1 Test Facility	2
2.2 Models	2
2.3 Test Procedure	3
3 RESULTS AND DISCUSSION	5
3.1 Environment Measurement Results	5
3.2 Foam Performance Results	7
4 CONCLUSIONS AND RECOMMENDATIONS	11
REFERENCES	

Tables

LIST OF TABLES

1	Densities for CPR-421 Samples Tested in Langley Mach 10 CFHT Facility	14
2	Stycast Model Thermal Property Parameter ($\sqrt{\rho C_p K}$) Versus Heating Rate for Two Phase-Change Coating Melt Temperatures (Measured by NASA-Langley and Reported in Ref. 3)	15
3	Average Minimum Recession and Maximum Recession at Three Locations on Each Sample	16
4	Average Minimum and Maximum Recession Rate; Cold-Wall and Hot-Wall Heating Rates at Each of Three Locations for Each Sample Tested	17

CONTENTS (Continued)

Figures		Page
LIST OF FIGURES		
1	Wedge Model with Foam Specimen Mounted in Flap — Bottom Side Only (NASA Photo)	18
2	Wedge Model Showing Top Surface with Flap Thin Skin Calorimeter Installed (NASA Photo)	19
3	Sketch of Model (from Ref. 2)	20
4	Predicted Cold Wall Heat Transfer Distribution on Flap	21
5	Predicted Pressure Distribution on Flap	22
6	Comparison of Predicted and Measured Cold Wall Heat Transfer Distributions on Flap	23
7	Comparison of Predicted and Measured Pressure Distributions on Flap	24
8	Calculated Shear Distribution on Flap (calculated using measured heating rates and calculated velocities)	25
9	Typical Post-Test Photograph of Foam Sample Which Did not Streak. (Sample Number CPRL-19 Tested at a Heating Rate of 5.9 Btu/ft ² -sec and a Shear of 2.3 lbf/ft ² for 15 Seconds)	26
10	Typical Post-Test Photograph of Foam Sample Which Did Streak (Sample Number CPRL-16; Tested at a Heating Rate of 13 Btu/ft ² -sec, and Shear of 4.5 lbf/ft ² , for 15 Seconds)	27
11	Minimum Average Recession Rate vs Cold Wall Heating Rate	28
12	Maximum Recession Rate vs Cold Wall Heating Rate	29
13	Minimum Average Recession Rate vs Hot Wall Heating Rate	30
14	Maximum Recession Rate vs Hot Wall Heating Rate	31
15	Recession at 1.0 in. from the Foam Leading Edge vs Time for $\delta = 10$ deg, $\alpha = 12$ deg	32
16	Recession at 2.5 in. from the Foam Leading Edge vs Time for $\delta = 10$ deg, $\alpha = 12$ deg	33
17	Recession at 3.75 in. from the Foam Leading Edge vs Time for $\delta = 10$ deg, $\alpha = 12$ deg	34
18	Recession at 1.0 in. from the Foam Leading Edge vs Time for $\delta = 15$ deg, $\alpha = 12$ deg	35

CONTENTS (Concluded)

Figures		Page
19	Recession at 2.5 in. from the Foam Leading Edge vs Time for $\delta = 15$ deg, $\alpha = 12$ deg	36
20	Recession at 3.75 in. from the Foam Leading Edge vs Time for $\delta = 15$ deg, $\alpha = 12$ deg	37
21	Recession at 1.0 in. from the Foam Leading Edge Time for $\delta = 20$ deg, $\alpha = 12$ deg	38
22	Recession at 2.5 in. from the Foam Leading Edge vs Time for $\delta = 20$ deg, $\alpha = 12$ deg	39
23	Recession at 3.75 in. from the Foam Leading Edge vs Time for $\delta = 20$ deg, $\alpha = 12$ deg	40
24	Approximate Char Thickness vs Heat Load for CPR-421 Samples	41

NOMENCLATURE

<u>Symbol</u>	<u>Description</u>
C_P	specific heat, Btu/lbm-°R
g_c	dimensional conversion factor, 32.2 lbm-ft/lbf-sec ²
H_{aw}	adiabatic wall enthalpy, Btu/lb
H_w	wall enthalpy, Btu/lb
M_∞	freestream Mach number
P_L	local pressure, lbf/in ²
P_o	total, pressure, lbf/in ²
Pr	Prandtl number
Q	heat load, Btu/ft ²
\dot{q}_{cw}	heating rate based on a wall temperature of 530°R, Btu/ft ² -sec
\dot{q}_{hw}	heating rate based on a wall temperature of 960°R, Btu/ft ² -sec
R	recession, in.
\dot{R}	recession rate, mils/sec
T_o	total temperature, °R
V_L	local velocity, ft/sec
<u>Greek</u>	
α	wedge model angle of attack, deg
δ	flap angle with respect to wedge model centerline
ρ	material density, lb/ft ³
τ	aerodynamic shear stress at the wall, lbf/ft ²

Section 1 INTRODUCTION

The Space Shuttle External Tank (ET) has an external insulation material known as CPR-421. This material serves both as a cryogenic insulation and a thermal protection system (TPS) material to protect the tank skin from aerodynamic heating during ascent. CPR-421 is sprayed directly onto the tank skin. It has a nominal density of two pounds per cubic foot.

Some of the initial convective heating tests of this material were conducted in the Langley Arc-Jet facility. In these tests the CPR-421 showed better performance, in general, than BX-250, the previous ET/TPS material. However, the CPR-421 developed streaks in its surface. At the time of these tests it was felt that these streaks might possibly be due to some anomalies in the arc-jet flow field such as turbulence, vortices, unsteadiness, pressure gradients, etc. Therefore it was decided that additional tests should be run in another facility. The Langley Mach-10 Continuous Flow Hypersonic Tunnel (CFHT) was selected for the next series of tests. These tests were conducted during December 1974.

The NASA-Langley Test Engineers on this project were Mr. J. Dunavant and Mr. T. Blackstock; the NASA-MSFC Test Engineer was Mr. R. Lopez, and the Lockheed-Huntsville Test Engineer was Mr. W. Dean.

Section 2 TECHNICAL DISCUSSION

2.1 TEST FACILITY

The Langley Mach 10 Continuous Flow Hypersonic Tunnel (CFHT) has a 31-inch square test section and operates at a nominal Mach number of 10.4. A detailed description of this tunnel is given in Ref. 1. For these particular tests the total temperature and pressure were approximately 1350°F and 900 psi, respectively for all runs.

2.2 MODELS

2.2.1 Wedge/Flap Model

Figures 1 and 2 show photographs of the stainless steel model used to hold and test the foam specimens during these tests. This model was furnished by Langley and had been used in previous tests in this same tunnel (see Ref. 2). Dimensions of this model are shown in Fig. 3. This model is basically a flat plate wedge with a flap at the rear. The flap can be deflected in both the positive and negative (up and down) directions. The gap between the flap and wedge was not sealed. (This was recommended by Langley personnel.) The wedge can also be run at positive and negative angles of attack. For these tests the wedge was run at +12 degrees and -12 degrees angle of attack. The flap was then deflected into the flow at 5, 10, 15 and 20 degrees from the wedge model centerline. Three rows of "trip strips" were also used on the model upstream of the flap to trip the boundary layer and obtain turbulent flow upstream of the flap. The trip roughness height was approximately .040 inch.

Modifications to the original model (as shown and used in Ref. 2) were made by the NASA-MSFC shops, according to the design changes and drawings made by Lockheed-Huntsville. These modifications consisted of providing a

recessed area in the lower portion of the flap in which the foam specimens were located and secured in place. This recessed area was six inches wide, five inches long, and one inch deep.

Also a calibration block was made to obtain heating rates in this region where the foam was to be placed. This Stycast block was cast against a piece of foam which had been tested in another facility. This gave it the same surface texture as a receding foam specimen surface.

Several thermocouples in the upper flap surface were used to obtain heating rates on that surface by the thin-skin calorimeter method. Pressures were also measured on this upper flap surface. Also a thin-skin calorimeter insert with four thermocouples was made for measuring the heating rates on the lower flap surface.

2.2.2 Foam Specimen Models

The Martin Marietta Corporation (MMC), Michoud Operations, furnished 38 samples of CPR-421 foam for these tests. The densities, and panel numbers of these samples are shown in Table 1 as provided by MMC. None of the foam specimens tested in this series of tests had "knit lines." These "knit lines" are seams between layers of the foam, caused by overlapping of the spray from different sprayer nozzles as they pass over a given point on the tank surface. These specimens were intentionally selected without "knit lines" because it was noted in previous tests that these "knit lines" are a different density and seemed to cause a different recession rate of the surface. It was hoped that the elimination of the knit lines would eliminate one of the variables in obtaining a recession rate prediction.

2.3 TEST PROCEDURE

The CFHT has a quick injection system which injects the model into the flow. The tunnel is started, the flow is established at the proper total conditions, and then the model is inserted into the flow field. Insertion time is

less than one second. This allows a step change in the heating rate to the model/specimen which is required for the thin-skin and Stycast/phase change heating rate measurement methods and also gives a time-zero for foam heating/recession effects data.

Section 3

RESULTS AND DISCUSSION

3.1 ENVIRONMENT MEASUREMENT RESULTS

Before the tests, the heating rates and pressures were predicted using data from Ref. 2. The data from Ref. 2 were obtained with turbulent flow and for tunnel conditions different from our planned run conditions. These data were converted to our planned total temperature and total pressure conditions for turbulent flow. The results of these predictions are shown as Figs. 4 and 5. During the tests, heating rates were measured on the upper flap surface using 10 thermocouples down the flap centerline. Next, the Stycast calibration block was used to obtain heating rates on the flap lower surface using the phase change coating/semi-infinite slab conduction technique. However there was some differences in the values measured on the top of the flap and on the bottom of the flap. Since the flow was axisymmetric and the flap angles and angles of attack were the same with respect to the flow, the heating rates should be the same on the top and bottom of the flap. At this point it was decided to make a thin-skin calorimeter insert to check the flap bottom side heating rates. This insert had four thermocouples down its centerline. Heating rates from this insert agreed more closely with the Stycast-measured heating rates than did the upper surface values. The reason for this difference between the top and bottom was never completely resolved. As a means of checking the Stycast heating rates, the following calibration procedure was used. A small sample, approximately 1.5 inches square, was cut from the Stycast model. This model was sent to the Langley phase-change technique calibration facility where the effective lumped thermal property, density, specific heat, and conductivity product ($\rho C_p K$), was determined. This is done by applying various known radiant heating rates to the sample surface and determining the melt times for various phase-change coating temperatures. The results of this effort are documented in Ref. 3 and presented in Table 2. Results of these heating rates measurement efforts are shown on Fig. 6. Also shown on Fig. 6 are the predicted values, for comparison purposes. Since Langley

personnel recommend use of the thin-skin upper surface data as being the most accurate, curves were faired through these data for use as the final heating rate values for use in the subsequent heating rate/recession rate correlations.

Measured pressures did not present any particular problem and are presented in Fig. 7 and compared to predicted values. As seen these agree quite well with predicted values.

Figure 8 presents the calculated shear levels on the flap at various flap angles. These values were determined using Reynold's analogy as follows:

$$\tau = \frac{\dot{q} V_L (Pr)^{2/3}}{(H_{aw} - H_w) g_c}$$

where

- τ = aerodynamic shear, lbf/ft²
- \dot{q} = heating rate, Btu/ft²-sec
- H_{aw} = adiabatic-wall enthalpy, Btu/lbm
- H_w = wall enthalpy, Btu/lbm
- g_c = dimensional conversion factor = 32.2 ft-lbm/lbf-sec²
- Pr = Prandtl number

The recovery temperature and enthalpy for these tests were approximately 1810°R and 410 Btu/lb, respectively.

The boundary layer thickness on the flap for these tests is undetermined. This is because there is a strong shock/boundary layer interaction at the flap/wedge junction. The high pressure behind the shock feeds upstream of the shock through the subsonic portion of the boundary layer, causing a significant

thickening of the boundary layer both upstream and downstream of the flap shock, and perhaps a separation bubble. This makes it very difficult, if not impossible, to calculate an accurate boundary layer thickness. Also no schlieren or shadowgraphs were taken because of the two end plates on either side of the flap.

3.2 FOAM PERFORMANCE RESULTS

3.2.1 General

A total of 23 foam specimens was tested in this series of runs. In general, the foam performance looked better than in the Arc-Jet environment. However, the material still "streaked" at the higher heating rate and shear levels. These "steaks" were observed to begin to take place at the flap angle of 15 degrees and were, of course, more pronounced and well defined at the maximum flap angle of 20 degrees. This was at heating rates at the foam center of approximately 9 and 13 Btu/ft²-sec for flap angles of 15 and 20 degrees, respectively. The corresponding shear levels are 3.3 and 4.6 lbf/ft². The maximum test time was 20 seconds because the tunnel was being run in the blowdown mode. Longer test times and bigger panels would be useful for evaluation of the further growth of the "streaks."

Figure 9 shows a typical post-test foam sample (Model CPRL 19). This model was tested for 15 seconds at a centerline heating rate of 5.9 Btu/ft²-sec and a shear level of 2.3 lbf/ft². As seen in Fig. 9 this sample did not develop any "streaks." Figure 10 shows a model which did develop "steaks" (Model CPRL-16). This model was tested for 15 seconds at a heating rate of 13.0 Btu/ft²-sec and a shear of 4.5 lbf/ft².

3.2.2 Correlations of Foam Recession Data

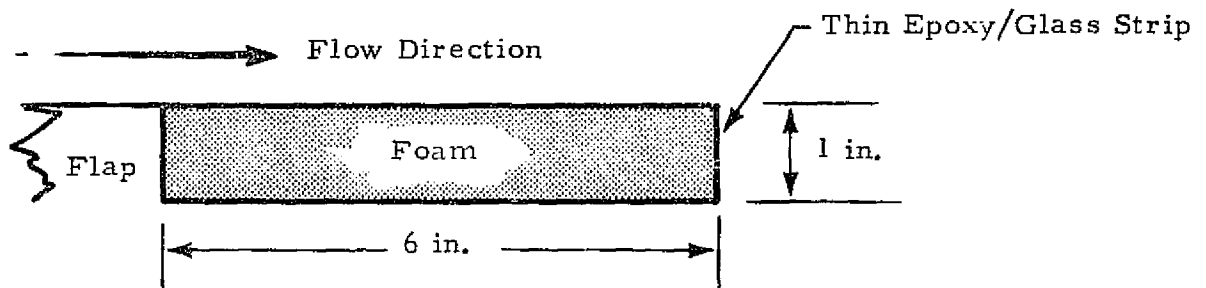
Quantitative results of these tests are shown in Tables 3 and 4. The initial thickness of each foam sample was measured at three places along its centerline. These locations are 1 inch from the leading edge, at the center,

and 3.75 inches from the leading edge. Post-test thicknesses were measured at these same locations. These post-test measurements were made by two methods. The first was to measure the "minimum average" recession. This was done by laying a thin metal strip across the sample and measuring the thickness at the top of the "humps" left by the streaks. (On samples where no "streaks" occurred this was, of course, just the sample thickness including the char layer.) The second method was to measure to the bottom of the deepest groove or "streak" to obtain the "maximum" recession. Results of these two measurements were then used to obtain a recession rate by simply dividing the total recession by the total run time. These recession rates were then used to plot against cold wall heating rates as shown in Figs. 11 and 12 for "minimum average" recession and maximum recession, respectively. The reason for attempting this method of correlation was that it worked well for a similar material (BX-250). However, as seen in Figs. 11 and 12 there is a large amount of scatter in these data. Attempts were made to reduce this scatter by remeasuring the sample final thicknesses but this did not help. Also the effect of run time on scatter was checked out. It was felt that perhaps the recession was not linear with time — which is assumed when determining the rate using the total run time. However no consistent effect of run time on scatter was found while examining the data. For example on a given run, (sample CPRL-8) there is a variation in the recession rate of from 14 to 52 mils per second with a heating rate variation of only 11.7 to 13.0 Btu/ft²-sec. Some of the scatter is due to the difficulties in obtaining a truly representative measurement of the post-test sample thickness due to the roughness of the samples and nonuniform recession in both streamwise and chordwise directions. Also some of the scatter is due to sample-to-sample variations. The amount attributed to each is, of course, unknown.

A straight line, least squares fit was taken for the data of Figs. 11 and 12, and the equations of these lines are shown on the figures. Figures 13 and 14 show this same type of an approach except that hot wall heating rates are used. These hot wall values are based on a wall temperature of 960°R.

Another approach to smoothing and correlating these data was also tried. This approach was successfully used in correlating the BX-250 foam recession data. In this approach the recession is plotted versus run time for all samples which are run at a given heating rate. The best straight line is then taken through these points and the slope of this line gives the average recession rate in mils per second. Figures 15 through 23 show the results of this attempted correlation. As seen from these figures it was not possible to obtain any reasonable straightline or slope from this method due to the data scatter. The third type correlation of these data was to plot char thickness versus total heat load. Results of this are shown in Fig. 24. Measurements were made at the center of each sample. Again there is a considerable amount of scatter in the measurements but an attempt was made to put curves through these data for each heating rate level.

On three of the samples (CPRL-16, 17, 18) an attempt was made to retard the streaking by bonding a thin strip of glass cloth, dipped in epoxy, on the downstream surface as shown in the following sketch:



The reason for doing this was that it was felt that the pressure gradient along the cracks or streaks greatly increased their rate of growth. That is, when a crack developed in the char layer, the flow down the crack was greatly accelerated when the downstream end of the crack "felt" the low back pressure at the base of the flap. This large pressure gradient, from the flap pressure to the base pressure, should normally cause a high flow rate and

high heating rate along the sides of the crack. This would be especially true in a situation with a thin boundary layer where the hot outer layers of the boundary layer could be drawn through the crack.

When models CPRL-16 and 17 were run it was not evident that the epoxy strips helped the "streaking" problem. Rather the epoxy strips eroded at about the same rate as the foam, and the models "streaks" still developed. (Model CPRL-18 was not tested.)

Section 4

CONCLUSIONS AND RECOMMENDATIONS

As a result of this series of tests, the following conclusions and recommendations are made:

- The CPR-421 foam streaks are not peculiar to the Arc Jet facility.
- The CPR-421 foam shows better recession performance than the BX-250 foam.
- There was a large amount of scatter in the data. This was apparently due to:
 - "sample-to-sample" variation
 - difficulty in obtaining a representative recession measurement due to nonuniform recession in both streamwise and chordwise directions
- Additional CPR-421 tests are needed in other facilities which would allow for:
 - Larger size panels
 - Longer test times
 - Smaller pressure gradients along the sample length
 - Thicker boundary layer.

This should help in the further understanding of the causes and possible solutions to the streaking problem. It will also allow for greater total recession and char layer thicknesses which will allow for more accurate measurements and, hopefully, less scatter.

- An attempt should be made to model the CPR-421 performance on a charring ablation computer code. Since the CPR-421 does char and not just "recede" as the BX-250 does, it cannot be expected to correlate with heating rate alone as was the case with the BX-250. (This modeling would, of course, be without regard to the streaks — just the normal ablative/charring process.)
- An attempt should be made to strengthen the hot char matrix to prevent initiation of cracks which can develop into streaks. This should be possible through the use of additives such as chopped silica fibers or other ingredients which will provide a high viscosity melt layer as the char forms and stabilizes.

REFERENCES

1. Dunavant, J.C., and H. W. Stone, "Effect of Roughness on Heat Transfer to Hemisphere Cylinder at Mach Numbers 10.4 and 11.4," NASA TN D-3871, 1967.
2. Hamilton, H. H., and J. D. Dearing, "Effect of Hinge Line Bleed on Heat and Pressure Distribution over a Wedge- Flap Combination at Mach 10.4," NASA TN D-4686, 1968.
3. NASA-Langley Research Center Letter 160A, 8 January 1975, from T. R. Creel, Jr., to W. G. Dean on Stycast sample thermal properties evaluation.

Table 1
DENSITIES FOR CPR-421 SAMPLES TESTED IN LANGLEY MACH 10 CFHT FACILITY

(Notes: Average density = 2.187 lbm/ft³; maximum density is 8.5% over average; minimum density is 6.1% less than average.)

CPRL Model Number	Density (lbm/ft ³)
1	2.054
2	2.173
3	2.074
4	2.153
5	2.106
6	2.100
7	2.277
8	2.168
9	2.107
10	2.191
11	2.160
12	2.071
13	2.299
14	2.118
15	2.191
16	2.249
17	2.162
18	2.212
19	2.317
20	2.257
21	2.120
22	2.289
23	2.285
24	2.328
25	2.237
26	2.133
27	2.279
28	2.218
29	2.140
30	2.115
31	2.162
32	2.165
33	2.184
34	2.372
35	2.160
36	2.212
37	2.116
38	2.150

REPRODUCIBILITY OF THE
ORIGINAL PAGE IS POOR

Table 2

STYCAST MODEL THERMAL PROPERTY PARAMETER ($\sqrt{\rho C_p K}$) VERSUS HEATING RATE FOR TWO PHASE-CHANGE COATING MELT TEMPERATURES (MEASURED BY NASA-LANGLEY AND REPORTED IN REF. 3)

Phase-Change Coating Melt Temperature (°F)	Heating Rate Input Level (Btu/ft ² -sec)	$\sqrt{\rho C_p K}$ (Btu/ft ² - °R-sec ^{1/2})
300 ↓ 500 ↓	4.2	.066
	4.7	.070
	6.2	.072
	7.9	.079
	8.2	.073
	9.0	.078
	13.2	.073
	13.6	.074
	5.3	.059
	6.3	.082
	8.5	.070
	9.5	.073
	13.2	.073
	13.6	.074
	15.2	.082

Table 3

AVERAGE MINIMUM RECESSION AND MAXIMUM RECESSION AT THREE
LOCATIONS ON EACH SAMPLE

RUN NO.	SAMPLE	INITIAL THICKNESS, IN.			AVG. MINIMUM RECESSION			MAX. RECESSION IN "STREAKS"			REMARKS	
		1" FROM L.E.	CENTER	3.75" FROM L.E.	1" FROM L.E.	CENTER	3.75" FROM L.E.	1" FROM L.E.	CENTER	3.75" FROM L.E.		
5	CPRL-1	No Data IN.	.959 IN.	No Data IN.	- IN.	-.011* IN.	- IN.	- IN.	- IN.	- IN.	DID NOT	"STREAK"
6	-2	.958	.957	.957	.000	.005	.006	-	-	-	" "	" "
7	-3	.962	.961	.962	.004	.012	.006	-	-	-	" "	" "
8	-4	.957	.961	.958	.043	.088	.120	.098	.273	.420		"STREAKED"
9	-5	.958	.962	.960	.009	.007	.008	-	-	-	DID NOT	"STREAK"
10	-6	.962	.960	.957	-.005	-.002	-.005	-	-	-	" "	" "
-	-7	.960	.961	.960							DID NOT	RUN
27	-8	.955	.957	.955	.070	.196	.264	.147	.272	.364		"STREAKED"
28	-9	.959	.960	.961	.073	.078	.269	.164	.290	.320		
29	-10	.958	.959	.958	.066	.153	.261	.120	.358	.412		
30	-11	.959	.961	.959	.075	.161	.242	.110	.300	.425		
31	-12	.960	.961	.960	.103	.253	.378	.180	.468	.523		
-	-13	.959	.960	.960							DID NOT	RUN
32	-14	.960	.960	.958	-.009	-.003	-.018	-	-	-	DID NOT	"STREAK"
33	-15	.960			.004	.016	.003	-	-	-	" "	" "
35	-16	.964			.092	.166	.308	.130	.450	.563		"STREAKED"
36	-17	.961			.065	.174	.296	.260	.460	.570		
-	-18	.955									DID NOT	RUN
34	-19	.957			.011	.018	.009	-	-	-	DID NOT	"STREAK"
37	-20	.960			.050	.145	.194	.100	.195	.347		"STREAKED"
38	-21	.961			.005	.046	.035	.028	.075	.123		
39	-22	.961			.011	.043	.101	.025	.119	.227		
40	-23	.961			.003	.011	.047	.016	.088	.156		
41	-24	.958			.038	.051	.070	.032	.111	.239		
42	-25	.959			.026	.027	.067	.030	.063	.116		
43	-26	.960			.025	.030	.061	.051	.101	.169		
-	-27	.959									DID NOT	RUN
-	-28	.956										
-	-29	.957										
-	-30	.952										

* SWELLED

Table 4
AVERAGE MINIMUM AND MAXIMUM RECESSION RATE, COLD-WALL AND HOT-WALL HEATING RATES
AT EACH OF THREE LOCATIONS FOR EACH SAMPLE TESTED

RUN NO	SAMPLE	RUN TIME	AVG MINIMUM RECESSION RATE, MILLS/SEC			MAX RECESSION RATE, MILLS/SEC			FLAP ANGLE, δ°	$\dot{Q}_{\text{COLD WALL, BTU/FT}^2\text{-SEC}}$			$\dot{Q}_{\text{HOT WALL, BTU/FT}^2\text{-SEC}}$		
			1" FROM L.E.	CENTER	3.75" FROM L.E.	1" FROM L.E.	CENTER	3.75" FROM L.E.		1" FROM L.E.	CENTER	3.75" FROM L.E.	1" FROM L.E.	CENTER	3.75" FROM L.E.
5	CPRL-1	15 sec.	No Data	swelled	No Data	-	-	-	5°	-	-	-	-	-	-
6	-2	15	0	33	4	-	-	-	10	5.0	5.9	6.1	3.04	3.59	3.71
7	-3	15	267	80	4	-	-	-	10	5.0	5.9	6.1	3.04	3.59	3.71
8	-4	15	2.87	5.87	8.0	6.53	18.2	28.0	20	11.7	13.0	12.6	7.12	7.91	7.67
9	-5	20	45	35	4	-	-	-	10	5.0	5.9	6.1	3.04	3.59	3.71
10	-6	20	-	-	-	-	-	-	10	↓	↓	↓	↓	↓	↓
-	-7	(DID NOT RUN)	-	-	-	-	-	-	-	-	-	-	-	-	-
27	-8	5	14.0	39	52.8	29.4	54.4	72.8	20	11.7	13.0	12.6	7.12	7.91	7.67
28	-9	5	14.6	15.6	53.8	32.8	58.0	64.0	20	↓	↓	↓	↓	↓	↓
29	-10	10	6.6	15.3	26.1	12.0	35.8	41.2	20	↓	↓	↓	↓	↓	↓
30	-11	10	7.5	16.1	24.2	11.0	30.0	42.5	20	↓	↓	↓	↓	↓	↓
31	-12	15	6.9	16.9	25.2	12.0	31.2	34.87	20	↓	↓	↓	↓	↓	↓
-	-13	(DID NOT RUN)	-	-	-	-	-	-	-	-	-	-	-	-	-
32	-14	20	-	-	-	-	-	-	10	5.0	5.9	6.1	3.04	3.59	3.71
33	-15	20	2	8	15	-	-	-	10	↓	↓	↓	↓	↓	↓
35	-16	15	6.1	11.1	20.5	8.67	30.0	37.53	20	11.7	13.0	12.6	7.12	7.91	7.67
36	-17	15	4.3	11.6	19.7	17.33	30.67	38.00	20	↓	↓	↓	↓	↓	↓
-	-18	(DID NOT RUN)	-	-	-	-	-	-	-	-	-	-	-	-	-
34	-19	15	73	12	60	-	-	-	10	5.0	5.9	6.1	3.04	3.59	6.10
37	-20	5	10.0	29.0	38.9	20.00	39.0	69.4	20	11.7	13.0	12.6	7.12	7.91	7.67
38	-21	15	33	31	2.33	1.87	5.0	8.2	15	9.1	9.0	9.1	4.43	5.48	5.54
39	-22	15	87	2.87	6.73	1.67	7.93	15.1	15	↓	↓	↓	↓	↓	↓
40	-23	10	30	1.10	4.70	1.60	8.8	15.6	15	↓	↓	↓	↓	↓	↓
41	-24	10	3.80	5.10	7.00	3.20	11.1	23.9	15	↓	↓	↓	↓	↓	↓
42	-25	5	5.20	5.4	13.40	6.00	12.6	23.2	15	↓	↓	↓	↓	↓	↓
43	-26	5	5.00	6.1	12.20	10.20	20.2	33.8	15	↓	↓	↓	↓	↓	↓
-	-27														
-	-28														
-	-29														
-	-30														

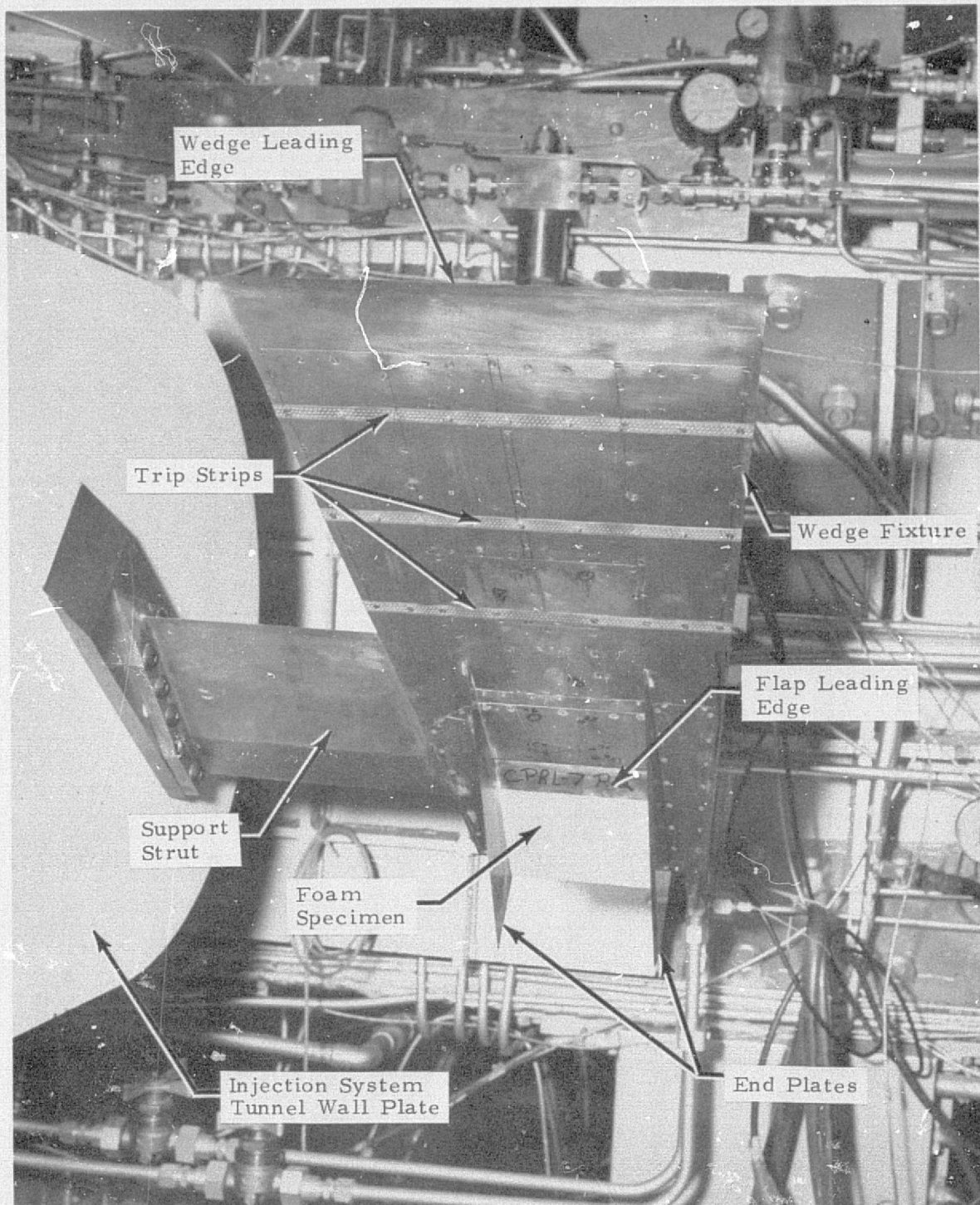


Fig. 1 - Wedge Model with Foam Specimen Mounted in Flap - Bottom Side Only (NASA Photo)

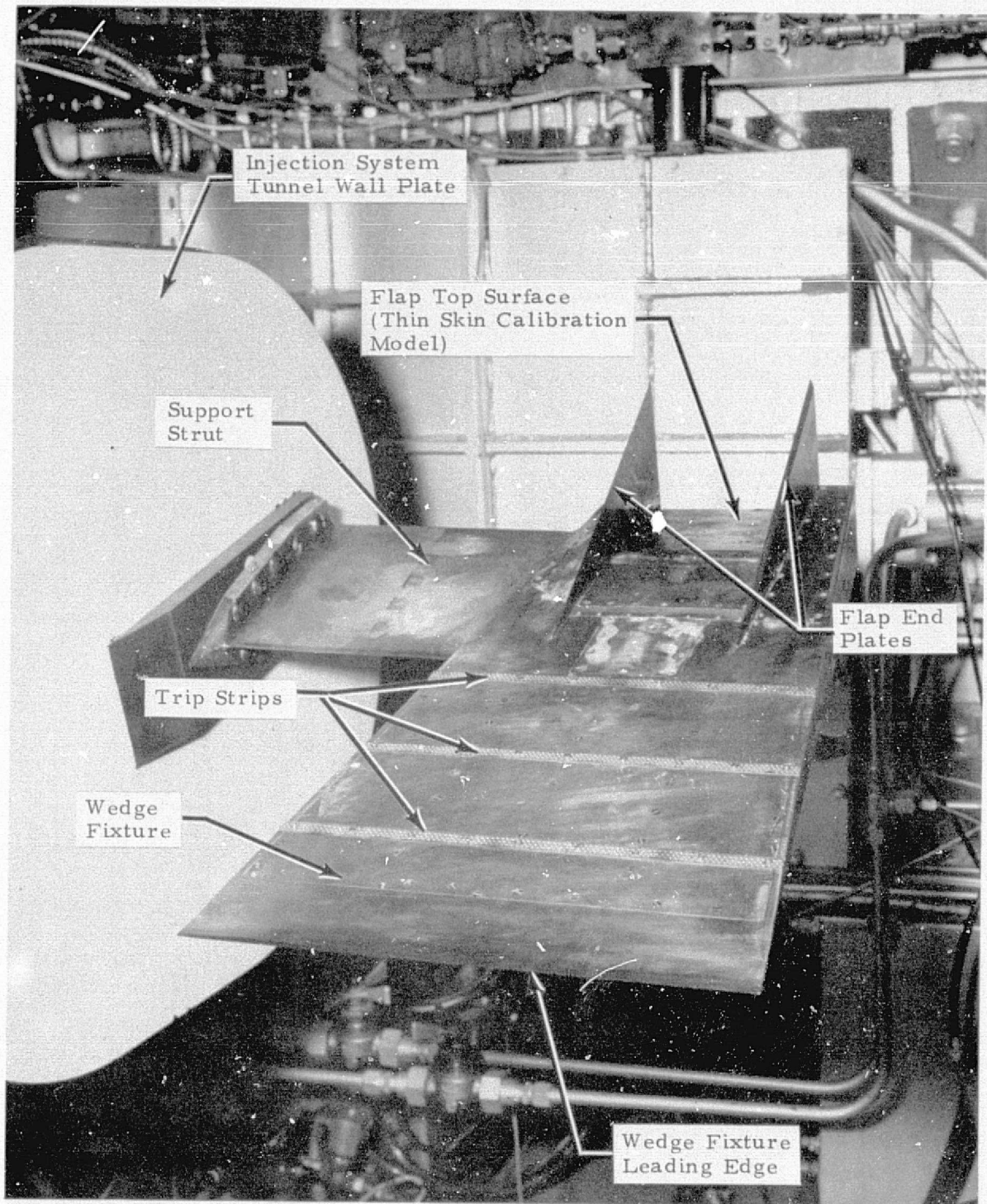


Fig. 2 - Wedge Model Showing Top Surface with Flap Thin Skin Calorimeter Installed (NASA Photo)

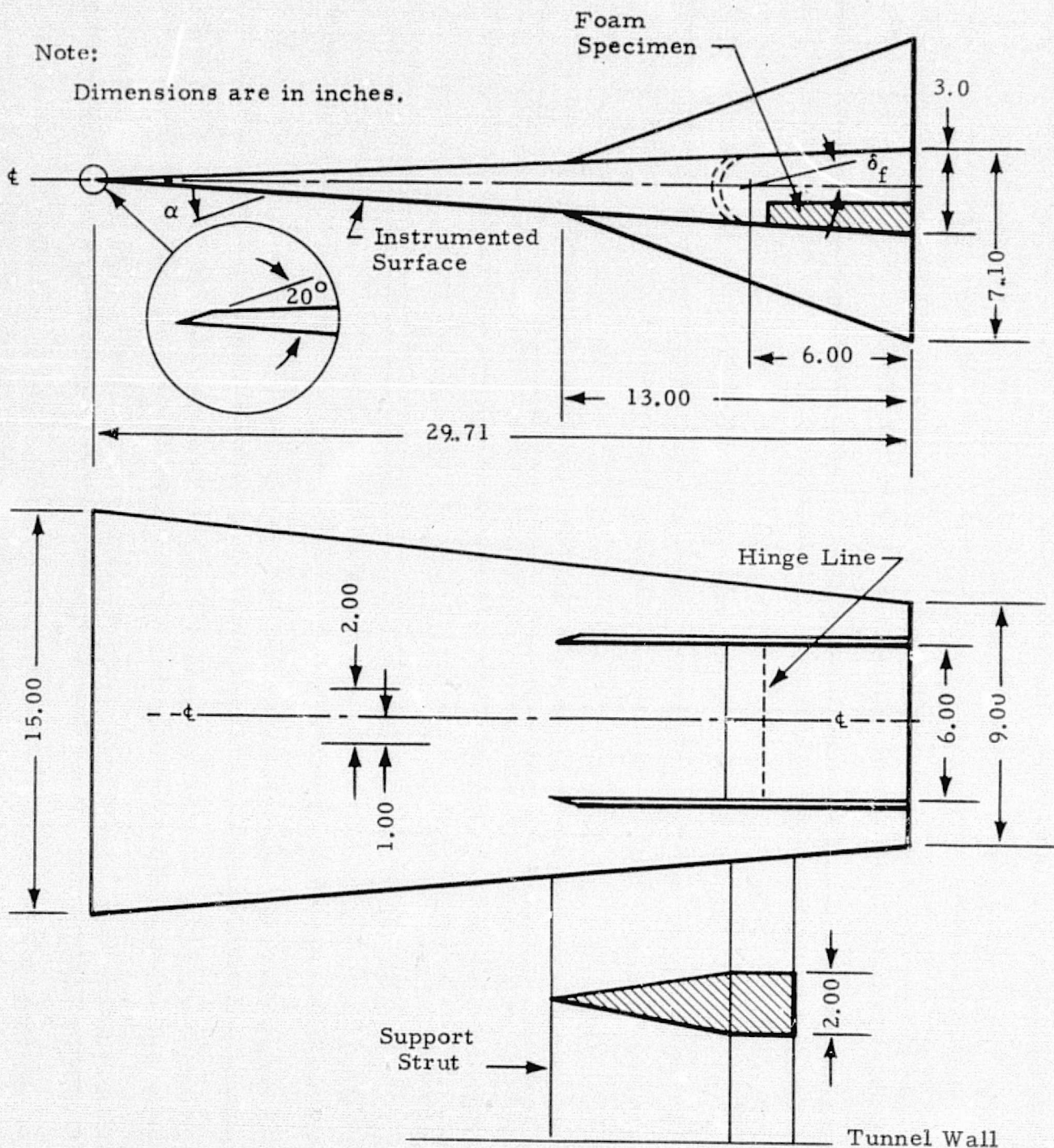


Fig. 3 - Sketch of Model (from Ref. 2)

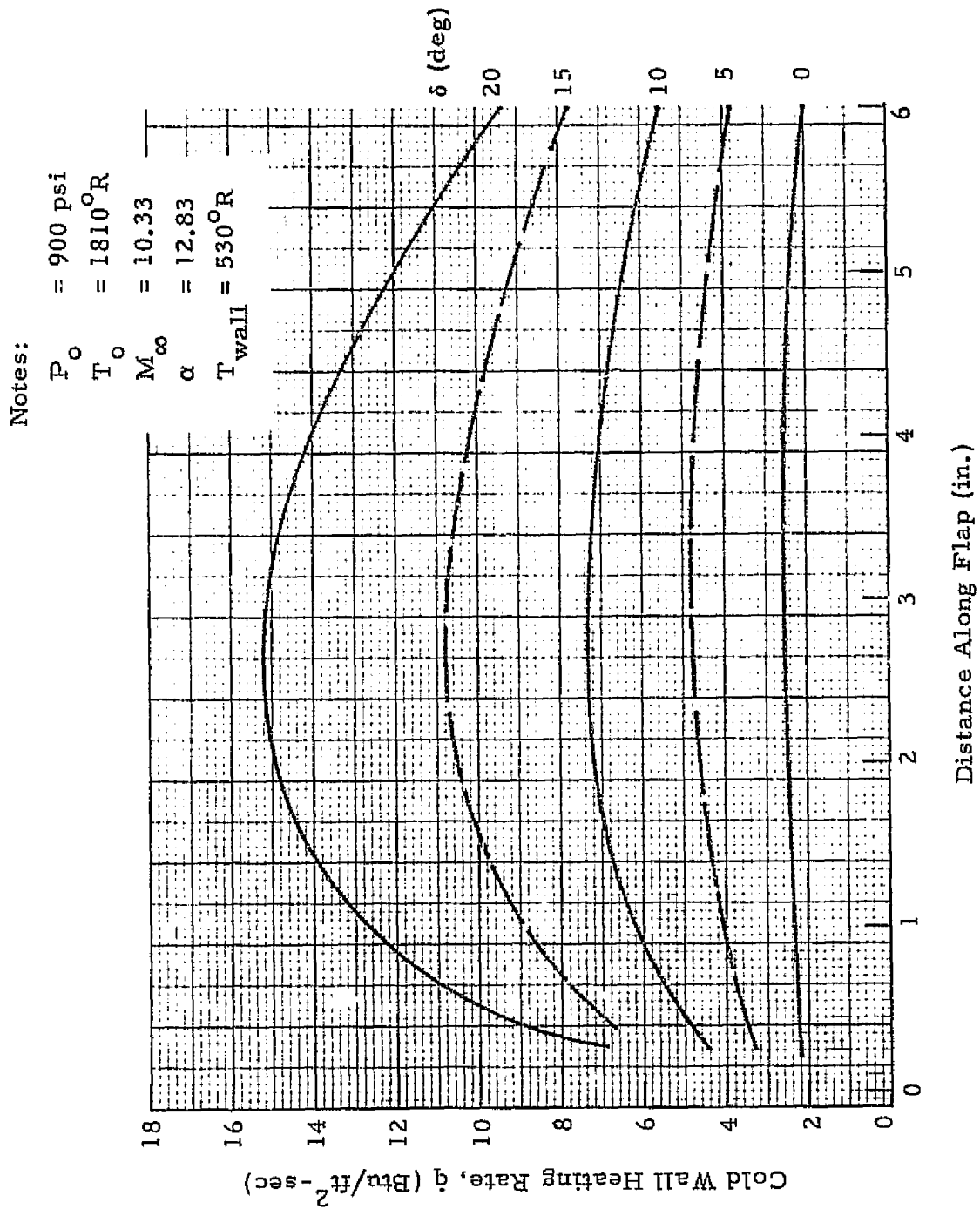


Fig. 4 - Predicted Cold Wall Heat Transfer Distribution on Flap

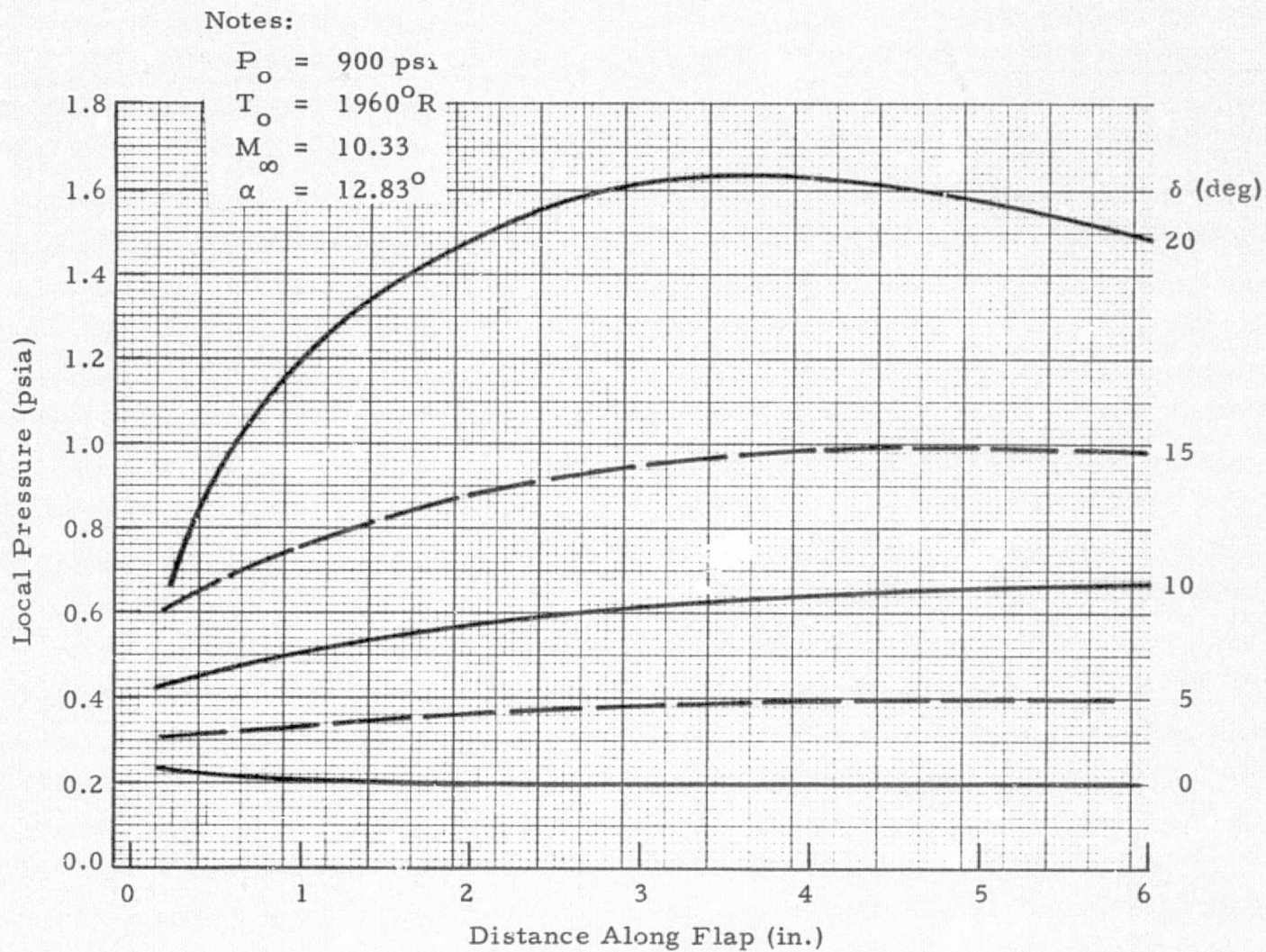
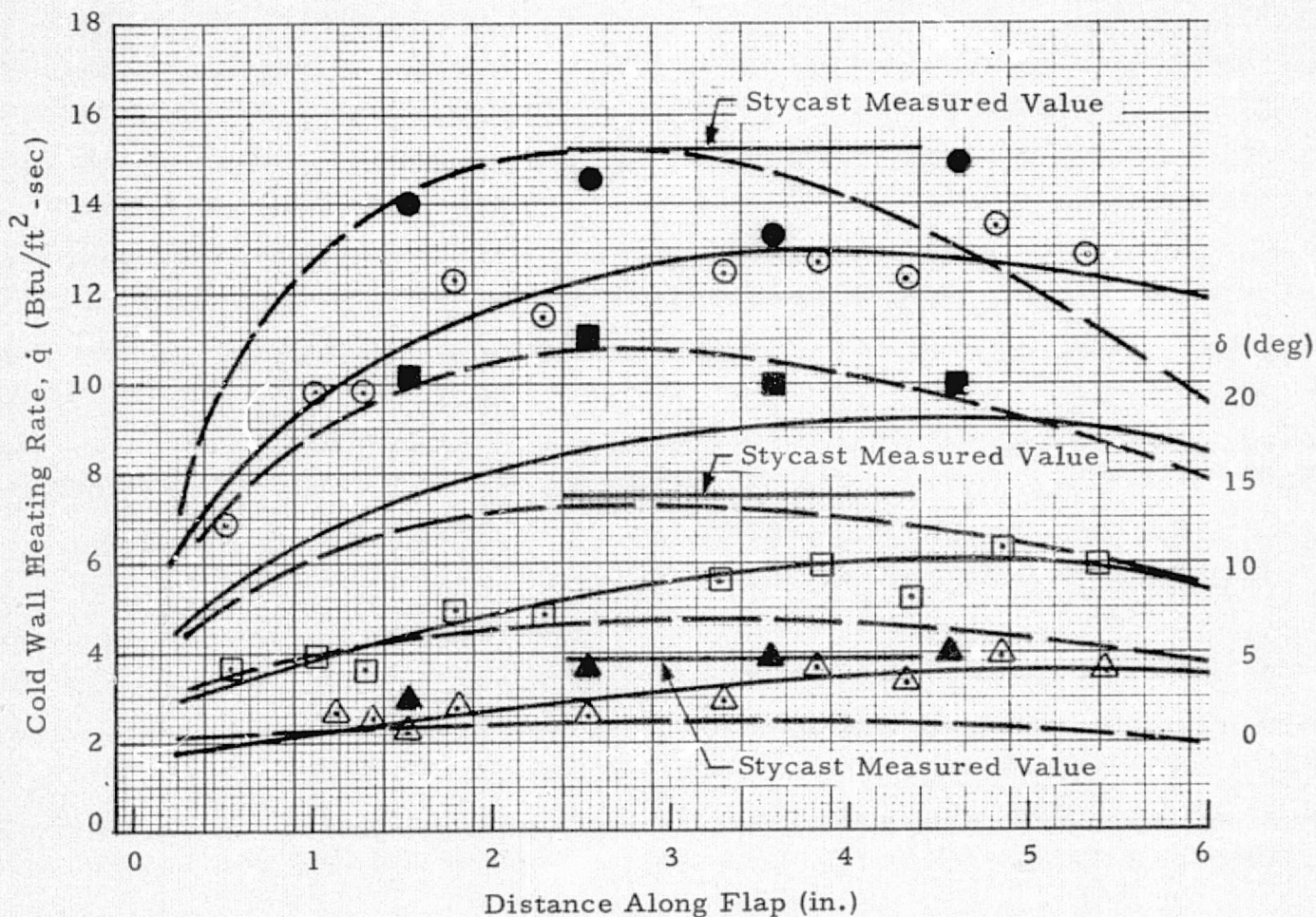


Fig. 5 - Predicted Pressure Distribution on Flap



Notes:

$$\begin{aligned}
 T_{\text{wall}} &= 530^{\circ}\text{R} \\
 P_o &= 900 \text{ psi} \\
 T_o &= 1810^{\circ}\text{R} \\
 \alpha &= 12.83^{\circ}
 \end{aligned}$$

Sym	δ (deg)
○	20 Top
●	20 Bottom
□	10 Top
△	5 Top
▲	5 Bottom
■	15 Bottom
—	Data Faired Curves
- - -	Predicted Curves

Fig. 6 - Comparison of Predicted and Measured Cold Wall Heat Transfer Distributions on Flap

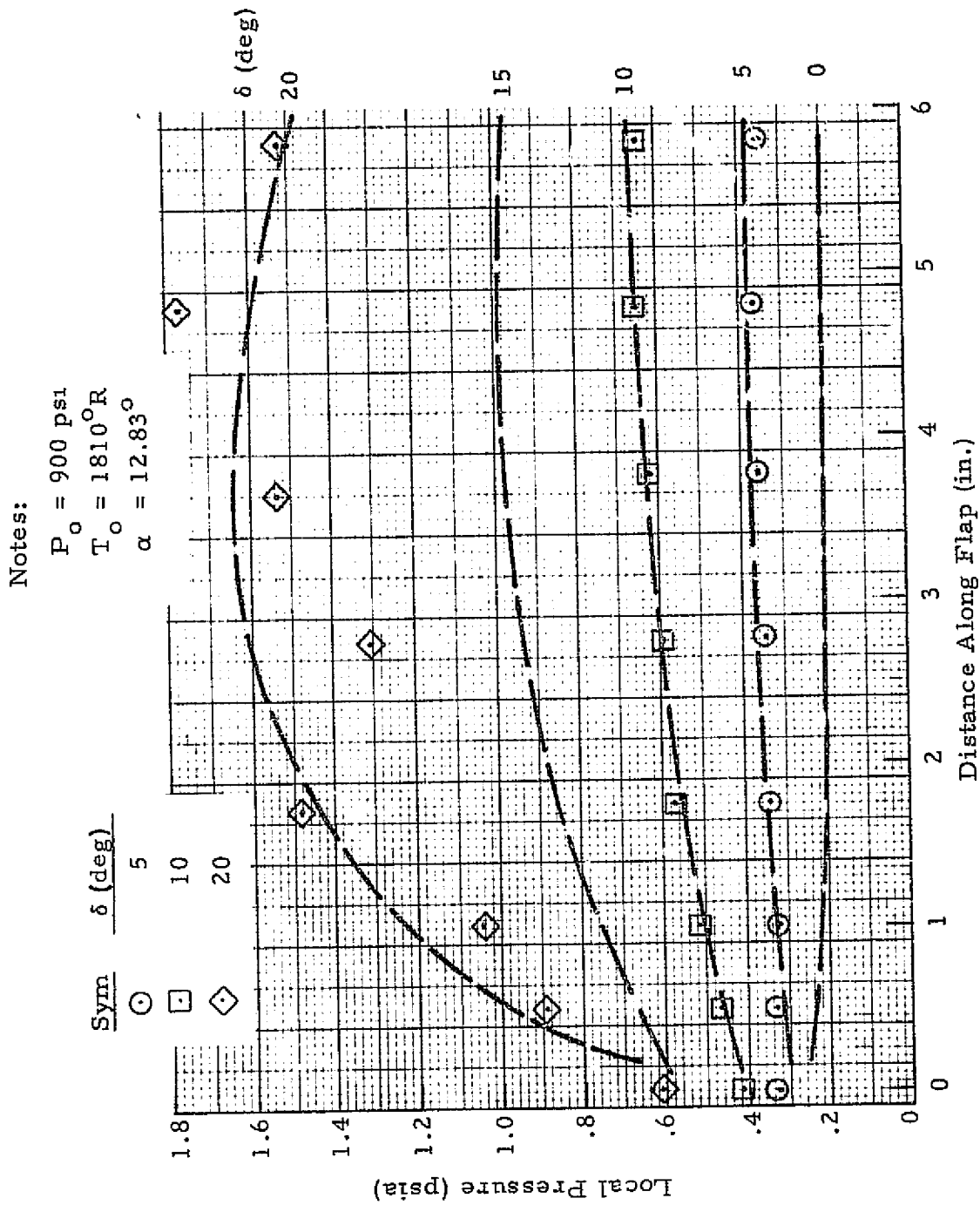


Fig. 7 - Comparison of Predicted and Measured Pressure Distributions on Flap

REPRODUCIBILITY OF THE
ORIGINAL PAGE IS POOR

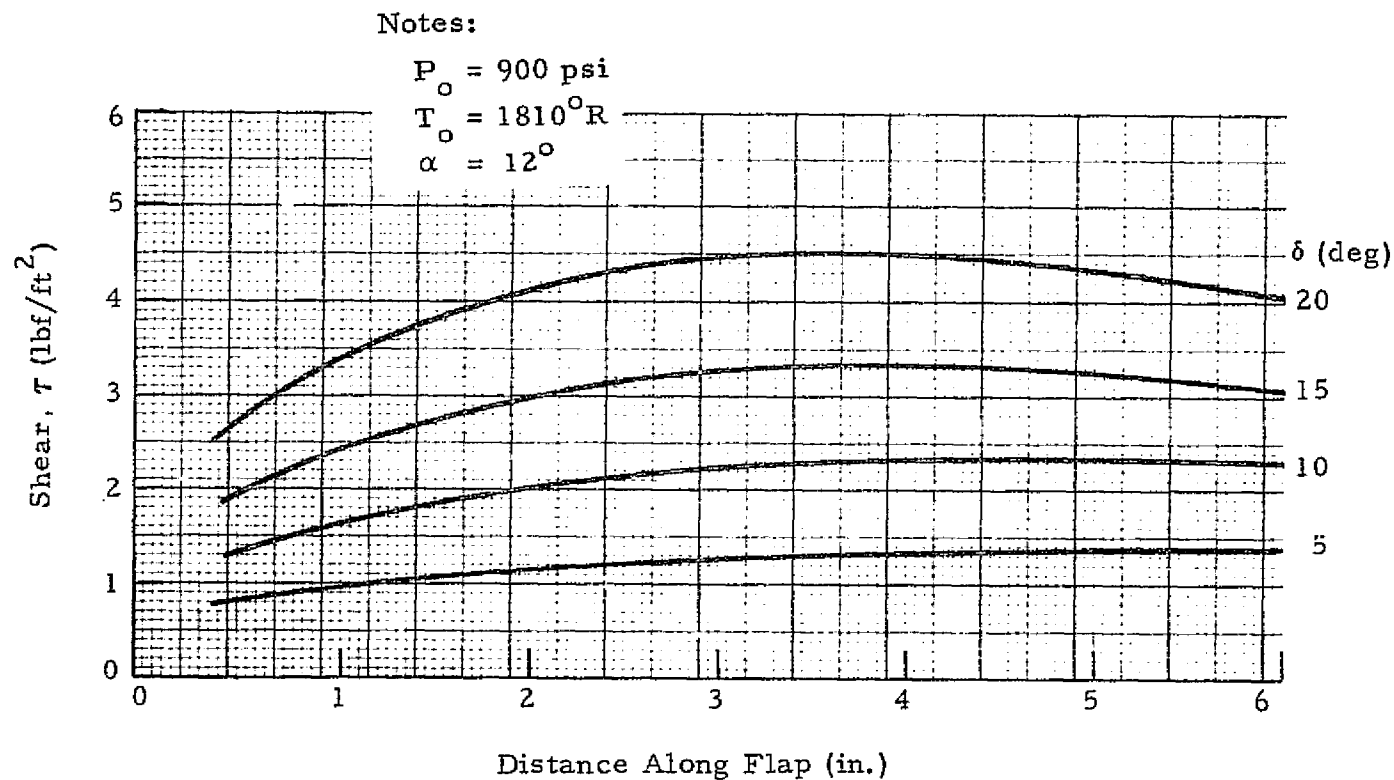


Fig. 8 - Calculated Shear Distribution on Flap (calculated using measured heating rates and calculated velocities)

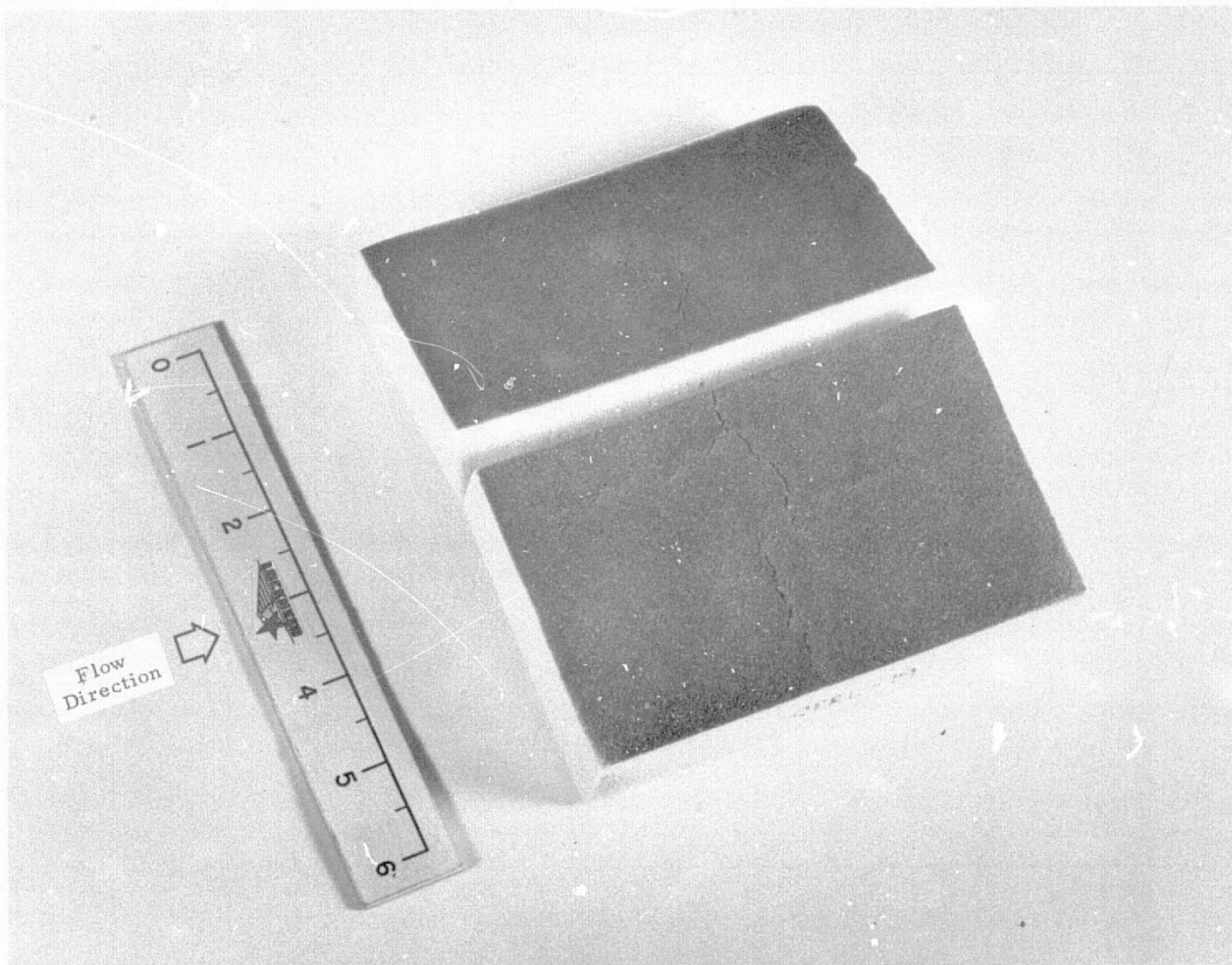


Fig. 9 - Typical Post-Test Photograph of Foam Sample Which Did Not Streak. (Sample Number CPRL-19 Tested at a Heating Rate of 5.9 Btu/ft²-sec and a Shear of 2.3 lbf/ft² for 15 Seconds)

REPRODUCIBILITY OF THE
ORIGINAL PAGE IS POOR

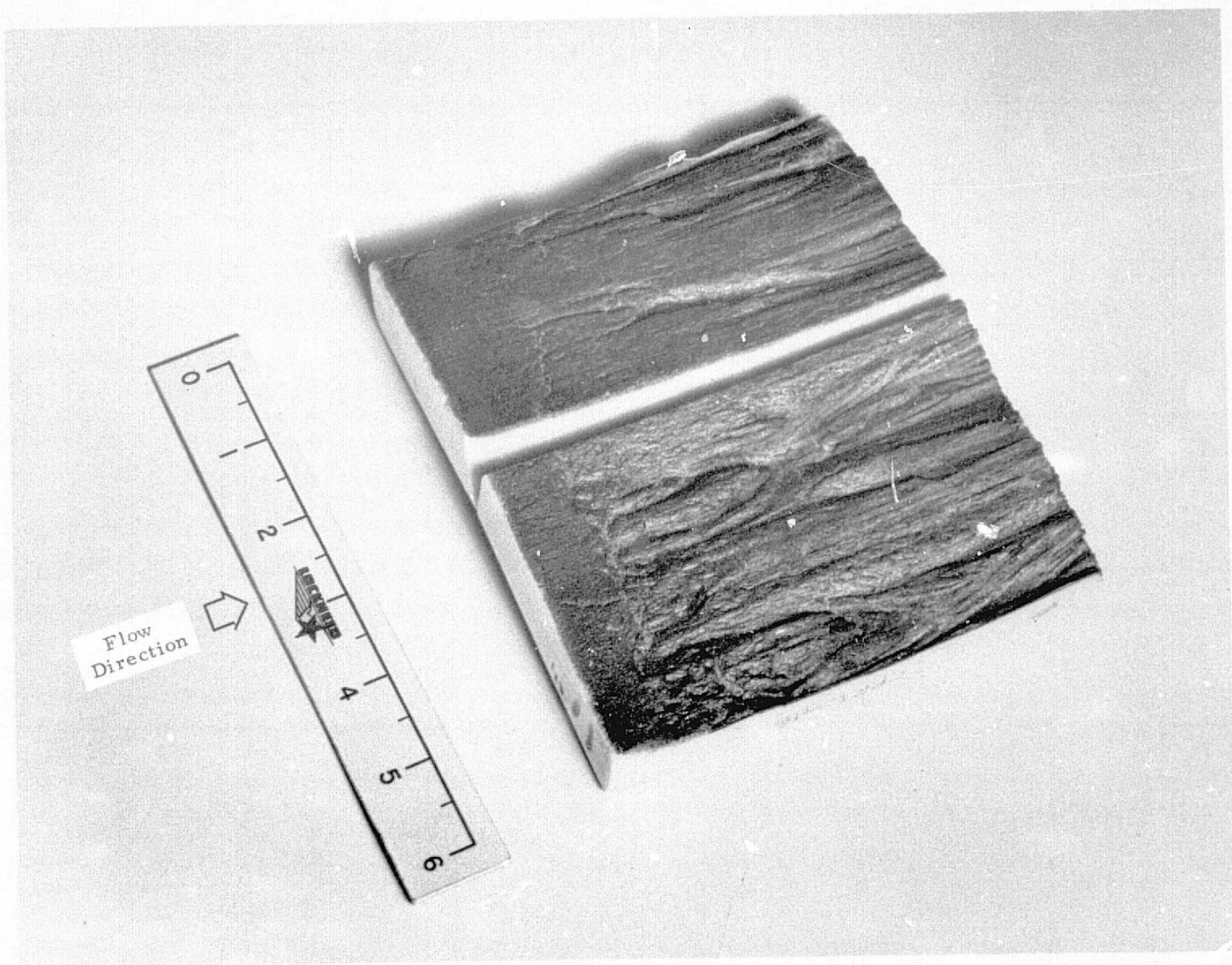


Fig. 10 - Typical Post-Test Photograph of Foam Sample Which Did Streak (Sample Number CPRL-16; Tested at a Heating Rate of 13 Btu/ft²-sec, and a Shear of 4.5 lbf/ft², for 15 Seconds)

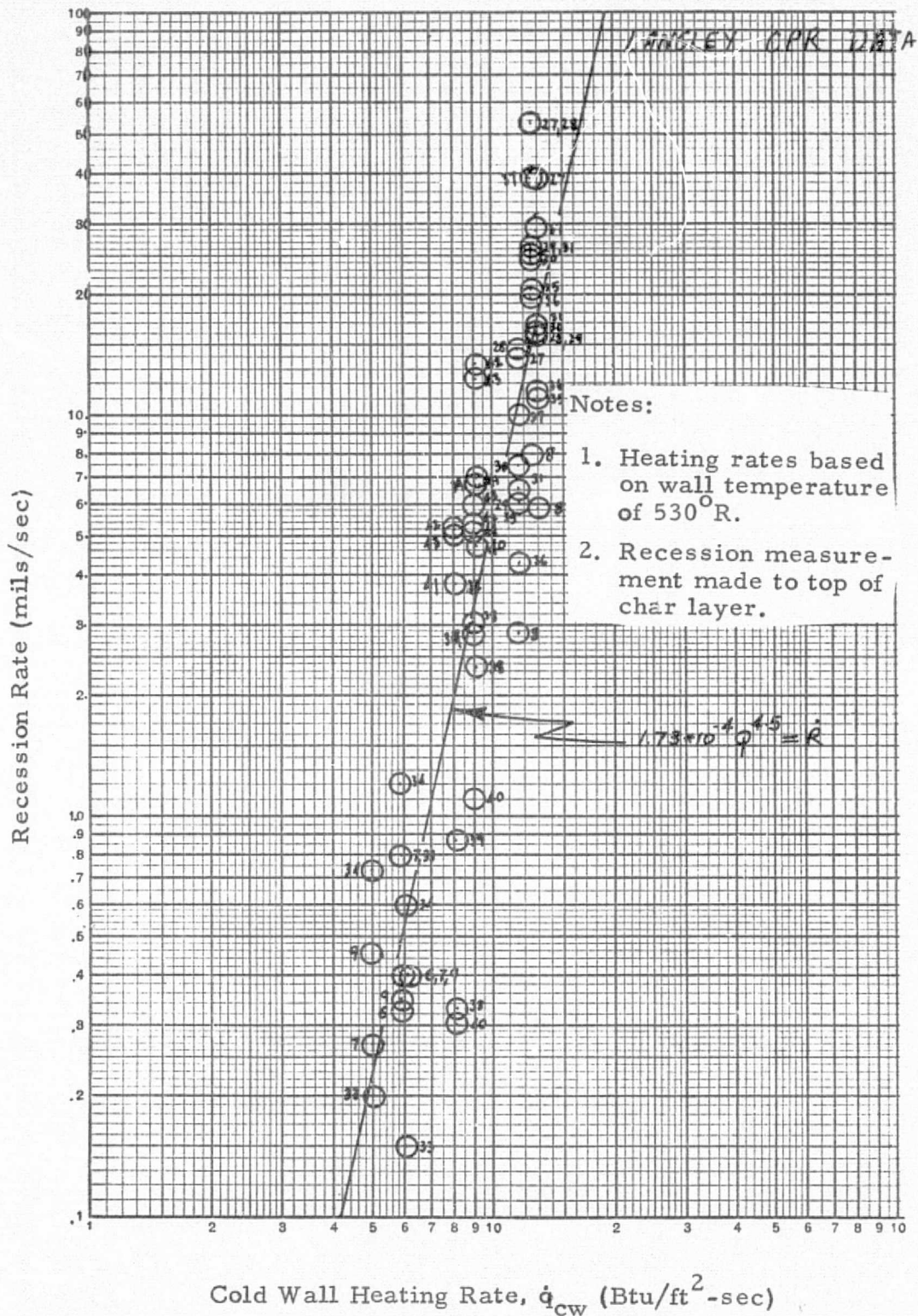


Fig. 11 - Minimum Average Recession Rate vs Cold Wall Heating Rate

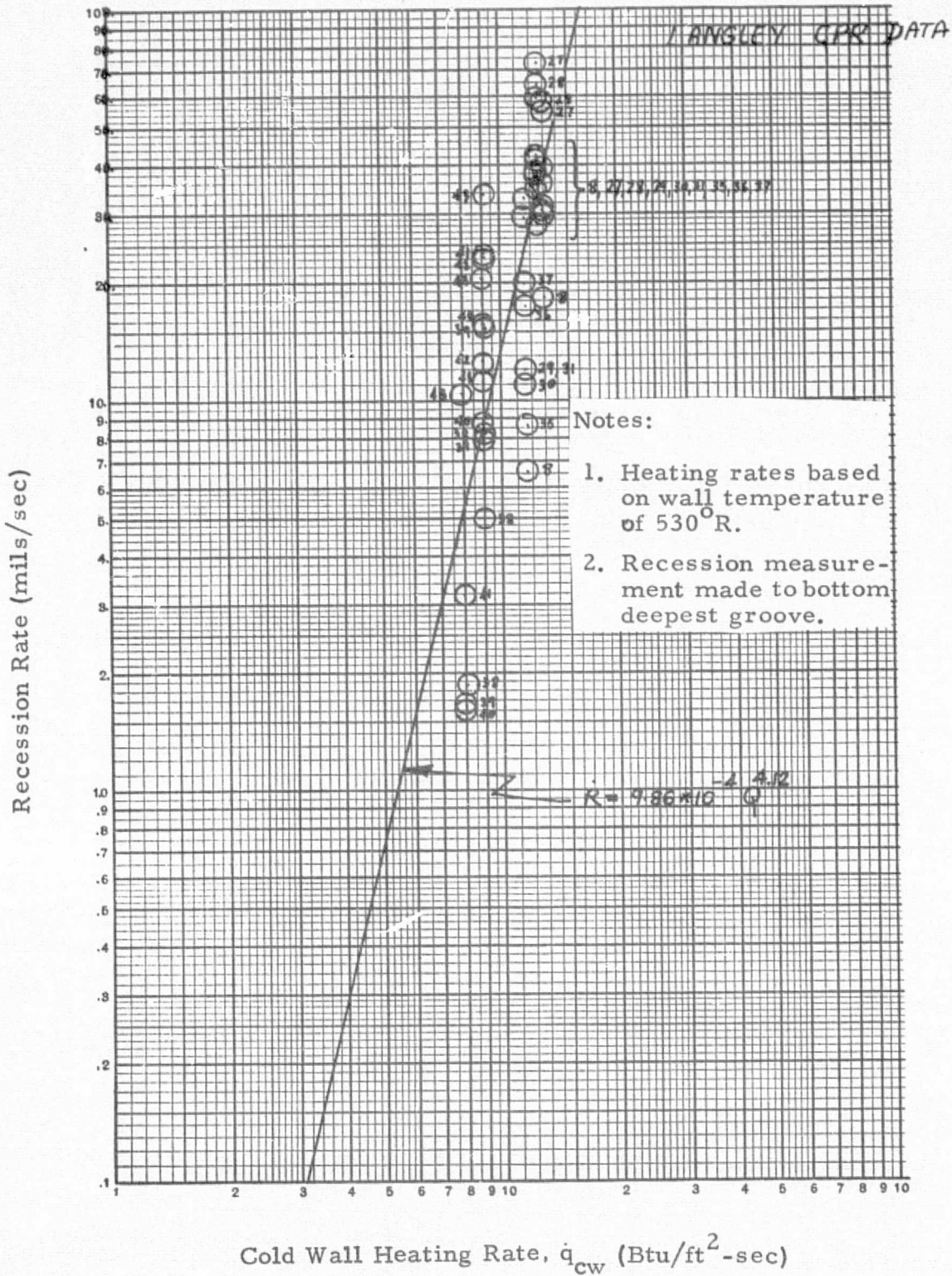
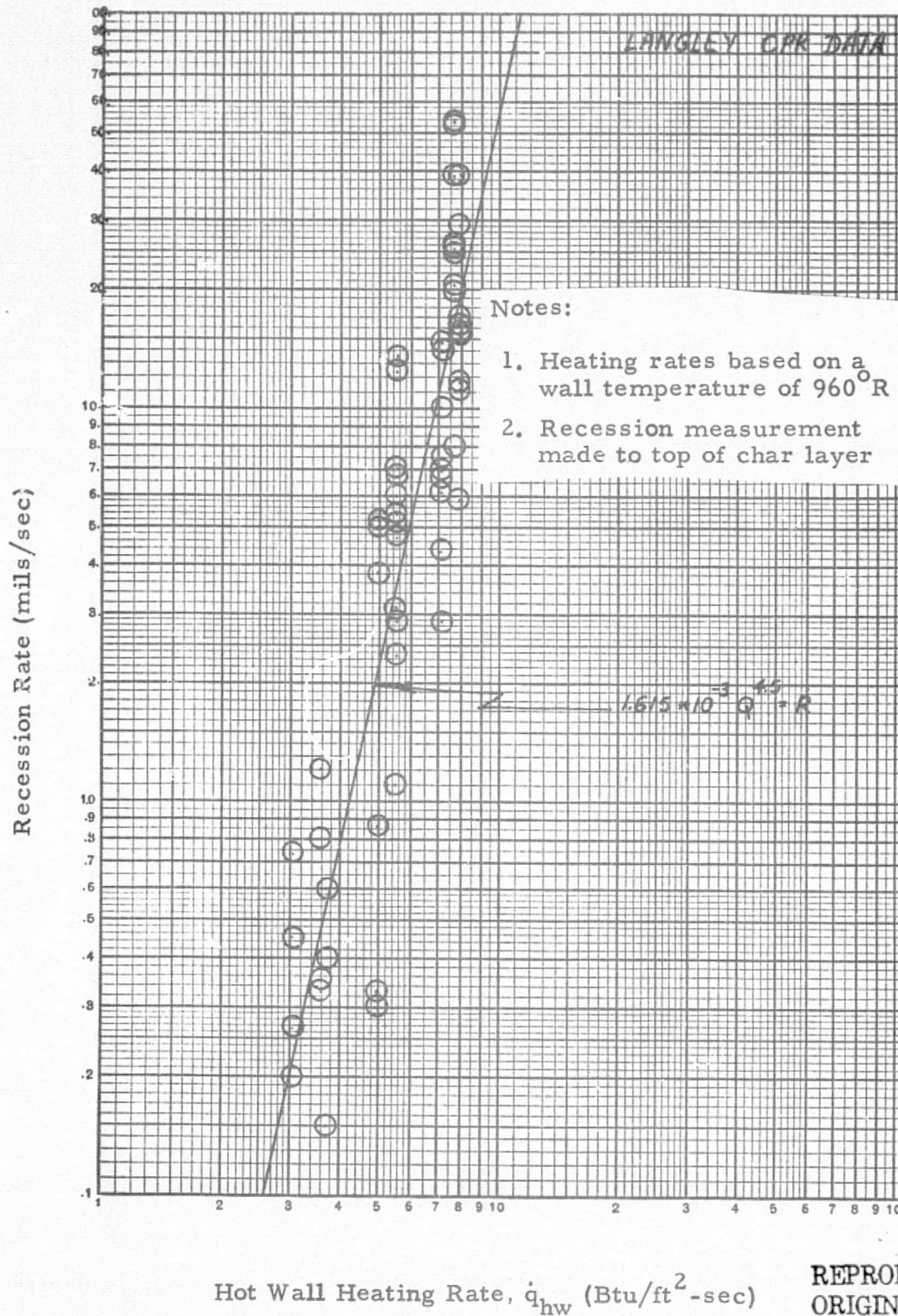


Fig. 12 - Maximum Recession Rate vs Cold Wall Heating Rate



REPRODUCIBILITY OF THE
ORIGINAL PAGE IS POOR

Fig. 13 - Minimum Average Recession Rate vs Hot Wall Heating Rate

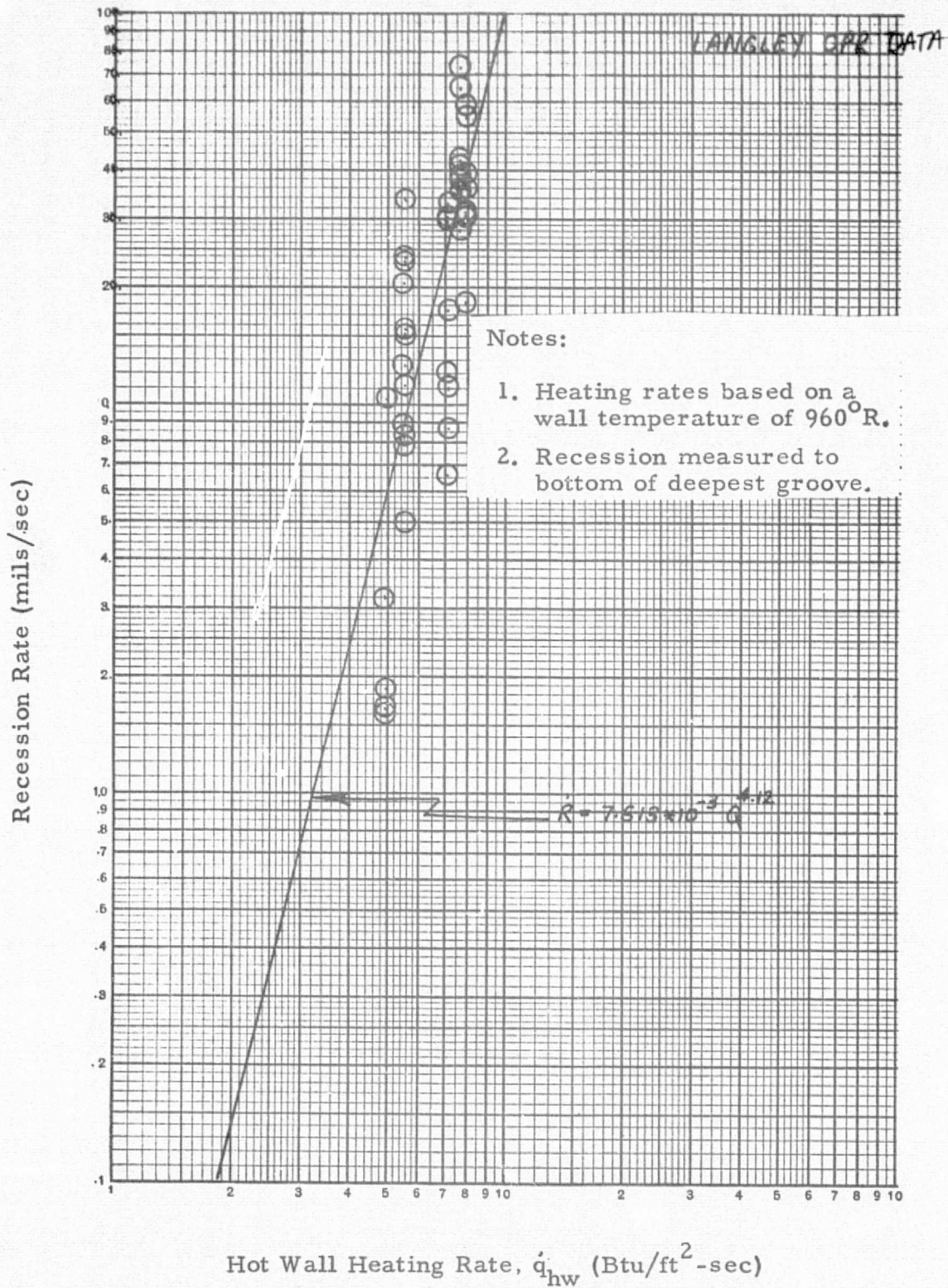


Fig. 14 - Maximum Recession Rate vs Hot Wall Heating Rate

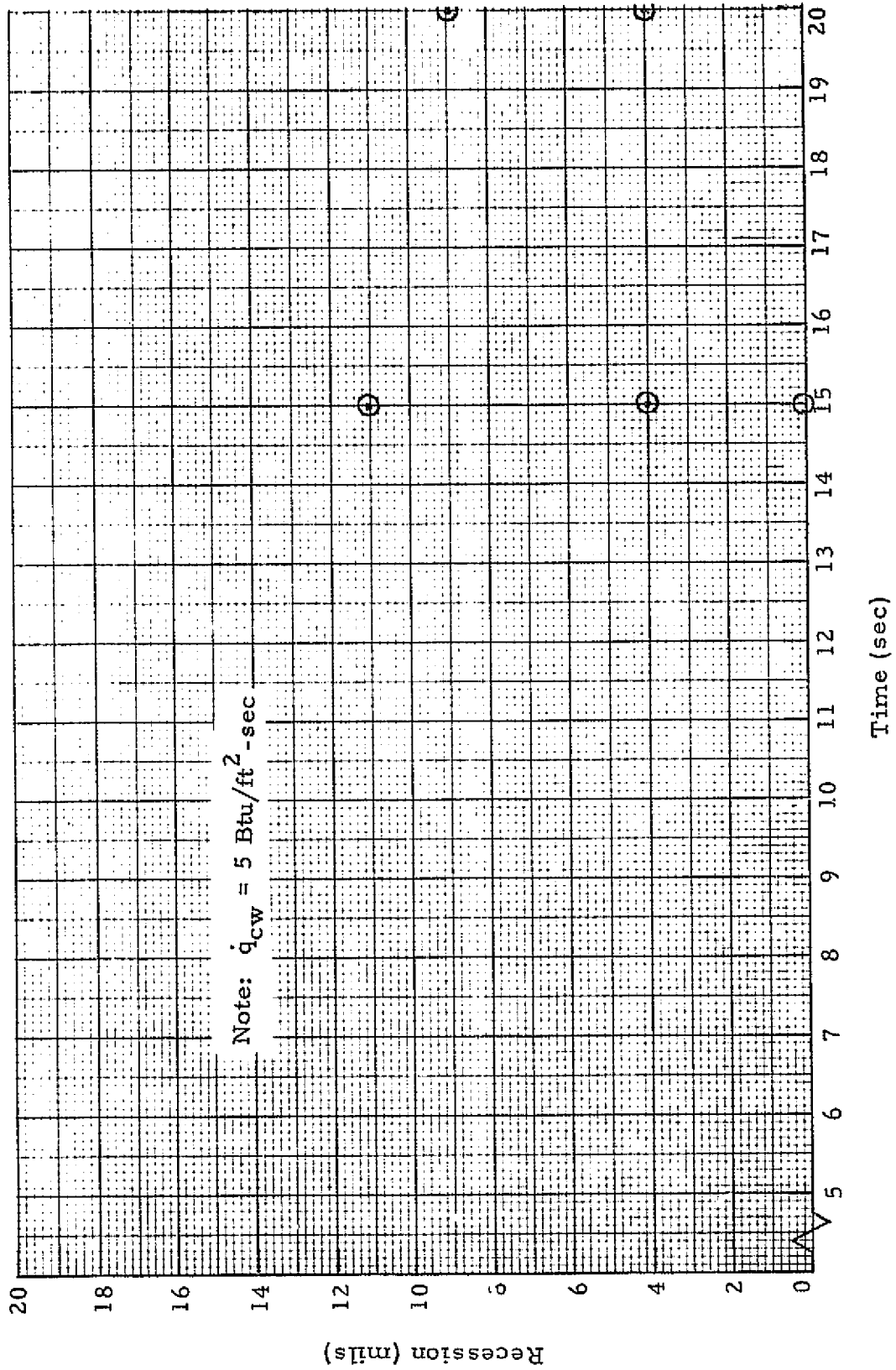


Fig. 15 - Recession at 1.0 in. from the Foam Leading Edge vs Time for $\delta = 10 \text{ deg}$, $\alpha = 12 \text{ deg}$

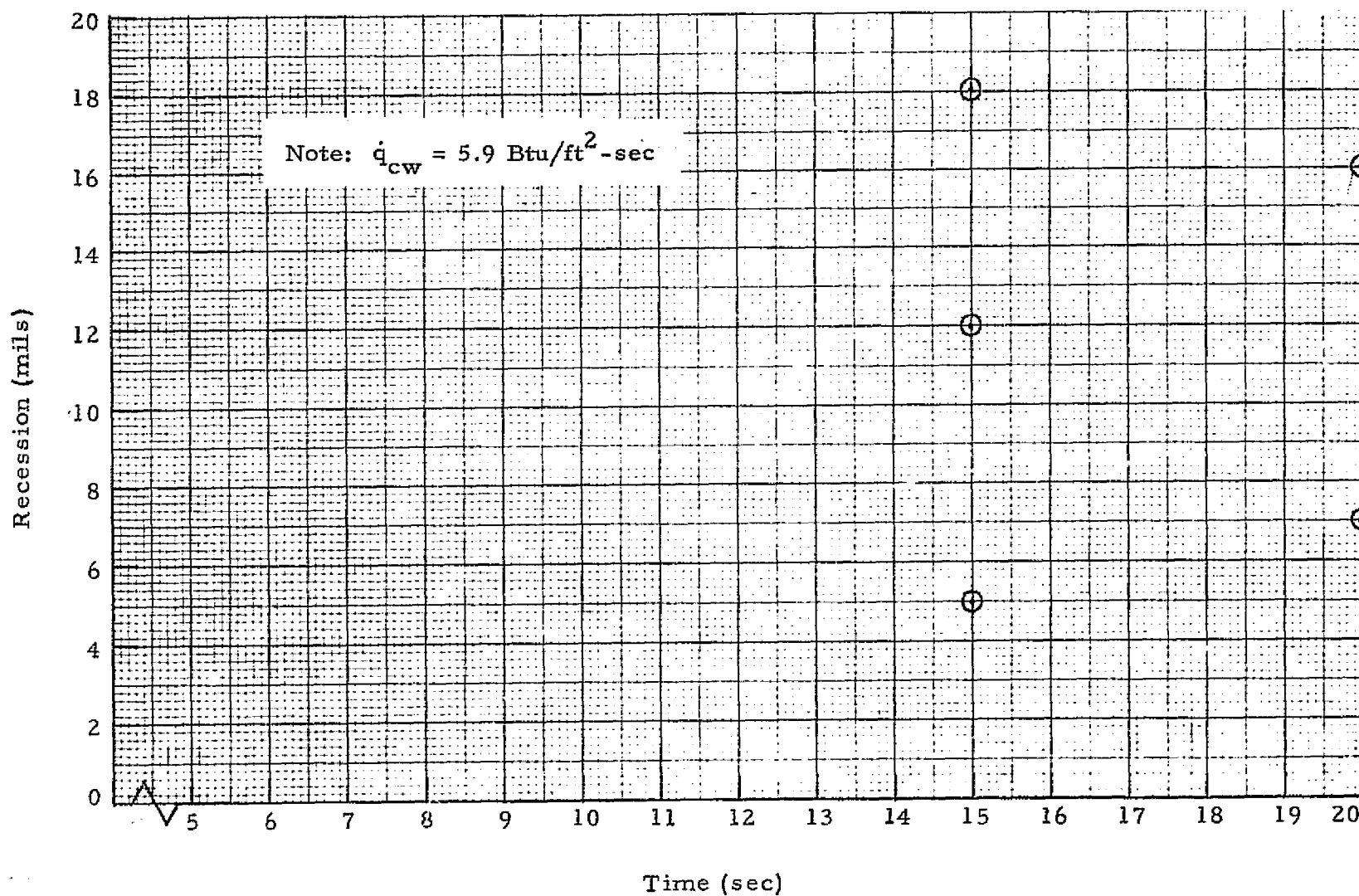


Fig. 16 - Recession at 2.5 in. from the Foam Leading Edge vs Time for $\delta = 10 \text{ deg}$, $\alpha = 12 \text{ deg}$

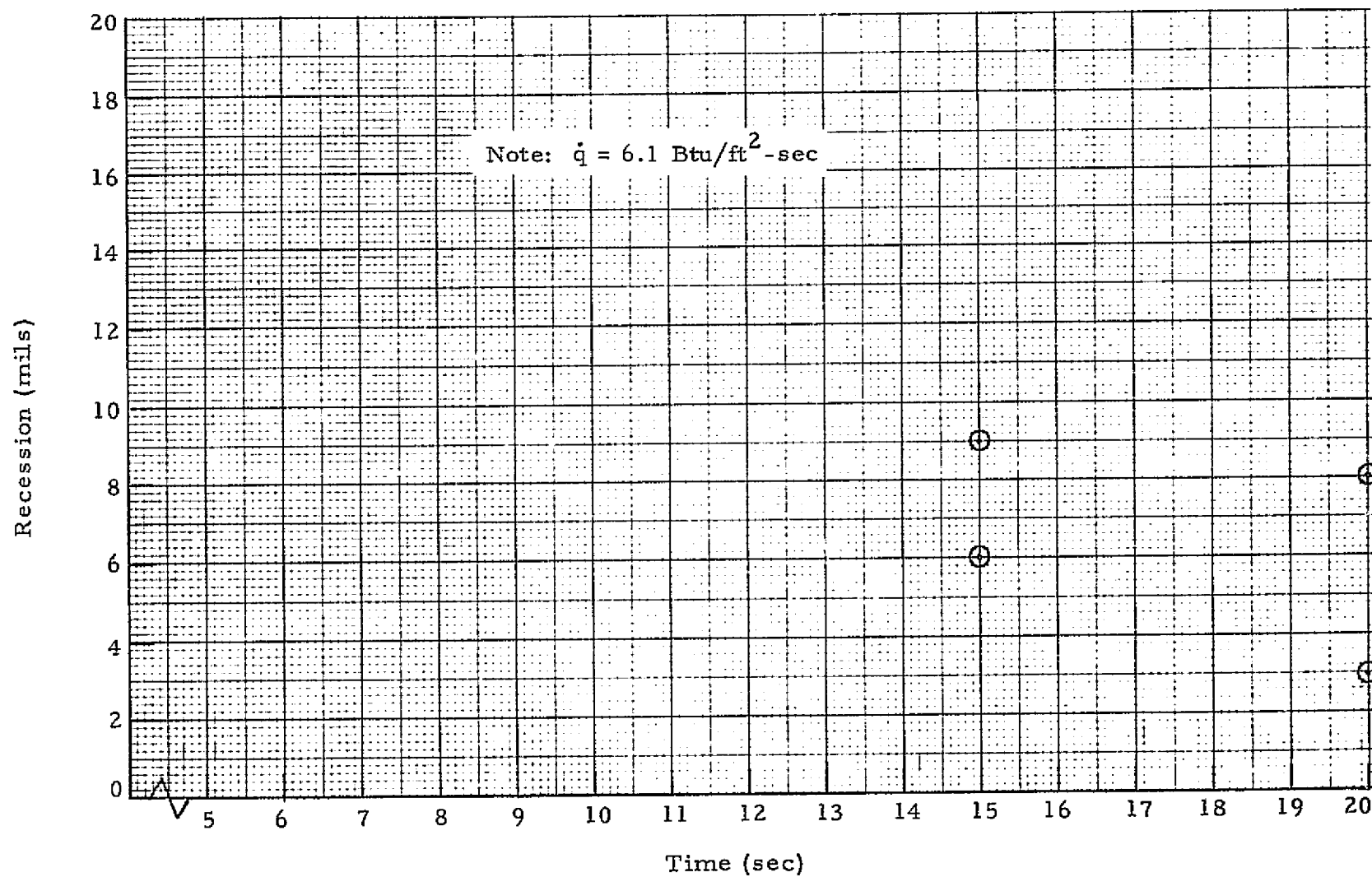


Fig. 17 - Recession at 3.75 in. from the Foam Leading Edge vs Time for $\delta = 10 \text{ deg}$, $\alpha = 12 \text{ deg}$

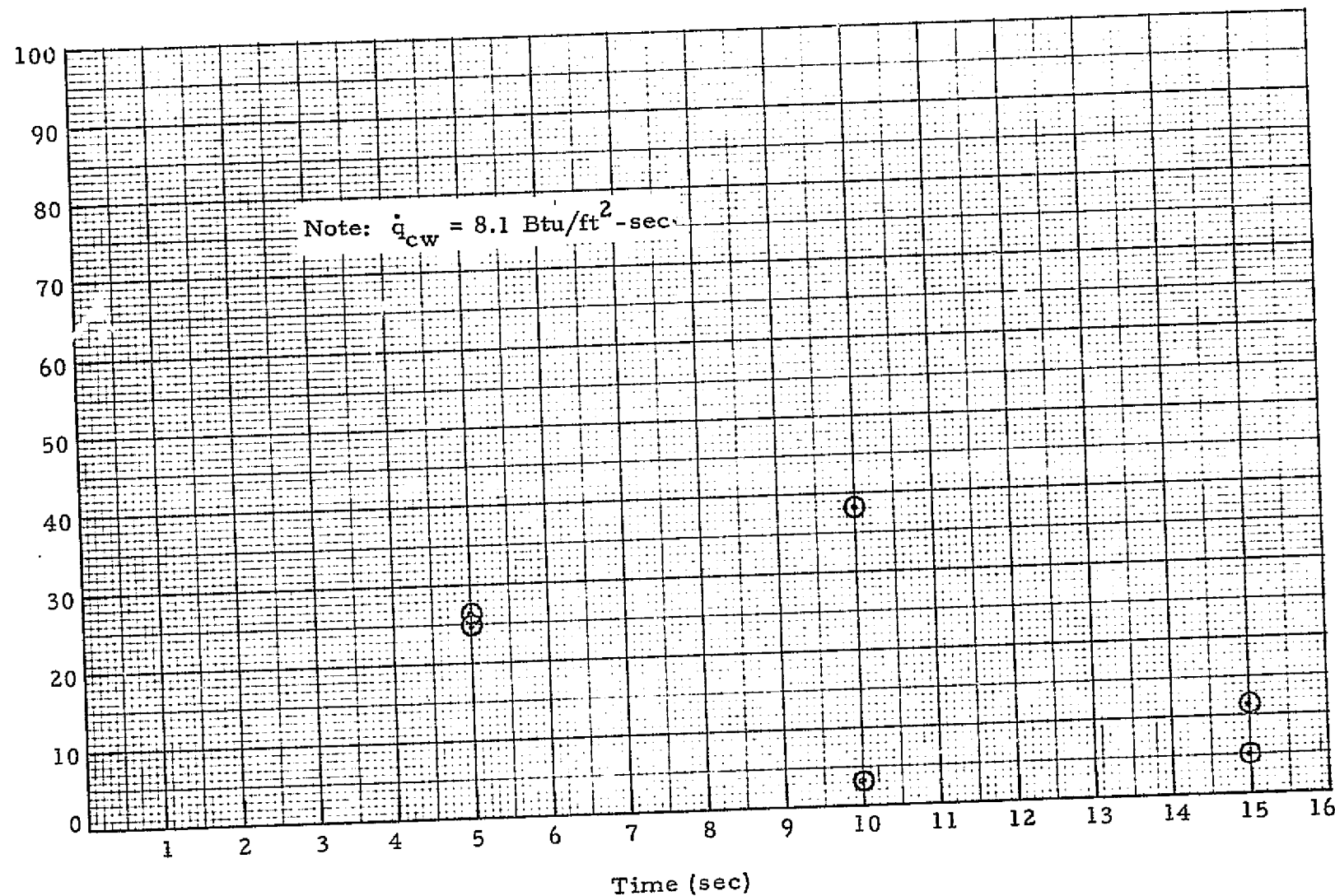


Fig. 18 - Recession at 1.0 in. from the Foam Leading Edge vs Time for $\delta = 15 \text{ deg}$, $\alpha = 12 \text{ deg}$

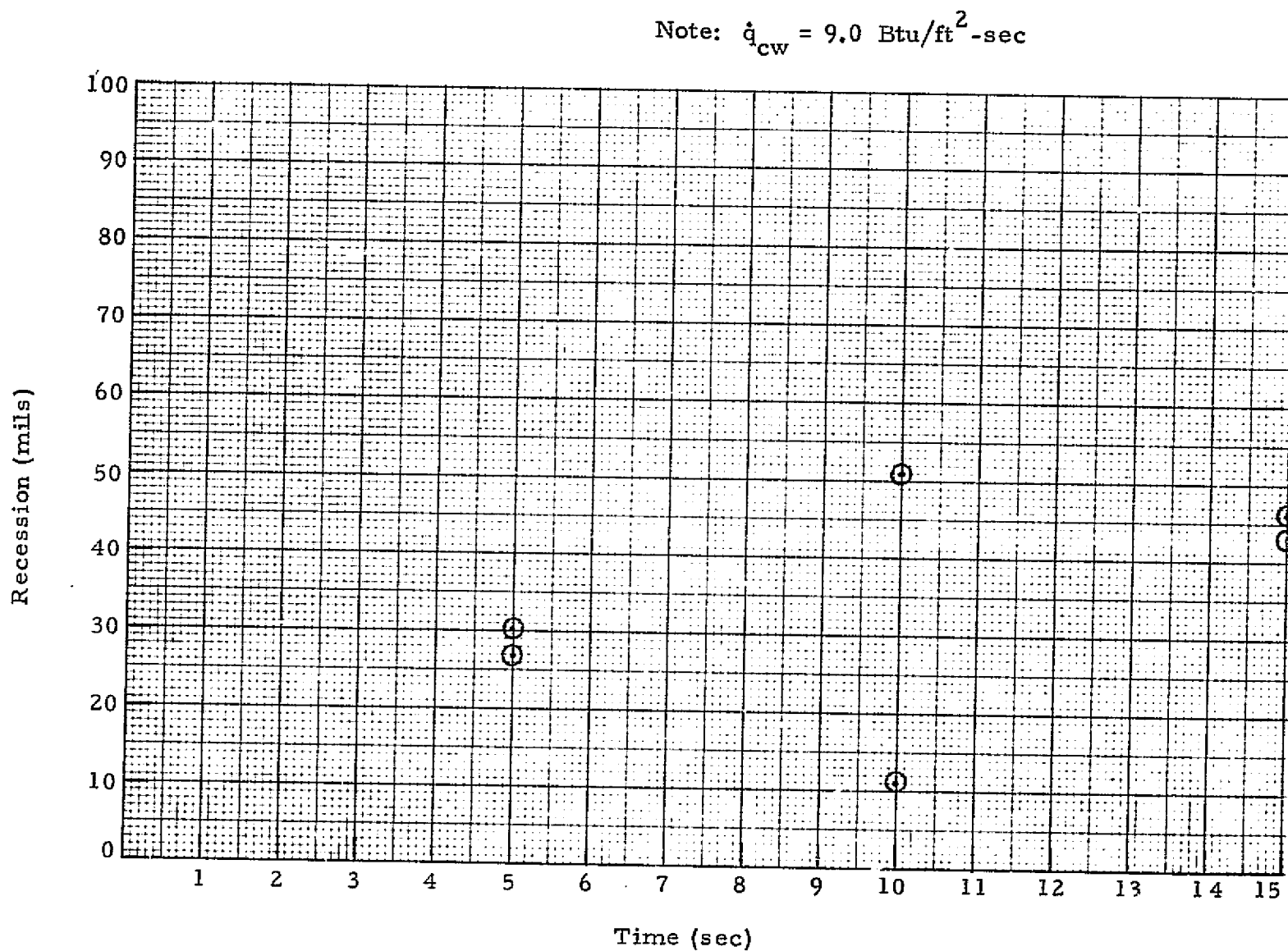


Fig. 19 - Recession at 2.5 in. from the Foam Leading Edge vs Time for $\delta = 15 \text{ deg}$, $\alpha = 12 \text{ deg}$

Note: $\dot{q} = 9.1 \text{ Btu/ft}^2\text{-sec}$

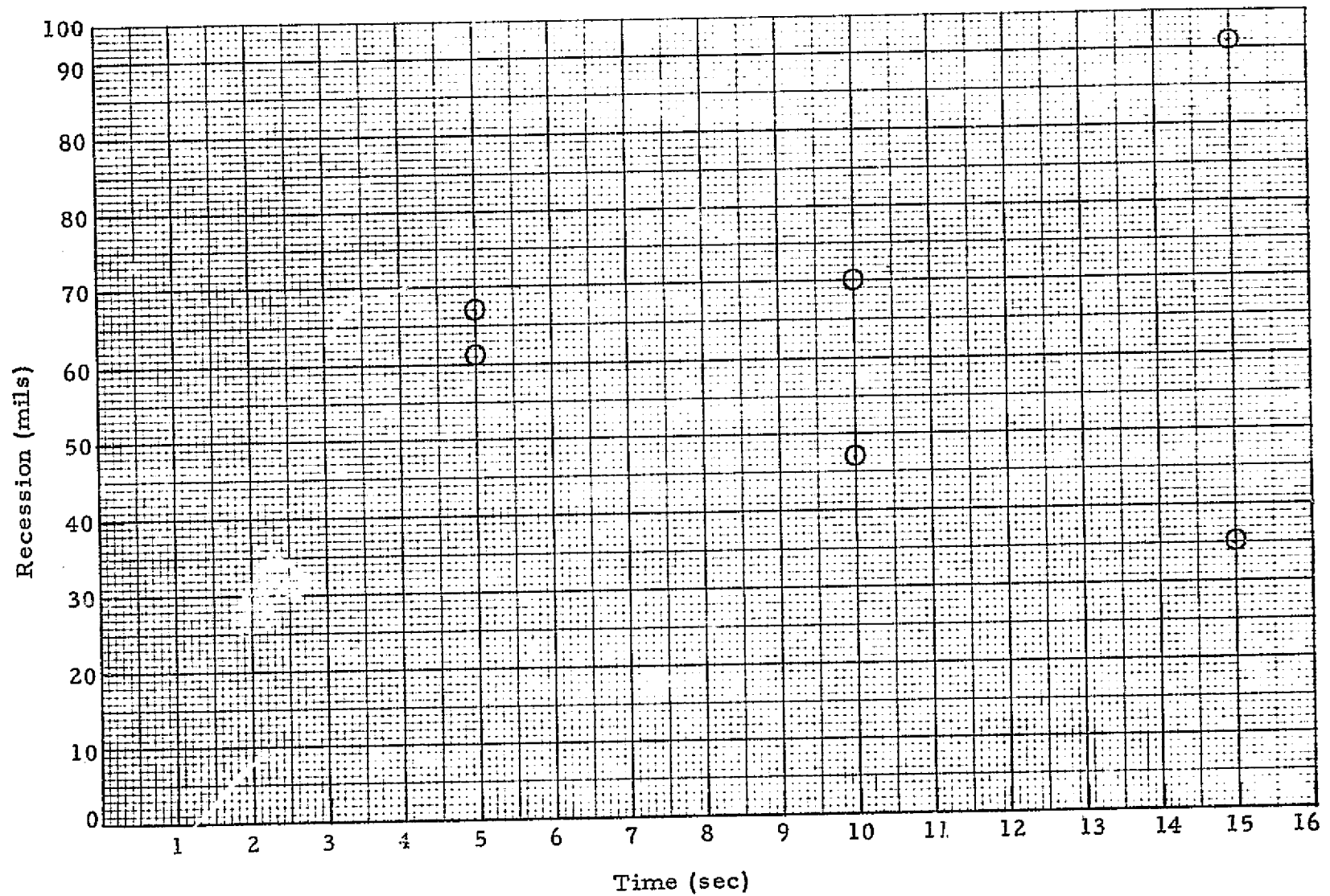


Fig. 20 - Recession at 3.75 in. from the Foam Leading Edge vs Time for $\delta = 15 \text{ deg}$, $\alpha = 12 \text{ deg}$

Note: $\dot{q} = 11.7 \text{ Btu/ft}^2\text{-sec}$

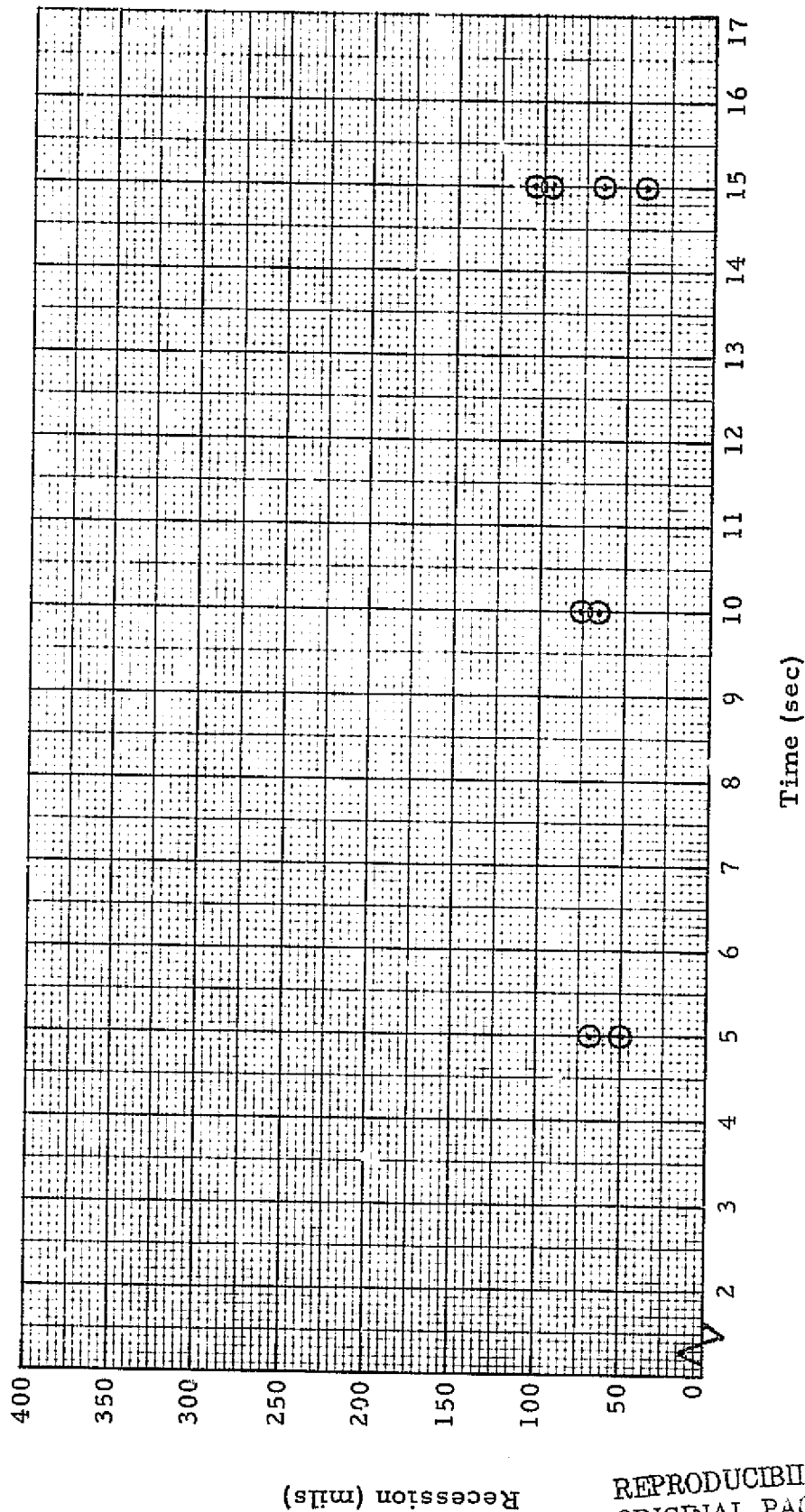


Fig. 21 - Recession at 1.0 in. from the Foam Leading Edge vs Time for $\delta = 20 \text{ deg}$, $\alpha = 12 \text{ deg}$

REPRODUCIBILITY OF THE
ORIGINAL PAGE IS POOR

Note: $\dot{q} = 13.0 \text{ Btu/ft}^2\text{-sec}$

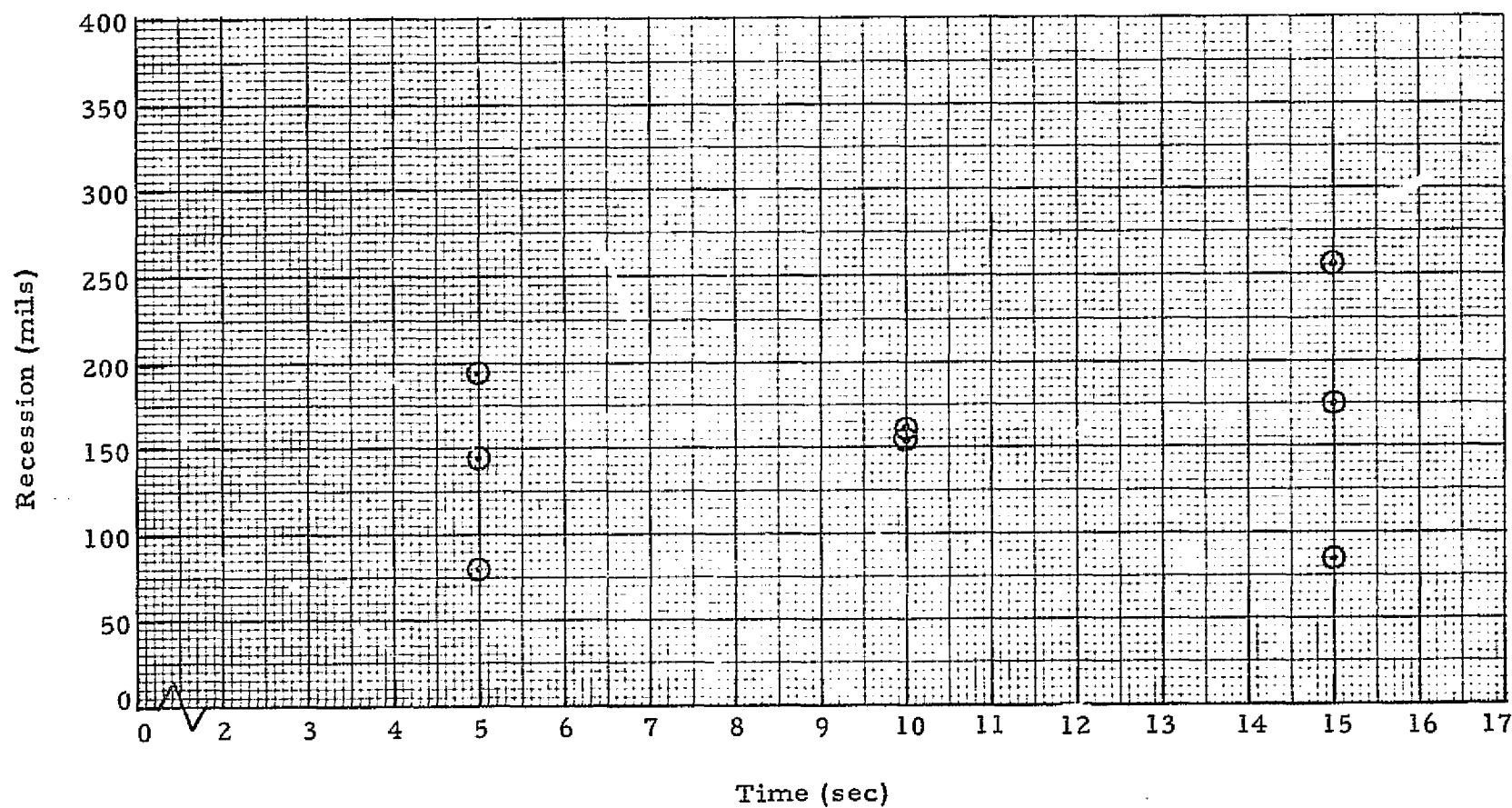


Fig. 22 - Recession at 2.5 in. from the Foam Leading Edge vs Time for $\delta = 20 \text{ deg}$, $\alpha = 12 \text{ deg}$

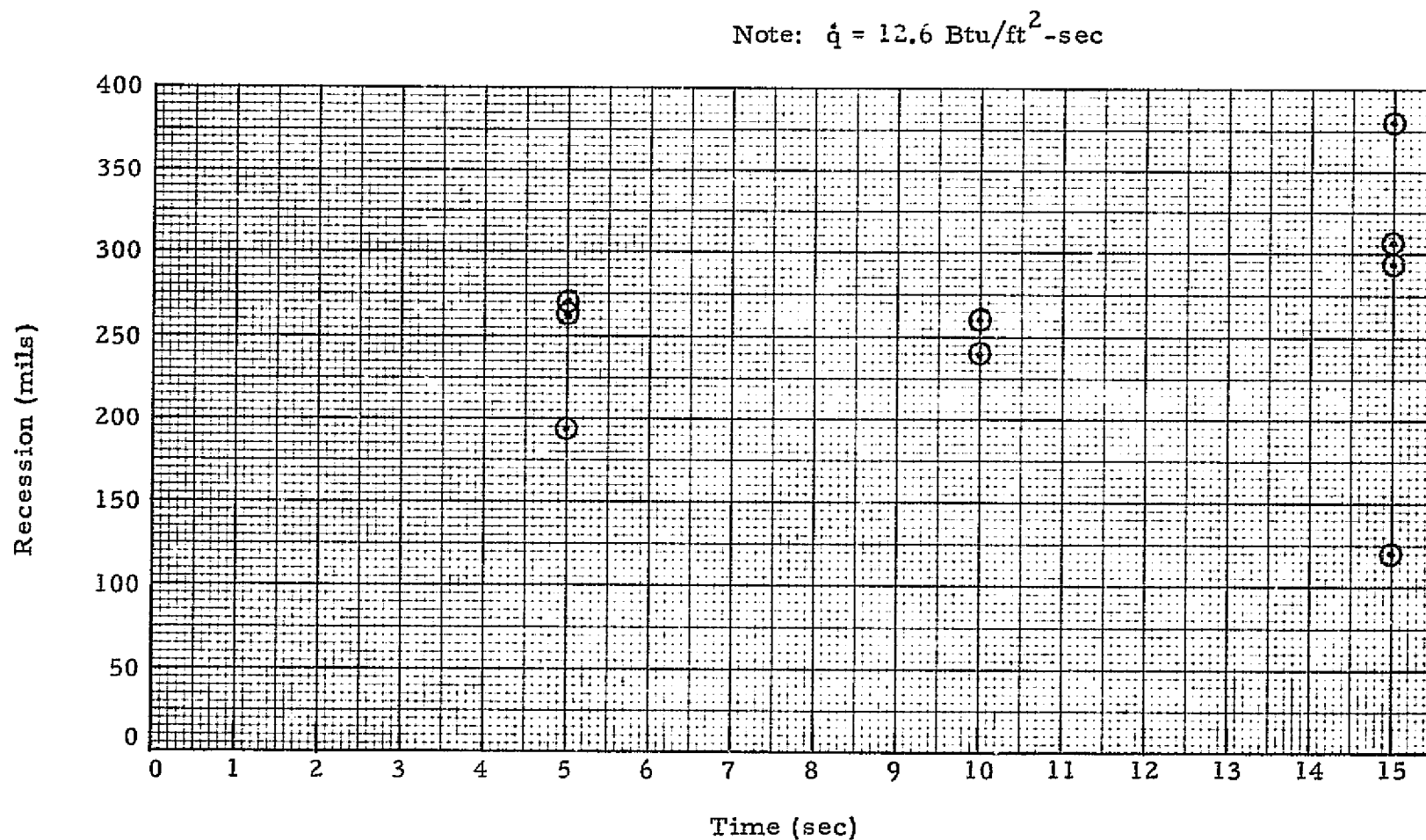


Fig. 23 - Recession at 3.75 in. from the Foam Leading Edge vs Time for $\delta = 20 \text{ deg}$, $\alpha = 12 \text{ deg}$

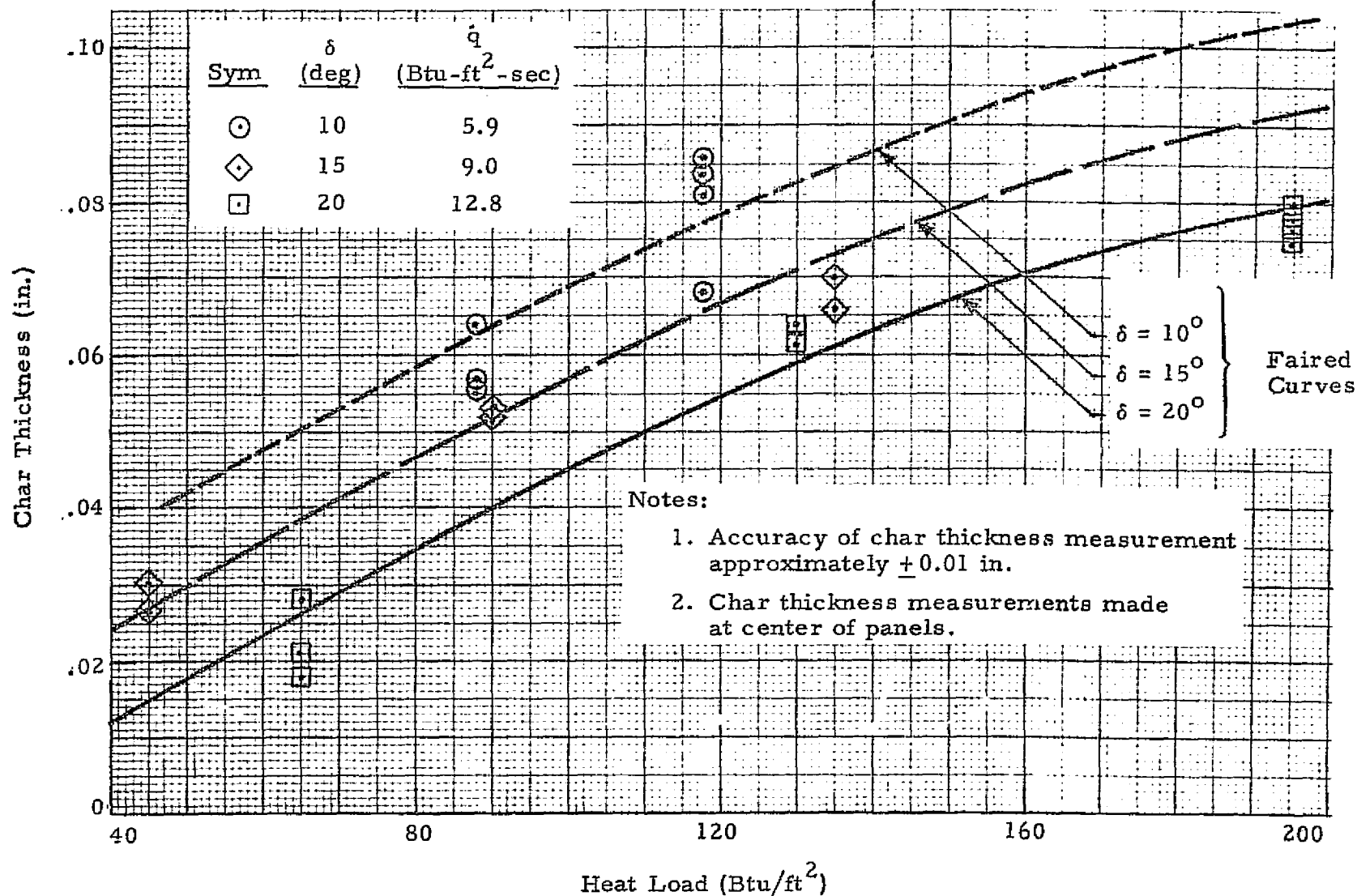


Fig. 24 - Approximate Char Thickness vs Heat Load for CPR-421 Samples

Appendix H

Dean, W. G., and Z. S. Karu, "Results of Space Shuttle External Tank Thermal Protection System Foam Tests in AEDC Tunnel C," LMSC-HREC TM D390783, Lockheed Missiles & Space Company, Huntsville, Ala., May 1975.

Lockheed

Missiles & Space Company, Inc.

HUNTSVILLE RESEARCH & ENGINEERING CENTER

Cummings Research Park
4800 Bradford Drive,
Huntsville, Alabama

RESULTS OF SPACE SHUTTLE
EXTERNAL TANK THERMAL
PROTECTION SYSTEM FOAM
TESTS IN AEDC
TUNNEL 'C'

May 1975

Contract NAS8-25569

Prepared for National Aeronautics and Space Administration
Marshall Space Flight Center, Alabama 35812

by

W.G. Dean
Z.S. Karu

APPROVED:

B. Hobson Shirley

B. Hobson Shirley, Supervisor
Engineering Sciences Section

FOREWORD

This report documents the results of a test program conducted in Tunnel "C" at the Arnold Engineering Development Center in support of the NASA-MSFC development of the Space Shuttle External Tank. Tests were conducted on the candidate thermal protection system materials. ARO personnel conducted the tests for NASA-MSFC with the Martin Marietta Corporation (MMC) furnishing the test specimens and serving as the prime test contractor. Lockheed-Huntsville assisted in planning the tests and reducing the data. On-site monitoring of the tests was done by personnel from NASA-MSFC, Martin-Marietta and Lockheed-Huntsville.

The Lockheed support was conducted under Contract NAS8-25569, "Space Shuttle Thermal Support." The NASA-MSFC Contracting Officer's Representative for this contract is Dr. Kenneth E. McCoy, EP-44. The NASA-MSFC Test Engineer for these tests was Mr. R. Lopez, EP-44; the AEDC/ARO Test/Project Engineer was Mr. R.K. Matthews; and the MMC Test Engineer was Mr. S. Copsey; the Lockheed-Huntsville Test Engineers were Mr. Z.S. Karu and Mr. W.G. Dean.

Acknowledgment is hereby given to AEDC/ARO and MMC for all specimen and facility photographs shown herein. They are used by permission of these organizations.

CONTENTS

<u>Section</u>		<u>Page</u>
	FOREWORD	ii
	NOMENCLATURE	iv
1	INTRODUCTION AND SUMMARY	1
2	TECHNICAL DISCUSSION	2
	2.1 Test Facility and Test Conditions	2
	2.2 Test Fixture Description	2
	2.3 Test Panel Description	3
	2.4 Test Procedure	5
	2.5 Data Taken	6
3	RESULTS	9
	3.1 Environment Prediction and Measurement Results	9
	3.2 Foam Panel Results	10
	3.3 Comparison of AEDC Data with Other Facility Data on CPR-421 Foam	20
	3.4 Foam 'Ablation' Products Contamination Effects	20
4	CONCLUSIONS AND RECOMMENDATIONS	21
	REFERENCES	23

NOMENCLATURE

Symbol

ET	External Tank of Space Shuttle vehicle
P_L	local pressure
P_o	total pressure
H_r	recovery enthalpy
\dot{q}_{cw}	cold wall heating rate
\dot{q}_{hw}	hot wall heating rate
\dot{q}_{turb}	turbulent heating rate
T_o	total temperature
T_r	recovery temperature
T_w	wall temperature
X	distance along wedge from leading edge
\dot{W}	streak width rate

Greek

δ	wedge angle
τ	aerodynamic shear

Section 1 INTRODUCTION AND SUMMARY

A series of tests was conducted at AEDC in Tunnel "C" on three candidate thermal protection system materials. Test conditions were selected which closely simulated the predicted flight values of heating rate, pressure, enthalpy and shear on selected points of the External Tank (ET). Tests were conducted in three phases on three separate dates, 6 January, 20 January and 12 February 1975. Sixty-two panels were tested. Of these, 58 were CPR-421, one was BX-250, and three were SLA-561s. Some of the CPR-421 panels had machined surfaces, some had "net sprayed" or "as-sprayed" surfaces, some were coated and some were uncoated. Both constant heating rate and trajectory type varying heating rate runs were made. The tunnel was run continuously and the samples were injected into the flow for each separate test.

Data taken included color movies, shadowgraphs, heating rates, pressures and foam recession measurements. This report presents the test environments, numerous pretest and post-test photographs of the panels, and recession measurements and correlations.

The CPR-421 material continued to "streak" in this test facility as it did previously in the Langley Arc Jet and Langley Mach 10 Continuous Flow Hypersonic Flow facilities. However, the data are used to better define some streaking boundaries for vehicle applications.

A comparison of the data taken in these tests and that from previous test programs is also presented.

Section 2

TECHNICAL DISCUSSION

2.1 TEST FACILITY AND TEST CONDITIONS

Tunnel "C" is a closed-circuit, hypersonic wind tunnel with a Mach number 10 axisymmetric contoured nozzle and a 50-in. diameter test section. The tunnel can be operated continuously over a range of pressure levels from 200 to 2000 psia with air supplied by the main compressor plant of the von Karman facility. Stagnation temperatures sufficient to avoid air liquefaction in the test section (up to 1900°R) are obtained through the use of a natural gas fired combustion heater in series with an electric resistance heater. The entire tunnel (throat, nozzle, test section and diffuser) is cooled by integral, external water jackets. The tunnel is equipped with a model injection system which allows the model to be removed from the test section while the tunnel remains in operation. A more complete description of the tunnel is available in the Test Facilities Handbook (Ref. 1).

Most of the tests were run at a total temperature of 1900°R and a total pressure of 1800 psi. However at the end of the last series of tests, two panels were run at a lower total temperature of 1500°R with the same total pressure to see what effect enthalpy might have on foam performance. The total enthalpy for the 1900°R case was 478 Btu/lb, and the recovery enthalpy was approximately 415 to 420 Btu/lb depending upon the wedge angle of the exposed foam surface. For the 1500°R total temperature runs, the total and recovery enthalpies were 370 Btu/lb and 315 to 325 Btu/lb, respectively.

2.2 TEST FIXTURE DESCRIPTION

Figure 1 shows a photograph of the test fixture used in this series of tests. This fixture, or model, is essentially a steel wedge with a recessed area for mounting the foam panels behind a sharp leading edge. The model

is approximately 17 inches wide and 22.7 inches long on its top surface. The recessed area takes a panel 17 x 14 inches and up to 1.75 inches thick. The model angle of attack was changed during the various tests to vary the local pressure, heating rate and shear values. This same wedge fixture was used in a previous test program (Ref. 2) and was modified to accept the foam panels for the present tests. The necessary design modification recommendations and drawings were made by Lockheed-Huntsville, and the shop work was done by NASA-MSFC. Reference 2 contains detailed dimensions of this wedge fixture.

During the second series of tests it was found that during some of the long runs the wedge was heating up under the foam due to heating to the sides, leading edge and bottom ramp angle surfaces. Therefore before the third series of tests, AEDC added some water cooling tubes and passages to the fixture. This solved the heating problem.

To ensure turbulent flow over the foam panels, a "trip strip" of spheres was placed across the wedge leading edge. This strip was about four inches from the front of the model. The spheres were about 0.040 inches in diameter.

2.3 TEST PANEL DESCRIPTION

Sixty-two panels were tested of which 58 were CPR-421 foam, one was BX-250 foam and three were SLA-561s material. Table 1 shows each panel number, when it was made, its thickness, density and weight, with remarks. Some of the panels listed in Table 1 were not tested but were made for this series of tests and are shown here for documentation purposes only. All panels were made by Martin Marietta Corporation (MMC) and were 17 x 14 inches except panels 58, 59 and 60 which were 17 x 26 inches. The 17-inch dimension was always perpendicular to the flow direction. All panels were mounted on aluminum plates approximately 0.1 inch thick. The panel approximate thicknesses, including the aluminum plate, were:

- SLA-561s 0.50 in.
- CPR-421 1.0 and 1.75 in.
- BX-250 1.0 in.

Some of the panels had a machined surface; others were "net sprayed" or "as sprayed." Also some CPR-421 panels had a white vinyl coating, designated v-445. All the SLA-561s panels had a white silicone coating, DC 92-007. Some of the foam panels had "knit" lines. These are seams that were caused by the overlapping of the spray pattern as the material was being made. On the vehicle the foam will be sprayed directly onto the tank using a number of sprayer heads mounted on a rack which moves up the outside of the tank as it turns. This results in an overlapping of layers of foam in what is known as the "barberpole" effect. Therefore the test panels need to have these same seams in them to determine how they may affect the foam recession characteristics. The orientation of these overlaps or "knit" lines with respect to the flow was the same for the tests as it will be on the vehicle in flight.

Figures 2 through 5 show some typical CPR-421 pretest photographs. Figure 2 is of a typical panel without knit lines. Figure 3 is of a typical panel with knit lines. Figure 4 shows a panel with small holes in its surface apparently due to quality control problems in the spraying process. Figure 5 shows a typical "net-spray surface" panel. On these "net spray" panels it was not possible to get a very accurate initial or pretest thickness due to the roughness of the surface.

A question was raised as to the effect of the foam "curing" or "aging" on its recession characteristics during testing. That is, it may be that some of the panels were not fully cured at the time of testing. What effect this may have had on the foam performance is not yet known. NASA-MSFC is presently making a study of this effect. The age at time of testing of each panel is shown on subsequent post-test photographs in Section 3 (Results). For example, panel CTC1-67 was less than one week old when tested. It was made on 7 February 1975 and tested on 12 February 1975. Also it is noted that these panels were stored in plastic bags (not sealed) for protection during this curing time. Whether this affects the curing is also unknown at present.

2.4 TEST PROCEDURE

At the beginning of the tests the wedge fixture was installed on the tunnel sting inside the test section tank or airlock beneath the tunnel test section. The tunnel was started and brought up to the operating condition of $T_o = 1900^{\circ}\text{R}$ and $P_o = 1800$ psia. The first foam panel was installed on the wedge fixture and the wedge injected into the flow. After the proper test time the fixture was retracted and the foam removed and replaced with a new panel. This process was continued until all panels were run while the tunnel was operated in the continuous, closed-loop mode.

During the time while the wedge was actually in the flow, it was run either at a constant or at a variable angle of attack. The variable angle of attack cases were used to simulate the variation of heating rate with time for selected points on the Shuttle External Tank (ET) surface. Figures 6 and 7 show the two heating rate versus time histories used during the tests conducted on 20 January 1975. These time variations were designated trajectories 1 and 2, respectively. Trajectory 1 simulates the heating rate to ET Body Point 7065 during the first heat pulse during launch. Trajectory 2 simulates the same body point but for the entire 605 seconds of launch. Figures 8, 9 and 10 present the variations used during the tests of 12 February 1975. These are designated trajectories A, B and C, respectively. Trajectories A and C again simulate Body Point 7065 for the first heat pulse and total heat pulse, respectively. Trajectory B simulates the first heat pulse for Body Point 7105. The heating rates presented are for a location on the foam approximately three inches from the foam leading edge. The flight heating rates being simulated are for the "55 Nautical Mile AOA" trajectory for vehicle configuration 500.

At the end of the last series of tests (on 12 February 1975) two panels were tested at lower tunnel total temperatures as the tunnel was being cooled off for shutdown. The purpose of these two tests was to determine what effect enthalpy might have on foam recession/performance.

Also several panels were tested with a "vortex generator" on the surface of the stainless steel leading edge part of the wedge. The location and size of this "vortex generator" is shown on Fig. 11. Two heights were used: 1/2 and 5/8 inch.

Two panels, one CPR-421, and one SLA-561s, were tested with a "shock generator" protruding through the panel. This configuration is shown in Fig. 12.

Table 2 gives the test run log for all tests.

2.5 DATA TAKEN

2.5.1 Environments Data

During the time of planning for these tests, predictions were made of the expected values of pressure, heating rate and shear. The results of this work are presented and are compared with measured values in the Results section of this report.

For the first series of tests (6 January 1975) a Stycast calibration slab was made for use in measuring the heating rates to the wedge surface where the foam panels were to be placed. This slab had five Gardon gage type calorimeters and two pressure taps installed in its surface. The reason for using the Stycast slab was to be able to get a good distribution of heating rates over the entire surface, not just the values at the five calorimeter locations. However, very little heating rate data were obtained during this first series of tests because this Stycast slab cracked around the mounting inserts which were cast into it for holding it onto the wedge fixture. This cracking was apparently due either to thermal stresses or to excessive torquing of the mounting studs, or perhaps due to some of both effects. To remedy this situation, a steel plate was made and the calorimeters and pressure taps installed in it. This worked satisfactorily and the required data were obtained. Figure 13 shows the dimensions, measurements, locations, etc., for these models.

2.5.2 Foam Panel Data

The data taken on the foam panels are divided into two categories: (1) qualitative and (2) quantitative. The qualitative data consisted of TV camera coverage (recorded on video tape for on-the-spot playback), 16 mm color movie coverage, and on-site observation by the Test Engineers monitoring the tests. Figure 14 shows a photograph of the test setup on the Tunnel "C" test section with each of the camera locations. The personnel observation area is located on the deck or catwalk over the test section, where there are two top windows about the same size as the side windows. The quantitative data obtained consisted of pretest and post-test thicknesses and time variation of the foam surface recession. This time varying recession was obtained using a simple but ingenious "grid-line" system developed by ARO/AEDC especially for these tests. This system is illustrated in Fig. 15, and consists of a 35 mm slide projector which projects lines onto the foam surface at an angle of about 45 degrees, and a 70 mm sequenced camera viewing the foam from above. As the foam recedes, the grid lines are displaced in the camera view (see detail A of Fig. 15). The amount of displacement or translation of the grid lines in the camera view can be related to the amount of actual surface recession if the required geometry and dimensions are known. The 70 mm sequenced camera takes pictures at known times (either 1 or 2 second intervals) and from the resulting photos the recession versus time curve can be obtained. In the actual practice of the data reduction, the geometry was not used but instead "tare shots" were made using a metal panel in place of foam which could be lowered to given "recession" depth locations. It was placed at given locations and the 70 mm sequenced camera fired to obtain the translation to recession ratio. This factor was then non-dimensionalized by dividing by the model span on the projected picture. This allowed the scale factor to be used with any projector which became quite useful because different viewers were used in the data reduction process. This resulted in different size models on the screen and different amounts of measured translation for a given recession on the actual foam surface. Figure 16 shows a plot of projected line scale factors from the tare shots versus wedge angle. It is noted that a set of tare

shots and scale factors were needed for each of the three series of tests since the camera, projector and model were moved after each test and not necessarily set back up in their original positions. The inflection points in the curves of Fig. 16 are apparently due to the complex motion of the surface of the foam as the sting mechanism articulates to achieve the different wedge angles. The accuracy of this grid line recession measurement is estimated by ARO/AEDC as being about 10 to 20%. Some difficulty was experienced in reduction of the data when there was a very minute amount of recession due to the "fuzz" on the projected lines being about the same as the recession. However, this system of measurement was, in general, very useful in determining what was happening to the foam during the test, especially in the "streaks." Figure 17 shows how the grid lines appear on the foam samples as mounted in the test position in the tunnel.

Section 3 RESULTS

3.1 ENVIRONMENT PREDICTION AND MEASUREMENT RESULTS

The environments predicted analytically for these tests are shown in Figs. 18, 19 and 20. These plots are of the turbulent heating rate (cold wall and hot wall), local static pressure on the wedge, and aerodynamic shear on the wedge surface, all versus distance along the wedge for different wedge surface angles. The heating rates were predicted using the Lockheed-Huntsville Multiple Pressure Gradient Program (Ref. 3). The flow was assumed turbulent due to the use of the trip spheres on the leading edge. The local pressures were predicted using the methods/tables of Ref. 4. The shear values were predicted using a modified Reynolds Analogy and the calculated heating rates. The values shown are for tunnel total conditions of 1900°R and 1800 psi.

For comparison with measured results, heating rates and pressures were plotted versus δ for fixed X locations corresponding to the Gardon gage calorimeter and pressure tap locations. Shear is also shown in this form although no shear measurements were made. These results are shown on Figs. 21, 22 and 23. Also shown on Figs. 21 and 22 are the measured values. The measured values are converted from the gage wall temperature to the "cold wall" temperature of 460°R . As seen, the agreement is good at the higher angles. However, at a wedge angle of 6 degrees the flow apparently was transitional rather than fully turbulent because the measured heating rate value was below the predicted turbulent level. The predicted laminar flow values are shown on Figs. 24 and 25.

The predicted heating rates and shear for the low temperature/low enthalpy ($T_0 = 1540^{\circ}\text{R}$) runs are also shown in Figs. 24 and 25, respectively.

The pressures for these cases are the same as for the high temperature runs because the total pressure was the same.

The local Reynolds number per foot for the 1900°R and 1540°R runs are shown as a function of δ in Fig. 26. The boundary layer velocity thicknesses along the wedge surface for various δ values are shown for the 1900°R and 1540°R runs are shown on Figs. 27 and 28, respectively. Figure 29 shows the recovery enthalpy and temperatures as a function of δ for the two run conditions; these values were obtained from ARO/AEDC. Figure 30 shows a typical shadowgraph.

3.2 FOAM PANEL RESULTS

The panel test results are divided into two categories — qualitative, i.e., pictures and observations, and quantitative, i.e., measured values of recession and streak width.

3.2.1 Qualitative Results

The post-test photographs of the various panels are divided into two categories, constant wedge angle runs and trajectory runs rather than in the order in which they were tested. The reader is referred to the run log (Table 2) for a complete listing of all runs made. The constant wedge angles used were: $\delta = 9, 12, 18, 20, 23.5$ and 38 degrees. As mentioned earlier the trajectory heating simulations were designated 1, 2, 3 and A, B and C.

To familiarize the reader with what he will be seeing in subsequent photographs, Fig. 31 is presented at this point. This is an overview of the wedge fixture retracted into the Tunnel "C" test tank with a foam sample still mounted in place. Note that the streaks in this sample are quite pronounced.

Figure 32 is shown to illustrate the overlay of tare shot grid lines with grid lines on the receding foam surface.

Typical constant-wedge-angle run panel photographs are shown in Figs. 33 through 55. The test group number (which is the same as the run number), the sample number, the test condition, heating rate, pressure and shear, test time, and remarks with the panel description are given with each photograph. Most photos were made after the tests and after the panels had been removed from the wedge fixture. However, some of the photos are taken from the 70 mm sequenced camera negatives, for example Fig. 33, because post-test photos were not made of all panels.

A 9-degree wedge angle case panel is shown on Fig. 33. Not much happened to this panel except that it "popcorned" early in the test, perhaps even before being inserted into the tunnel due to the low pressure in the test tank.

Figures 34, 35 and 36 show several 12 degree wedge angle cases. The panel of Fig. 34 seemed to perform better than the other panels shown except for the two large chunks which came out during or after retraction. The reason for this better performance is not really known, perhaps panel CTC1-11 was worse because of its lower density (1.85 lb/ft^3 versus 2.29 lb/ft^3 for panel CTC1-5). Also the knit lines of panel CTC1-12 (Fig. 36) caused it to perform worse than the panel of Fig. 34.

Several 18-degree wedge angle cases were selected for presentation here and these are grouped in Figs. 37 through 47. The panels of Figs. 37 through 40 experienced the streaking problem mentioned earlier in this report. These streaks are clearly seen in the post-test photos. The development and growth of these streaks seems to be, in general, a random process. They may appear at various times in the run and at various locations on the sample surface. They usually start after the initial char layer has had time to build up and start to protect the underlayers of material. Then suddenly a streak will appear and start to grow toward the downstream edge of the sample. They usually grow in both depth and width and grow quite rapidly until a certain size is reached and then tend to slow down or completely stop

growing. For the reader who is interested in further insight on the development of these streaks, both movie film and TV video tape are available from essentially all the tests conducted.

Figures 41 and 42 present additional 18-degree wedge angle cases but with the "vortex generator" in place on the forward stainless steel leading edge of the wedge fixture upstream of the foam. (See Fig. 11 for details of this set-up.) The peculiar thing about these two panels is that the first tested (Fig. 41) did streak behind the vortex generator while the second panel (Fig. 42) did not streak behind the vortex generator but off to the left side of it. This is not explained at the present time. It was felt before the tests that perhaps some flow disturbance might be contributing to the streaking phenomena. Therefore, this type test was suggested to check that possibility. However, since observing the results of the tests it is apparent that flow disturbances are not the primary cause of the streaks.

Figure 43 shows a long panel tested at an 18-degree wedge angle. This panel was 17 inches wide and 26 inches along the flow direction whereas the other panels were 17 x 14 inches. The reason for testing this configuration was to see just what happens to the streaks as they grow farther downstream. From the 14-inch panels of the initial tests it was seen that the streaks grew wider and deeper as they proceeded along the panel length. The questions which naturally arose were:

- "What is going to happen on the vehicle where we have many feet of panel for the streaks to run down"?
- "Do they continue to grow until they wipe out the foam completely — or just what will happen?"

After testing this panel it is seen that the streaks did continue to grow wider and deeper as they proceeded all the way to the back edge of this 26-inch panel. This points up the real need for further tests of still bigger panels to further study this problem. (In the quantitative results section a plot of streak width and depth versus distance is presented to graphically show this

problem.) Also this long panel had a number of knit lines coming through to the surface. It had been suggested that perhaps these knit lines, being a higher density material than the rest of the foam, might help retard or slow down the streak growth rate. However, this effect was not observed in this test — or in any of the tests for that matter. The streaks just "walked" right on through the knit lines.

Results of one of the low temperature/low enthalpy run are shown in Fig. 44. There was a noted difference in the performance and appearance of this panel from those tested at the higher temperatures. Very little if any surface recession occurred, and the "char" color was light brown as opposed to almost black for the higher temperature runs. (For comparison purposes the recovery enthalpy for this test was about 320 Btu/lb as opposed to 420 Btu/lb for the higher temperature runs.) This panel "popcorned" some near the knit line and tried to streak in some locations.

Results of the run with the shock generator are shown in Fig. 45. This was a very dramatic test. This shock generator configuration created a very severe pressure gradient across the normal shock ahead of its upstream side. The result was that the foam receded through to the aluminum backup plate very rapidly and the cavity in the foam ahead of the cylinder could be seen proceeding forward during the test. In connection with this test calculations were made to determine the actual severity and magnitude of the pressure gradient across the shock. Results of this are shown in Fig. 46. The wedge shock and cylinder bow shocks are shown with the calculated pressures in front of and behind these shocks. The pressure behind the normal shock on the foam surface is about 18.2 psi while that in front of the shock is only 0.78 psi. This large pressure gradient feeds upstream through the subsonic portion of the boundary layer causing a reverse flow which quickly chews out the foam. This problem is not expected to be as severe on the vehicle even in the regions of attachments, protuberances, etc., because the boundary layer on the vehicle in most locations will be much thicker than in this test. However, the general effect of this type problem was well illustrated by this test, showing the need for a "hard" ablator in such regions.

Figure 47 shows a similiar test result with a shock generator but with the SLA-561s material. This test was not as dramatic as with the CPR-421 material but the panel did burn through to the aluminum, and large chunks came out. This panel also had "built-in" defects or cracks in the SLA-561s that went through to the aluminum. The shock generator would probably not have had as much of an effect on the material response if the defects had not been present.

The only BX-250 sample tested is shown in Fig. 48. As seen, this material receded all the way through to the aluminum in several places. Its recession rate was significantly greater than any of the CPR-421 samples. Note also that the BX-250 surface had a distinct diamond shape pattern on it. This same type pattern has been observed on many other ablative material surfaces in previous tests and development programs and is known as "cross hatching."

Three 20-degree wedge angle cases are shown in Figs. 49, 50 and 51. The first two are without knit lines and the last figure has one knit line. Again the streaks are quite pronounced in these tests. In Fig. 51 the streaks only occurred downstream of the knit line. Figure 49 shows some remains of the Tempilaq coating stripes. This was used in an effort to determine the foam surface temperature. It was not really conclusive as to what was happening to the Tempilaq during the run. To one observer it seemed to melt and disappear almost instantly after injection but to this writer it was not that clear whether it was melting or blowing away. Anyway, this did not prove to be a very satisfactory way way to measure the foam surface temperature. It is recommended that a non-contact infrared thermometer (similiar to the one presently being used by MMC (Ref. 5) be used in future tests to try to measure surface temperature. Incidentally, it was not mentioned in the test measurement section but an attempt was made to use a pyrometer to measure foam surface temperature in some of the early tests; this did not yield any data because its range was too high.

Figures 52, 53 and 54 show the results of some 23.5 degree wedge angle runs. The panel of Fig. 52 did not streak but most of the char layer was lost

on retraction. The panel of Fig. 53 had a knit line and there was a vast difference in the response of the foam upstream and downstream of the knit line. The foam did streak downstream of the knit line, and there was some "popcorning" at the knit line. The panel of Fig. 54 did not streak like the one of Fig. 53, but seemed to have a large number of small streaks that all ran together.

Figure 55 shows the only panel run at a wedge angle of 38 degrees. This panel receded very rapidly and only a thin sheet was left at the end of the run of about 10 seconds. This thin sheet delaminated from the aluminum and was blown away (except for the leading edge part as seen in Fig. 55) on or immediately after retraction from the tunnel. However, it is pointed out that the heating rate in this case was quite high — about $16 \text{ Btu/ft}^2\text{-sec}$ — which is higher than that expected in areas of the vehicle where CPR-421 will be used. This run was made to determine if the CPR-421 could have possibly been used in these high heating areas, and it does not look feasible after seeing the results.

Some of the vehicle trajectory heating simulation run results are shown in Figs. 56 through 69. These are grouped in the following order: trajectories 1, 2, A, B and C. (Also see Figs. 6 through 10 for the time history of each of these trajectories.) The trajectory 1 cases are shown on Figs. 56, 57 and 58. The first two of these panels had no knit lines, the third did have a knit line. All three panels streaked but the streaks did not go all the way through to the aluminum backup plate. It is noted here that there was a thin layer of foam adjacent to the aluminum which appeared to be a higher density, stronger material than most of the panel. It is possible that this "rind" may have prevented the streaks from reaching all the way to the aluminum. These panels were all one-inch thick — including the 0.1-inch aluminum. Figure 58 also illustrates a type of streak which resembles a feather in that it grew somewhat laterally as well as longitudinally. (This is the third streak from the right on this panel.) This type streak appeared on a number of the panels throughout the test program. Note also on this panel that the streaks did not

occur just behind the knit line but upstream of it and grew right on through the knit line.

Figure 59 shows the remains of a panel which was to have been tested for a full 600 second trajectory 2. However, the test was cut short during the long low heating time to be simulated. It is noted that this simulation was not necessarily representative of the flight during the periods between the first and second heat pulses because although the heating rate and pressure are about the same as in flight the shear is higher than on the vehicle. This causes a lot of "buffeting" of the foam. The foam also seemed to swell laterally quite a bit also in some of these long trajectory runs, possibly causing the loss of chunks of material from the sides of the panel as the foam projected itself over the sides of the wedge fixture and caught the flow. This swelling laterally was also observed in the other long trajectory tests (trajectory C), discussed later. Another possible cause of the loss of such large chunks on this panel (Fig. 59) was the heating up of the aluminum backup plate from heat being conducted into it from the wedge fixture during these long run times. The bottom of the wedge was at about a 30 degree angle of attack when the foam was at 0 degree angle of attack. This heating caused the wedge to get very hot and this may have heated up the aluminum, causing debonding of the foam. This problem was eliminated before the last series of tests (12 February 1975) by adding water cooling to the wedge fixture. No debonding was observed on the trajectory C cases which ran over 600 seconds.

Figures 60 through 67 show some typical trajectory A run results. The first three panels show a comparison of surfaces. These panels' surfaces are: (1) as-sprayed; (2) machined and coated, and (3) as-sprayed with a coating in Figs. 60, 61 and 62, respectively. All three panels were nominally 1-3/4 inch thick initially. Qualitatively speaking the as-sprayed surfaces seemed to hold up better than the machined surfaces. That is, by watching the tests and reviewing the movies the as-sprayed surfaces seemed to have a heavier, thicker, glossy-black char layer which held up and protected the underlying foam better than the machined surface panels. However, the quantitative comparison of the

measured recession (discussed later) did not necessarily show that the as-sprayed samples were better. This was partly due to the difficulty in obtaining an accurate initial thickness of the as-sprayed surfaces due to their roughness and waviness. Also, these as-sprayed panels did not seem to streak as severely as the machined panels. The effect of the coating was that it seemed to hold the surface together better early in the test and then the surface started coming out in "flakes" but the overall response was about the same with and without the coatings.

Figure 63 shows a panel which failed apparently due to a pressure build-up between the foam and the aluminum backup plate. This panel was not sprayed directly onto the aluminum plate used in the test. It was sprayed, removed, trimmed and then bonded to this plate. This was necessary to obtain the desired initial thickness since the spray process does not always give the desired "rise" thickness. This is called a "secondary bond" and all panels having this are noted in Table 1. (Note the knit lines exposed in the foam where the "plug" came out in Fig. 63.)

Figure 64 is a CPR-421 panel which had built-in defects to see what affect these might have on the foam recession and streaks. Three panels similar to this were tested. They were made by breaking the foam into four pieces and then bonding them to the aluminum. When these panels were injected into the flow, the swelling of the foam tended to close and "heal" these cracks. The first panel tested did not streak at the crack (Group 56). The second and third panels (Groups 57, 58) had a streak which followed the cracks. The third panel (Group 58) had a knit line and "popcorned" excessively with the streaks forming mostly from the "popcorned" areas. It did not seem to be affected by the defect cracks.

Figures 65 and 66 show results of an attempt to determine the effects of the vortex generator, situated on the wedge leading edge, on the foam and the streaks. Again the results are not too conclusive, because one of these started streaking in a location not directly behind the vortex generator. However, both had streaks which were behind the vortex generator.

Figure 67 shows an SLA-561s panel tested with defects. The defects seemed to have little or no effect on the panel. It did not look much different after the test than before.

A trajectory B simulation panel is shown on Fig.68. This was an as-sprayed panel 1-3/4 inches thick. It held up quite well in this reduced heating environment. It has a glossy black char layer much like that seen for the as-sprayed panels tested using trajectory A.

A trajectory C run panel is shown on Fig.69. This panel was 1.0 inch thick with the aluminum and it held up very well for this long heating situation (over 600 seconds). It did not burn through to the aluminum. It had a machined surface and was coated. Needless to say, the results of this run were very encouraging — to see less than one inch of foam survive a Body Point 7065 full heating simulation while about 2 inches will be applied on the vehicle.

3.2.2 Quantitative Results

Results of the data taken and reduced from the "grid line" system are presented in this section. Recession was measured for each panel which was run at constant heating rate levels. The measured recession was then plotted versus time and a slope was taken to obtain a recession rate. Four grid lines were used on most panels giving data at four slightly different heating rate and shear levels. The changes in wedge angle gave the major change in heating rate. These recession rates were then used to plot the values seen on Figs. 70 through 83.

Two types of recession were measured, average minimum recession and recession in the streaks. The minimum values were taken at a location along the width of the panel where there was only flat foam, i.e., no streaks. When a streak developed, the recession to the bottom of the streak was also measured. Results of these measurements were plotted versus both cold wall and hot wall heating rates as seen in Figs.70 through 73. The heating rates used in the plots are to a smooth flat surface, not the heating rate inside

the streak since there is no way to measure this. The cold wall heating rates used in these plots were based on $T_w = 530^\circ\text{R}$ to be consistent with the way the Langley $M = 10$ data were presented. Least squares fit curves were determined for all these curves. However, due to the scatter in the data, some of these curves had a negative slope. The curve fits were presented on the plots when they had a positive slope, and where the slopes were negative they were omitted. It is also noted that some of the panels that were run at the lower heating rates experienced swelling (negative recession) during their tests. Recession rate values for these cases are presented for completeness below the lower margin on the log-log plots, for example, Groups 77, 27 and 6 on Fig. 70.

As seen on these recession rate curves, there is a lot of scatter in the data. Efforts were made to reduce this scatter by reviewing the data in an attempt to determine if the "grid line" system accuracy was the cause of this. It was decided that the scatter is due to the random foam response more than to accuracy of the system.

An effort was also made to determine if distance along the foam panel length made a difference in the recession rates. Results of this are shown in Figs. 74 and 75. Figure 74 is for a distance of two inches from the trailing edge while Fig. 75 is for a distance of about five inches from the trailing edge. (A limited amount of data was available at constant locations because the "grid-lines" or shadows move as the sting changes angle of attack.) From these plots it is not obvious that location along the panel affects the recession rate or causes the scatter.

Similiar plots were also made for streak width rate versus heating rate as seen in Figs. 76 and 77. This is the rate at which the streaks are growing in width. Again a large amount of scatter is present in the data. Figures 78 and 79 present the effect of panel location on these results. Figure 78 is for a distance of two inches from the trailing edge and Fig. 79 is for a location of about five inches from the trailing edge. Again it is not apparent that panel location has any effect on streak width rate.

The streak data are also presented in the form of streak depth versus distance along the streaks for a constant time for several panels. These results are shown on Figs. 80 and 81. In general the streaks get deeper as they proceed toward the rear of the panel as expected, although there are a few exceptions, for example, Group 64.

Figures 82 and 83 show still another form of the streak data, that is, streak depth and width versus time. Both these curves are for a location on the panels of about two inches from the trailing edge. Some of the streaks seem to decrease in growth rate as time increases while others do not.

Figure 84 presents an attempt to correlate time to start streaking versus heating rate. Here again there is a lot of scatter in the data but it is concluded that if the heating rate is about $5 \text{ Btu/ft}^2\text{-sec}$ then the time to start a streak is long (100 seconds or more) almost as long as the time of the first heat pulse on the vehicle.

3.3 COMPARISON OF AEDC DATA WITH OTHER FACILITY DATA ON CPR-421 FOAM

Figures 85 and 86 present comparisons of this AEDC Tunnel "C" data with Langley Arc Jet Facility, and Langley Mach 10 Continuous Flow Hypersonic Tunnel data and the Martin "design" curve. Both average minimum recession and recession in the streaks are presented. It is seen that, within the scatter, the data agree reasonably well. Also the Martin "design" curve appears to be conservative.

3.4 FOAM 'ABLATION' PRODUCTS CONTAMINATION EFFECTS

Figure 87 shows two Tunnel "C" sting adaptor sections which were exposed to the foam ablation products. The deposits resulting from these products can be seen on these sections by noting the one on the right where the deposits were scraped off. These removed deposits were taken by MMC to their labs for analysis. For further information on these results the reader is referred to the MMC Project Engineer, Steve Copsey.

Section 4

CONCLUSIONS AND RECOMMENDATIONS

The following conclusions are drawn from the results of these tests:

- The CPR-421 foam definitely has better recession characteristics than the BX-250 foam.
- There is a lot of scatter in the CPR-421 foam recession response.
- A one-inch thick foam panel withstood the simulated total heat pulse for Body Point 7065 on the ET LOX tank without burning through.
- There are still quality control problems in producing the CPR-421 panels.
- The streaking problem is not caused by flowfield disturbances.
- Pretest defects (cracks) in the CPR-421 foam panels did not necessarily cause any detrimental effects on the foam performance.
- The "shock" generator caused a rapid burn-through of the foam, but this simulation is much worse than that expected on the vehicle.
- The "as-sprayed" panel surfaces apparently held up better than the machined surfaces.
- The panel surface coatings did not significantly affect the overall foam performance.
- Panel age effects were not determined in these tests.
- The SLA-561s material survived these environments with little effects.

As a result of these tests it is recommended that the following actions be considered:

- Expose the panels in future tests to a vacuum environment before testing to see if this will eliminate "popcorning."

- Perform additional tests to determine the effects of aging on foam performance.
- Conduct tests on longer panels to determine whether the streaks continue to grow wider and deeper down the panel and vehicle.
- Develop better simulation to determine the effects of shocks on the foam.
- Study the effects of additional wall cooling (nearer cryogenic temperatures) on foam performance.

REFERENCES

1. Arnold Engineering Development Center, Test Facilities Handbook -- Tenth Edition, Arnold Air Force Station, Tenn., May 1974.
2. Matthews, R.K., "Experimental Investigation of Water Ejection from a Wedge Model at Mach Number 6," AEDC-TR-71-26, ARO, Inc., Tullahoma, Tenn., April 1971.
3. Blackledge, M.L., and C.J. Wojciechowski, "Real Gas Multiple Pressure Gradient Heating Rate Program," LMSC-HREC A783781, Lockheed Missiles & Space Company, Huntsville, Ala., May 1967.
4. Ames Research Staff, "Equations, Tables and Charts for Compressible Flow," NACA R-1135 (1953).
5. IR Industries, Inc., "Thermodot[®] Model TD-17 Non-Contact Infrared Thermometer," Brochure IR 1972, Santa Barbara, Calif.
6. Dean, W.G., "Results of Tests of CPR-421 Foam in the Langley Mach 10 Continuous Flow Hypersonic Wind Tunnel," LMSC-HREC TM D390678, Lockheed Missiles & Space Company, Huntsville, Ala., February 1975.

Table 1
 DESCRIPTIONS OF PANELS USED IN THIS TEST PROGRAM

Model	Batch	Av. Thickness		Size (in.)	Material	Density (lb/ft ³)	Panel Wt. (gm)	Remarks	
		L/E**	T/E**						
CTC1-	1	12-10-74	0.952	0.954	14 x 17	CPR-421	2.03	1187	Many Small Holes
	2	12-10-74	0.950	0.950			2.09	1182	
	3	12-16-74	0.941	0.940			2.15	1112	
	4*	12-9-74	0.963	0.953			2.31	1210	
	5	12-7-74	0.955	0.964			2.29	1185	
	6	12-7-74	0.962	0.965			2.26	1188	
	7	12-14-74	0.962	0.964			1.95	1172	
	8*	12-9-74	0.958	0.959			2.30	1213	
	9	12-14-74	0.957	0.951			1.97	1181	
	10	12-14-74	0.944	0.943			2.03	1174	
	11	12-14-74	0.963	0.941			1.85	1176	
	12*	12-9-74	0.966	0.969			2.28	1203	
	13	12-14-74	0.961	0.958			2.03	1179	
	14	12-14-74	0.939	0.929			1.89	1173	
	15	12-14-74	0.956	0.958			1.93	1167	
	16*	12-9-74	0.958	0.900			2.14	1194	
	17	12-14-74	0.964	0.955			2.03	1192	
	18	12-14-74	0.967	0.935			2.03	1178	
	19	12-14-74	0.967	0.944			2.00	1194	
	20*	12-9-74	0.962	0.957			1.97	1197	
	21	12-14-74	0.948	0.950			1.95	1177	
	22	12-14-74	0.949	0.951			1.97	1167	
	23	12-14-74	0.954	0.953			2.08	1184	
	24*	12-9-74	0.965	0.986			2.22	1202	
	25	12-14-74	0.965	0.945			2.03	1169	
	26	12-14-74	0.953	0.946			1.99	1183	
	27	12-14-74	0.967	0.956			1.96	1181	Coated v-455
	28*	12-9-74	0.958	0.941			2.14	1198	
	29	12-16-74	0.966	0.954			2.10	1188	
	30	12-16-74	0.960	0.942			1.99	1191	
	31	12-16-74	0.969	0.970			2.01	1194	
	32*	12-9-74	0.970	0.967			2.28	1203	
	33	12-16-74	0.968	0.966			2.07	1197	
	34	12-16-74	0.944	0.948			2.09	1187	
	35	12-16-74	0.965	0.960			1.86	1177	
	36*	12-9-74	0.968	0.967			2.55	1118	
	37	12-16-74	0.957	0.955			2.03	1195	
	38	12-14-74	0.952	0.950			1.86	1175	Coated v-455
	39	12-16-74	0.956	0.955			2.21	1198	
	40*	12-9-74	0.953	0.922			2.50	1213	
	41	12-16-74	0.956	0.966			2.04	1185	
	42	12-16-74	0.942	0.957			2.07	1188	
	43	12-14-74	0.956	0.952			1.86	1175	
	44*	12-9-74	0.960	0.941			2.43	1211	Coated v-455
	45	12-16-74	0.964	0.960			2.10	1189	
	46	12-16-74	0.966	0.966			2.21	1192	Broken + Coated Broken + Coated Broken + Coated
	47	12-16-74	0.960	0.960			1.99	1193	
	48*	12-9-74	0.970	0.966			2.56	1210	
	49	12-16-74	0.961	0.967			2.23	1190	
	50	12-16-74	0.966	0.965			2.09	1184	Coated v-455
	51	12-16-74	0.962	0.965			2.21	1193	
	52*	12-9-74	0.956	0.957			2.08	1206	Coated v-455
	53	12-14-74	0.962	0.967			1.86	1173	
	54	12-16-74	0.948	0.942			2.03	1184	
	55	12-16-74	0.957	0.965			1.98	1186	
	56	12-16-74	0.927	0.938			1.98	1189	
	57*	1-11-75	1.745	1.747			17 x 26	2.30	1103
	58*	1-11-75	1.746	1.742	2.22			1297	
	59*	1-14-75	1.242	1.243	2.17			2333	
	60*	1-14-75	1.247	1.249	14 x 17		2.17	2308	Primary Bond Primary Bond Secondary Bond Sec. Bond v-455 Coated Sec. Bond
	61	2-3-75.1	1.57	1.39			2.62	1331	
	62	2-3-75.2	1.64	1.69			2.45	1350	
	63	2-3-75.3	1.45	1.37			2.28	1388	
	64	2-3-75.4	1.55	1.13			2.28	1415	
	65	2-3-75.5	1.59	1.75			2.35	1431	

* These panels have knit lines.

** L/E = leading edge, T/E = trailing edge.

Table 1 - (Continued)

Model	Batch	Av. Thickness		Size (in.)	Material	Density (lb/ft ³)	Panel Wt. (gm)	Remarks
		L/E	T/E					
CTC1-66	2-3-75.6	1.57	1.80	14 x 17 ↓	CPR-421	2.30	1434	Sec. Bond v-455 Coated
↓ 67	2-7-75.3	1.700	1.695		↓	2.27	1300	Primary Bond
↓ 68	2-7-75.2	1.676	1.682		↓	2.33	1352	Pri. Bond v-455 Coated
↓ 69	2-7-75.1	1.700	1.680		↓	2.34	1297	Primary Bond
BTC1- 1	6-174-	0.960	0.967		BX-250	2.30	1215	
↓	44181-A/ L896128							
↓ - 2	"	0.961	0.968			2.34	1218	
↓ - 3	"	0.960	0.967			2.25	1218	
↓ - 4	"	0.964	0.967			2.25	1220	
STC1- 1	MTPS 110	0.5356	-		SLA-561s	15.9	1650.0	Sprayed 1/29/75
↓	111				↓			
↓	113							
↓ - 2	MTPS 110	0.5354	-			16.0	1630.2	Sprayed 1/29/75
↓	111							
↓ - 3	MTPS 110	0.5277	-			16.0	1610.5	Sprayed 1/29/75
↓	111							
↓	113							

Table 2a
AEDC TUNNEL 'C' ET/TPS MATERIALS TEST
RUN LOG FOR 6 JANUARY 1975

Contractor: Martin-Marietta
Representatives: Steve Copsey,
Bill Dean,
Zain Karu,
Raoul Lopez

Test Title: NASA/Martin Insulation
Project: V41C-91A
Test Personnel: R. K. Matthews,
Capt. Harper

Run/Gp	Configuration	Mach No.	P _o (psia)	T _o (°F)	α (deg)	δ (deg)	Time (CST)	Remarks
1	7000	10.0	1800	1440	-.26	—	2233	TPC = 200°F
2	7000	↓	↓	↓	-.26	—	2244	
3	7000	↓	↓	↓	+9.0	+18	0317	
4	1	↓	↓	↓	+9.0	↓	0018	
5	2	↓	↓	↓	+9.0	↓	0048	
6	4	↓	↓	↓	+9.0	↓	0040	
7	101	↓	↓	↓	+9	↓	—	BX-250
8	3	↓	↓	↓	+3.5	+23.5	0103	
9	5	↓	↓	↓	+15	+12	0110	
10	8	↓	↓	↓	+9	+18	0128	
11	6	↓	↓	↓	-11	+38	0133	TPC = 700

Table 2b

AEDC TUNNEL 'C' ET/TPS MATERIALS TEST RUN LOG FOR 20 JANUARY 1975

Contractor: Martin-Marietta
 Representatives: Steve Copsey
 Bill Dean
 Raoul Lopez

Test Title: NASA/Martin Insulation
 Project: V41C-91A
 Test Personnel: R. K. Matthews
 Capt. Harper

Run/Gp	Configuration	Mach No.	P _o (psia)	T _o (°F)	α (deg)	δ (deg)	Time (CST)	Remarks
12	7000	10.16	1800	1440	12.0	0.0	0128	-22 deg PB
13	GPSE				6.0	6.0	0133	
14					0.0	12.0	0143	
15					-3.0	15.0	0153	
16					-6.0	18.0	0200	
17					-8.0	20.0	0207	
18					-11.5	23.5	0214	
19					+3.0	90.0	0217	
20					-11.5	23.5	0223	
21					-11.0	23.0	0232	
22	8000				-8.0	20.0	0238	Gps. 27-28-29 taken in Model 1. Mode 2 starting Gp. 30 Painted Samples:* First Stripe from rear 932°F Second Stripe from rear 1100°F Third Stripe from rear 1300°F First Stripe to Front 1450°F
23	Pressure				-6.0	18.0	0243	
24					-3.0	15.0	0246	
25					0.0	12.0	0250	
26	(Samples)				6.0	6.0	0254	
27	10				0.0	12.0	0341	
28	11				0.0	12.0	0354	
29	12				0.0	12.0	0412	
30	14				-6.0	18.0	0428	
31	15*				-8.0	20.0	0440	
32	17*				-8.0	20.0	0451	Variable Wedge Run 1 Variable Wedge Run 1 Variable Wedge Run 1 Sample Failed Before Injection Variable Wedge Run 2 ±12 deg ~ 3 min. Gp.
33	20				-8.0	20.0	0458	
34	19*				-11.5	23.5	0508	
35	21*				-11.5	23.5	0514	
36	24				-11.5	23.5	0524	
37	22				Var.	Var.	0538	
38	23				Var.	Var.	0550	
39	32				Var.	Var.	0559	
40	57				-11.5	23.5	0612	
41	58				Var.	Var.	0644	
42	60				-6.0	18.0	0725	

*Painted with phase-change coating, "Tempilaq"

REPRODUCIBILITY OF THE
 ORIGINAL PAGE IS POOR

Table 2c

AEDC TUNNEL 'C' ET/TPS MATERIALS TEST RUN LOG FOR 12 FEBRUARY 1975

Contractor: Martin-Marietta
 Representatives: Steve Copsey
 Bill Dean
 Raoul Lopez

Test Title: NASA/Martin Insulation
 Project: V41C-91A
 Test Personnel: R.K. Matthews
 Capt. Harper

Run/Gp	Configuration	Mach No.	P _o (psia)	T _o (°F)	α (deg)	δ (deg)	Time (CST)	Remarks
43	67	10.16	1800	1440	Var.	A	2220	Remove Shims
44	62				Var.	A	2237	
45	68				Var.	A	2302	
46	64				Var.	A	2311	
47	66				Var.	A	2325	
48	61				Var.	A	2333	
49	63				Var.	C	2345	
50	63				Var.	C	2350	
51	65				Var.	B	0042	
52	69				-6	18	0053	
53	27				-6	18	0106	
54	38				Var.	A	0113	
55	40				Var.	A	0120	
56	46				Var.	A	0130	
57	47				Var.	A	0138	
58	48				Var.	A	0147	
59	31				Var.	B	0157	
60	33				Var.	B	0207	
61	42				Var.	B	0217	
62	44				Var.	B	0223	
63	51				-6	18	0229	
64	35				-6	18	0237	
65	37				-6	18	0744	
66	43				Var.	A	0253	
67	45				Var.	A	0303	
68	50				Var.	A	0316	
69	52				Var.	A	0322	
70	49				Var.	B	0329	
71	202				Var.	A	0339	
72	201				Var.	A	1350	
73	30				Var.	A	0408	
74	39				Var.	A	0413	
75	41				Var.	C	0423	
76	34				Var.	C	0520	
77	26				+3	9	0607	
78	29				+3	9	0616	
79	203				-6	18	0627	
80	36	10.16	1800	1080	-6	18	0795	Vortex Gen. on Sample
81	7	10.16	1800	1080	-11	23	0719	

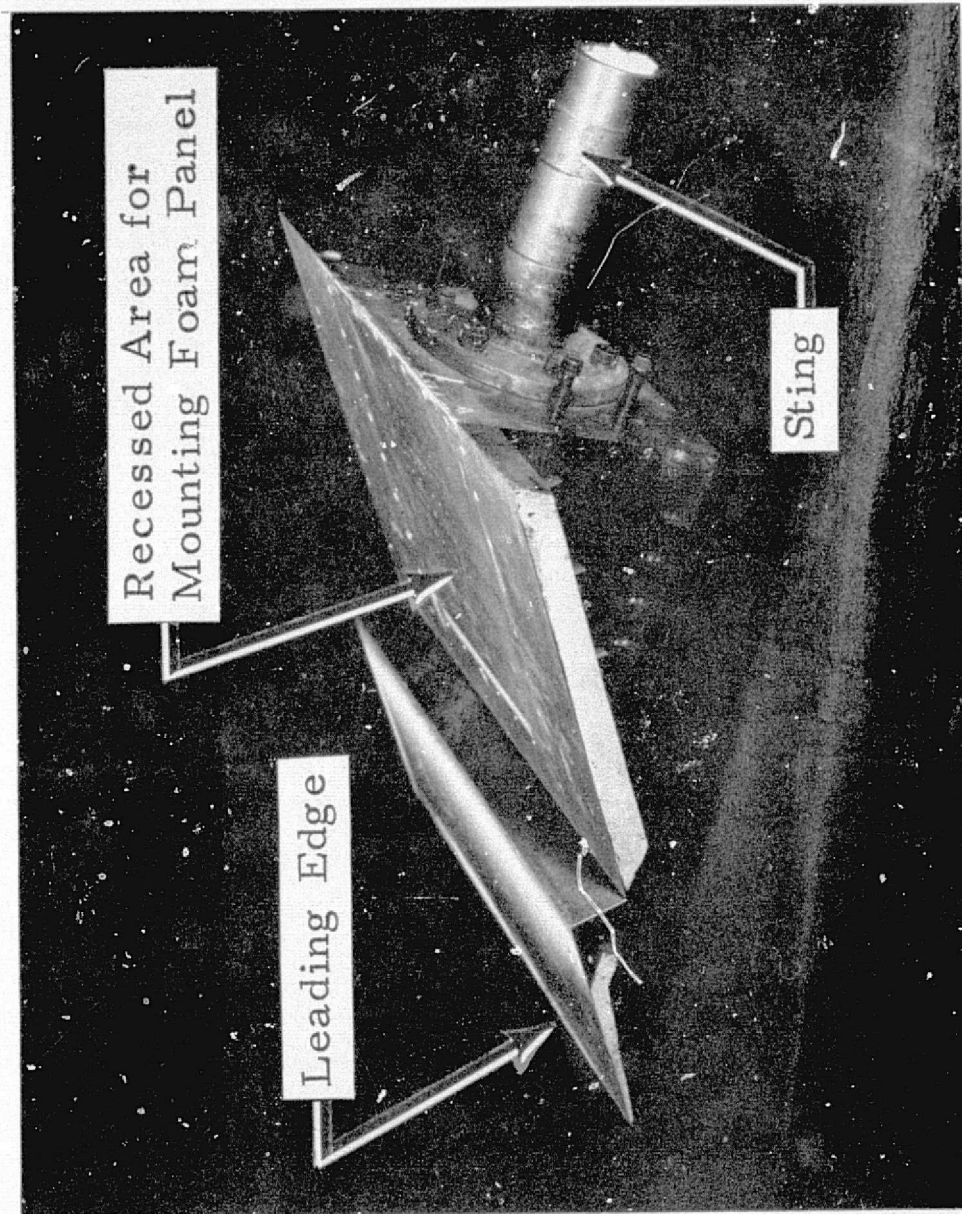


Fig. 1 - Steel Wedge Test Fixture Used for Holding Foam Panels During Tests

**REPRODUCIBILITY OF THE
ORIGINAL PAGE IS POOR**

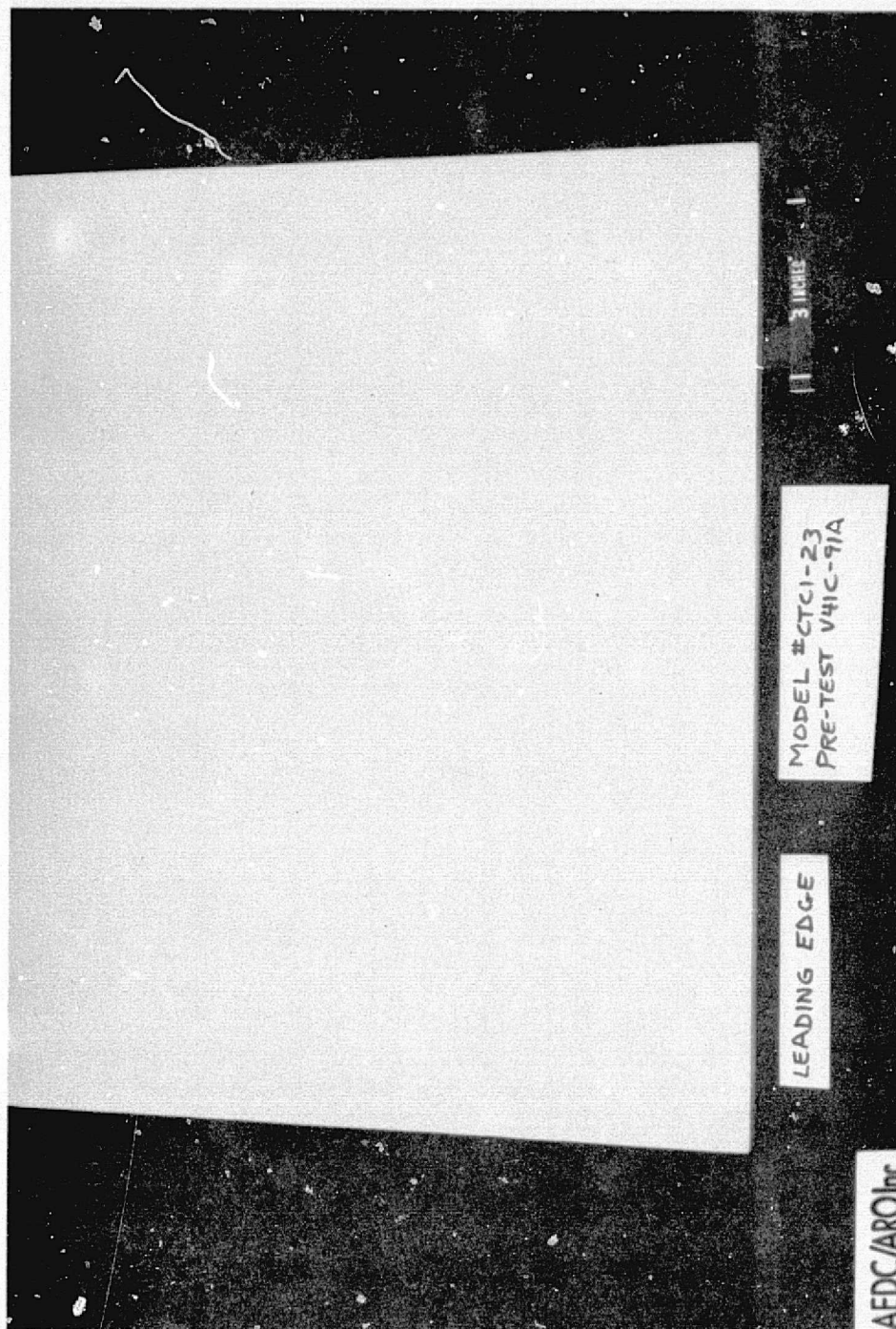


Fig.2 - Pretest Photograph of Typical CPR-421 Foam Panel Without Knit Lines

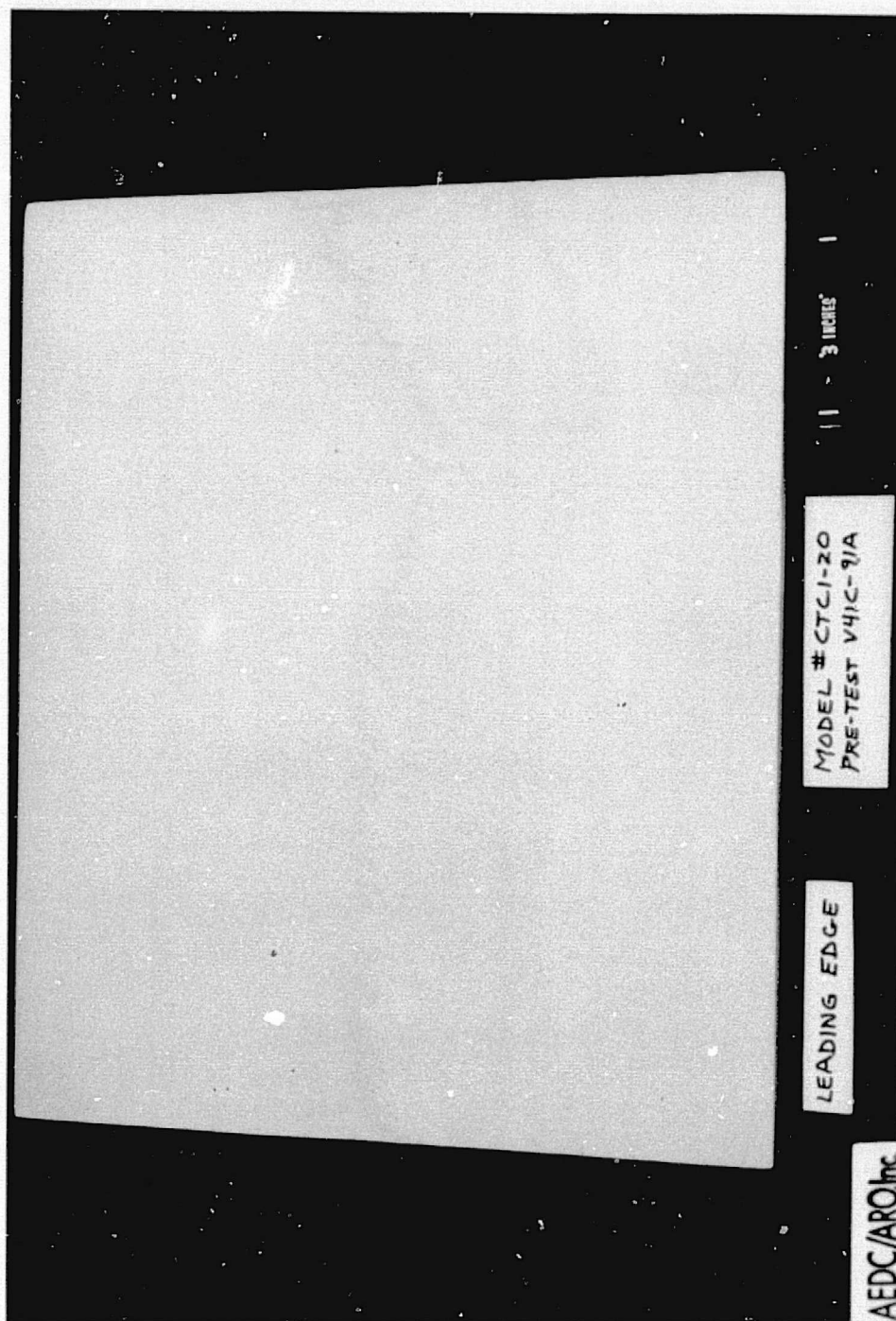


Fig. 3 - Typical Pretest Photograph of CPR-421 Foam Panel with Knit Line
(Near center of panel, running laterally)

REPRODUCIBILITY OF THE
ORIGINAL PAGE IS POOR

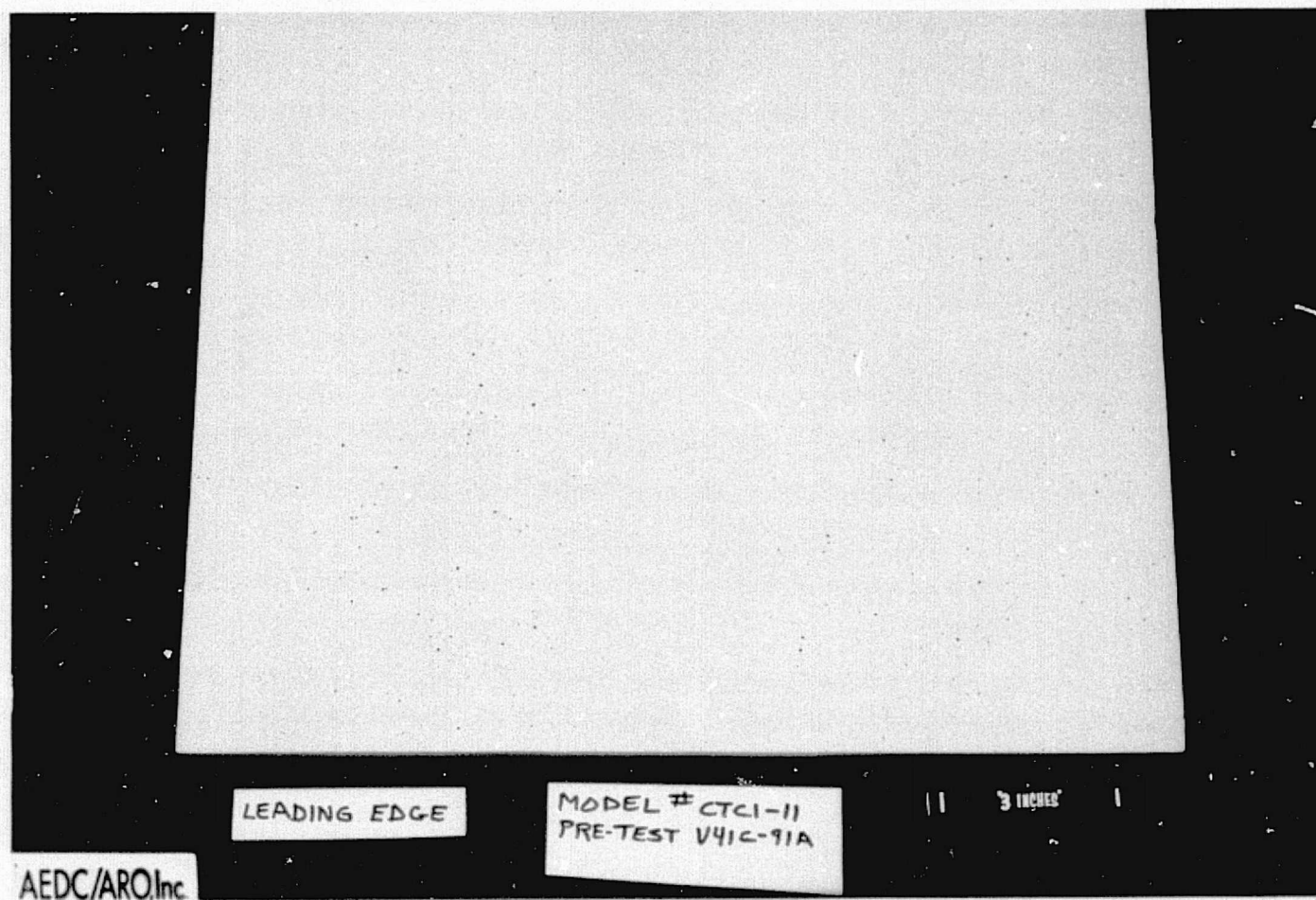


Fig. 4 - Typical Pretest Photograph of CPR-421 Foam Panel
with Small Voids or Holes in Surface



Fig. 5 - Typical Pretest Photograph of CPR-421 Foam Panel with "As-Sprayed" or "Net-Spray" Surface

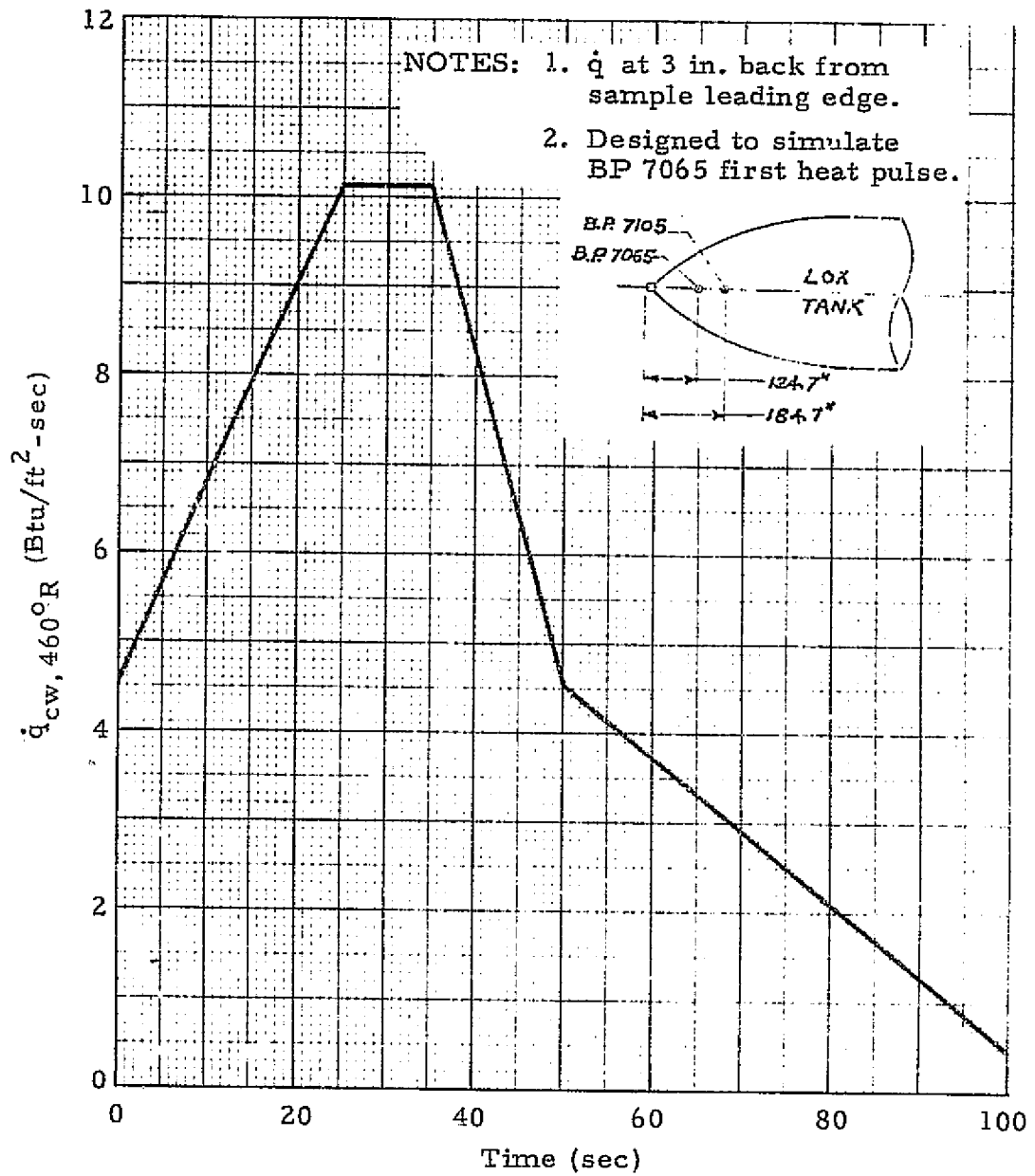


Fig. 6 - Trajectory 1 Heating Rate vs Time

REPRODUCIBILITY OF THE
ORIGINAL PAGE IS POOR

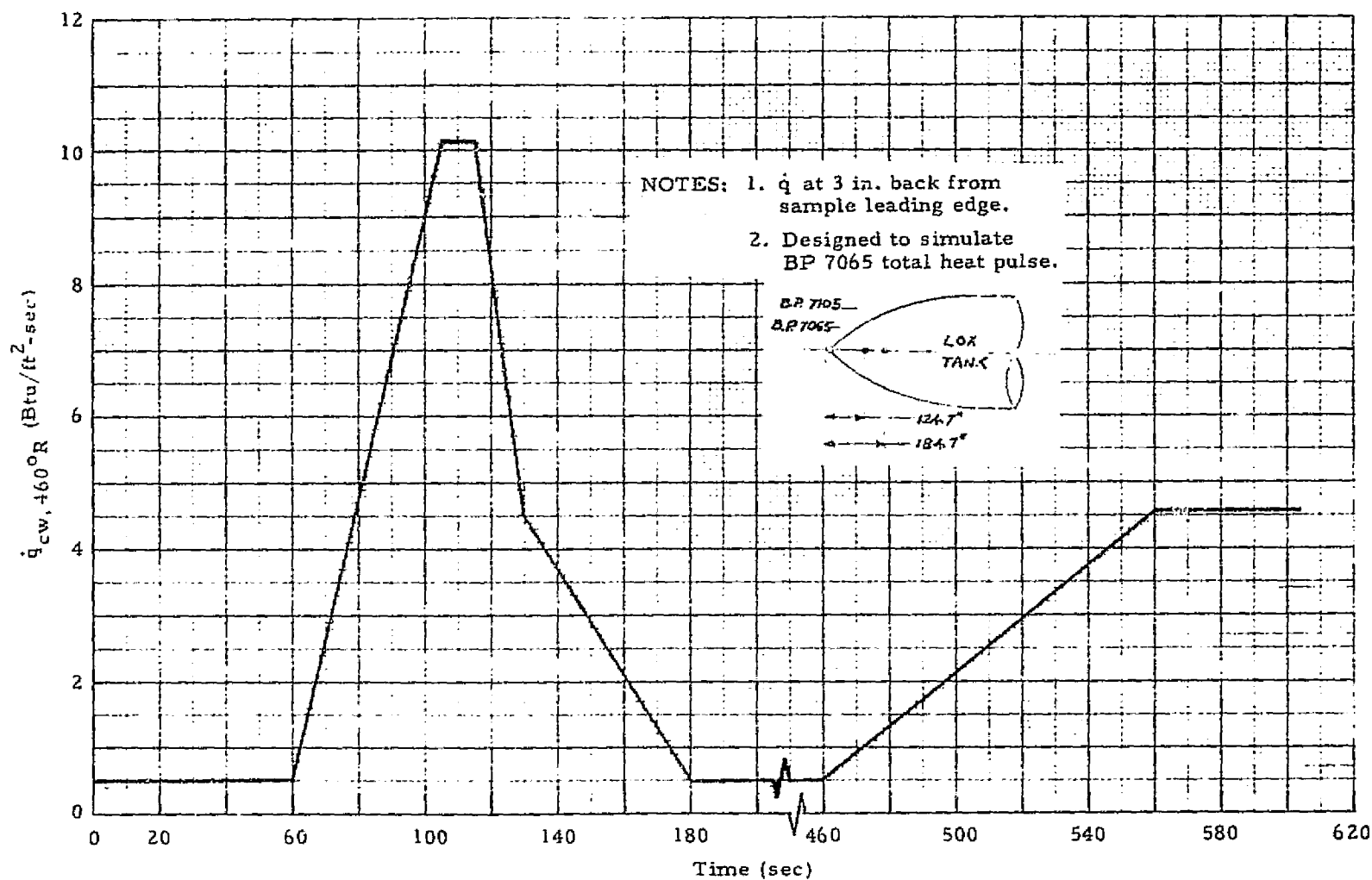


Fig. 7 - Trajectory 2 Heating Rate vs Time

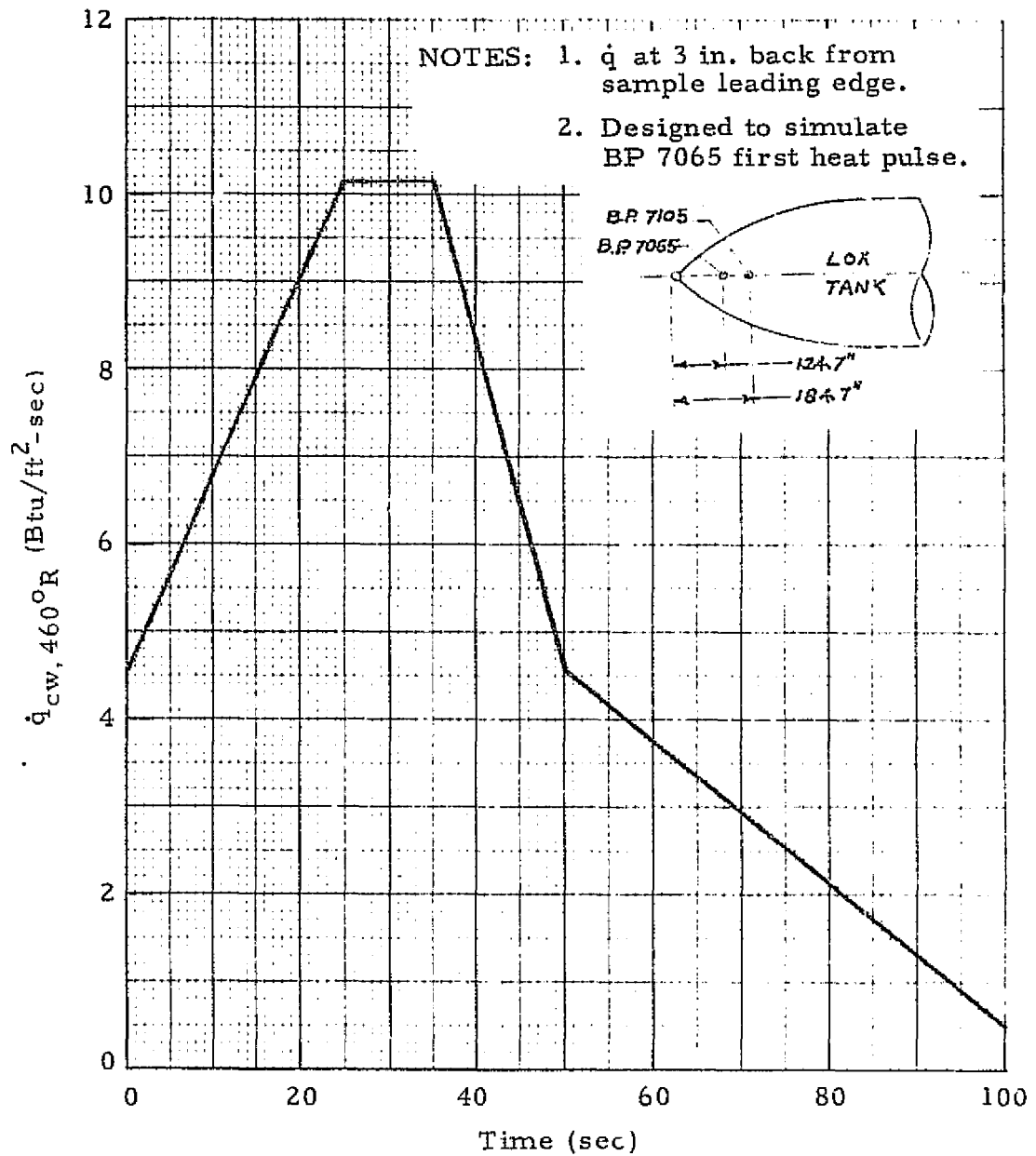


Fig. 8 - Trajectory A Heating Rate vs Time

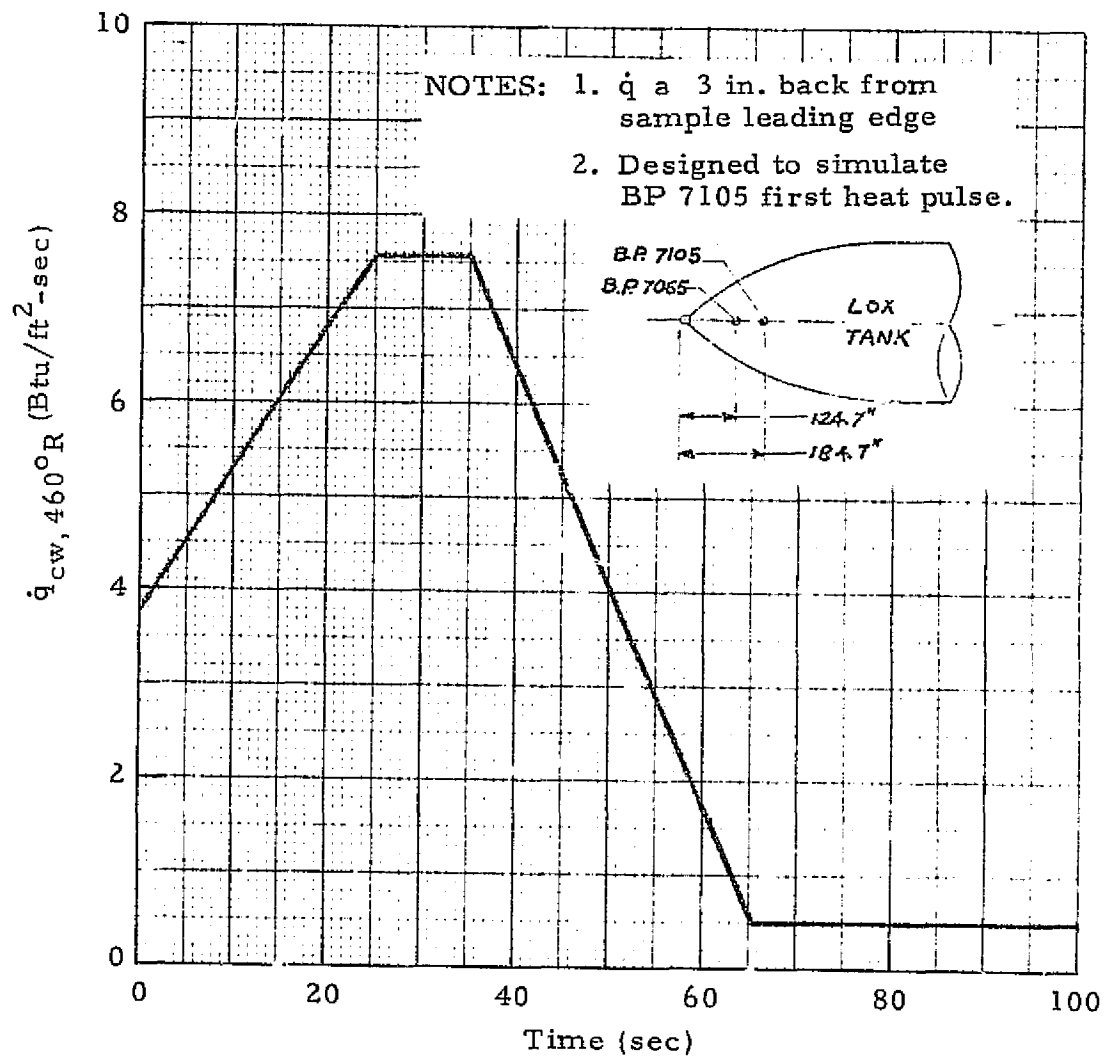


Fig.9 - Trajectory B Heating Rate vs Time

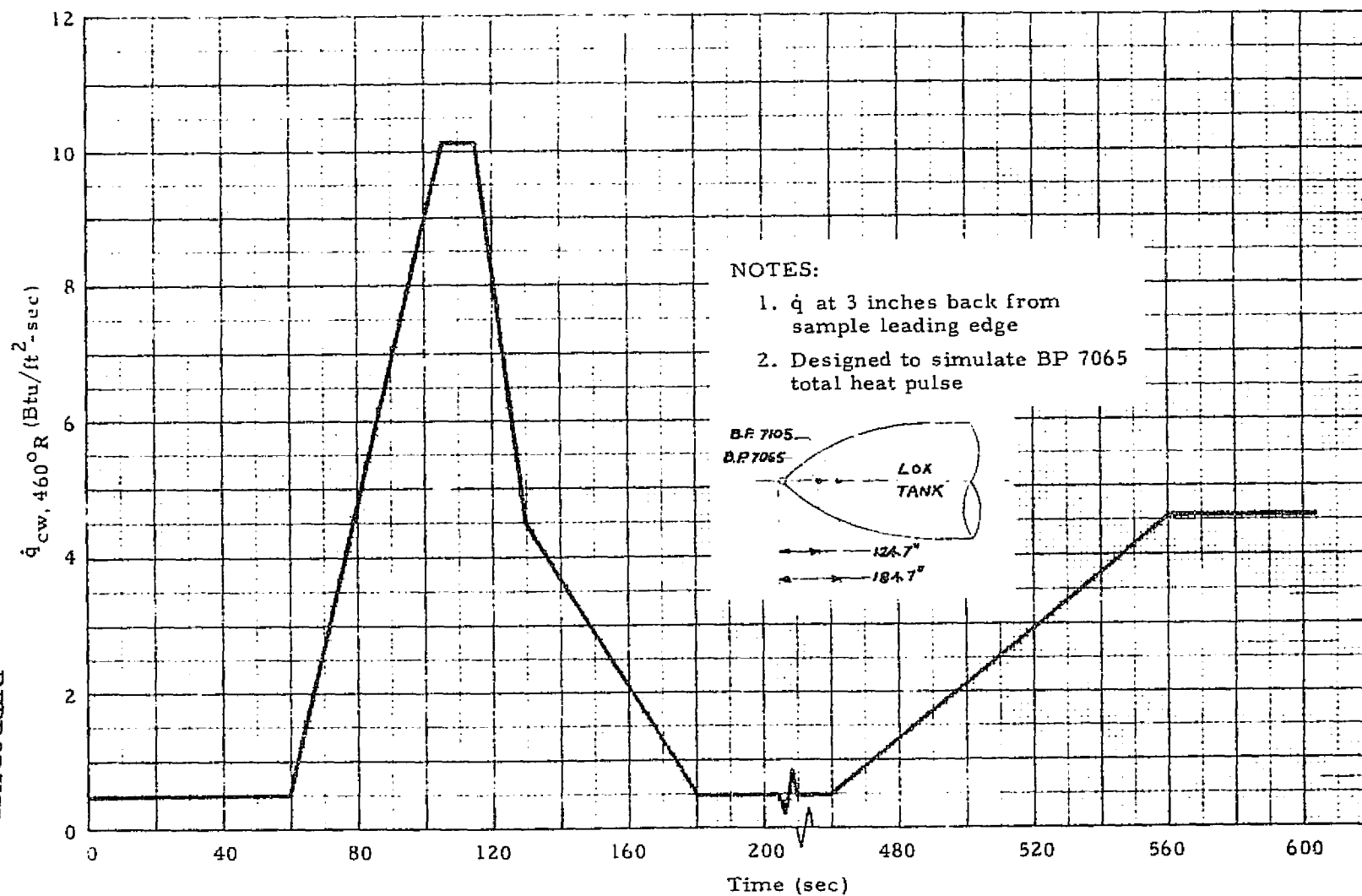
REPRODUCIBILITY OF THE
ORIGINAL PAGE IS POOR


Fig. 10 - Trajectory C Heating Rate vs Time

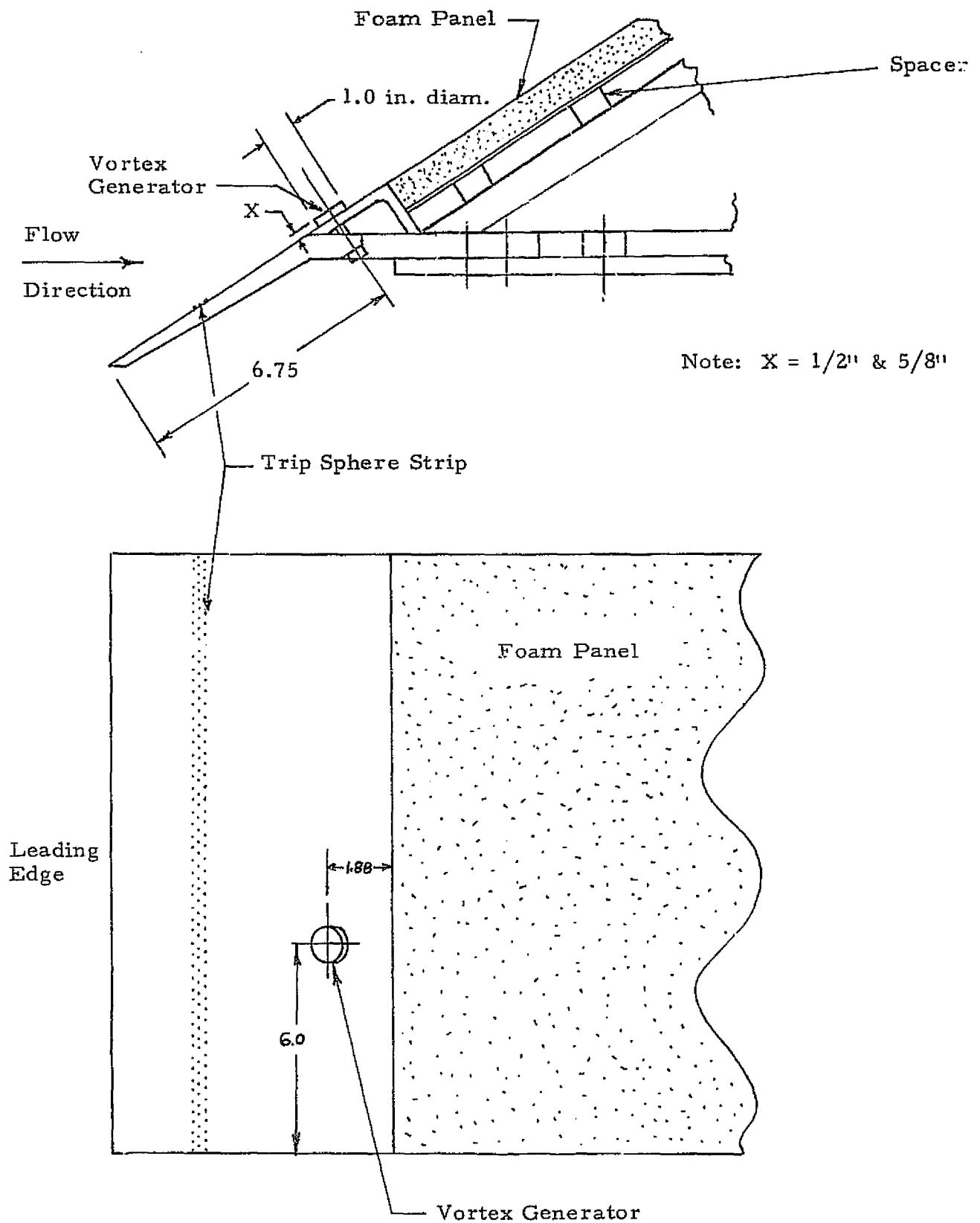


Fig. 11 - Sketch of Wedge-Fixture with Foam Panel Showing Vortex Generator Mounted on Stainless Steel Leading Edge

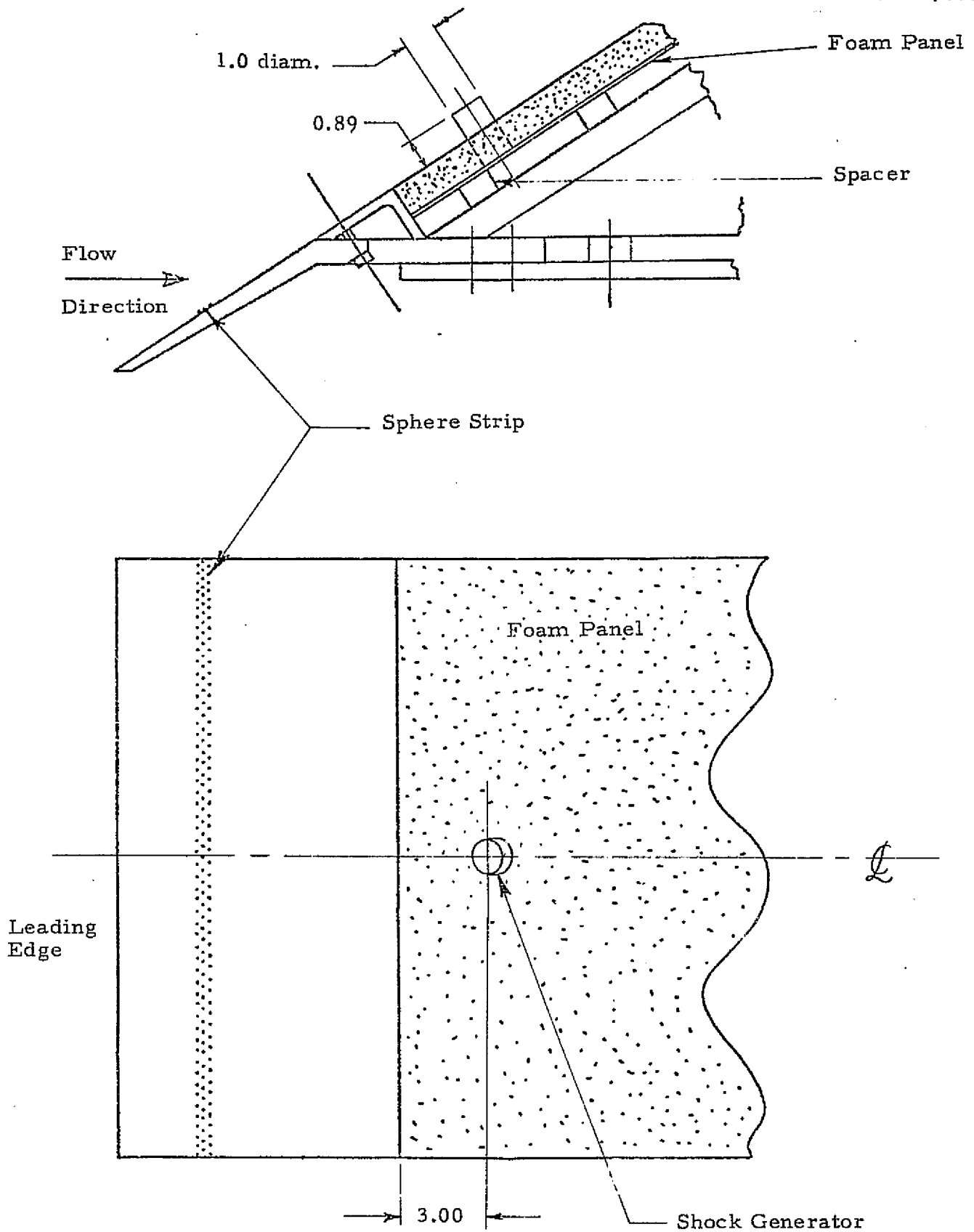


Fig. 12 - Sketch of Wedge Fixture and Foam Panel Showing Size and Location of "Shock" Generator

- NOTES: 1. Dimensions in inches.
 2. C = Calorimeter Locations.
 3. P = Pressure Tap Locations.

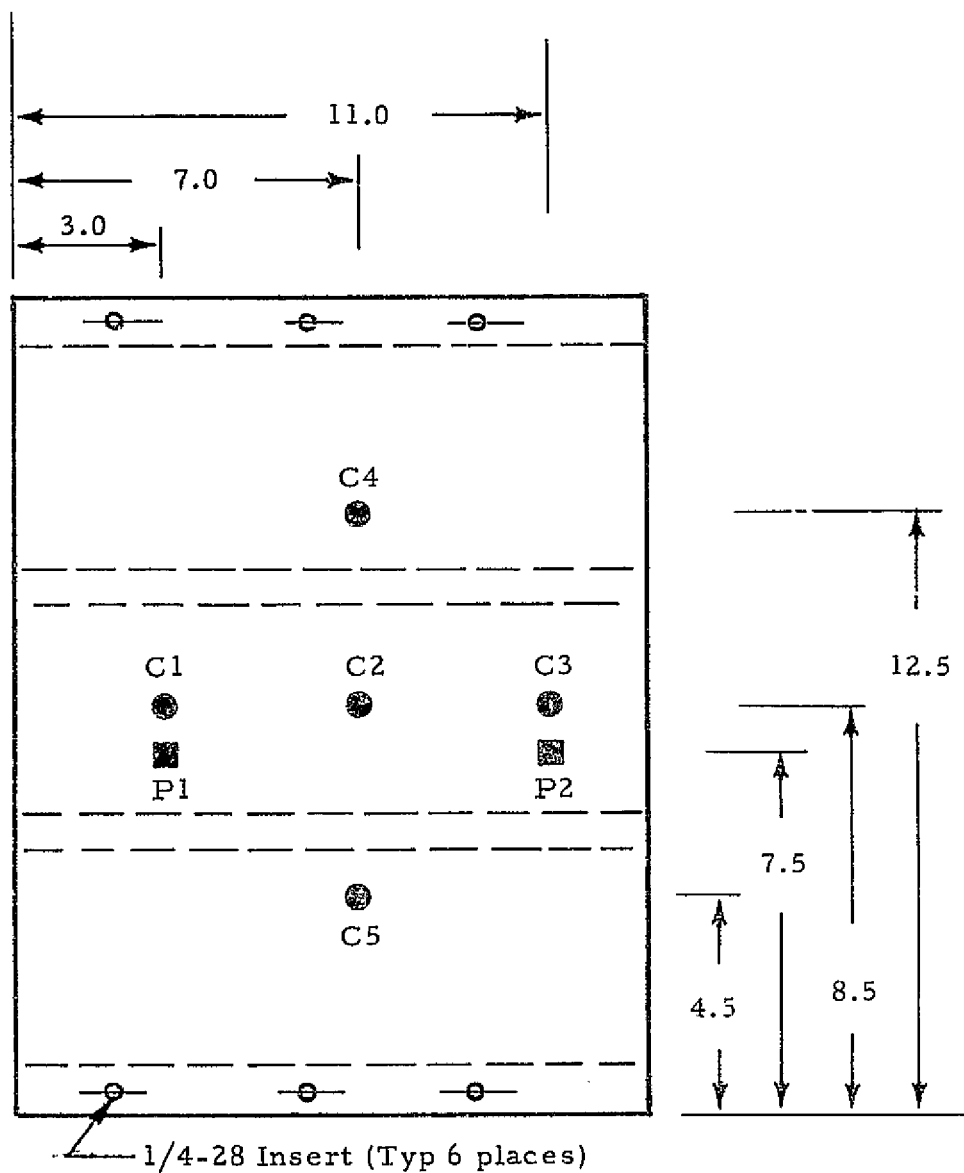


Fig. 13 - Calorimeter and Pressure Tap Locations on the Stycast and Steel Calibration Panels

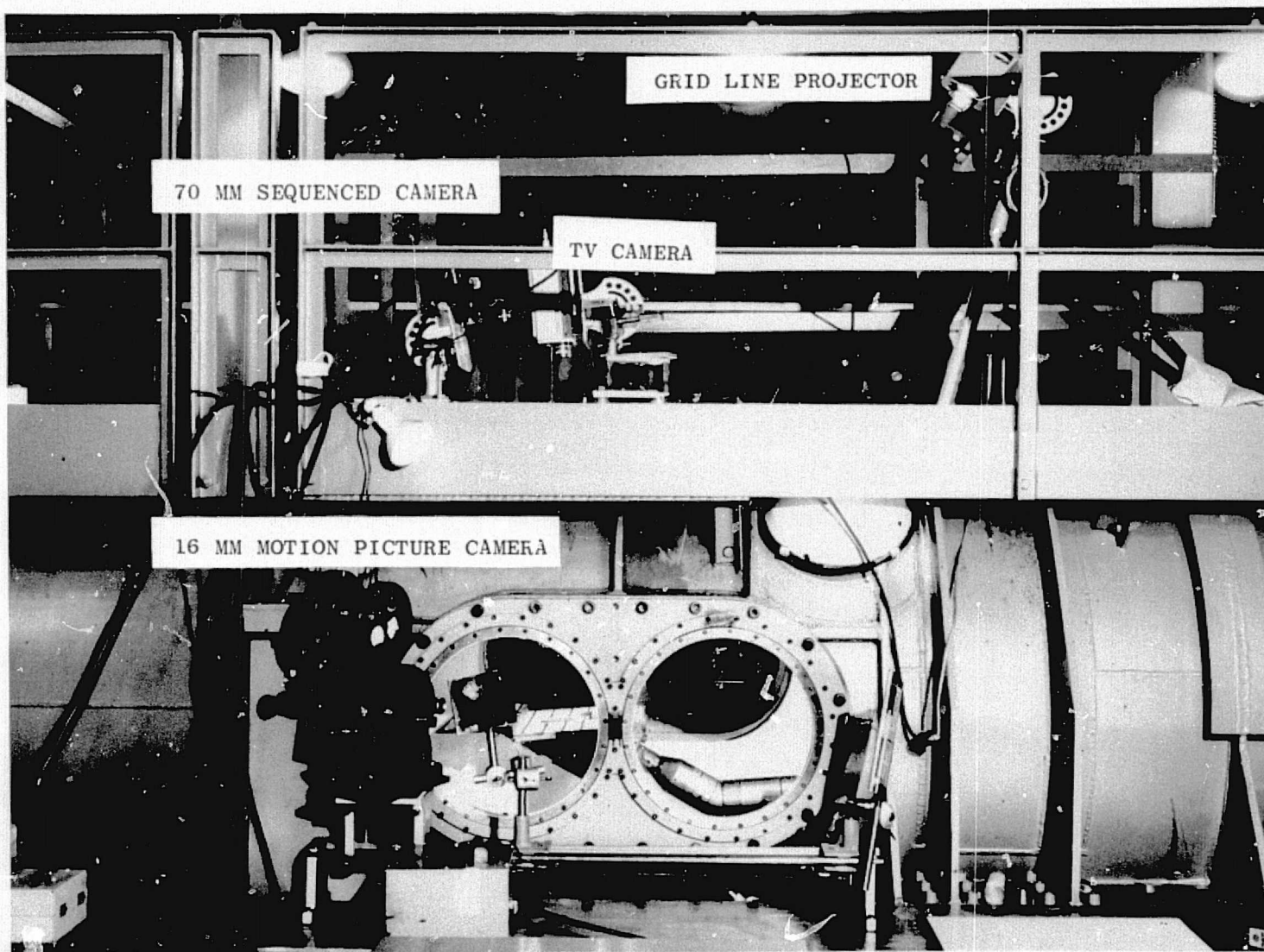


Fig. 14 - AEDC Tunnel "C" Test Section Showing Wedge in Tunnel and Camera Locations

LMSC-HREC TM D390783

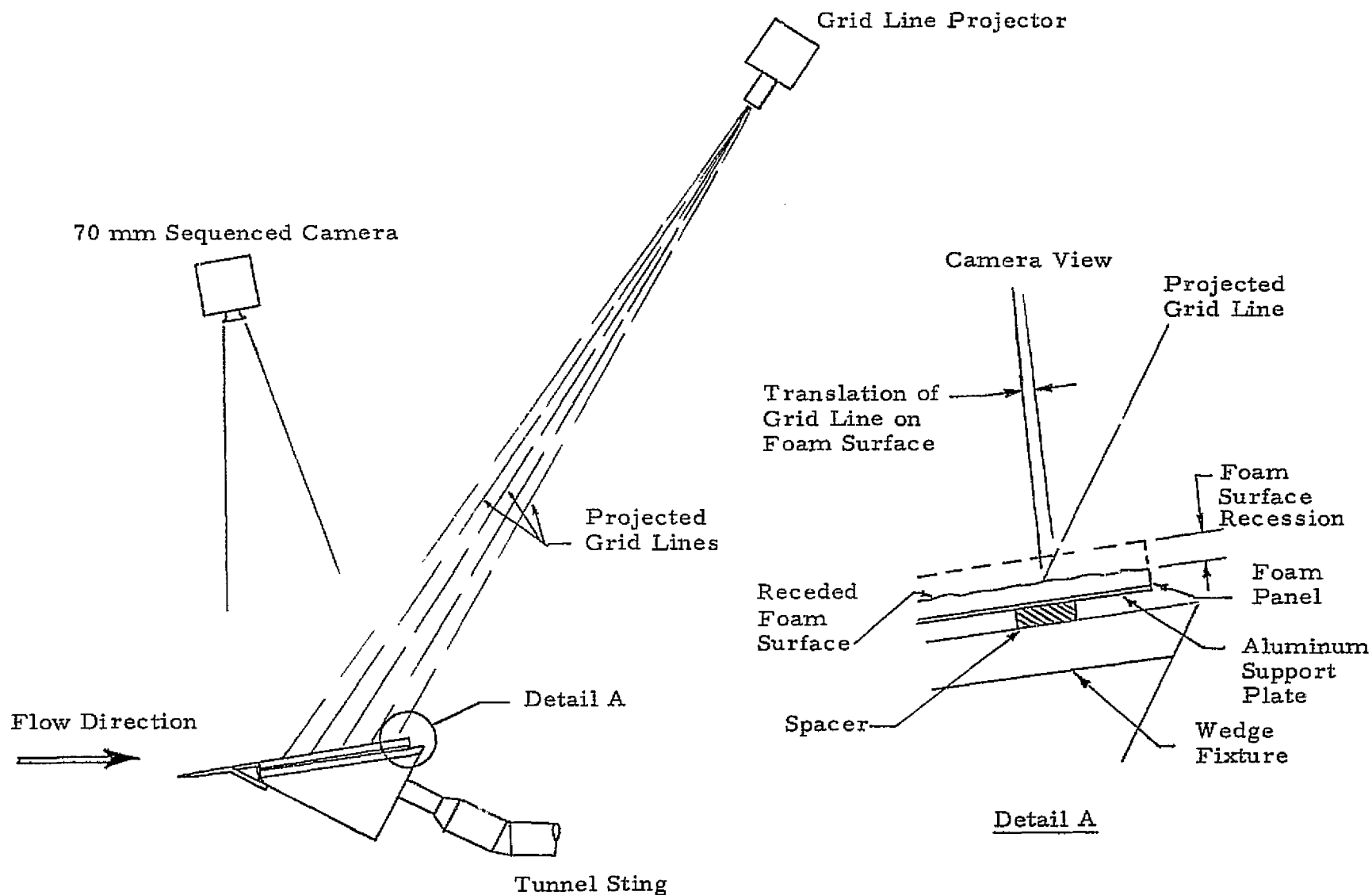


Fig. 15 - Illustration of ARO/AEDC Grid Line Projection System for Obtaining Foam Surface Recession vs Time During the Run

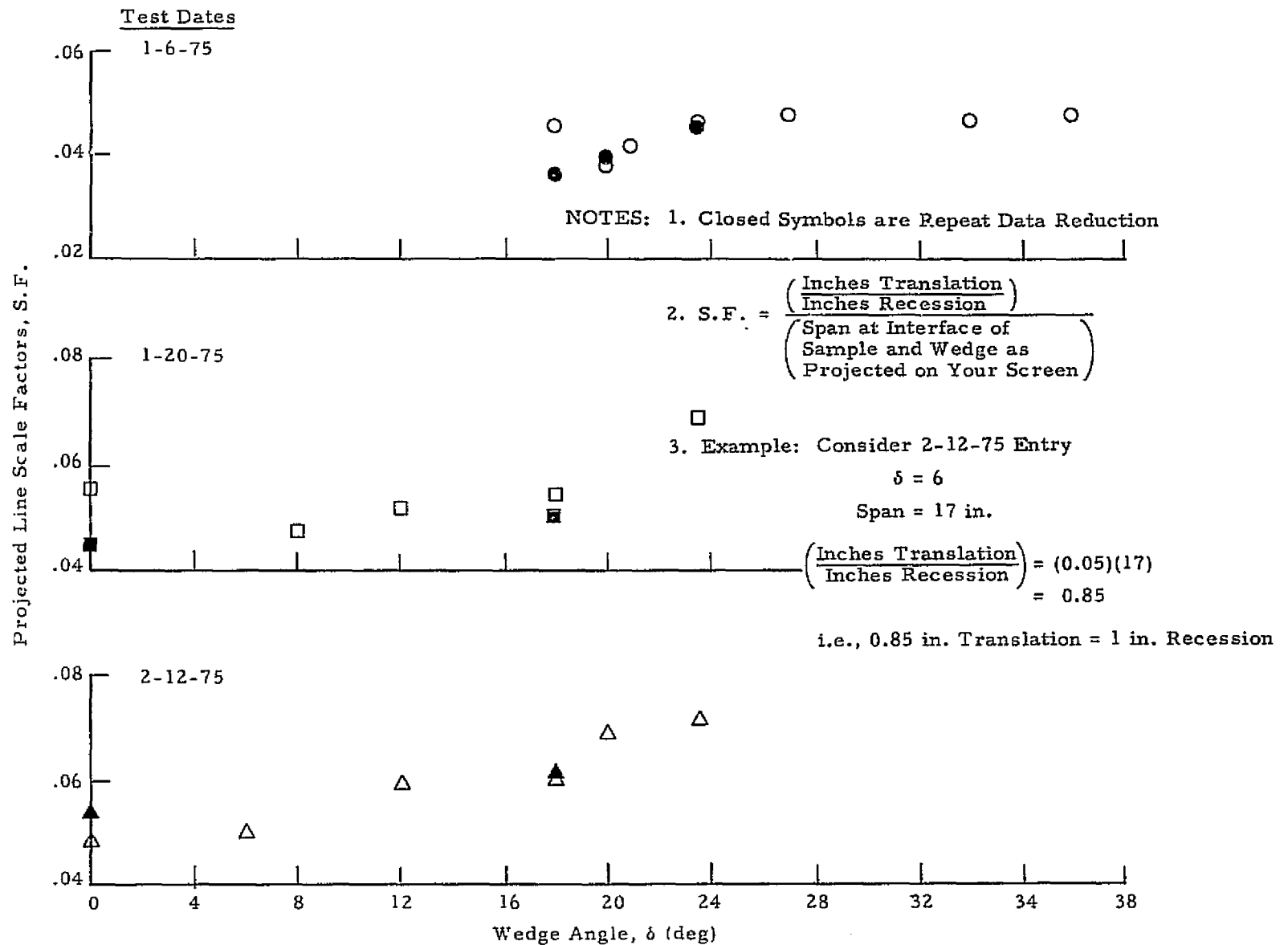


Fig. 16 - Results of Calibration Data for Projected Grid Lines



Fig. 17 - View of Foam Panel Mounted in Tunnel Showing Grid Lines on Foam Surface

AEDC/ARO Inc

REPRODUCIBILITY OF THE
ORIGINAL PAGE IS POOR

NOTES: 1. $P_o = 1800$ psi; $T_o = 1900^\circ\text{R}$; $T_w = 460^\circ\text{R}$.

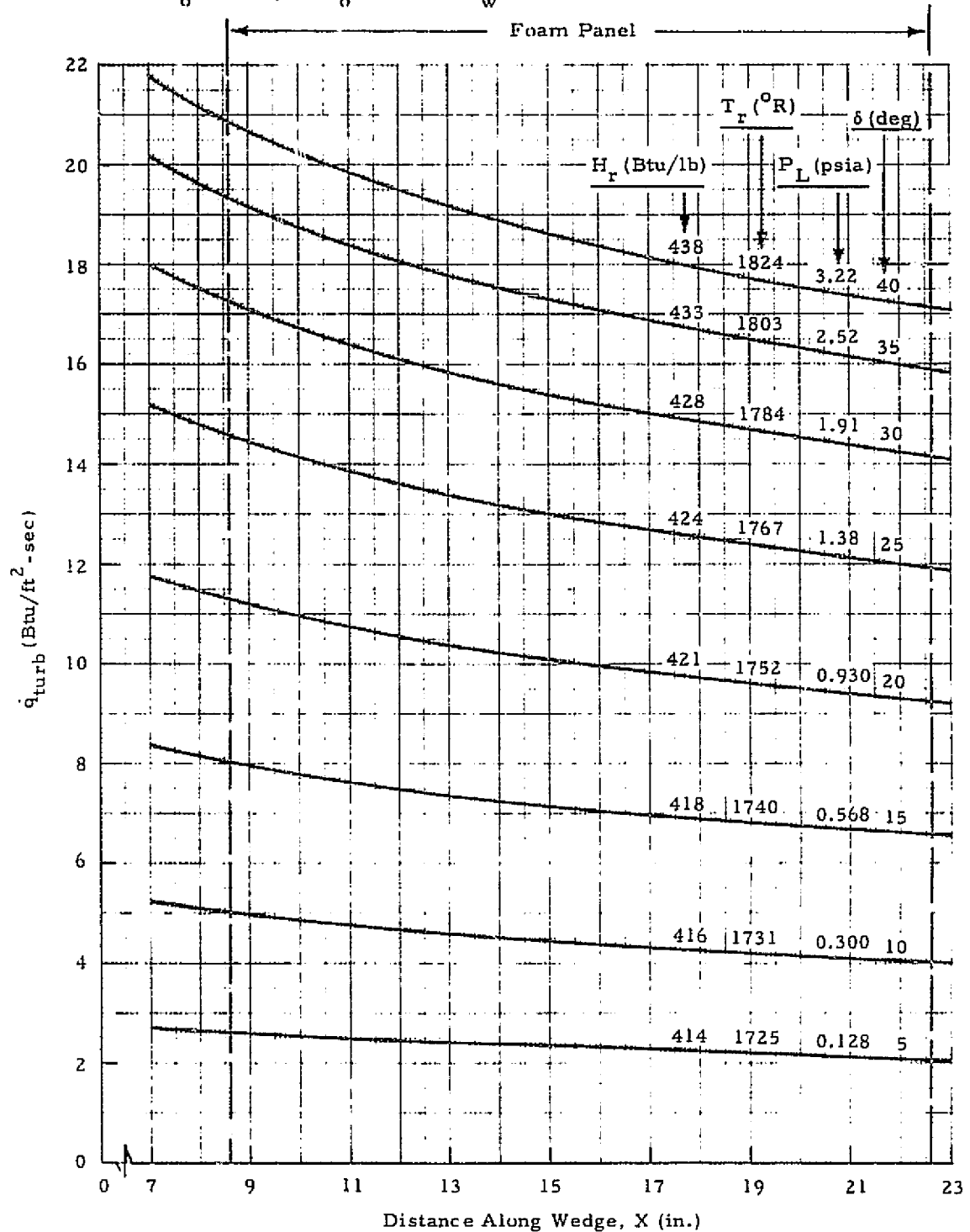


Fig. 18 - Cold Wall Heating Rate vs Distance Along Wedge for Various Wedge Angles

- NOTES: 1. $P_o = 1800$ psi
 2. $T_o = 1900^\circ\text{R}$
 3. $T_w = 960^\circ\text{R}$

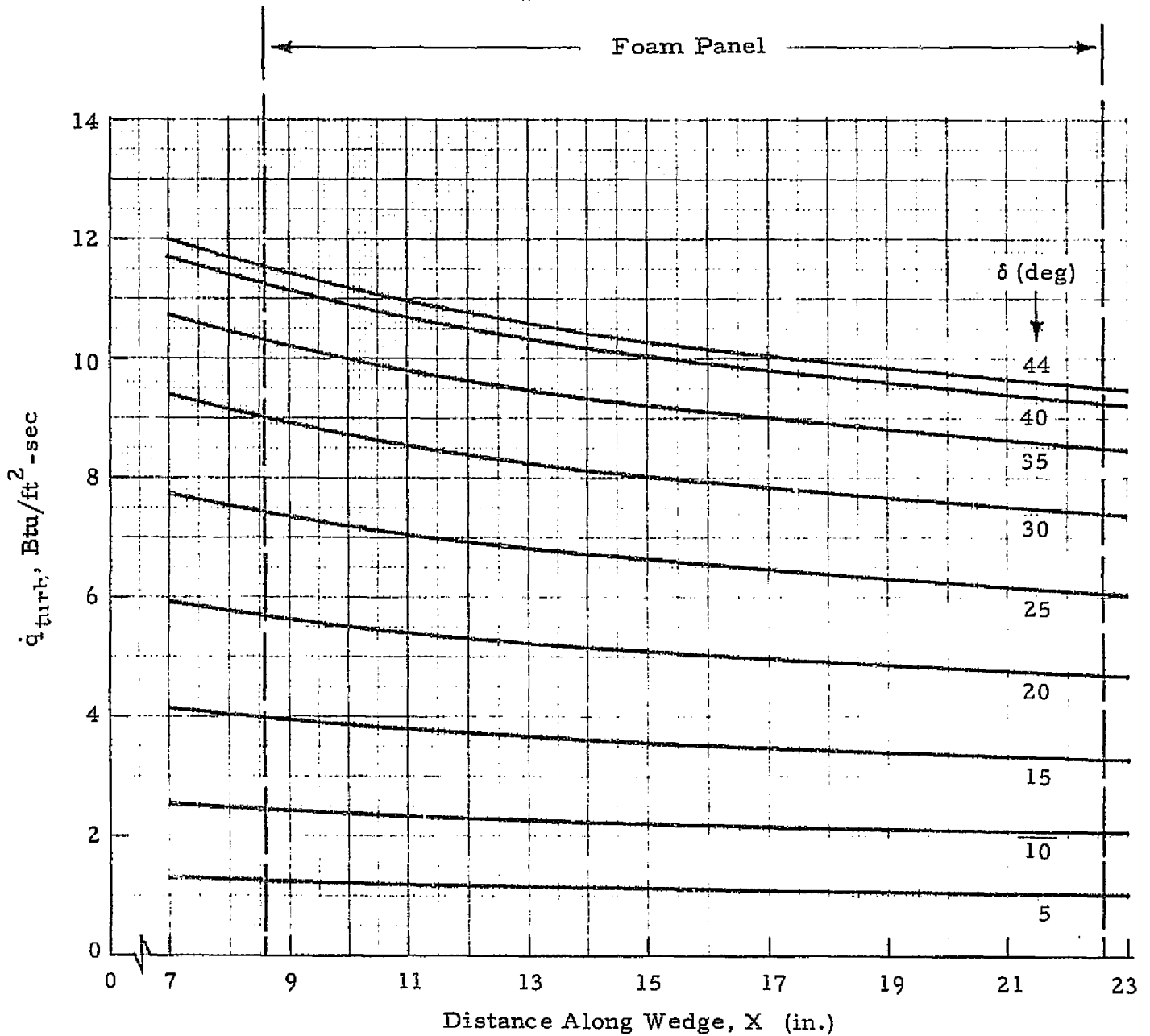


Fig. 19 - Hot Wall Heating Rate vs Distance Along Wedge for Various Wedge Angles

NOTES:

1. $T_o = 1900^{\circ}\text{R}$
2. $P_o = 1800 \text{ psi}$
3. $T_w = 460^{\circ}\text{R}$

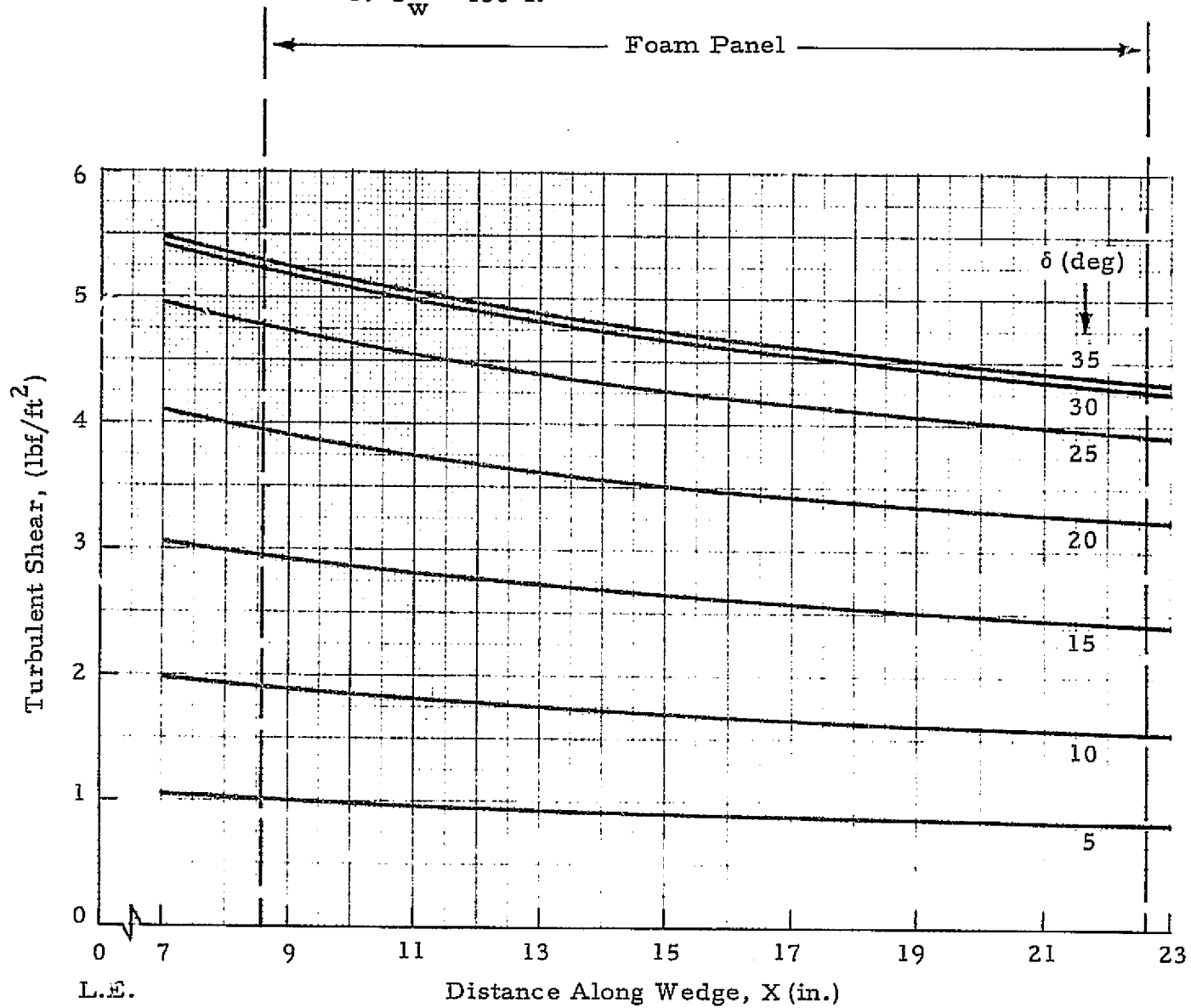


Fig. 20 - Cold Wall Shear vs Distance Along Wedge for Various Wedge Angles

NOTES:

1. $T_o = 1900^{\circ}\text{R}$
2. $P_o = 1800 \text{ psi}$
3. Upstream Gardon Gage Location

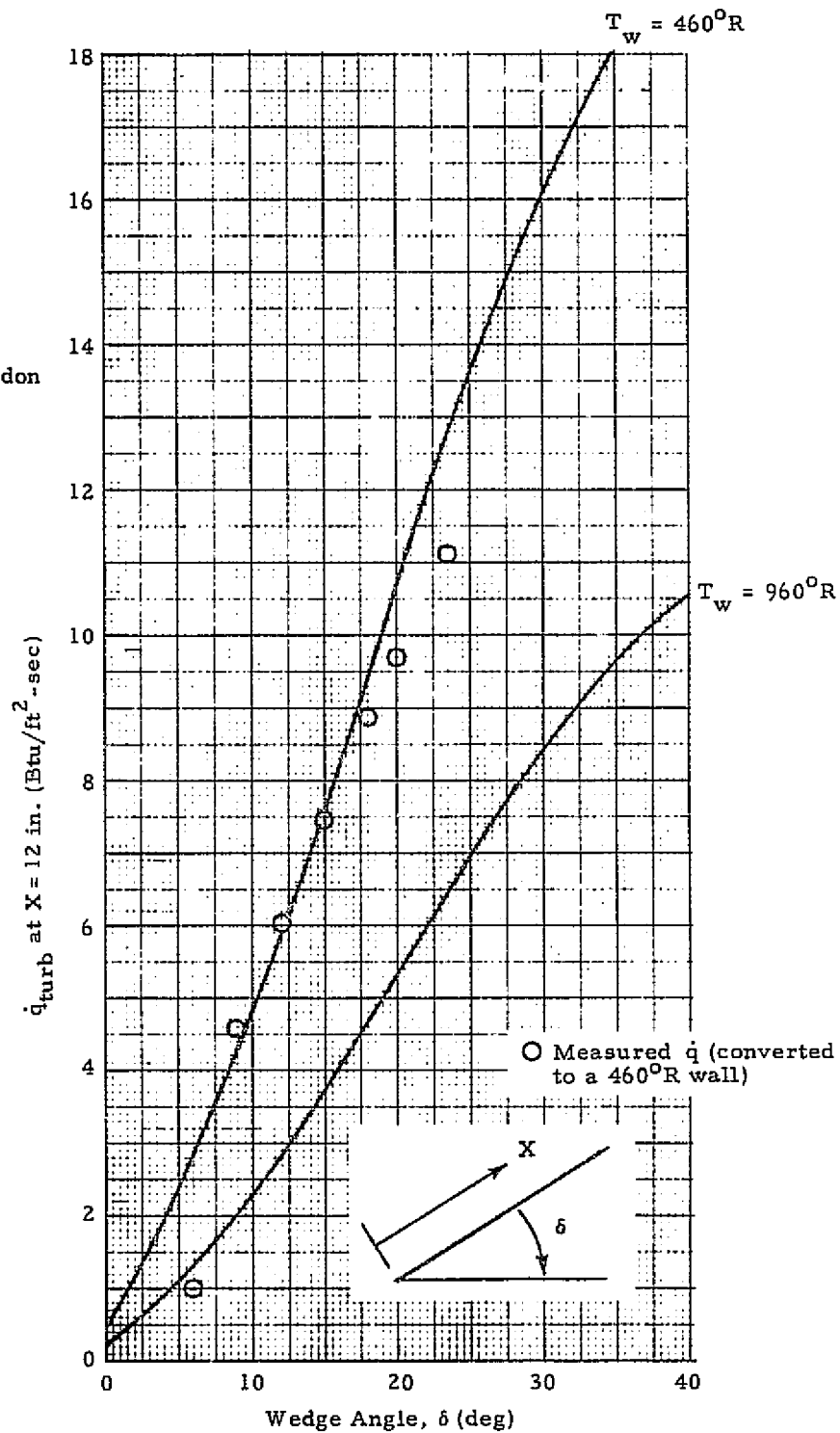


Fig. 21a - Calculated Turbulent Heating Rate vs Wedge Angle for Two Wall Temperatures Compared with Measured Values at $X = 12 \text{ in.}$

NOTES:

1. $T_o = 1900^\circ R$
2. $P_o = 1800$ psi
3. Center Gardon Gage Location

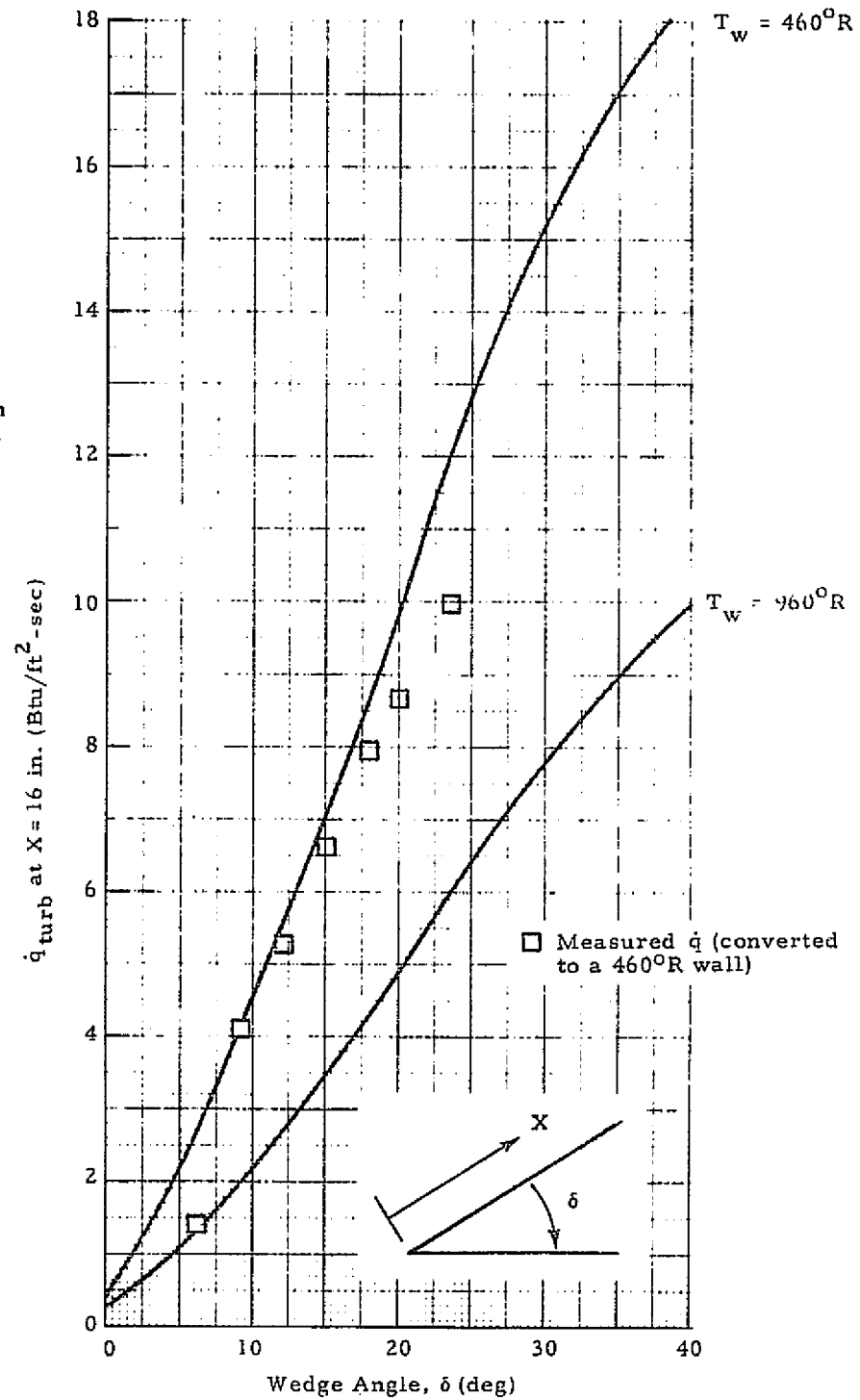


Fig. 21b - Calculated Turbulent Heating Rate vs Wedge Angle for Two Wall Temperatures Compared with Measured Values at $X = 16$ in.

REPRODUCIBILITY OF THE
ORIGINAL PAGE IS POOR

NOTES:

1. $T_o = 1900^{\circ}\text{R}$
2. $P_o = 1800 \text{ psi}$
3. Downstream
Gardon Gage
Location

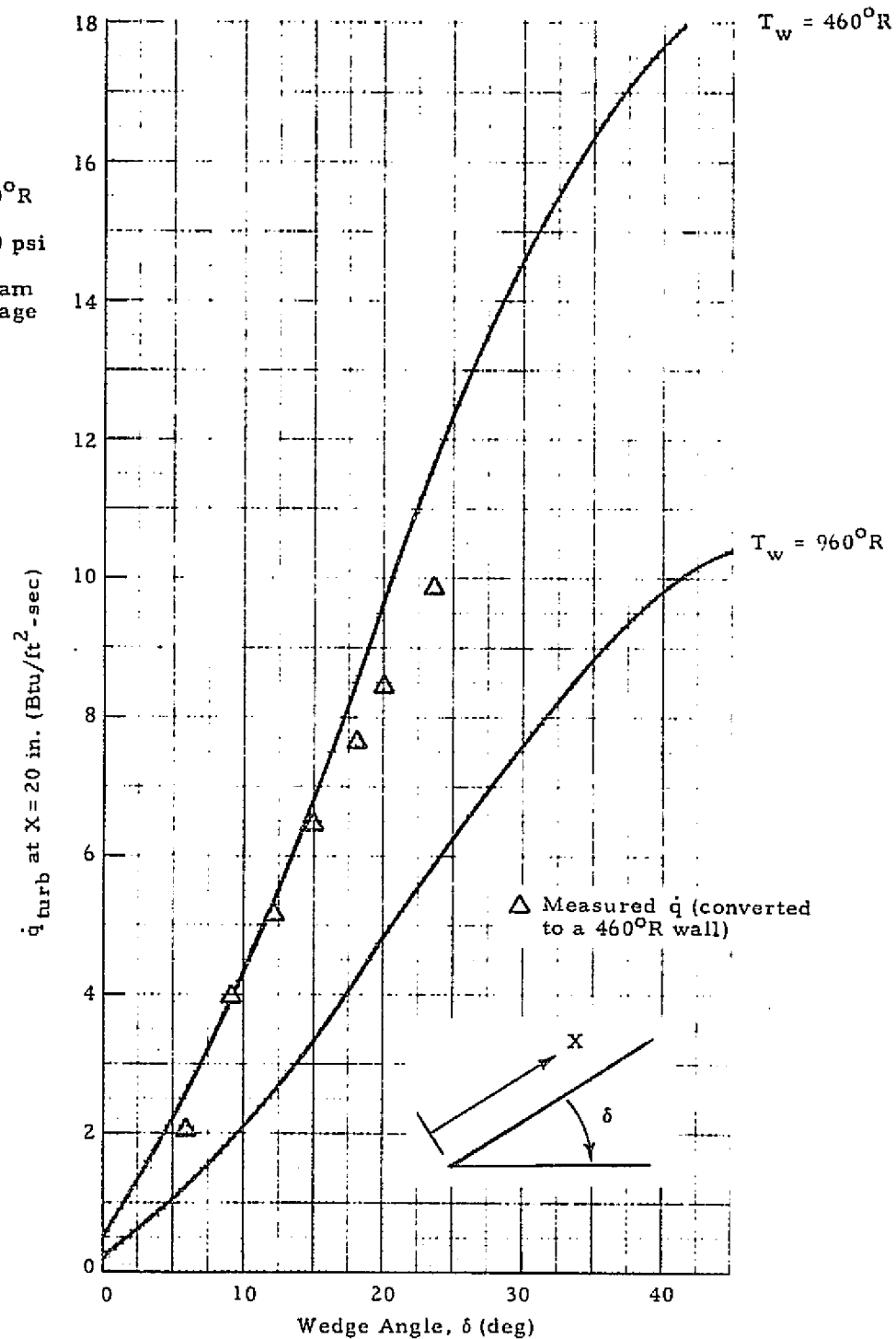


Fig. 21c - Calculated Turbulent Heating Rate vs Wedge Angle for Two Wall Temperatures Compared with Measured Values at $X = 20 \text{ in.}$

◇ Measured at Pressure Tap P_1

○ Measured at Pressure Tap P_2

See Fig. 13 for Locations of Pressure Taps P_1 and P_2

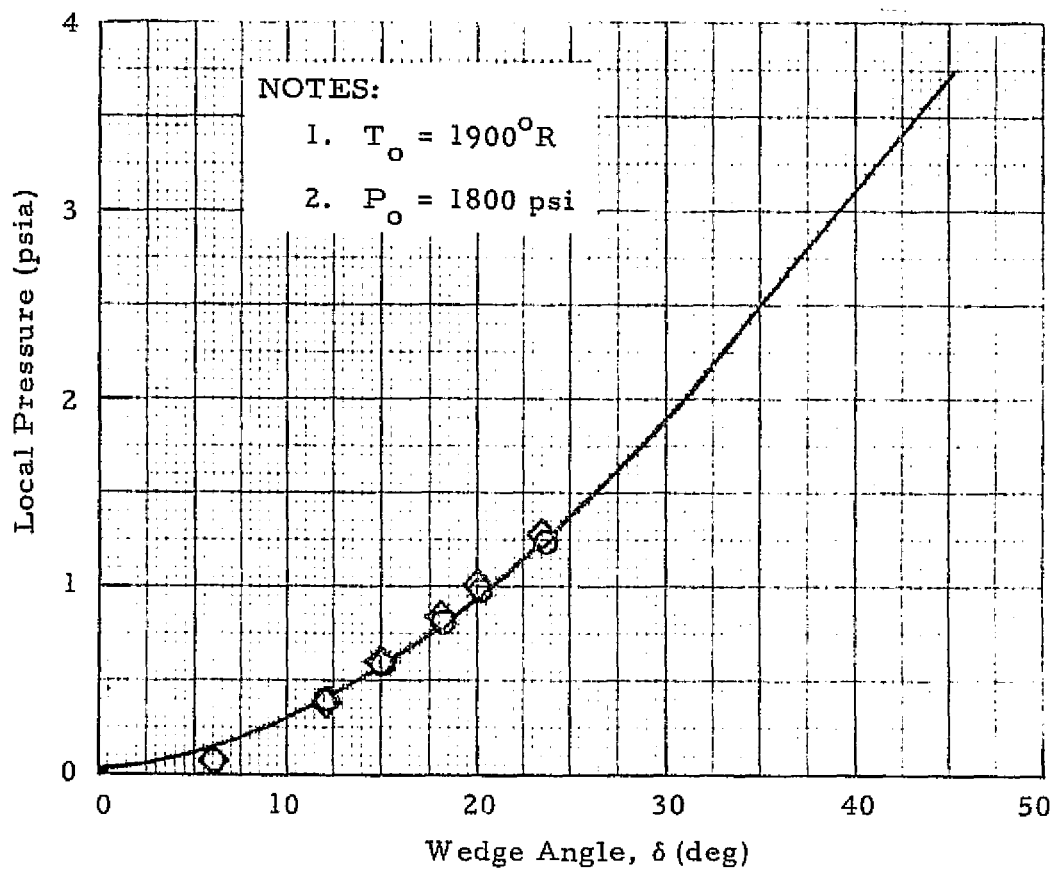


Fig. 22 - Calculated and Measured Local Pressure on Wedge vs Wedge Angle

NOTES:

1. $T_o = 1900^{\circ}\text{R}$
2. $P_o = 1800 \text{ psi}$

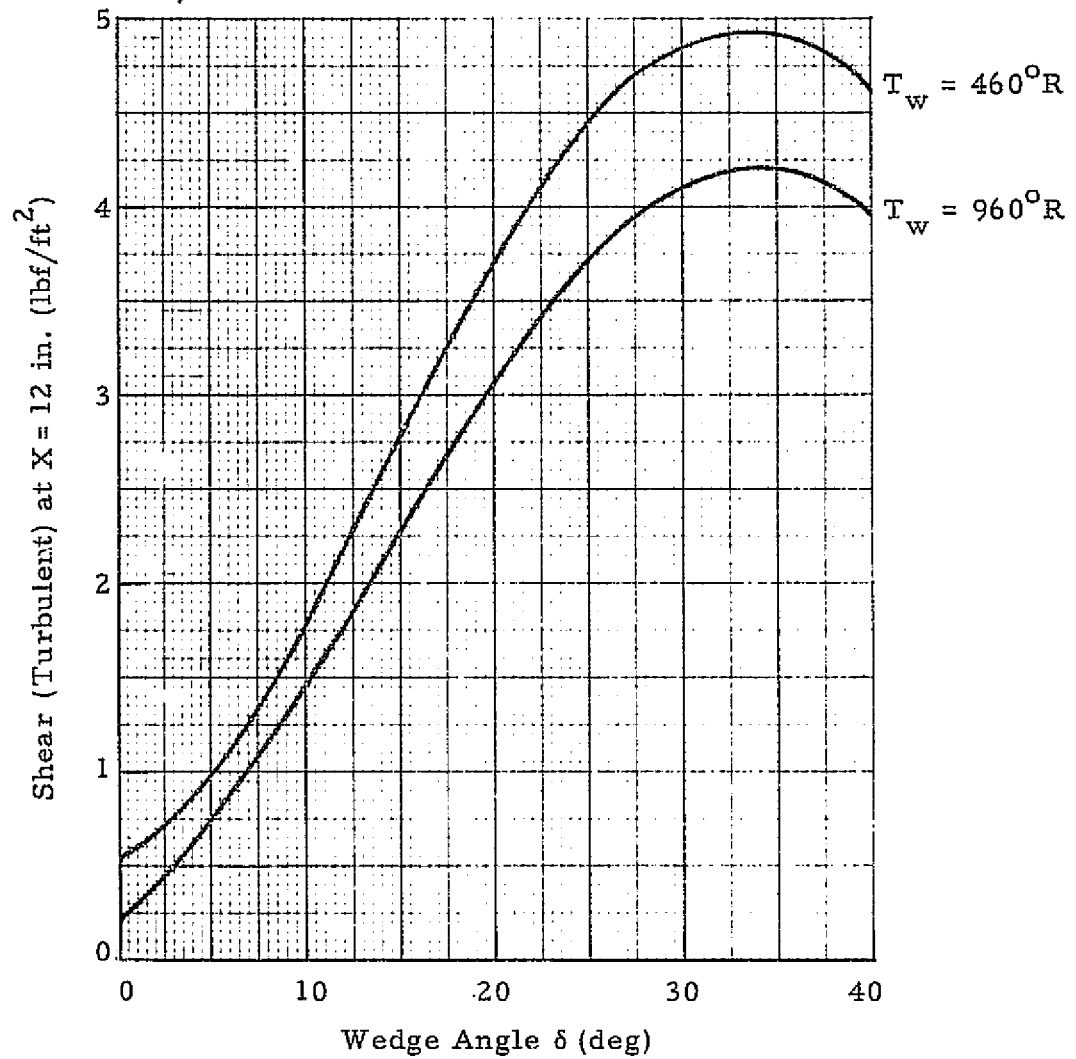


Fig. 23a - Turbulent Shear vs Wedge Angle for Two Wall Temperature Values at $X = 12 \text{ in.}$

REPRODUCIBILITY OF THE
ORIGINAL PAGE IS POOR

NOTES:

1. $T_o = 1900^{\circ}\text{R}$
2. $P_o = 1800 \text{ psi}$

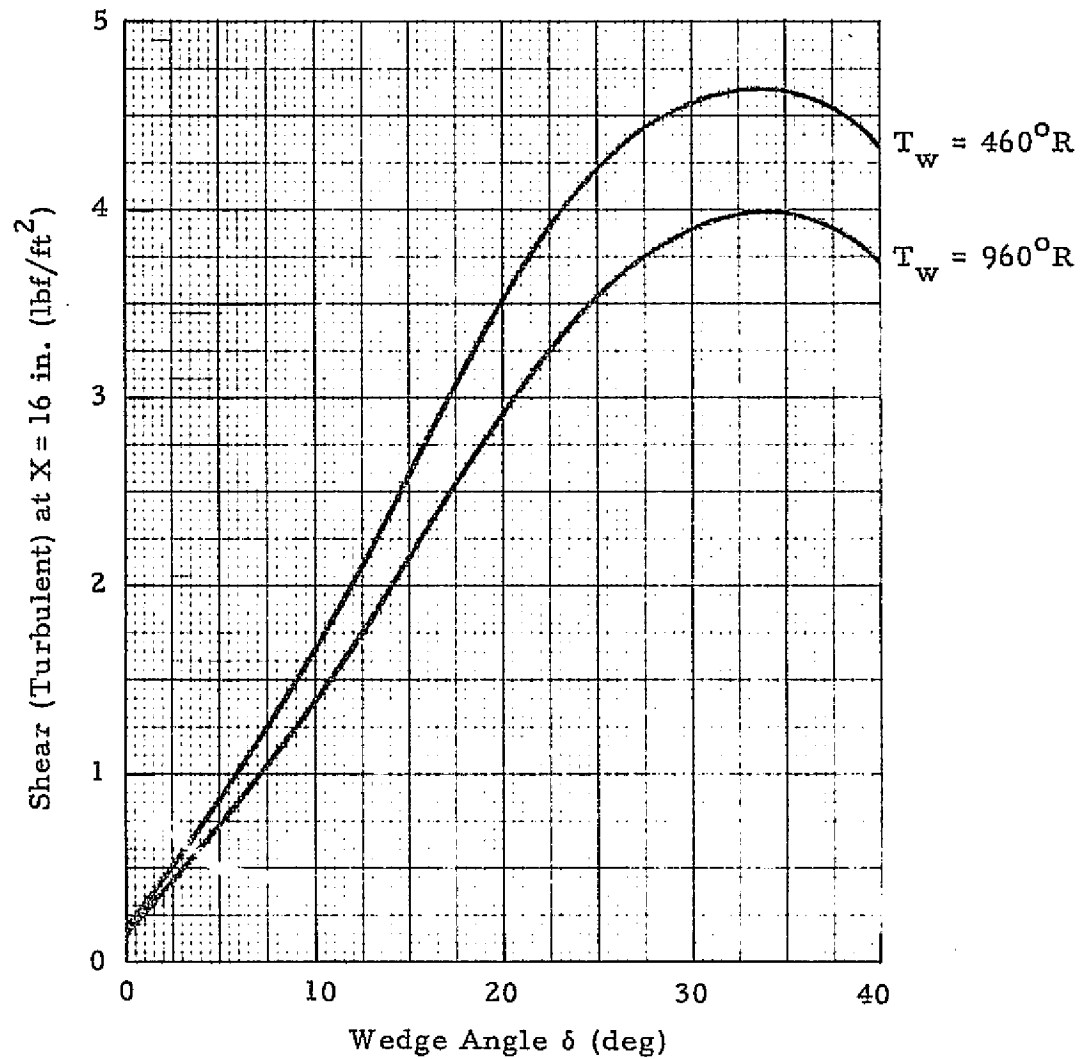


Fig. 23b - Turbulent Shear vs Wedge Angle for Two Wall Temperature Values at $X = 16 \text{ in.}$

NOTES:

1. $T_o = 1900^{\circ}\text{R}$
2. $P_o = 1800 \text{ psi}$

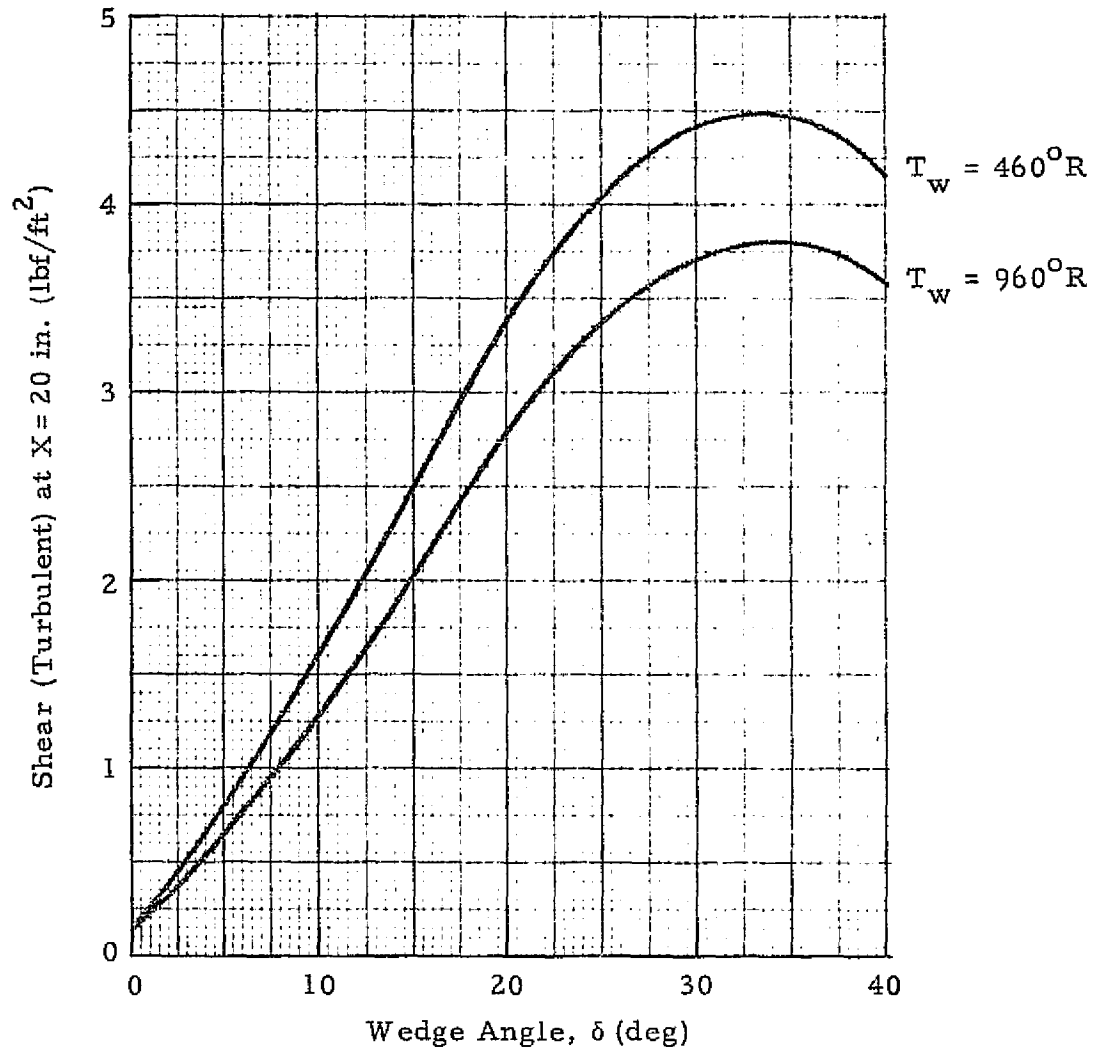


Fig. 23c - Turbulent Shear vs Wedge Angle for Two Wall Temperature Values at $X = 20 \text{ in.}$

NOTES:

1. $P_o = 1800$ psi
2. $T_w = 460^\circ R$

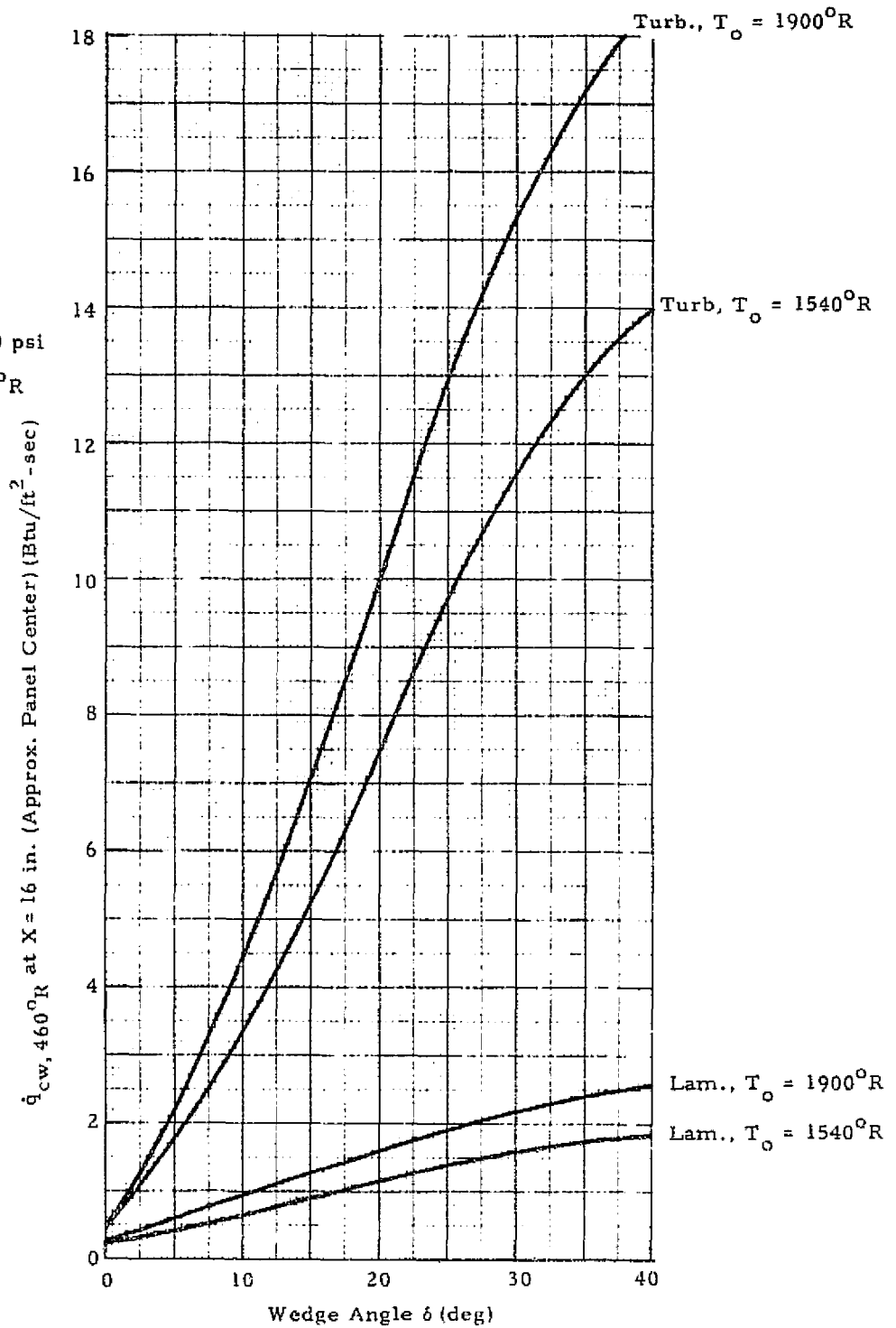


Fig. 24a - Comparison of Laminar and Turbulent Cold Wall Heating Rate vs Wedge Angle for Two Total Temperature Values (at center of panel)

REPRODUCIBILITY OF THE
ORIGINAL PAGE IS POOR

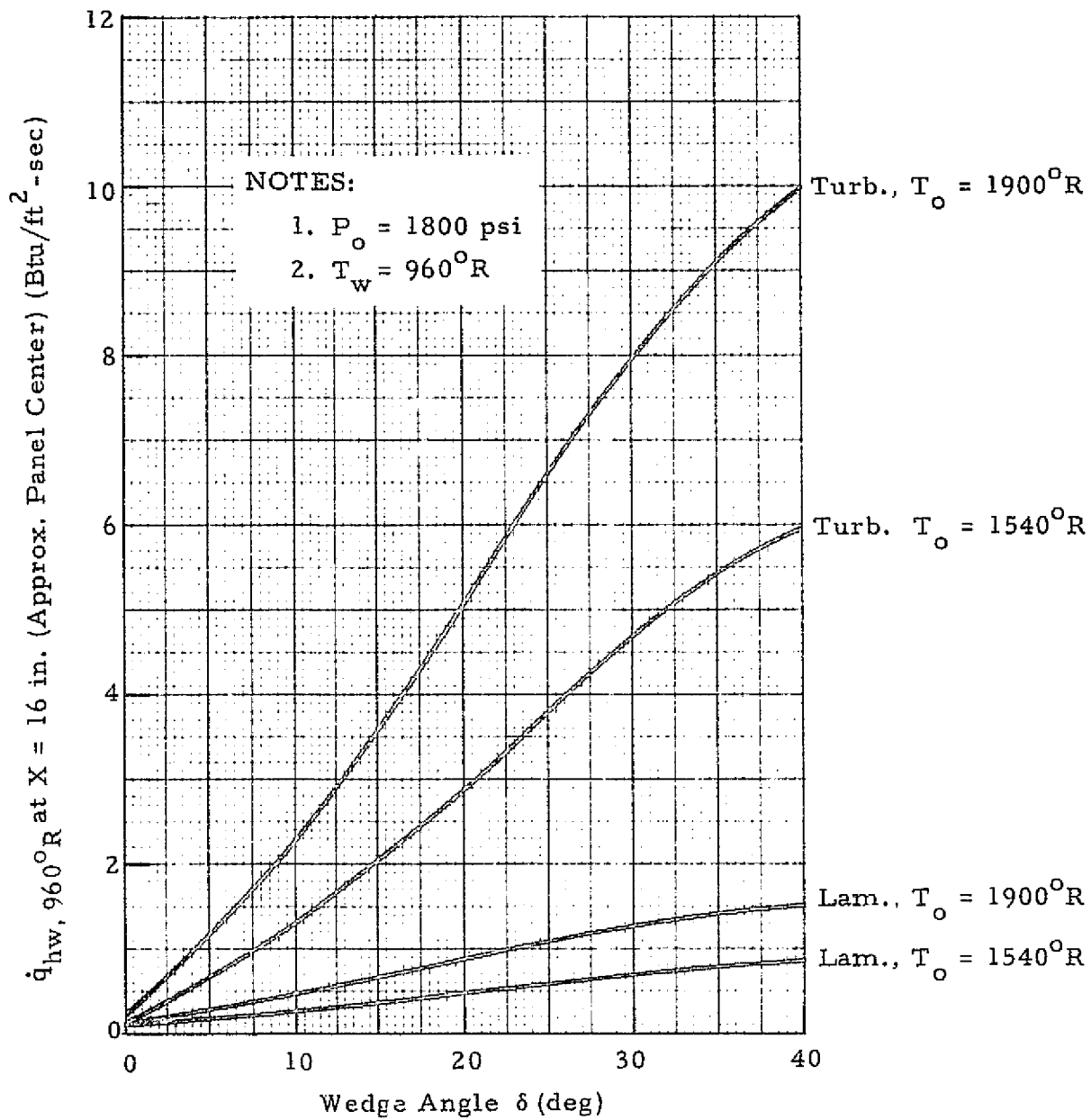


Fig. 24b - Comparison of Laminar and Turbulent Hot Wall Heating Rate vs Wedge Angle for Two Total Temperature Values (at center of panel)

NOTES:

1. $P_o = 1800$ psi
2. $T_w = 460^\circ R$

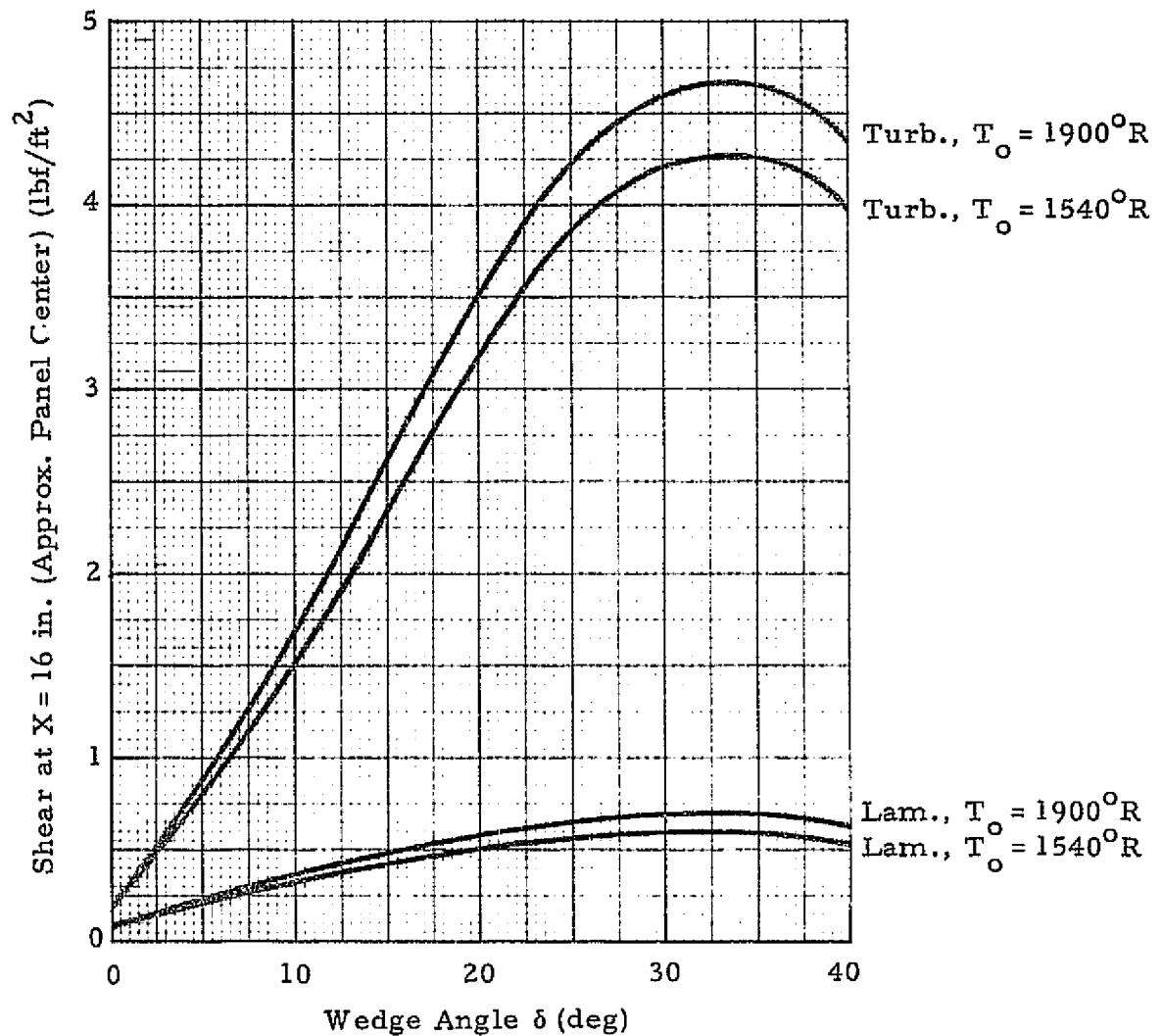


Fig. 25a - Cold Wall Laminar and Turbulent Shear vs Wedge Angle for Two Total Temperature Values (at center of panel)

NOTES:

1. $P_o = 1800 \text{ psi}$
2. $T_w = 960^\circ\text{R}$

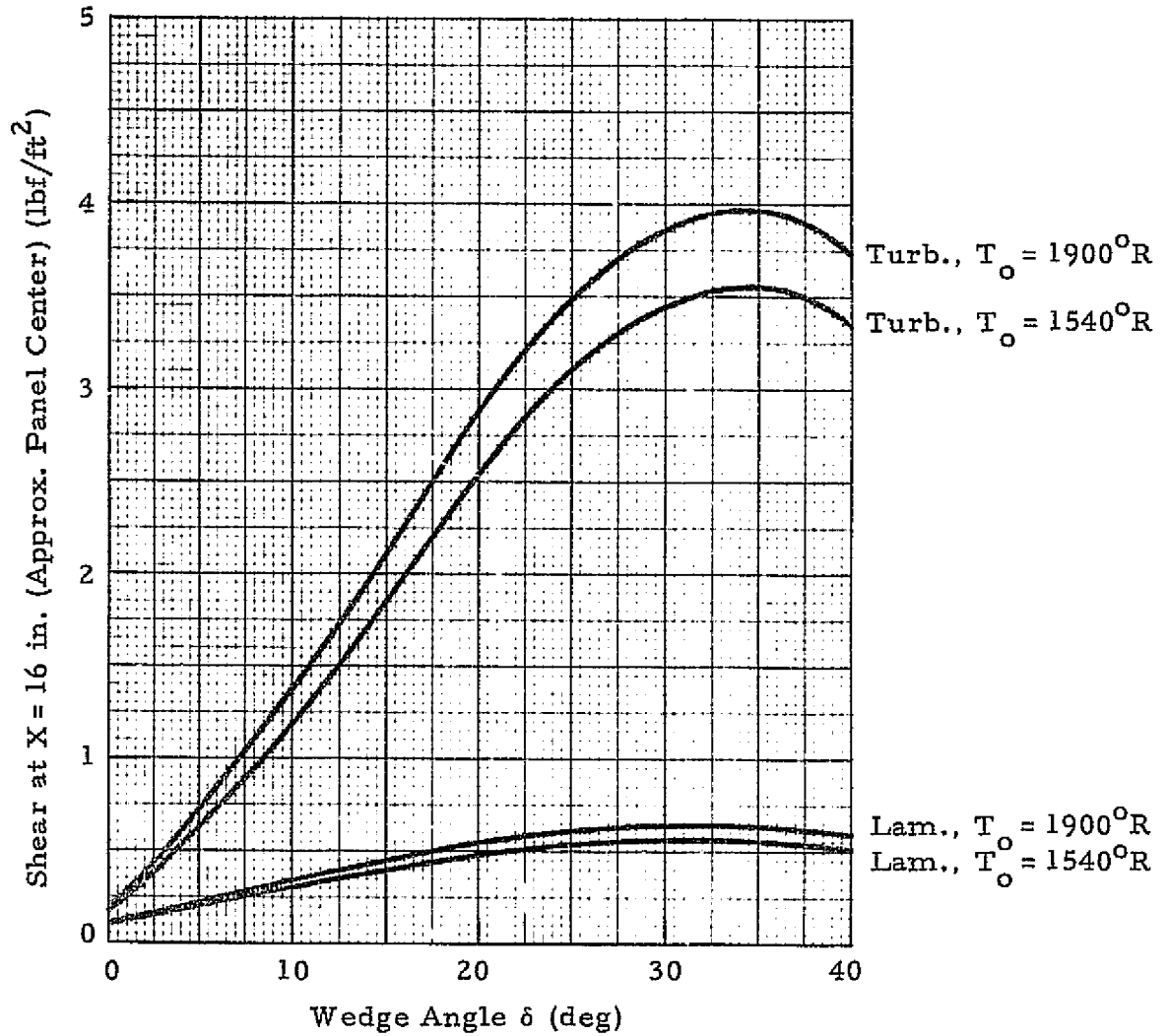


Fig. 25b - Hot Wall Laminar and Turbulent Shear vs Wedge Angle for Two Total Temperature Values (at center of panel)

NOTE:

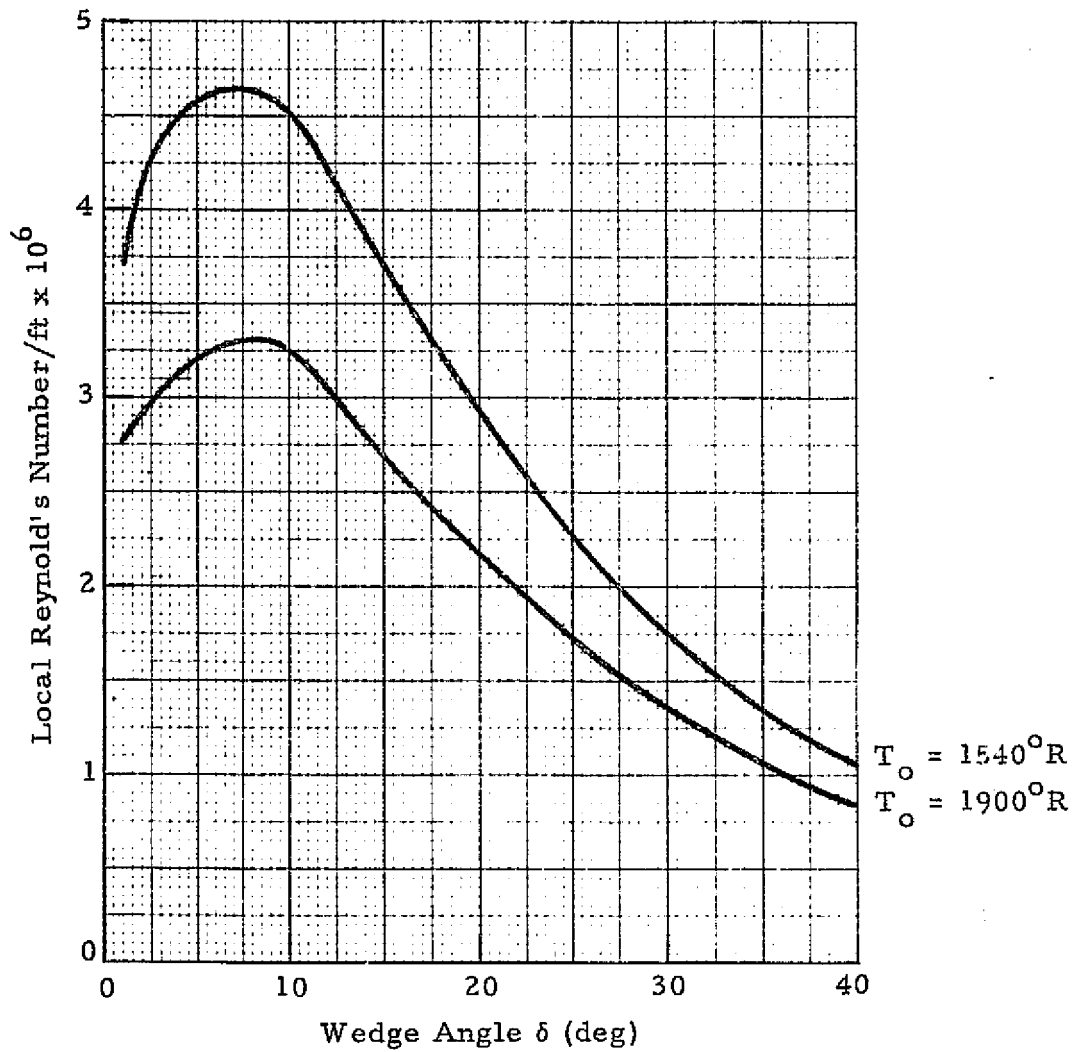
1. $P_o = 1800$ psi

Fig. 26 - Local Reynolds Number per Foot vs Wedge Angle for Two Total Temperature Values

NOTES:

1. $T_o = 1900^\circ R$
2. $P_o = 1800$ psi

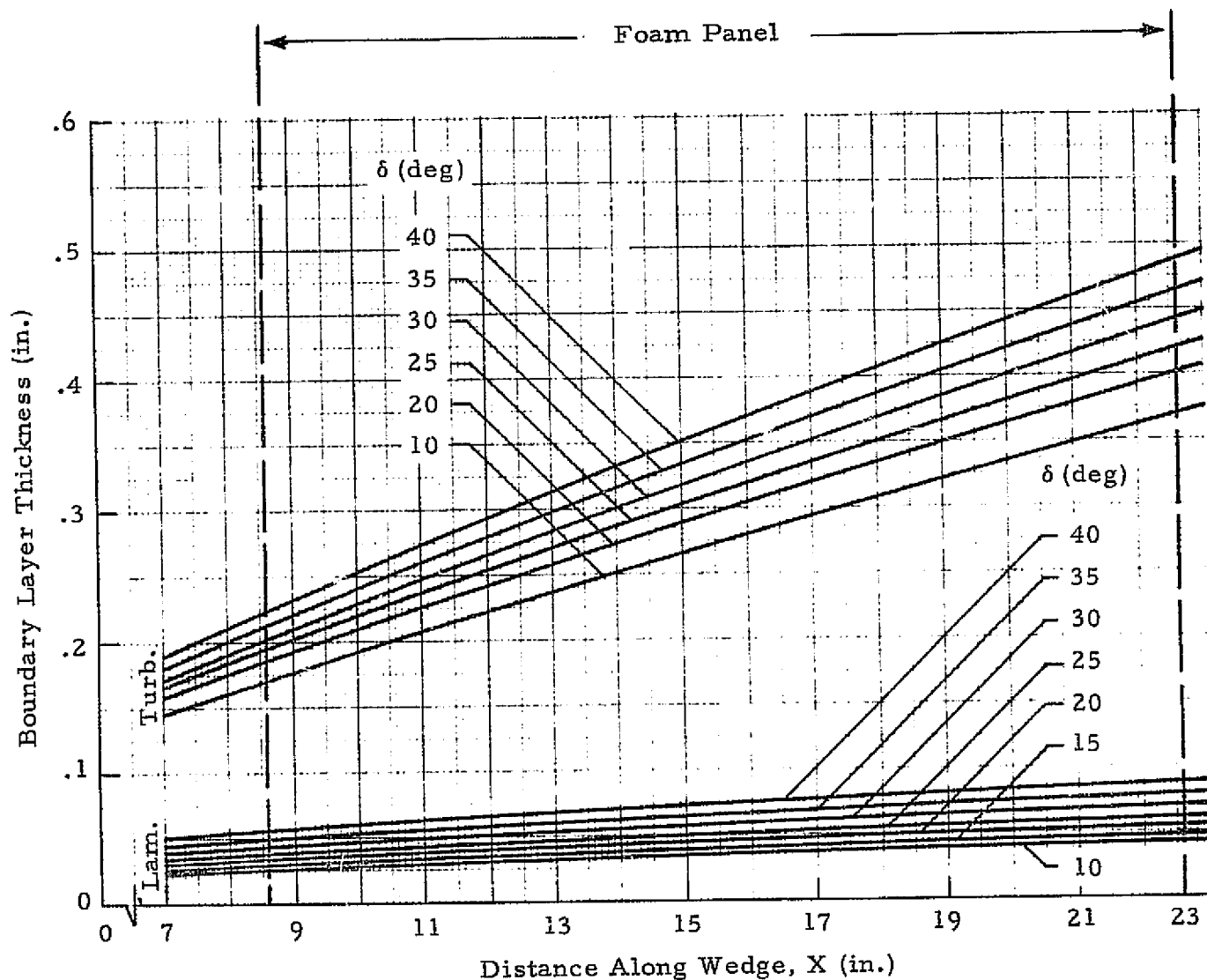


Fig. 27 - Laminar and Turbulent Boundary Layer Thickness vs Distance Along Wedge for $T_o = 1900^\circ R$, $P_o = 1800$ psi

REPRODUCIBILITY OF THE
ORIGINAL PAGE IS POOR

NOTES:

1. $T_o = 1540^\circ R$
2. $P_o = 1800$ psi

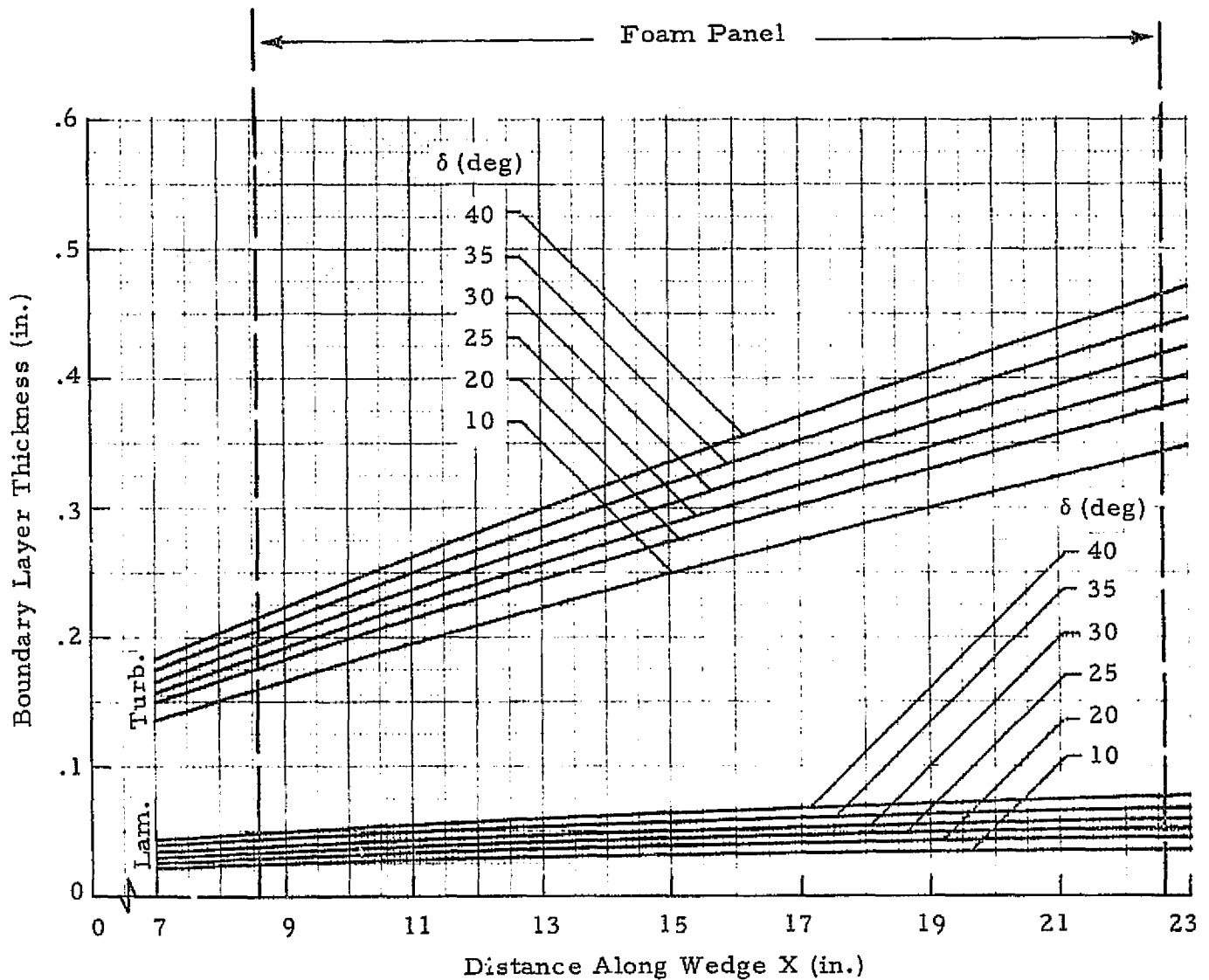


Fig.28 - Laminar and Turbulent Boundary Layer Thickness vs Distance Along Wedge for $T_o = 1540^\circ R$, $P_o = 1800$ psi

NOTES:

1. $P_o = 1800$ psi

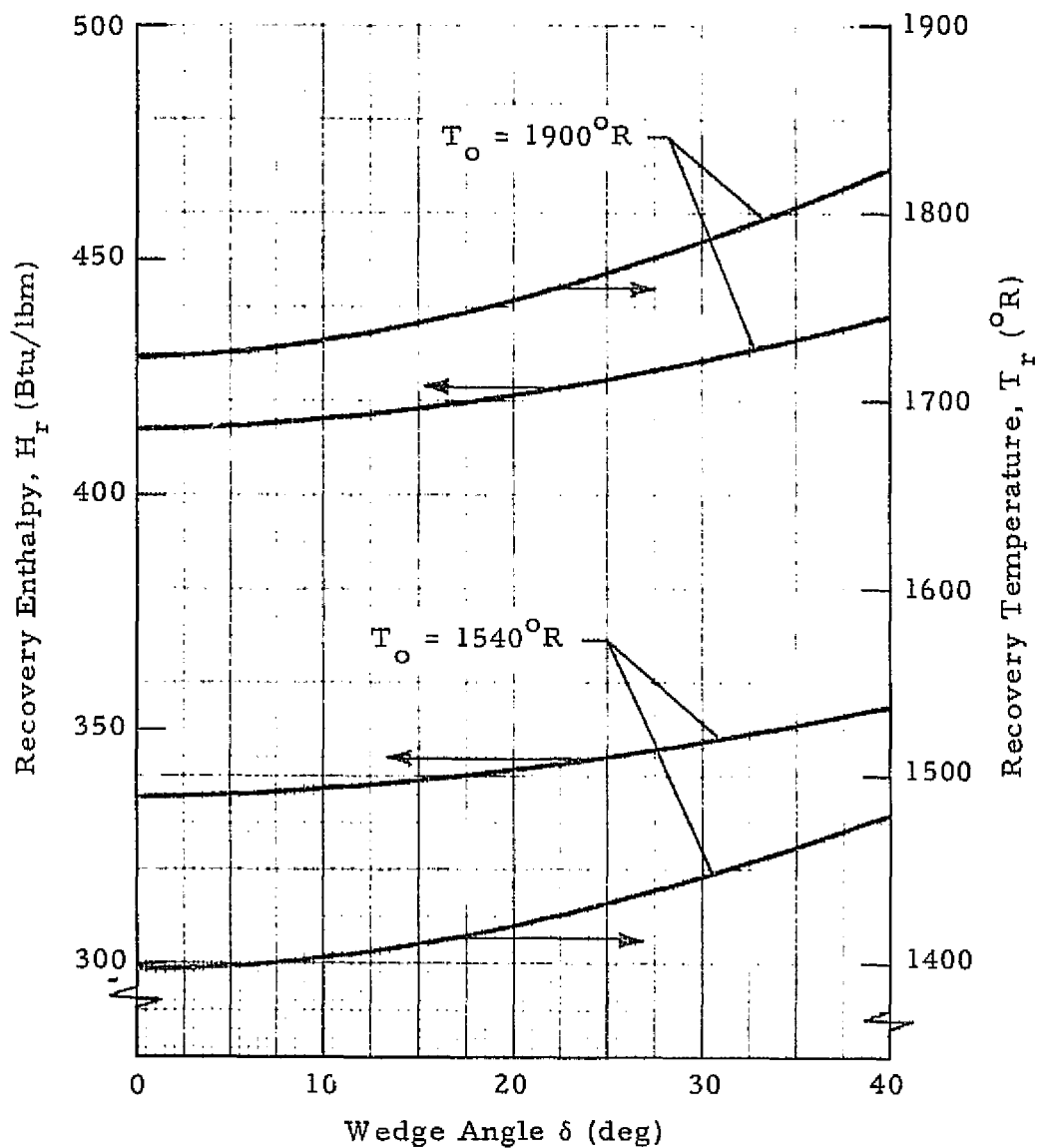


Fig. 29 - Recovery Enthalpy and Recovery Temperature for the Two Run Conditions Used

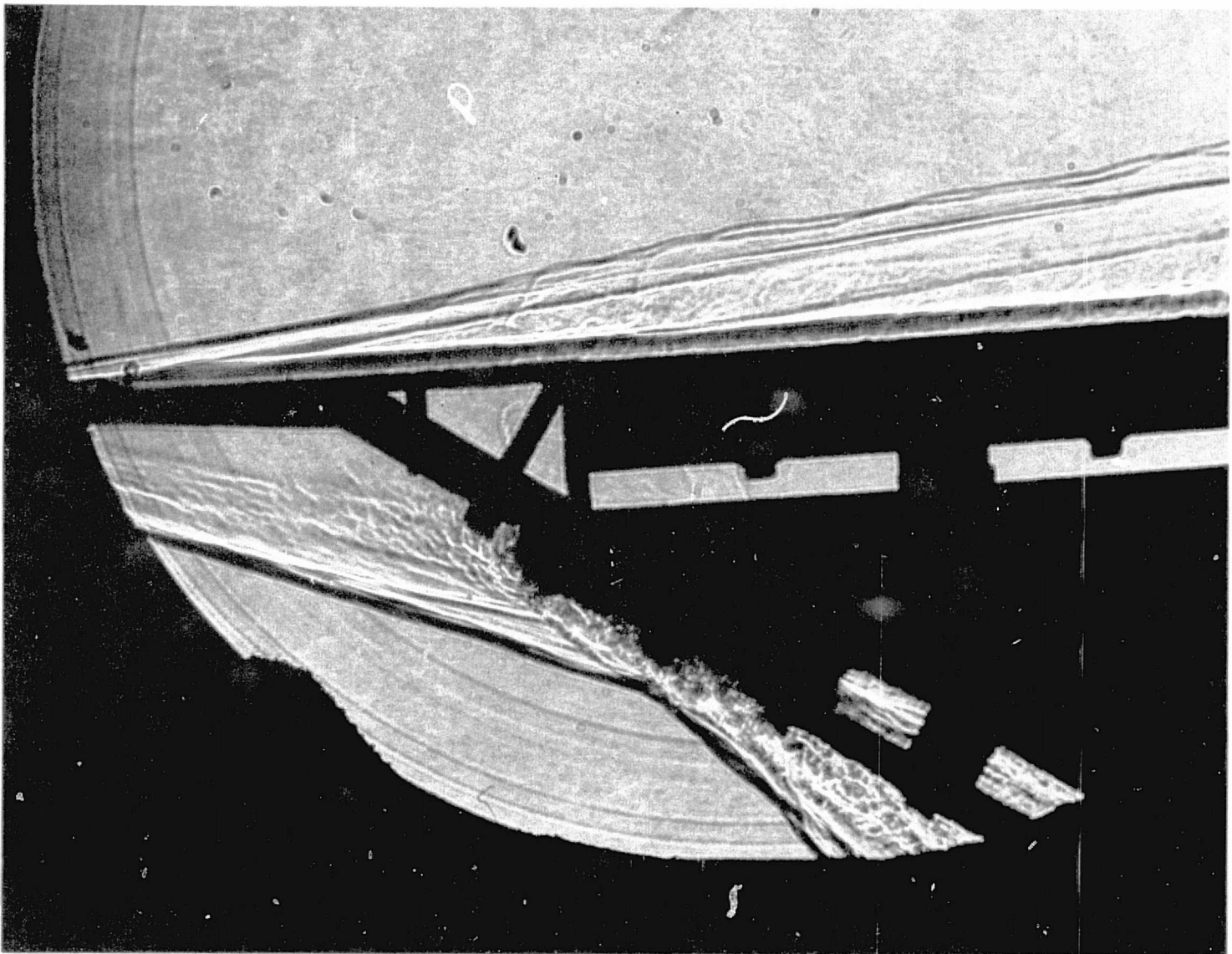


Fig. 30 - Typical Shadowgraph of Wedge Fixture/Steel Calibration Panel with a Wedge Angle of About 6 deg (Group 26)

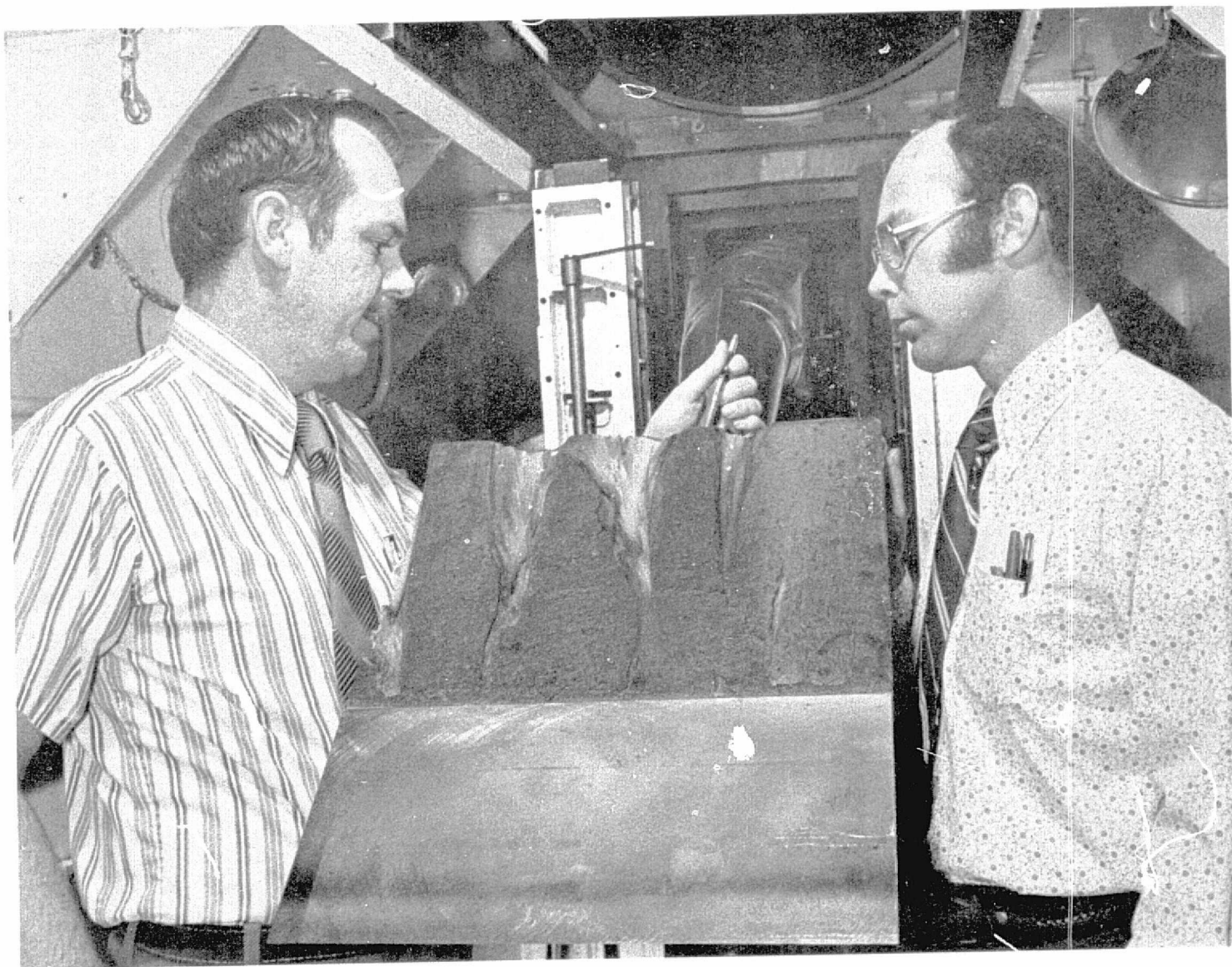


Fig.31 - Typical Post-Test Panel in Tunnel C Test Tank Before Detaching from Wedge Fixture

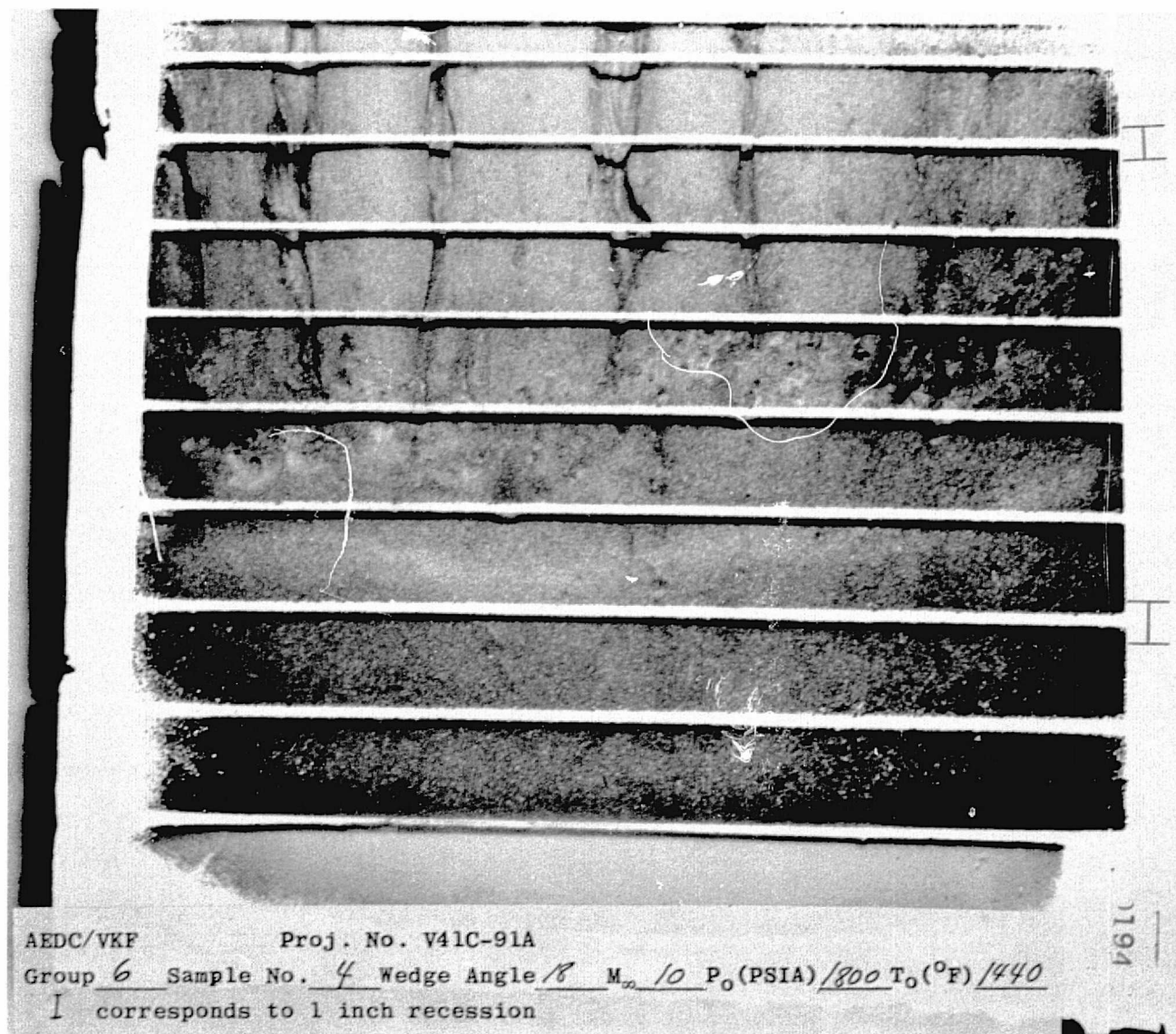


Fig. 32 - "Overlay" Photograph or Double Exposure Superimposing the Tare Shot Grid Lines (White Lines) over the Run Grid Lines (Black Lines). (Note distances marked on right which correspond to 1.0 in. recession.)

Flow
Direction

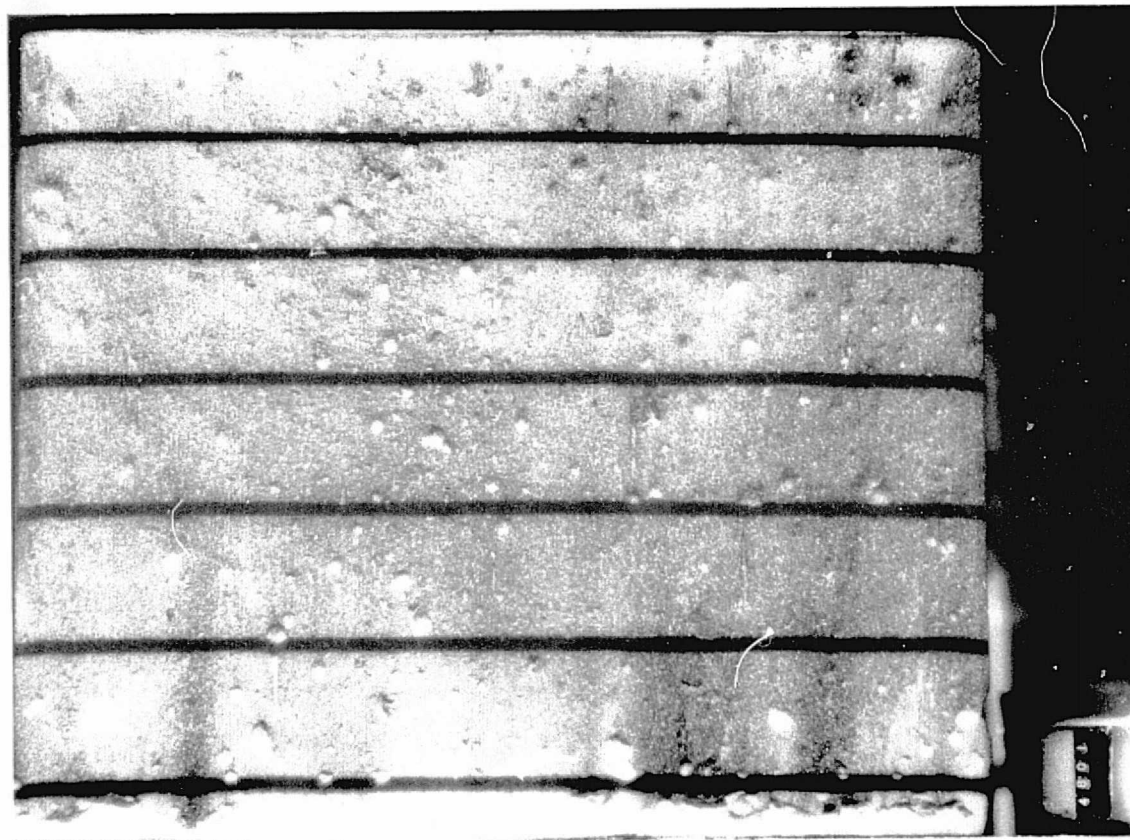


FIGURE 33

Remarks: Some "popcorning." Not much happened to the panel due to heating.

GROUP 77

Sample Description

No. CTC1-26

Matl. CPR-421

Thickness ~ 0.85 in.

Age at Time of Test 61 days

Surface

Machined x

Coated

As-Sprayed

Test Conditions

δ = 9 deg

\dot{q}_{cw} = 4.1 Btu/ft²-sec

P_L = 0.25 psi

τ = 1.5 psf

Test Time

~155 sec

LMSC-HREC TM D390783



FIGURE 34

Remarks: Missing chunks of material on right were lost during or after retraction.

GROUP 9

Sample Description

No. CTC1-5

Matl. CPR-421

Thickness ~ 0.85 in.

Age at Time
of Test 25 days

Surface

Machined x

Coated

As-Sprayed

Test Conditions

δ = 12 deg

\dot{q}_{cw} = 5.2 Btu/ft²-sec

P_L = 0.4 psi

τ = 2.0 psf

Test Time

~125 sec



FIGURE 35

Remarks: Started to streak early in the test but streaks did not seem to grow as fast as at the higher heating rates.

GROUP 28

Sample Description

No. CTC1-11

Matl. CPR-421

Thickness ~ 0.85 in.

Age at Time
of Test 38 days

Surface

Machined x

Coated

As-Sprayed

Test Conditions

δ = 12 deg

\dot{q}_{cw} = 5.2 Btu/ft²-sec

P_L = 0.4 psi

τ = 2.0 psf

Test Time

~ 87 sec

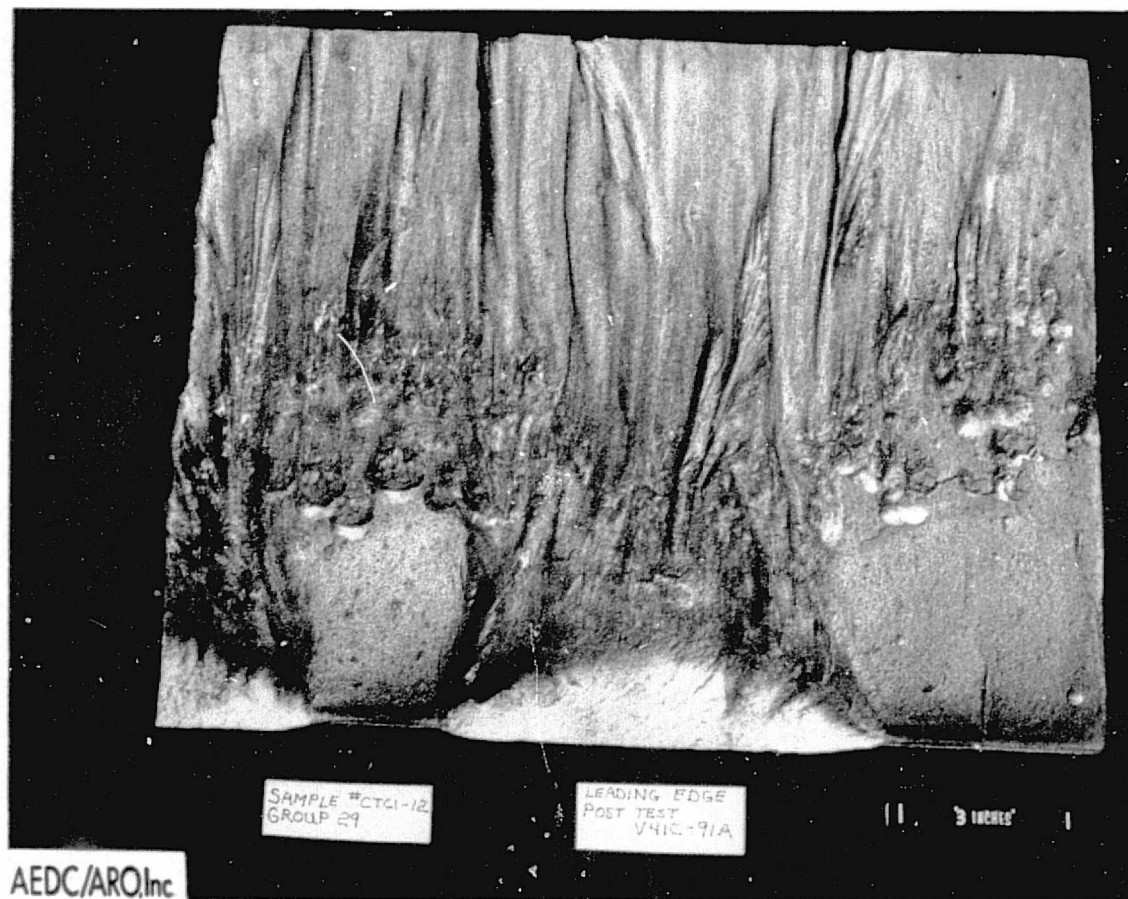


FIGURE 36

Remarks: Chunk came out when tunnel doors were opened.
"Popcorned" at knit line.

GROUP 29Sample DescriptionNo. CTC1-12Matl. CPR-421Thickness ~ 0.85 in.Age at Time
of Test 43 daysSurfaceMachined xCoated As-Sprayed Test Conditions $\delta = 12 \text{ deg}$ $\dot{q}_{cw} = 5.2 \text{ Btu/ft}^2\text{-sec}$ $P_L = 0.4 \text{ psi}$ $\tau = 2.0 \text{ psf}$ Test Time~ 58 sec

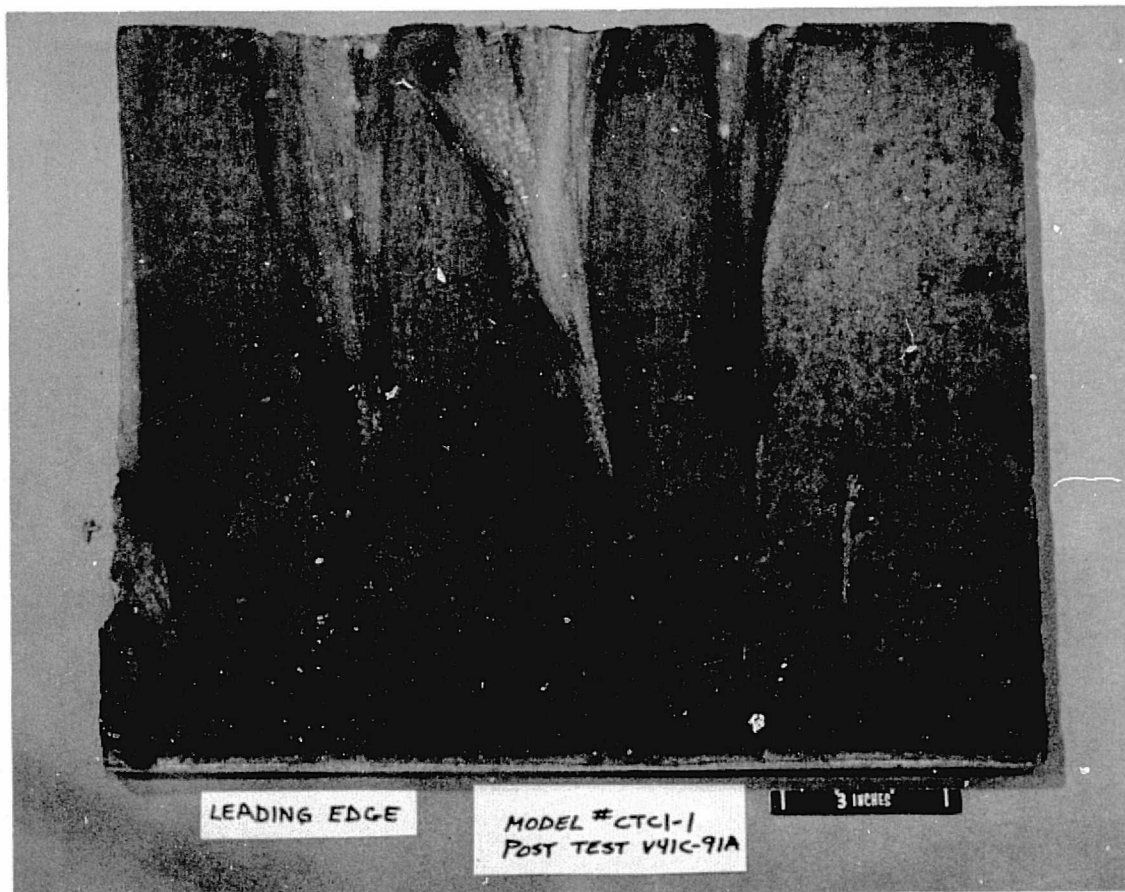


FIGURE 37

Remarks: Panel looked good except for streaks.

GROUP 4

Sample Description

No. CTC1-1

Matl. CPR-421

Thickness ~ 0.85 in.

Age at Time
of Test 28 days

Surface

Machined x

Coated

As-Sprayed

Test Conditions

δ = 18 deg

\dot{q}_{cw} = 7.9 Btu/ft²-sec

P_L = 0.8 psi

τ = 3.2 psf

Test Time

~ 69 sec

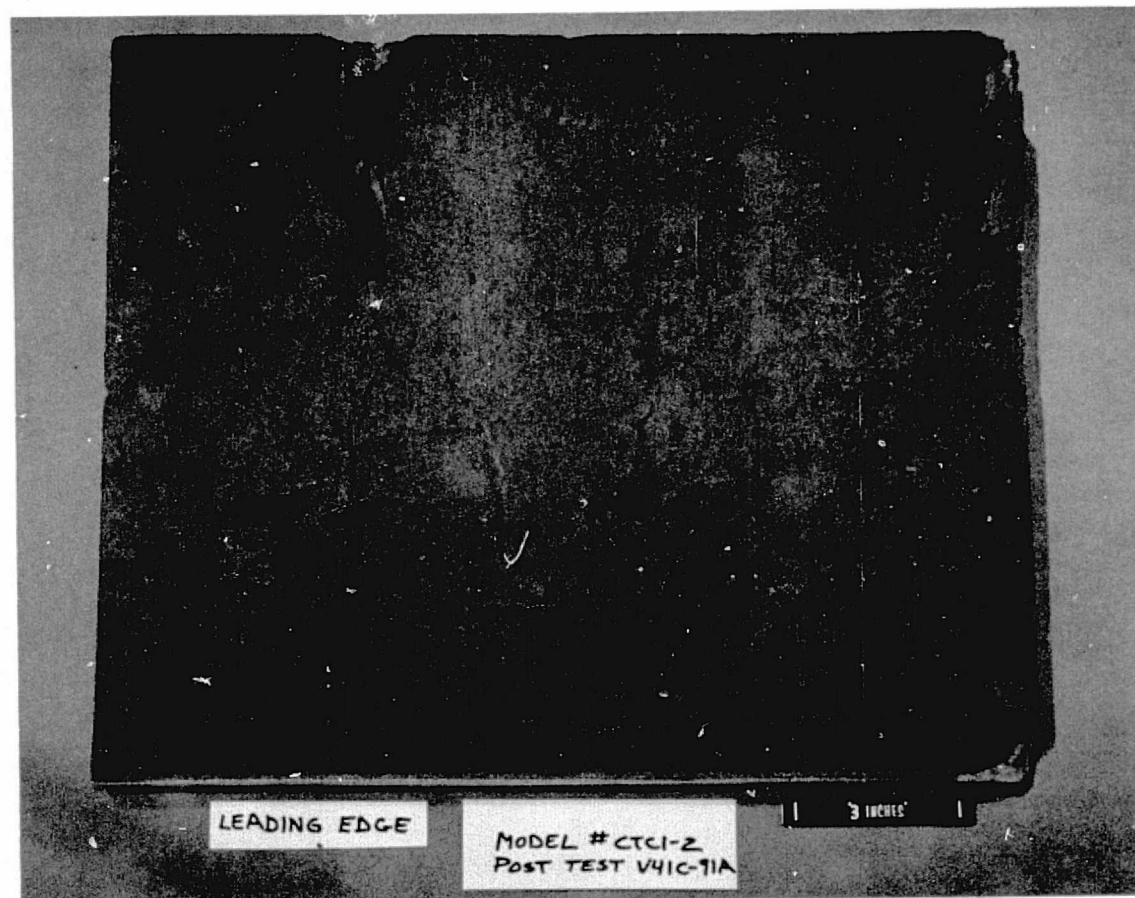


FIGURE 38

GROUP 5Sample DescriptionNo. CTC1-2Matl. CPR-421Thickness ~ 0.85 in.Age at Time
of Test 28 daysSurfaceMachined xCoated As-Sprayed Test Conditions $\delta = 18 \text{ deg}$ $\dot{q}_{cw} = 7.9 \text{ Btu/ft}^2\text{-sec}$ $P_L = 0.8 \text{ psi}$ $\tau = 3.2 \text{ psf}$ Test Time~ 40 sec

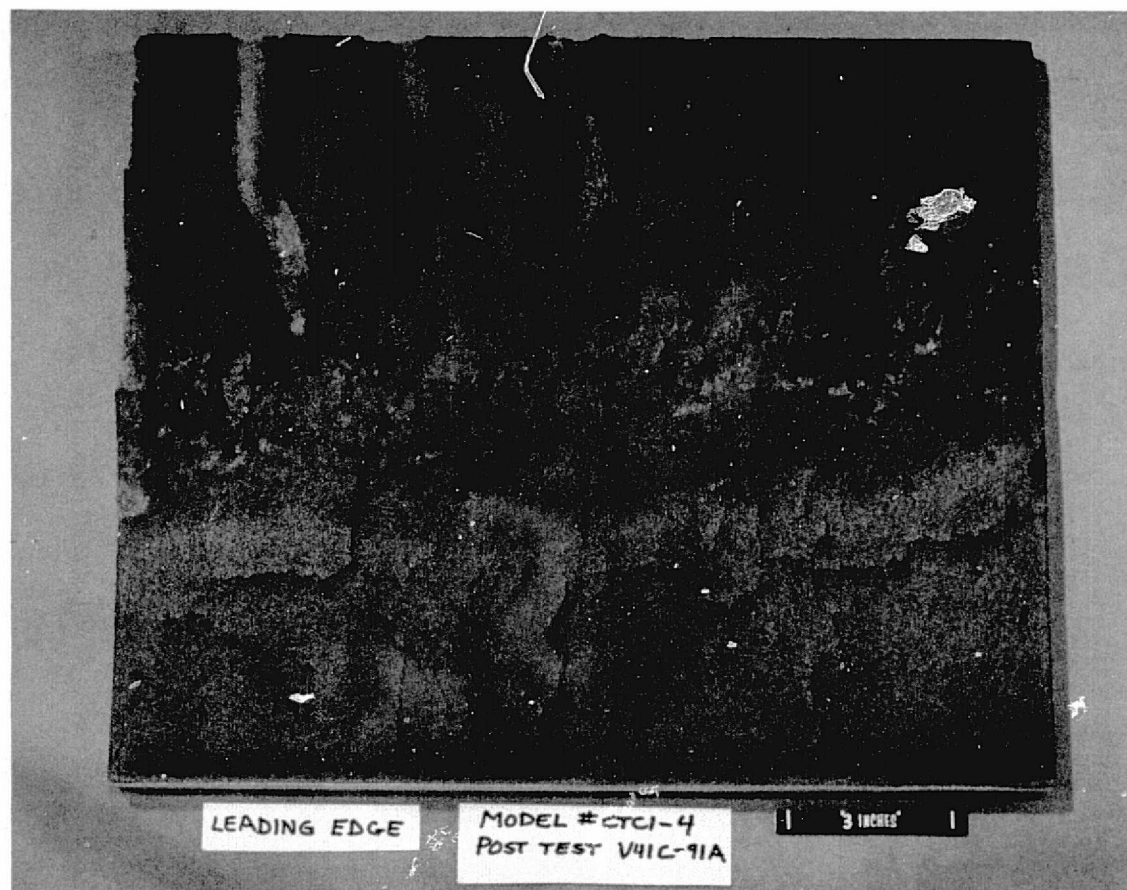


FIGURE 39

Remarks: "Popcorned" right after injection near knit line. Notice difference in char downstream and upstream of knit line.

GROUP 6

Sample Description

No. CTC1-4

Matl. CPR-421

Thickness ~ 0.85 in.

Age at Time
of Test 29 days

Surface

Machined x

Coated

As-Sprayed

Test Conditions

δ = 18 deg

\dot{q}_{cw} = 7.9 Btu/ft²-sec

P_L = 0.8 psi

τ = 3.2 psf

Test Time

~ 42 sec



FIGURE 40

Remarks: Streaks seemed to start from cracks in the char.

GROUP 30

Sample Description

No. CTC1-14

Matl. CPR-421

Thickness ~ 0.85 in.

Age at Time
of Test 38 days

Surface

Machined x

Coated

As-Sprayed

Test Conditions

δ = 18 deg

\dot{q}_{cw} = 7.9 Btu/ft²-sec

P_L = 0.8 psi

τ = 3.2 psf

Test Time

~ 63 sec

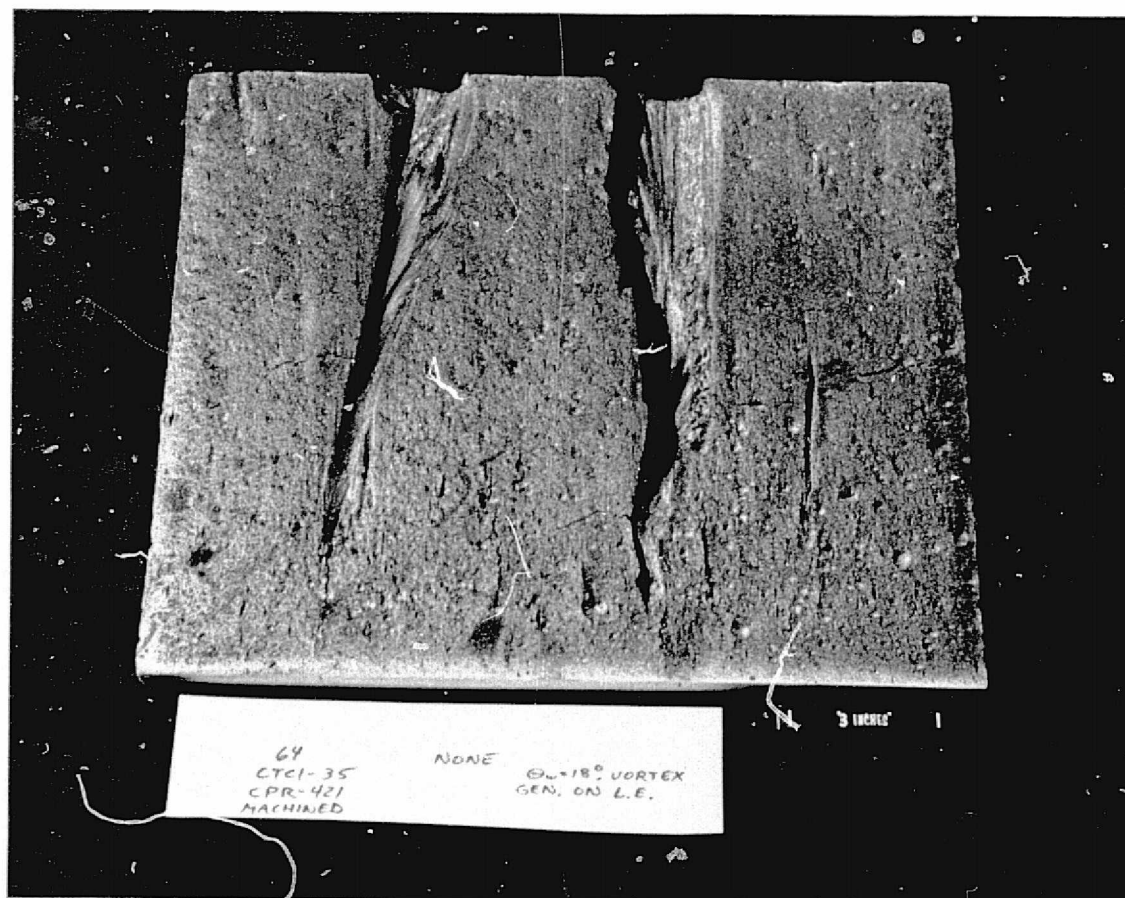


FIGURE 41

Remarks: Test run with 0.25 inch high vortex generator on wedge leading edge. Streaks on right side of panel occurred behind the vortex generator.

GROUP 64Sample DescriptionNo. CTC1-35Matl. CPR-421Thickness ~ 0.85 in.Age at Time
of Test 59 daysSurfaceMachined xCoated As-Sprayed Test Conditions $\delta = 18 \text{ deg}$ $\dot{q}_{cw} = 7.9 \text{ Btu/ft}^2\text{-sec}$ $P_L = 0.8 \text{ psi}$ $\tau = 3.2 \text{ psf}$ Test Time~ 62 sec

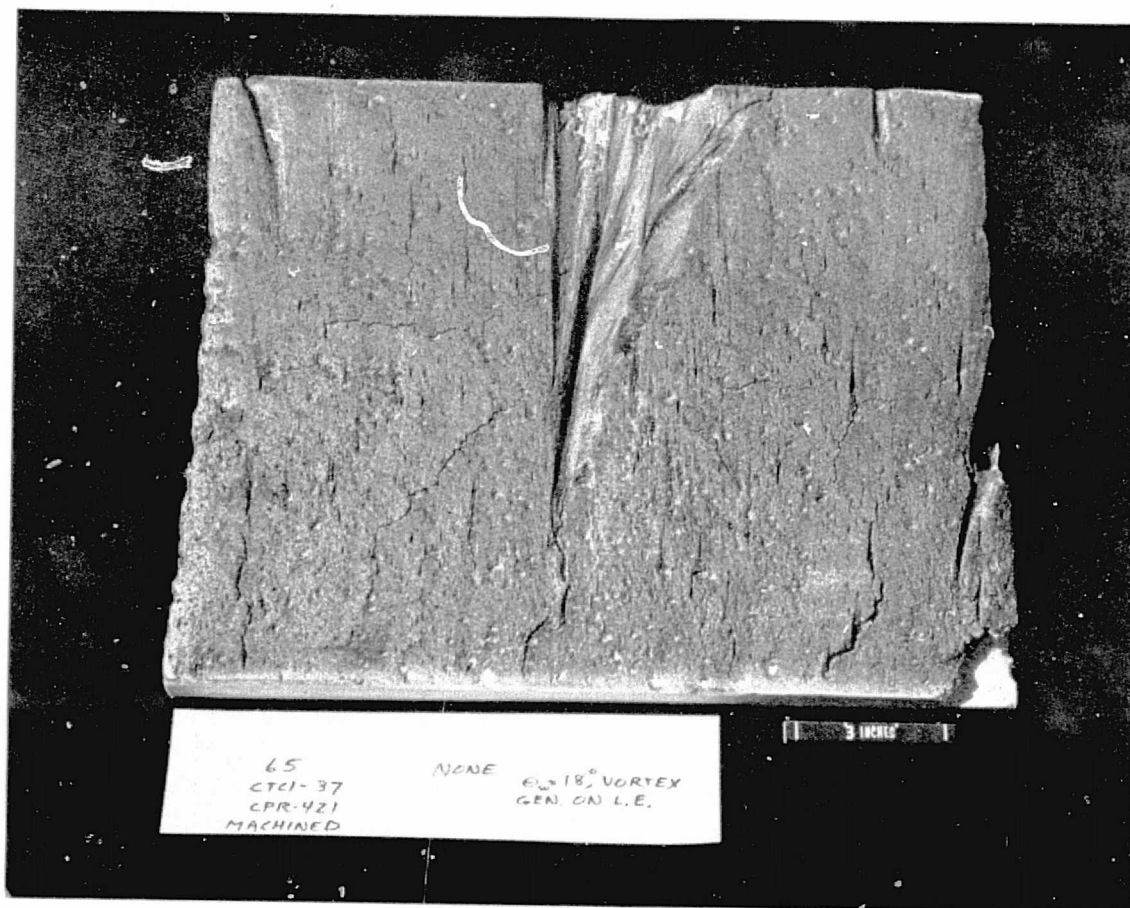


FIGURE 42

Remarks: Test run with a 0.25 inch high vortex generator on wedge leading edge. Streak did not occur right behind the vortex generator.

GROUP 65Sample DescriptionNo. CTC1-37Matl. CPR-421Thickness ~ 0.85 in.Age at Time
of Test 59 daysSurfaceMachined xCoated As-Sprayed Test Conditions $\delta = 18 \text{ deg}$ $\dot{q}_{cw} = 7.9 \text{ Btu/ft}^2\text{-sec}$ $P_L = 0.8 \text{ psi}$ $\tau = 3.2 \text{ psf}$ Test Time~ 85 sec

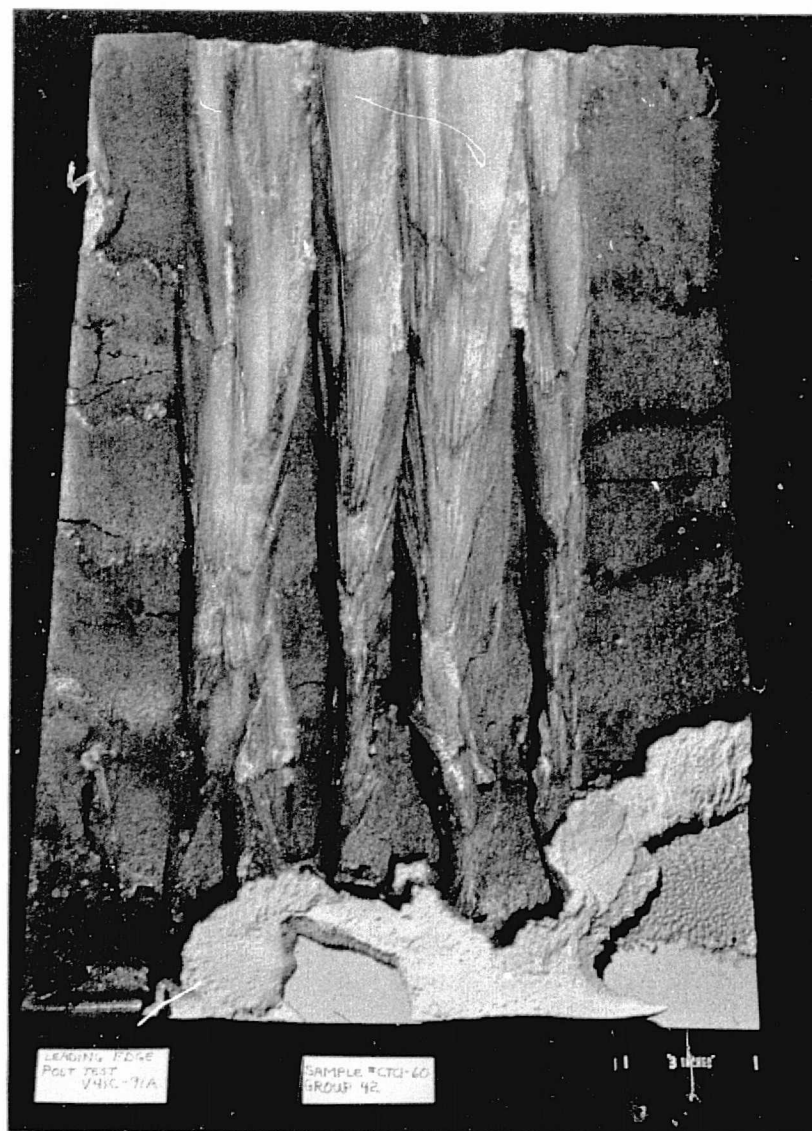


FIGURE 43

Remarks: Streaks got wider and wider as they proceeded toward the trailing edge of the panel. Panel "debonded" from the aluminum after retraction from the tunnel in some areas. Panel size = 17 wide x 26 inches long.

GROUP 42Sample DescriptionNo. CTC1-60Matl. CPR-421Thickness ~ 0.85 in.Age at Time
of Test 7 daysSurfaceMachined xCoated As-Sprayed Test Conditions $\delta = 18 \text{ deg}$ $\dot{q}_{cw} = 7.9 \text{ Btu/ft}^2\text{-sec}$ $P_L = 0.8 \text{ psi}$ $\tau = 3.2 \text{ psf}$ Test Time~ 62 sec

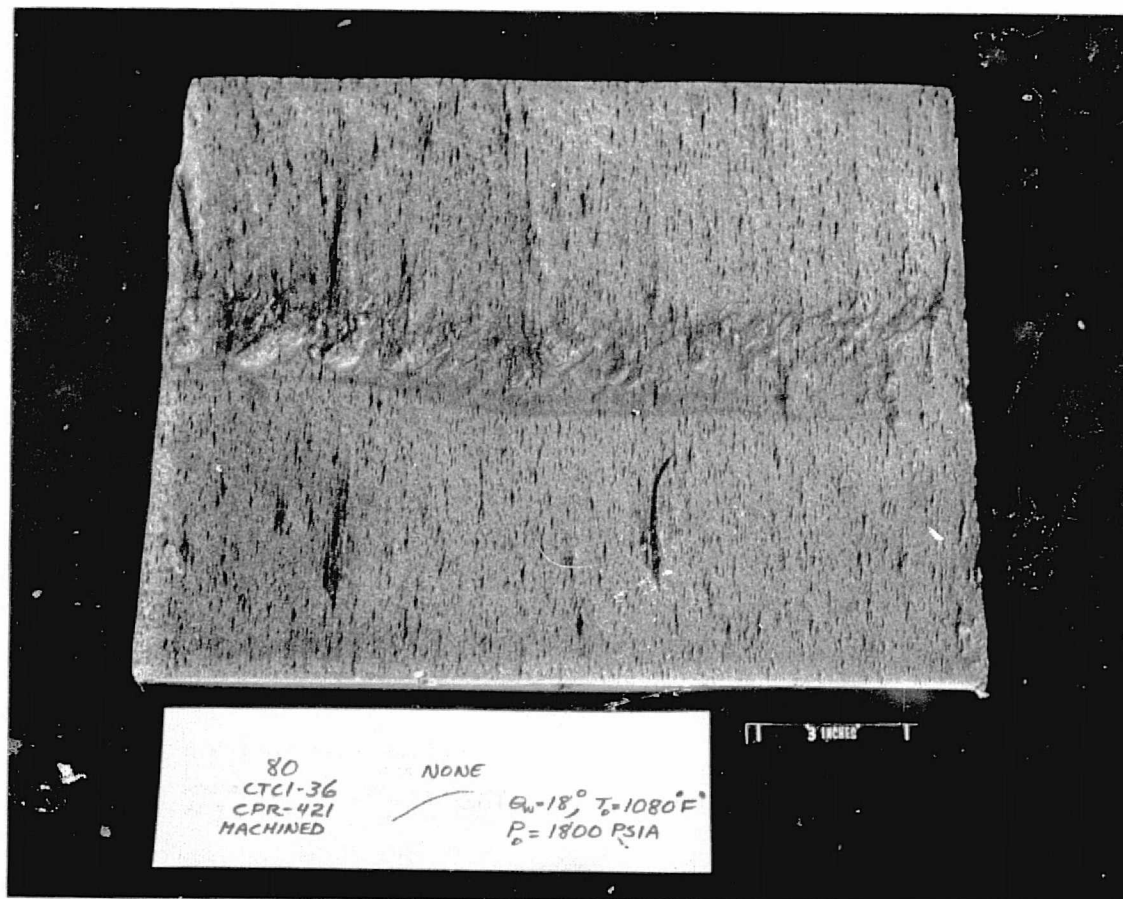


FIGURE 44

Remarks: This panel was run at $T_0 = 1500^\circ\text{R}$. "Popcorned" some at knit line. Some streaks tried to form. Panel char layer had a distinctly different color which was a much lighter brown than the panel run at the 1900°R total temperature.

GROUP 80Sample DescriptionNo. CTC1-36Matl. CPR-421Thickness ~ 0.85 in.Age at Time
of Test 66 daysSurfaceMachined xCoated As-Sprayed Test Conditions $\delta = 18 \text{ deg}$ $\dot{q}_{cw} = 7.6 \text{ Btu/ft}^2\text{-sec}$ $P_L = 0.8 \text{ psi}$ $\tau = 3.2 \text{ psf}$ Test Time~ 144 sec

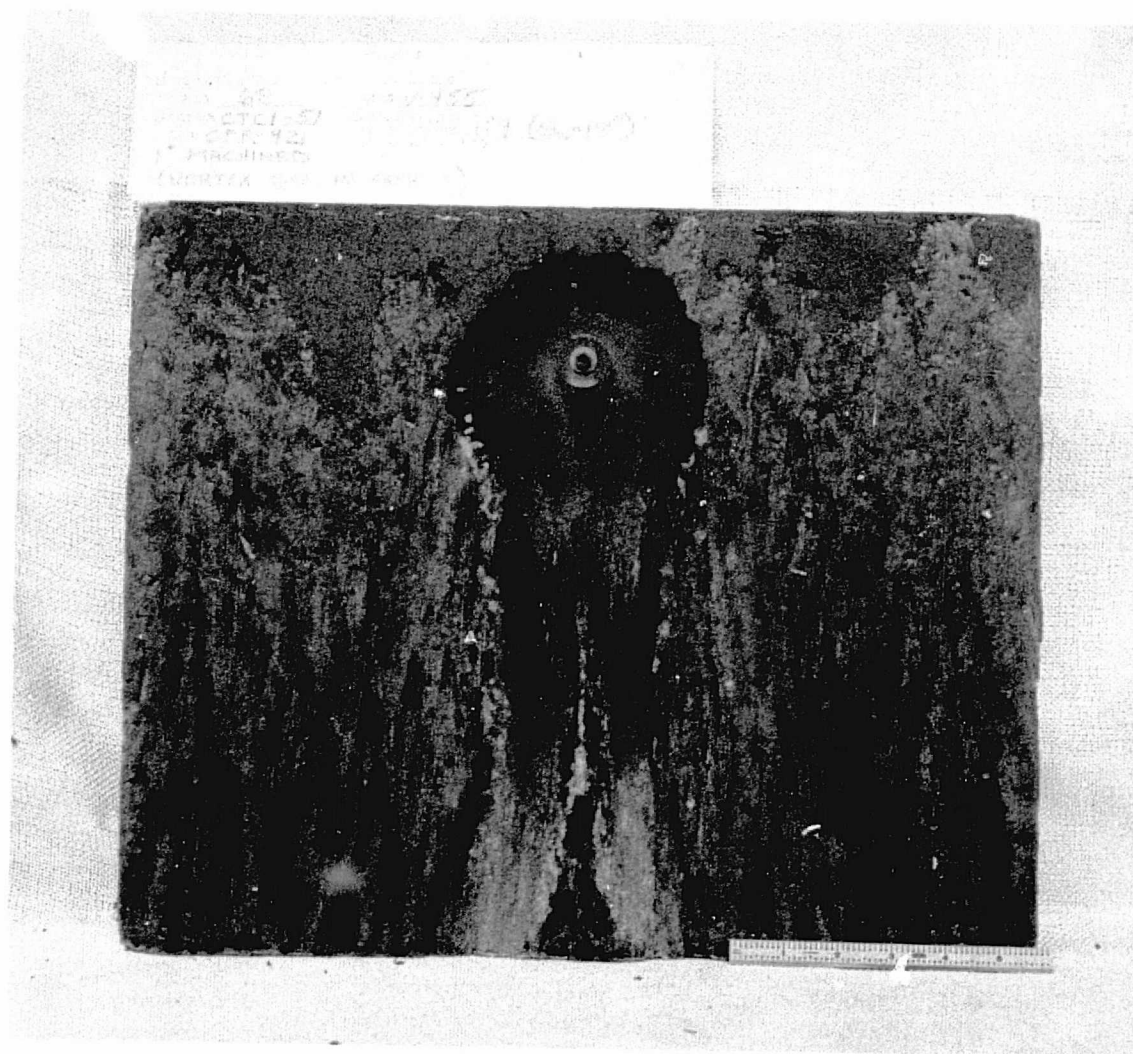


FIGURE 45

Remarks: Panel burned through to the aluminum very rapidly. Note some coating remaining near leading edge. Flow direction is from top to bottom in this photo.

GROUP 63Sample DescriptionNo. CTC1-51Matl. CPR-421Thickness ~ 0.85 in.Age at Time
of Test 59 daysSurfaceMachined xCoated xAs-Sprayed Test Conditions $\delta = 18 \text{ deg}$ $\dot{q}_{cw} = 7.9 \text{ Btu/ft}^2\text{-sec}$ $P_L = 0.8 \text{ psi}$ $\tau = 3.2 \text{ psf}$ Test Time~ 20 sec

NO

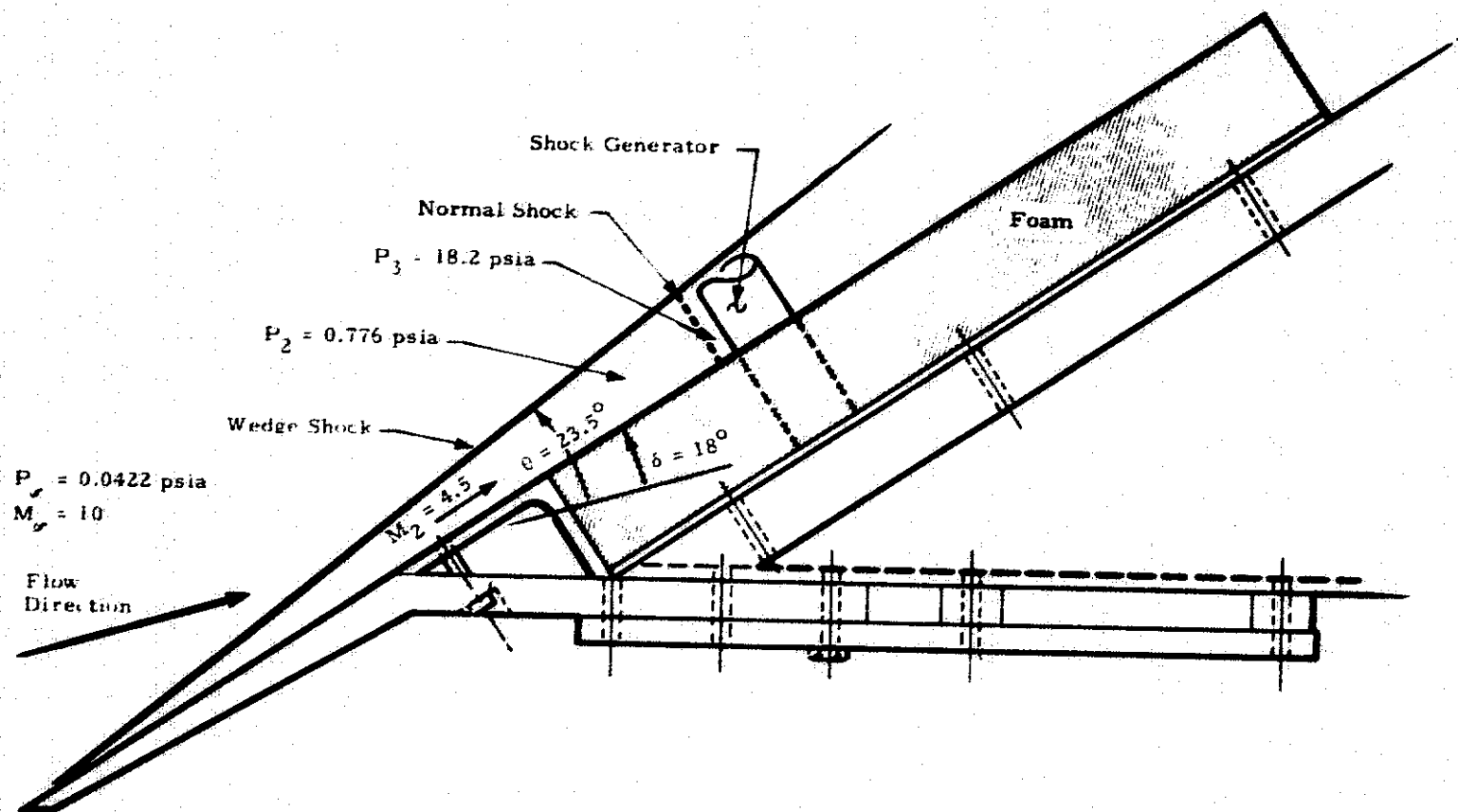


Fig. 46 - Comparison of Pressures Before and After Normal Shock in Front of Shock Generator in Foam for a Wedge Angle of 18 deg

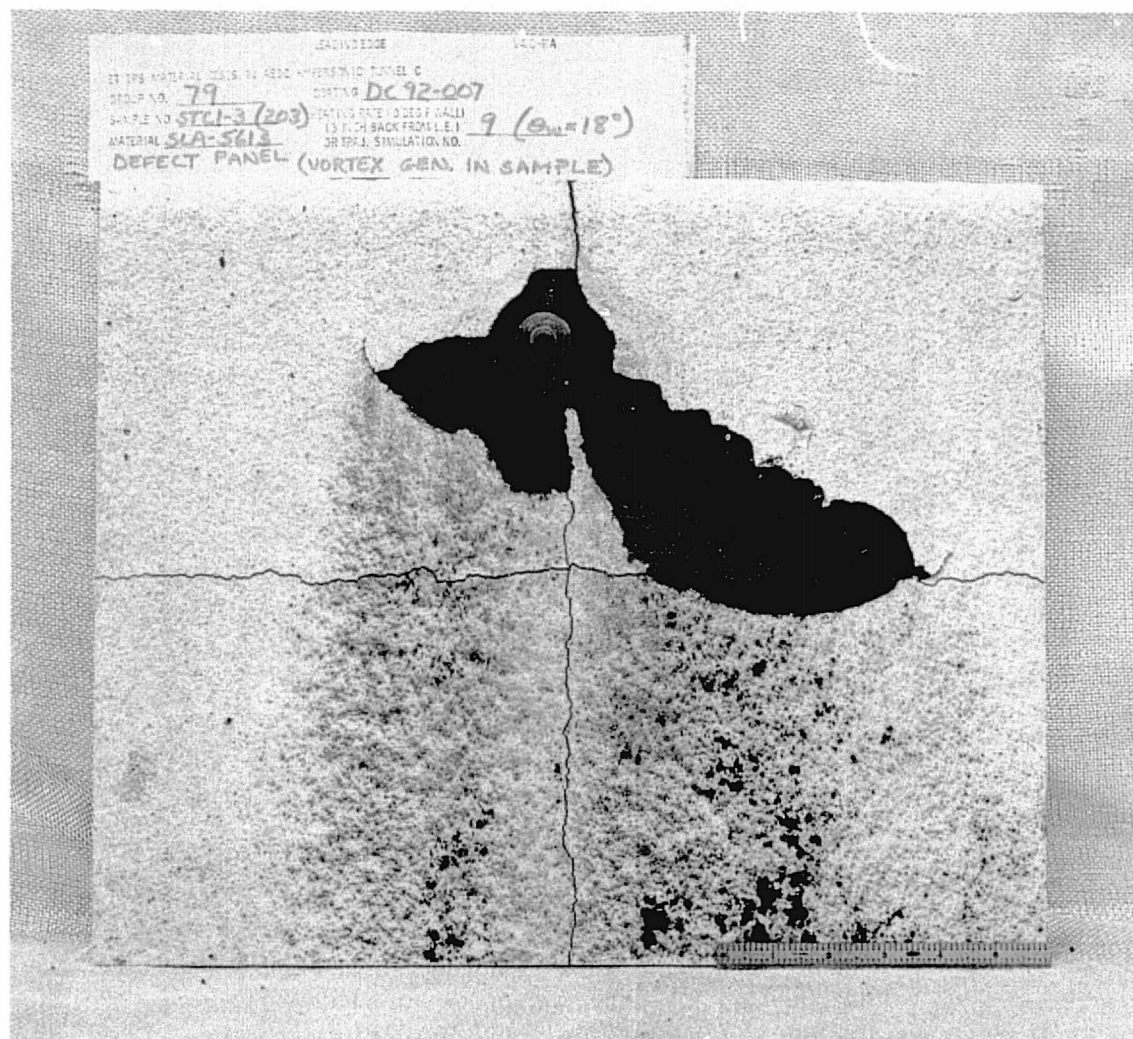


FIGURE 47

Remarks: SLA-561 panel with pretest cracks and shock generator mounted on aluminum and protruding through panel surface. Panel burned through to aluminum in front of protuberance. Shock generator protruded about 0.50 inches above SLA surface.

GROUP 79

Sample Description

No. STC1-3 (203)

Matl. SLA-561s

Thickness ~ 0.5 in.

Age at Time
of Test -

Surface

Machined -

Coated x

As-Sprayed x

Test Conditions

$\delta = 18 \text{ deg}$

$\dot{q}_{cw} = 7.9 \text{ Btu/ft}^2\text{-sec}$

$P_L = 0.8 \text{ psi}$

$\tau = 3.2 \text{ psf}$

Test Time

~ 60 sec

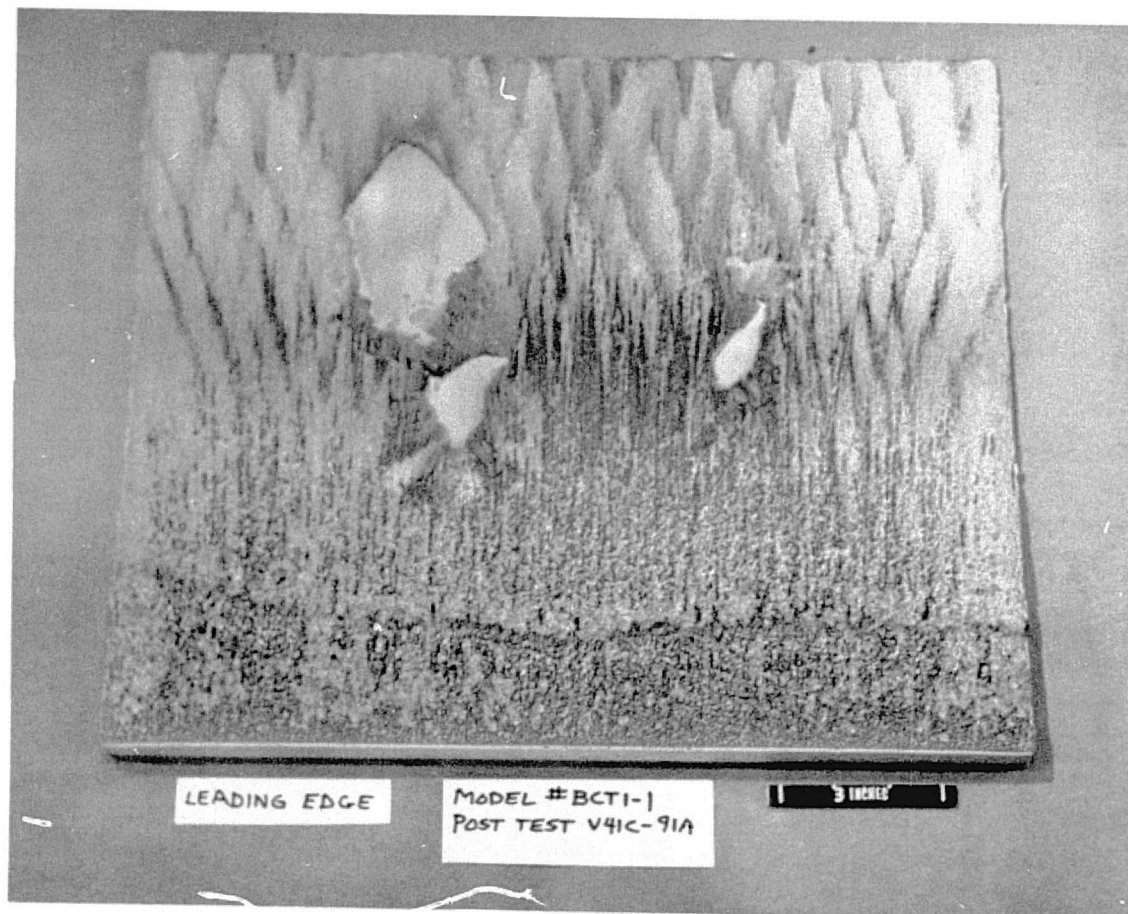


FIGURE 48

Remarks: BX-250. Panel receded through to the aluminum backup plate.

GROUP 7

Sample Description

No. BCT1-1

Matl. BX-250

Thickness ~ 0.85 in.

Age at Time
of Test -

Surface

Machined x

Coated -

As-Sprayed -

Test Conditions

$\delta = 18$ deg

$\dot{q}_{cw} = 7.9$ Btu/ft²-sec

$P_L = 0.8$ psi

$\tau = 3.2$ psf

Test Time

~ 37 sec

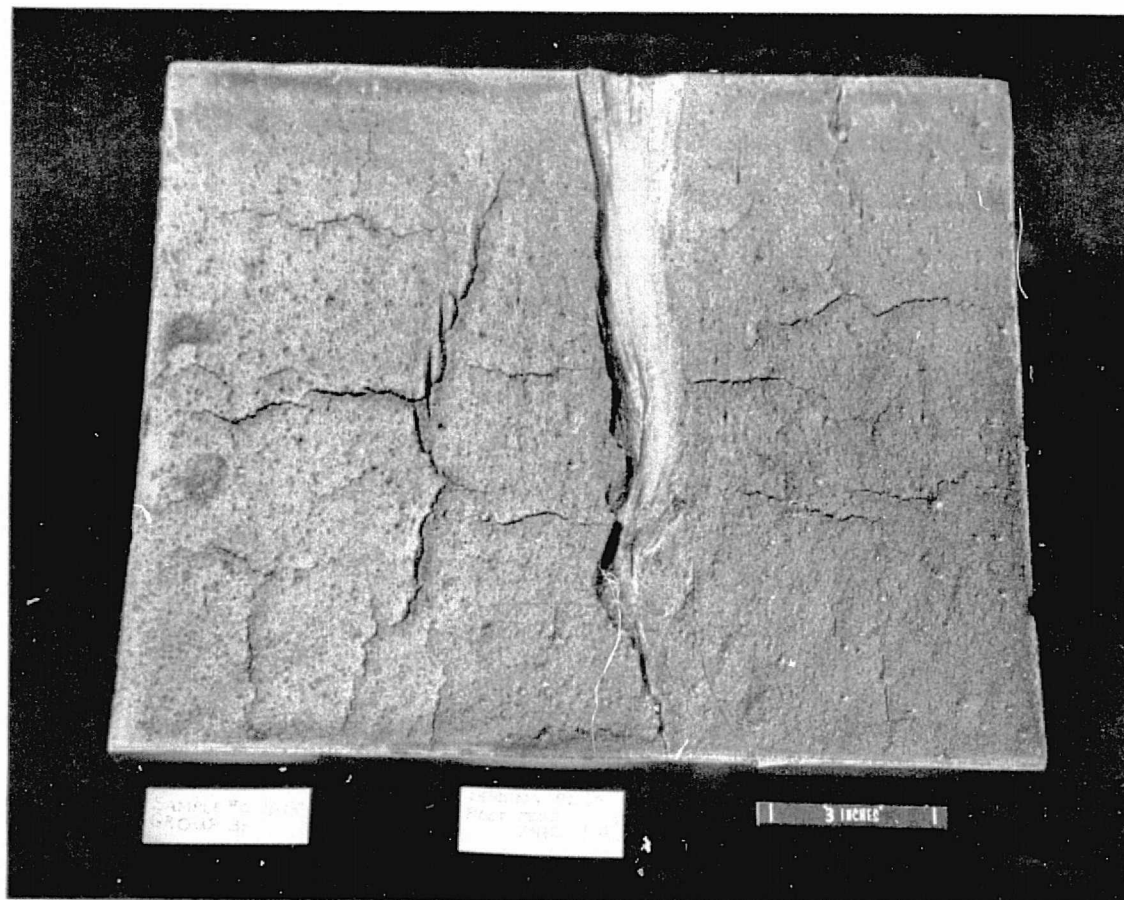


FIGURE 49

Remarks: Note some remains of Tempilaq phase change coating stripes near trailing edge.

GROUP 31Sample DescriptionNo. CTC1-15Matl. CPR-421Thickness ~ 0.85 in.Age at Time
of Test 38 daysSurfaceMachined xCoated As-Sprayed Test Conditions $\delta = 20$ deg $\dot{q}_{cw} = 8.7$ Btu/ft²-sec $P_L = 1.0$ psi $\tau = 3.5$ psfTest Time~ 57 sec

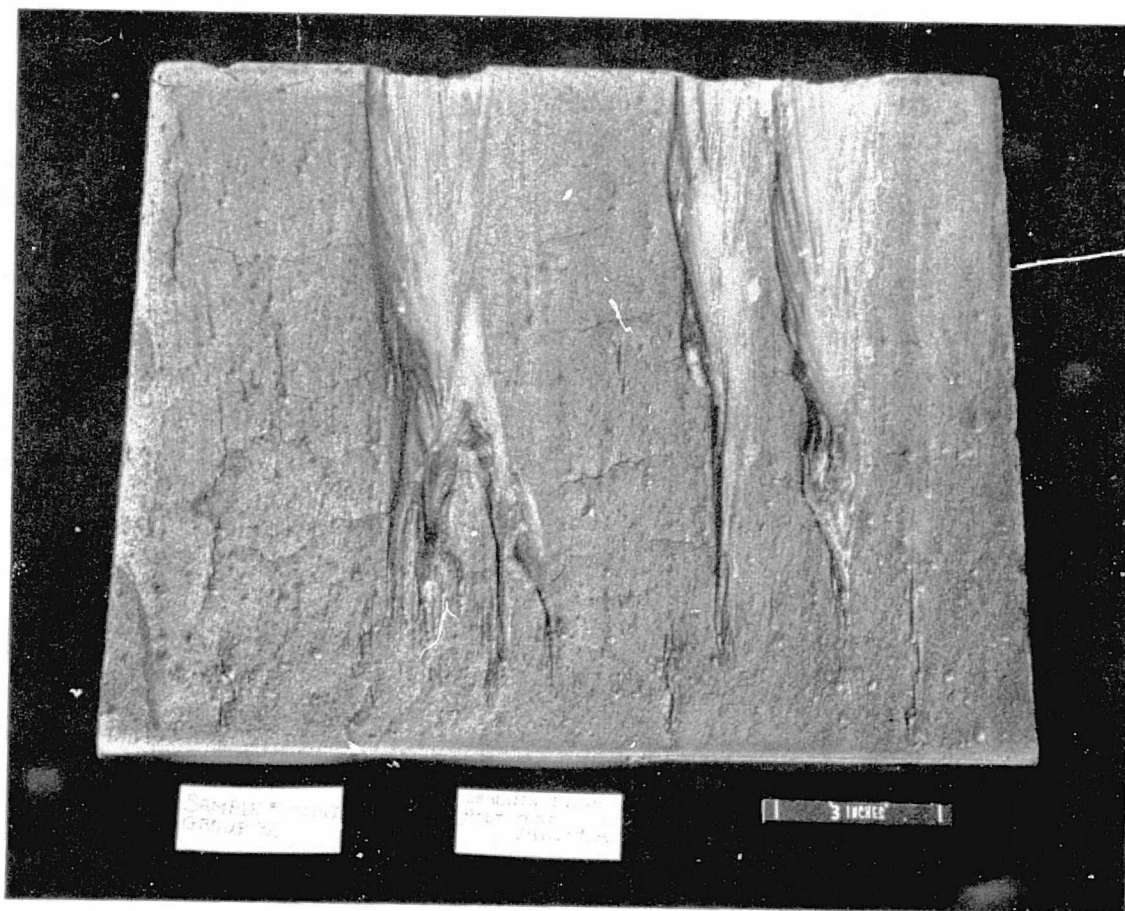


FIGURE 50

Remarks: Tempilaq seemed to disappear very quickly. Streaks were growing without having a preceding crack in the char layer.

GROUP 32Sample DescriptionNo. CTC1-17Matl. CPR-421Thickness ~ 0.85 in.Age at Time
of Test 38 daysSurfaceMachined xCoated As-Sprayed Test Conditions $\delta = 20$ deg $\dot{q}_{cw} = 8.7$ Btu/ft²-sec $P_L = 1.0$ psi $\tau = 3.5$ psfTest Time~ 36 sec

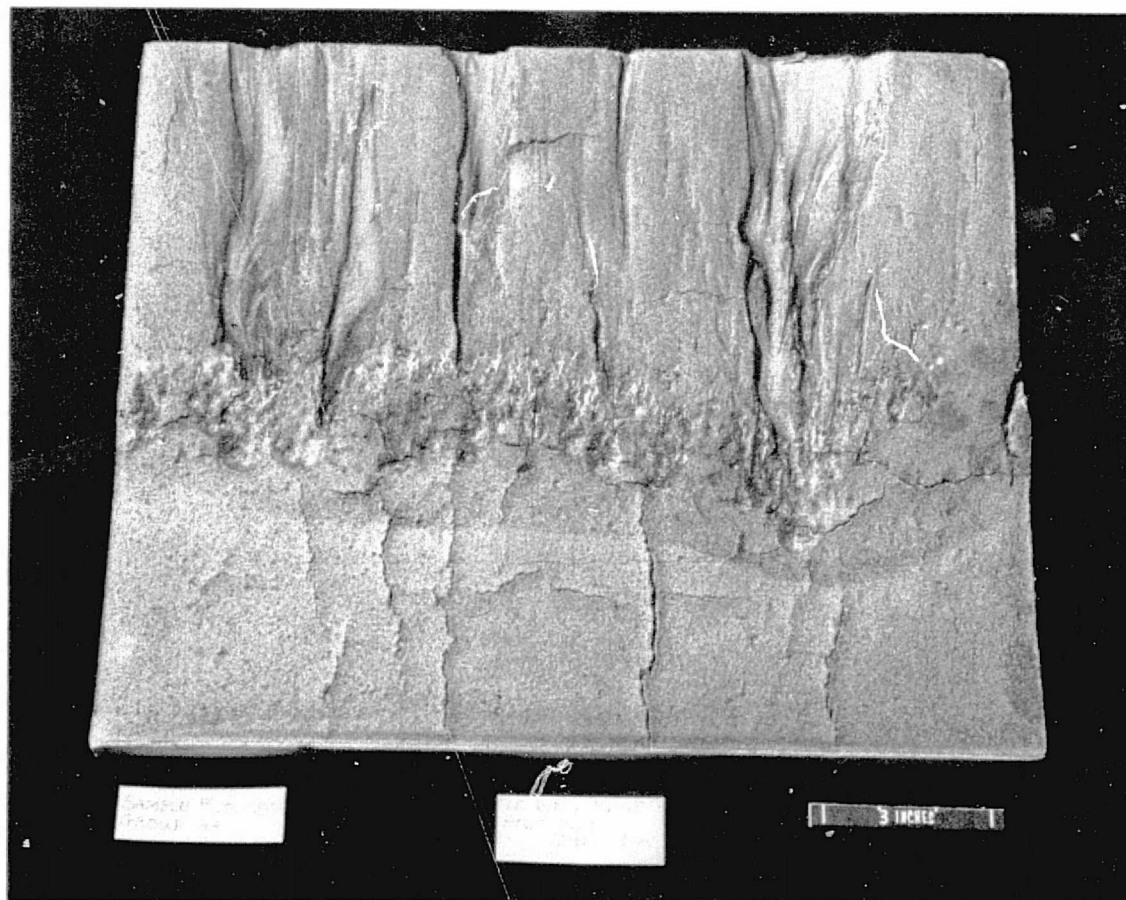


FIGURE 51

Remarks: Some chunks or "popcorn" came out at knit line before injection.

GROUP 33Sample DescriptionNo. CTC1-20Matl. CPR-421Thickness ~ 0.85 in.Age at Time
of Test 43 daysSurfaceMachined xCoated As-Sprayed Test Conditions $\delta = 20 \text{ deg}$ $\dot{q}_{cw} = 8.7 \text{ Btu/ft}^2\text{-sec}$ $P_L = 1.0 \text{ psi}$ $\tau = 3.5 \text{ psf}$ Test Time~ 39 sec

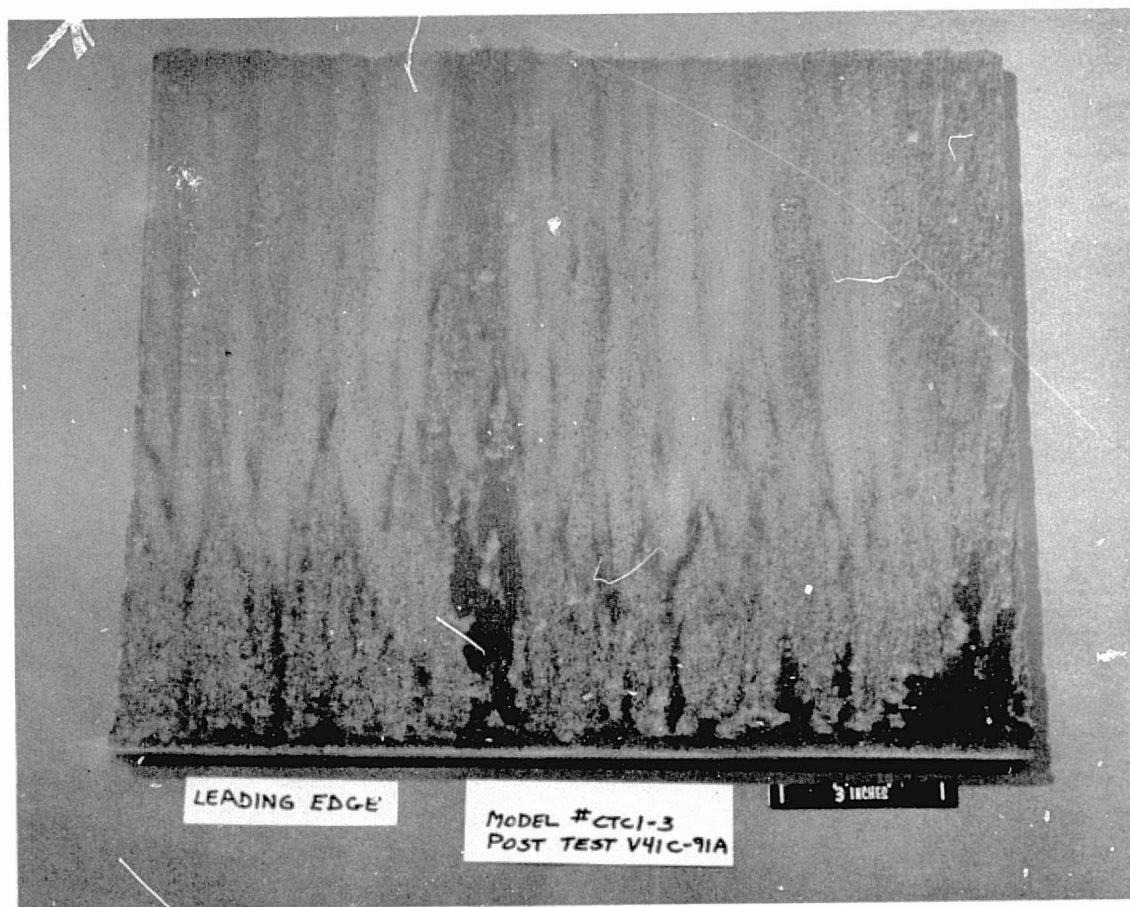


FIGURE 52

Remarks: Lost most of char on retraction.

GROUP 8Sample DescriptionNo. CTC1-3Matl. CPR-421Thickness ~ 0.85 in.Age at Time
of Test 16 daysSurfaceMachined xCoated As-Sprayed Test Conditions $\delta = 23.5 \text{ deg}$ $\dot{q}_{cw} = 10 \text{ Btu/ft}^2\text{-sec}$ $P_L = 1.25 \text{ psi}$ $\tau = 4.0 \text{ psf}$ Test Time~ 15 sec

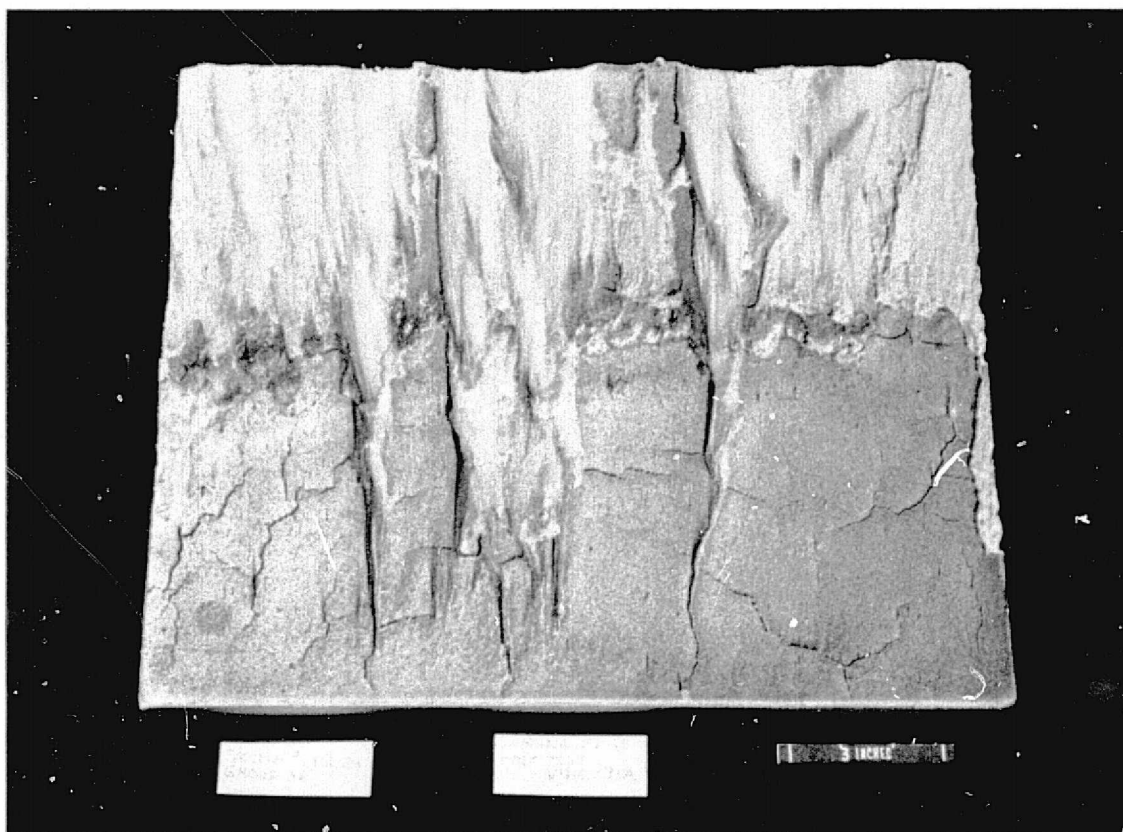


FIGURE 53

Remarks: Note difference in appearance in panel/char in front of and behind knit line.

GROUP 36

Sample Description

No. CTC1-24

Matl. CPR-421

Thickness ~ 0.85 in.

Age at Time
of Test 43 days

Surface

Machined x

Coated

As-Sprayed

Test Conditions

δ = 23.5 deg

\dot{q}_{cw} = 10 Btu/ft²-sec

P_L = 1.25 psi

τ = 4.0 psf

Test Time

~ 30 sec

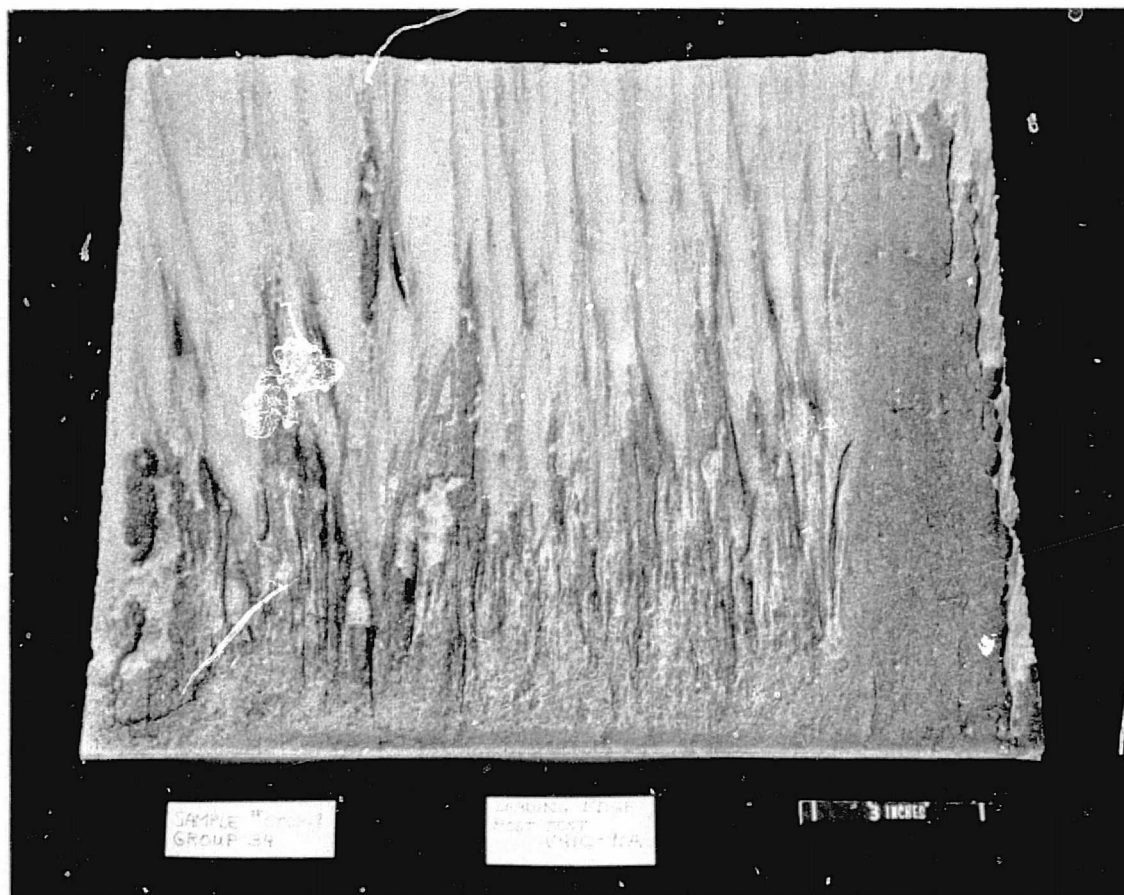


FIGURE 54

Remarks: Used Tempilaq strips on rear of model to try to determine surface temperature.

GROUP 34

Sample Description

No. CTC1-19

Matl. CPR-421

Thickness ~ 0.85 in.

Age at Time
of Test 38 days

Surface

Machined x

Coated

As-Sprayed

Test Conditions

δ = 23.5 deg

\dot{q}_{cw} = 10 Btu/ft²-sec

P_L = 1.25 psi

τ = 4.0 psf

Test Time

~ 22 sec

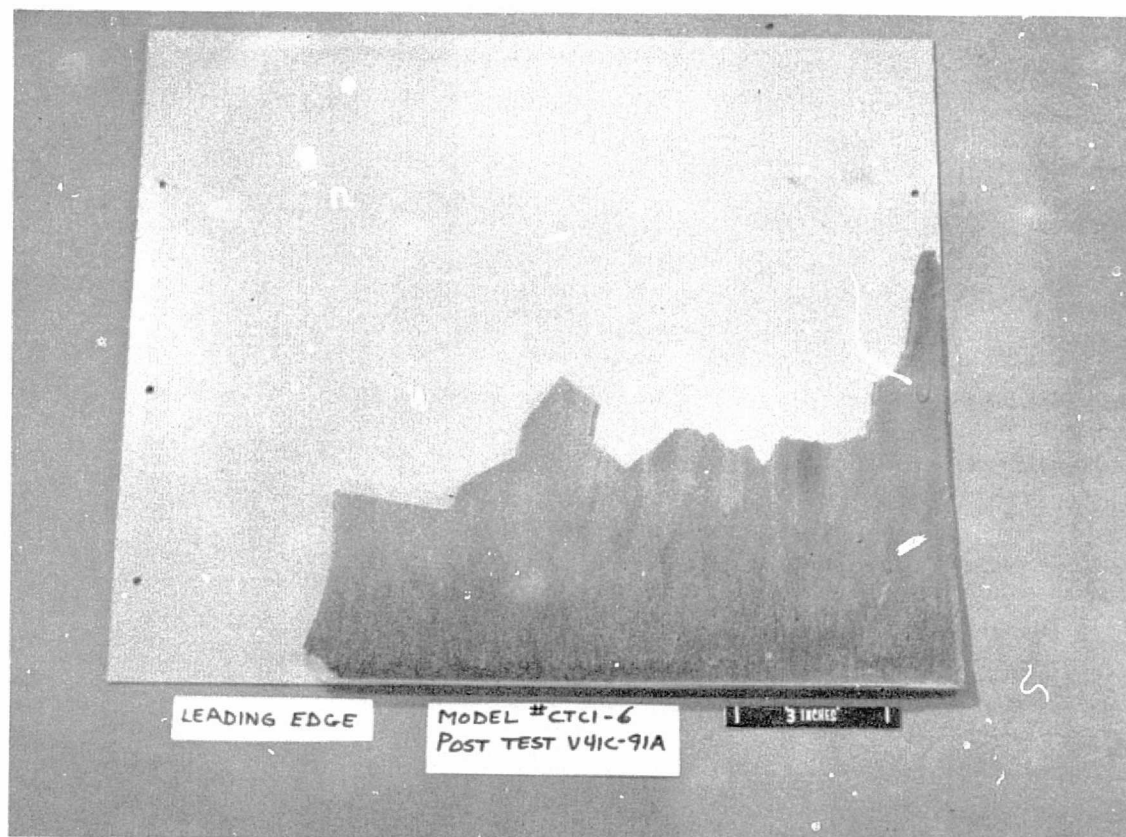


FIGURE 55

Remarks: Foam receded very rapidly over entire surface rather than streaking. Thin layer of foam was left at end of run but delaminated and blew away and left the bare aluminum on retraction or while in tank before tunnel doors were closed.

GROUP 11Sample DescriptionNo. CTC1-6Matl. CPR-421Thickness ~ 0.85 in.Age at Time
of Test 25 daysSurfaceMachined xCoated As-Sprayed Test Conditions $\delta = 38 \text{ deg}$ $\dot{q}_{cw} = 16^* \text{ Btu/ft}^2\text{-sec}$ $P_L = 2.9 \text{ psi}$ $\tau = 4.5 \text{ psi}$ Test Time~ 10 sec

* From extrapolated
measured values.

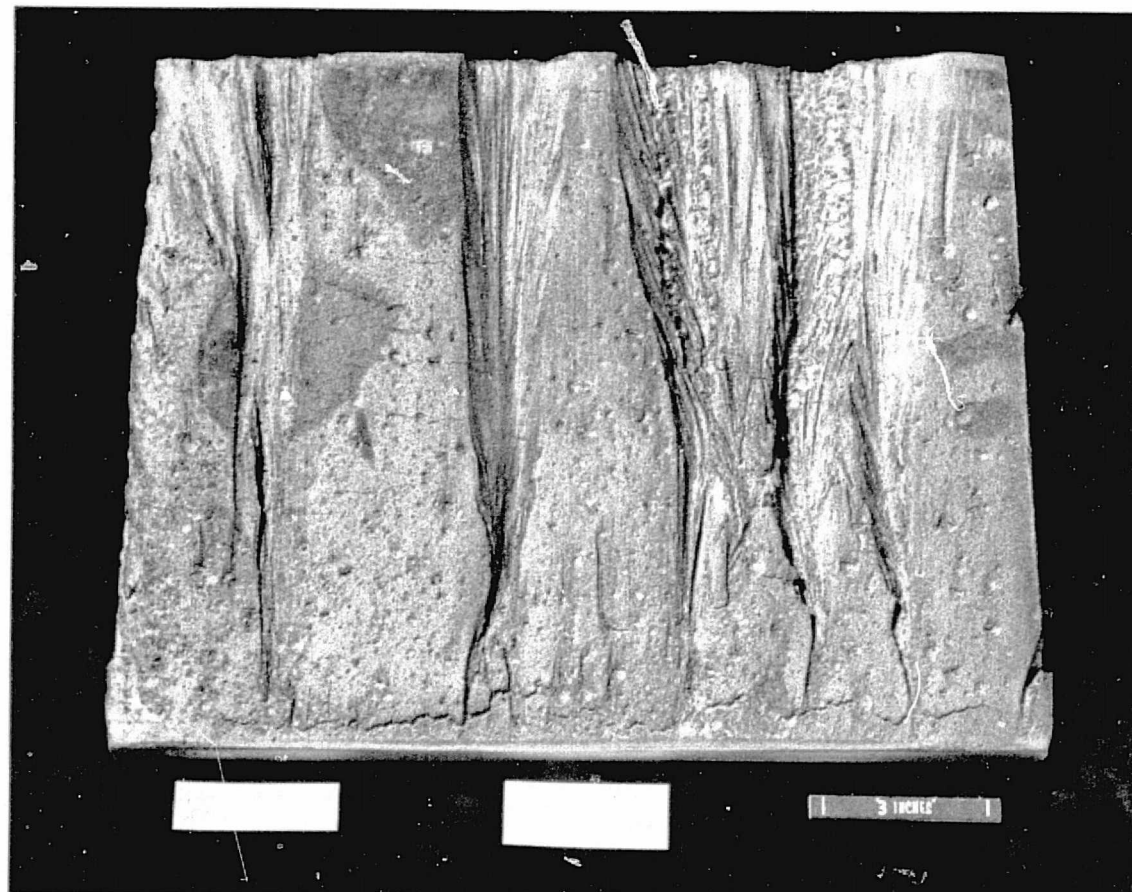


FIGURE 56

Remarks: These streaks went almost through to the aluminum. (Note one human shoeprint on upper left corner.)

GROUP 37

Sample Description

No. CTC1-22

Matl. CPR-421

Thickness ~ 0.85 in.

Age at Time
of Test 38 days

Surface

Machined x

Coated

As-Sprayed

Test Conditions

δ = Traj. 1

\dot{q}_{cw} = Btu/ft²-sec

P_L = psi

τ = psf

Test Time

~ 137 sec

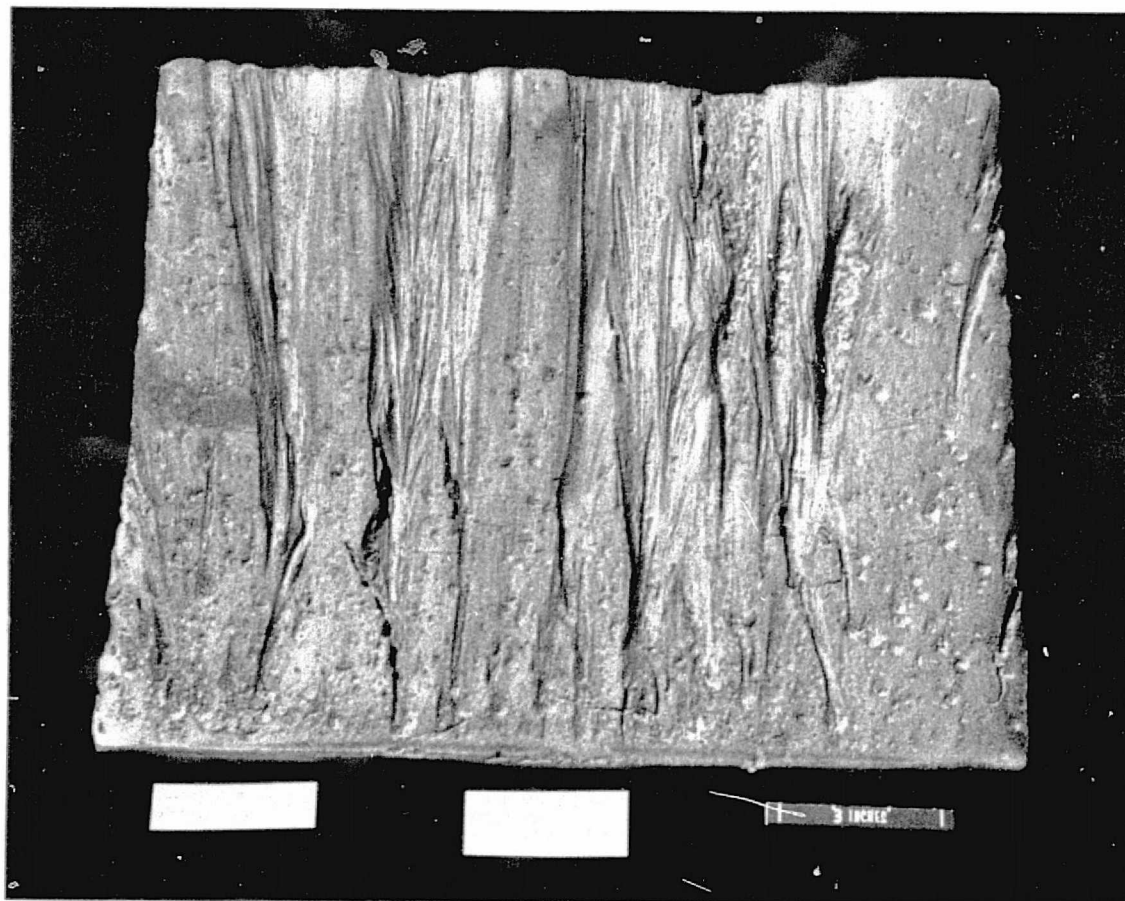


FIGURE 57

Remarks: Streaks went almost through to the aluminum. Would possibly have receded all the way through to the aluminum except for the "rind" or higher density foam layer adjacent to the aluminum.

GROUP 38Sample DescriptionNo. CTC1-23Matl. CPR-421Thickness ~ 0.85 in.Age at Time
of Test 38 daysSurfaceMachined xCoated As-Sprayed Test Conditions δ = Traj. 1 \dot{q}_{cw} = Btu/ft²-sec P_L = psi τ = psfTest Time~ 105 sec



FIGURE 58

Remarks: The knit line did not seem to retard the streaks at all, but panel did look better than CTC1-23 after the test.

GROUP 39

Sample Description

No. CTC1-32

Matl. CPR-421

Thickness ~ 0.85 in.

Age at Time
of Test 43 days

Surface

Machined x

Coated

As-Sprayed

Test Conditions

 δ = Traj. 1
 \dot{q}_{cw} = Btu/ft²-sec

 P_L = psi

 τ = psf

Test Time

~ 105 sec

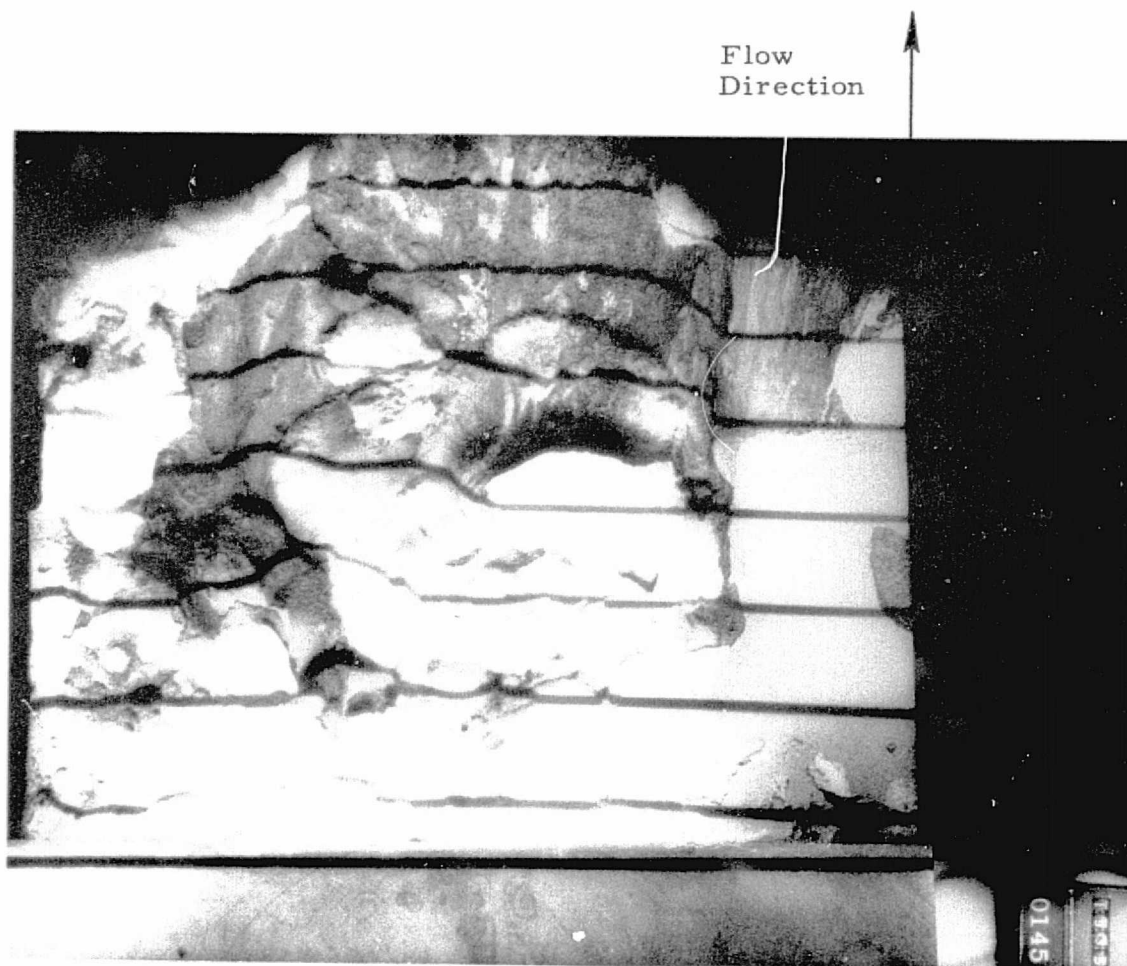
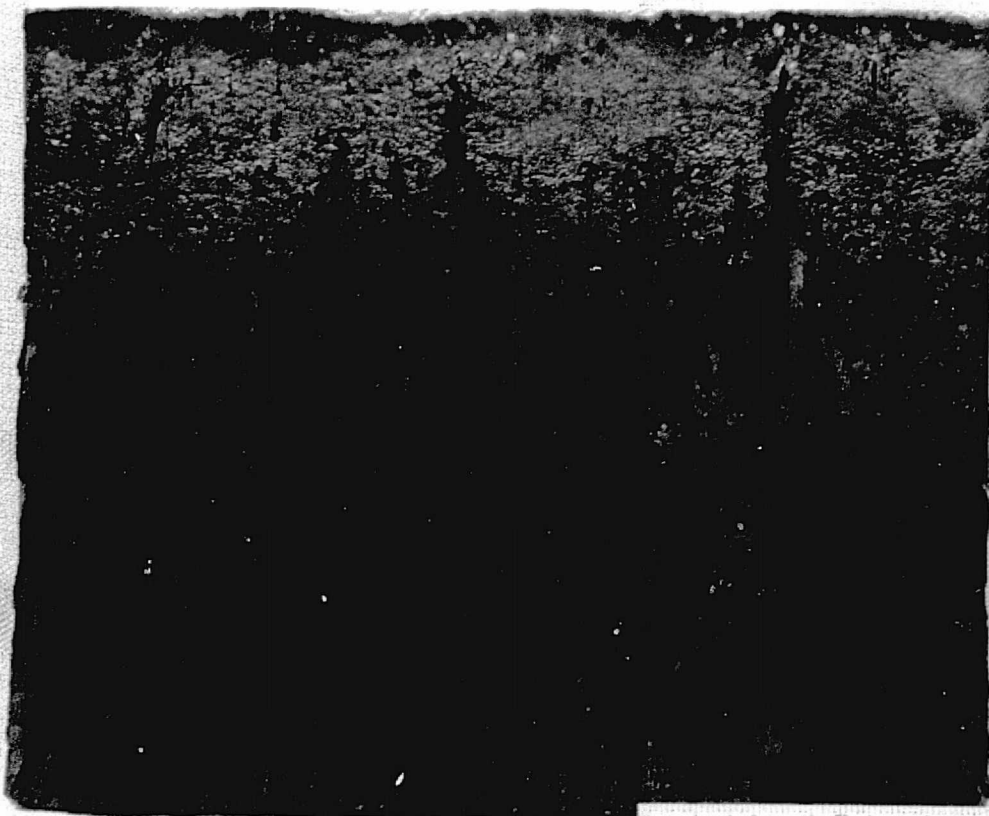


FIGURE 59

Remarks: Foam came off in large chunks - all the way through to the aluminum in some cases.

GROUP 41Sample DescriptionNo. CTC1-58Matl. CPR-421Thickness ~ 1.65 in.Age at Time
of Test 10 daysSurfaceMachined xCoated As-Sprayed Test Conditions δ = Traj. 2 \dot{q}_{cw} = Btu/ft²-sec P_L = psi τ = Test Time~ 337 sec

Flow Direction



GROUP 44

Sample Description

No. CTC1-62

Matl. CPR-421

Thickness ~ 1.65 in.

Age at Time
of Test 11 days

Surface

Machined

Coated

As-Sprayed x

Test Conditions

δ = Traj. A

\dot{q}_{cw} = Btu/ft²-sec

P_L = psi

τ = psf

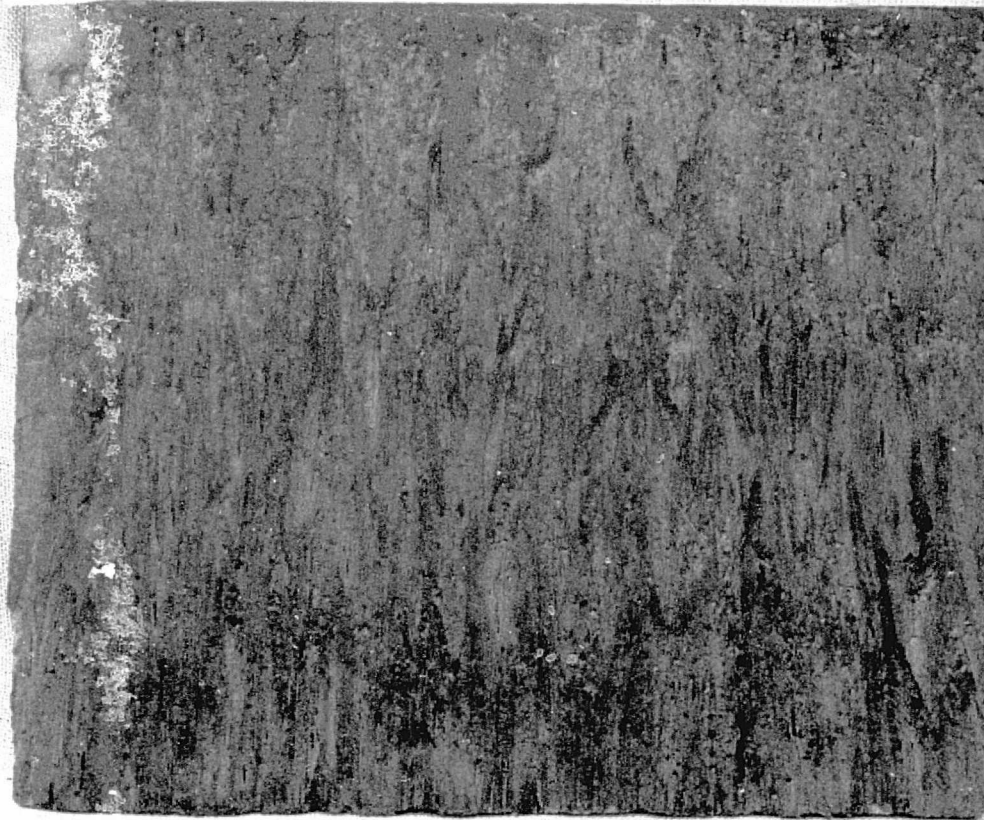
Test Time

~ 104 sec

FIGURE 60

Remarks: Net sprayed panel. Note glossy char near leading edge. Char looked much blacker and stronger during the test than the machined panel char. For pretest photo, see Fig. 5.

Flow Direction



GROUP 45

Sample Description

No. CTC1-68

Matl. CPR-421

Thickness ~ 1.57 in.

Age at Time
of Test 6 days

Surface

Machined x

Coated x

As-Sprayed

Test Conditions

δ = Traj. A

\dot{q}_{cw} = Btu/ft²-sec

P_L = psi

τ = psf

Test Time

~ 104 sec

FIGURE 61

Remarks: Panel was machined and coated and had knit lines. Note that some of coating still remains.

REPRODUCIBILITY OF THE
ORIGINAL PAGE IS POOR

Flow Direction



FIGURE 62

Remarks: Coating seemed to protect the foam in beginning of test.
Seemed to have a heavy, black protective char during test.

GROUP 46Sample DescriptionNo. CTC1-64Matl. CPR-421Thickness ~ 1.55 in.Age at Time
of Test 11 daysSurfaceMachined Coated x As-Sprayed x Test Conditions δ = Traj. A \dot{q}_{cw} = Btu/ft²-sec P_L = psi τ = Test Time~ 105 sec

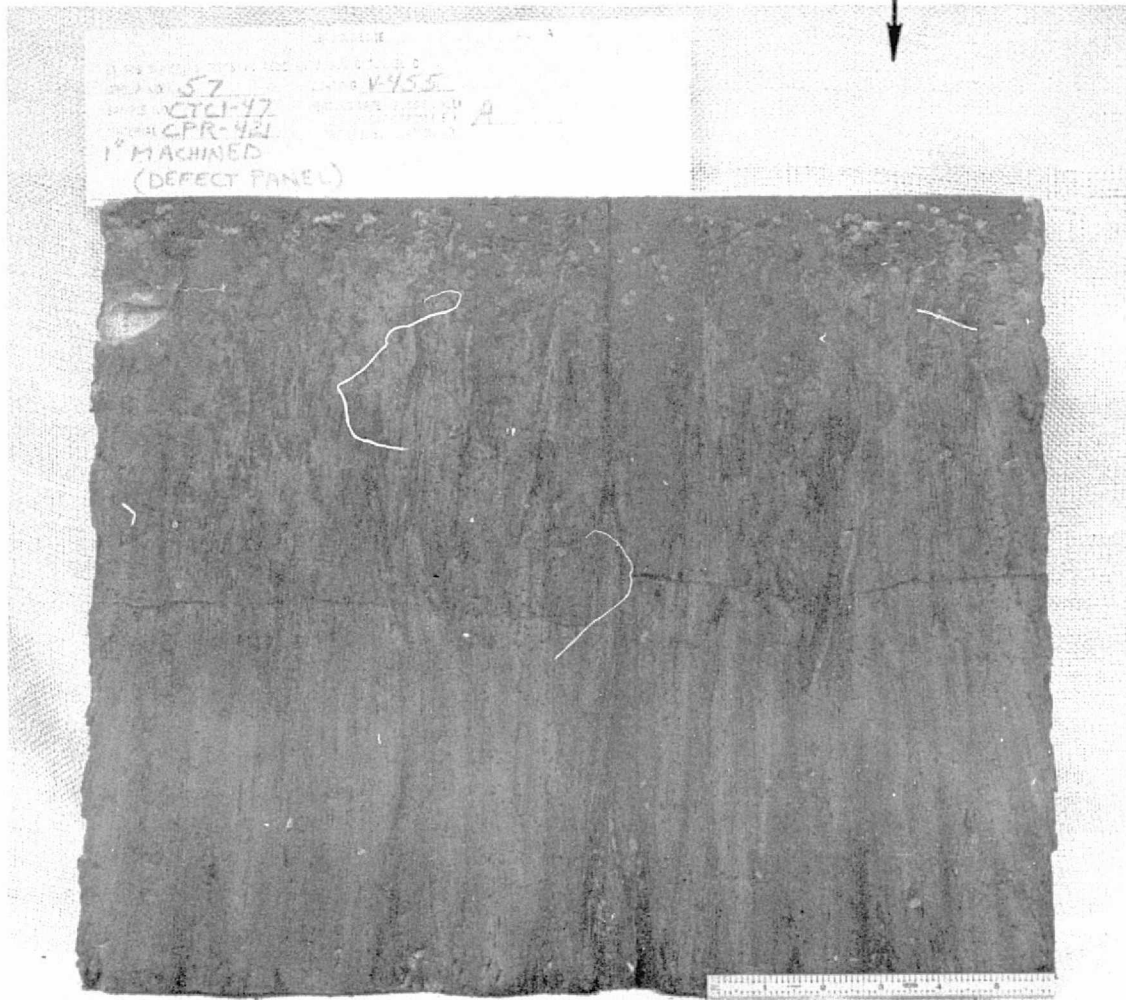
Flow Direction

GROUP 47Sample DescriptionNo. CTC1-66Matl. CPR-421Thickness ~ 1.55Age at Time
of Test 11 daysSurfaceMachined Coated x As-Sprayed x Test Conditions δ = Traj. A \dot{q}_{cw} = Btu/ft²-sec P_L = psi τ = psfTest Time ~ 104 sec

FIGURE 63

Remarks: Panel was looking good during test until large plug blew out of center. Failure was apparently due to buildup of pressure under panel — possibly due to heat-up of wedge fixture under aluminum panel. (Note: The foam panel was sprayed on another surface then removed and bonded to this aluminum plate. This was necessary to come out with about the right total panel thickness because the as-sprayed thickness is not accurately controllable.)

Flow Direction



GROUP 57

Sample Description

No. CTC1-47

Matl. CPR-421

Thickness ~ 0.95 in.

Age at Time
of Test 59 days

Surface

Machined x

Coated x

As-Sprayed

Test Conditions

δ = Traj. A

\dot{q}_{cw} = Btu/ft²-sec

P_L = psi

τ = psf

Test Time

~ 104 sec

FIGURE 64

Remarks: Panel had pretest cracks through the entire thickness of the foam. Streak in the middle followed the pretest crack. Note that some coating still remains on the panel surface near the leading edge.



FIGURE 65

Remarks: Test run with 5/8 inch high vortex generator on wedge leading edge. Streaked first to the left of the vortex generator, then directly behind the vortex generator. Receded almost to the aluminum.

GROUP 66Sample DescriptionNo. CTC1-43Matl. CPR-421Thickness ~ 0.85 in.Age at Time
of Test 61 daysSurfaceMachined xCoated As-Sprayed Test Conditions δ = Traj. A \dot{q}_{cw} = Btu/ft²-sec P_L = psi τ = psfTest Time~ 106 sec

100



FIGURE 66

Remarks: Test run with 5/8 inch vortex generator on wedge leading edge. Streaked some behind vortex generator. Some coating remained on panel near leading edge after the test.

GROUP 69Sample DescriptionNo. CTC1-52Matl. CPR-421Thickness ~ 0.85 in.Age at Time
of Test 66 daysSurfaceMachined xCoated xAs-Sprayed Test Conditions δ = Traj. A \dot{q}_{cw} = Btu/ft²-sec P_L = psi τ = psfTest Time~ 104 sec

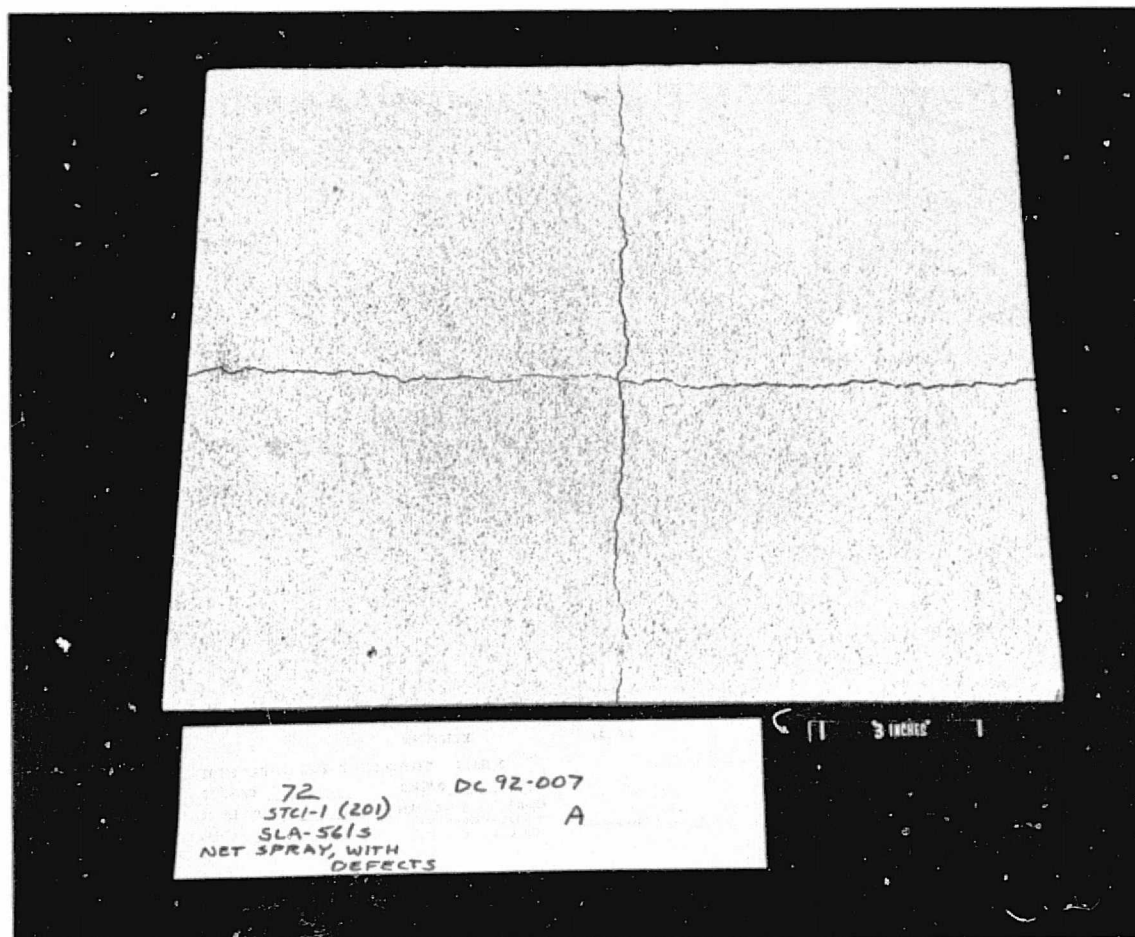


FIGURE 67

Remarks: Very little change in panel appearance during test. Pretest defects did not seem to affect performance.

GROUP 72Sample DescriptionNo. STC1-1 (201)Matl. SLA-561sThickness ~ 0.43 in.Age at Time
of Test —SurfaceMachined —Coated xAs-Sprayed xTest Conditions δ = Traj. A \dot{q}_{cw} = — Btu/ft²-sec P_L = — psi τ = — psfTest Time~ 98 sec

Flow
Direction

FIGURE 68

Remarks: Panel looked good after test. Had a glossy black, strong looking char layer that held up well.

GROUP 51Sample DescriptionNo. CTC1-65Matl. CPR-421Thickness ~1.57 in.Age at Time
of Test 11 daysSurfaceMachined Coated As-Sprayed xTest Conditions δ = Traj. B \dot{q}_{cw} = Btu/ft²-sec P_L = psi τ = psiTest Time~104 sec

Flow
Direction

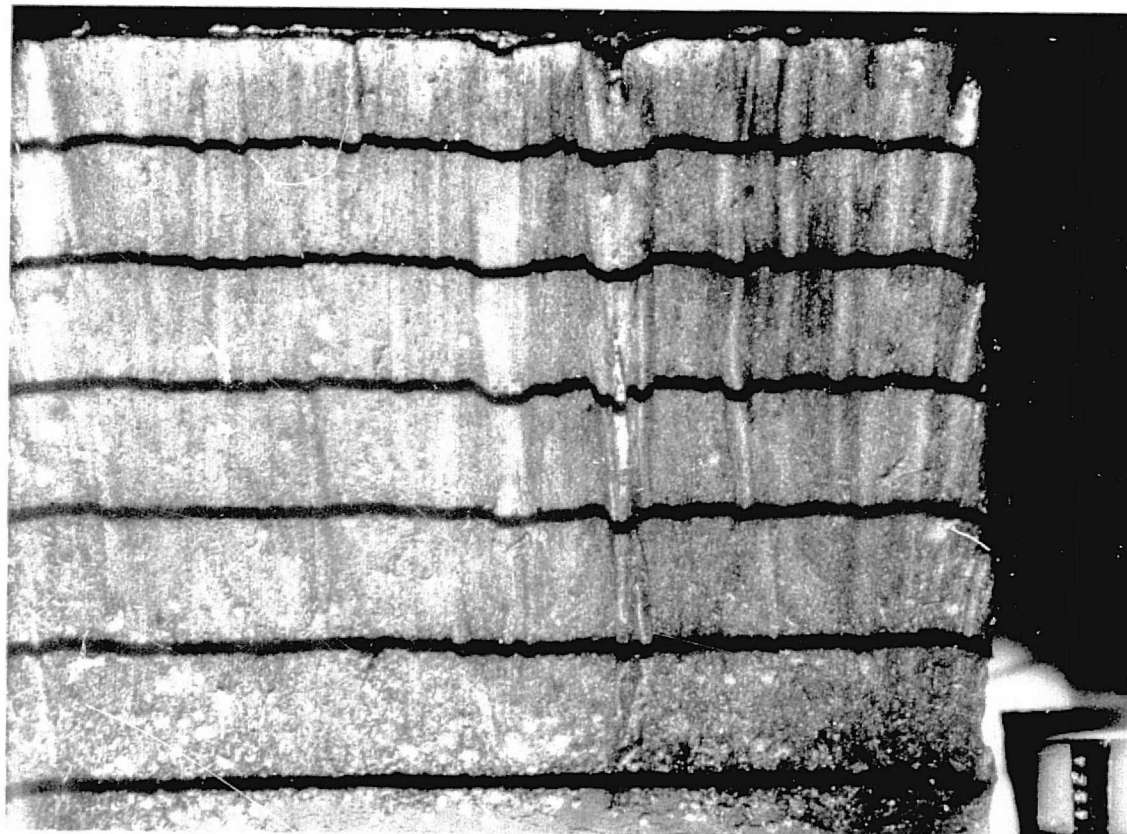


FIGURE 69

Remarks: Panel did not burn all the way through!!!

GROUP 75

Sample Description

No. CTC1-41

Matl. CPR-421

Thickness ~ 0.85 in.

Age at Time
of Test 59 days

Surface

Machined x

Coated

As-Sprayed

Test Conditions

δ = Traj.C

\dot{q}_{cw} = Btu/ft²-sec

P_L = psi

τ =

Test Time

~625 sec

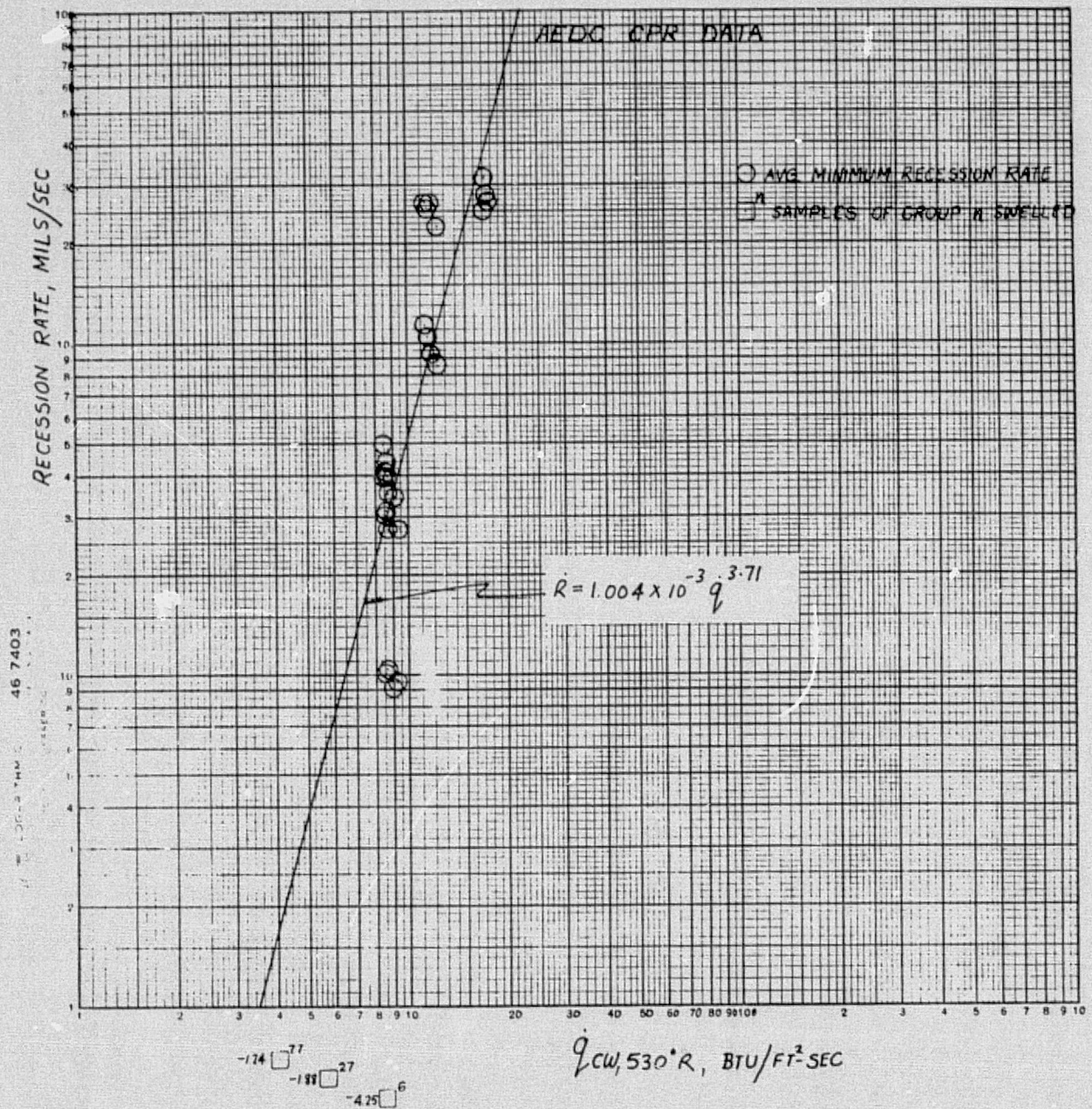
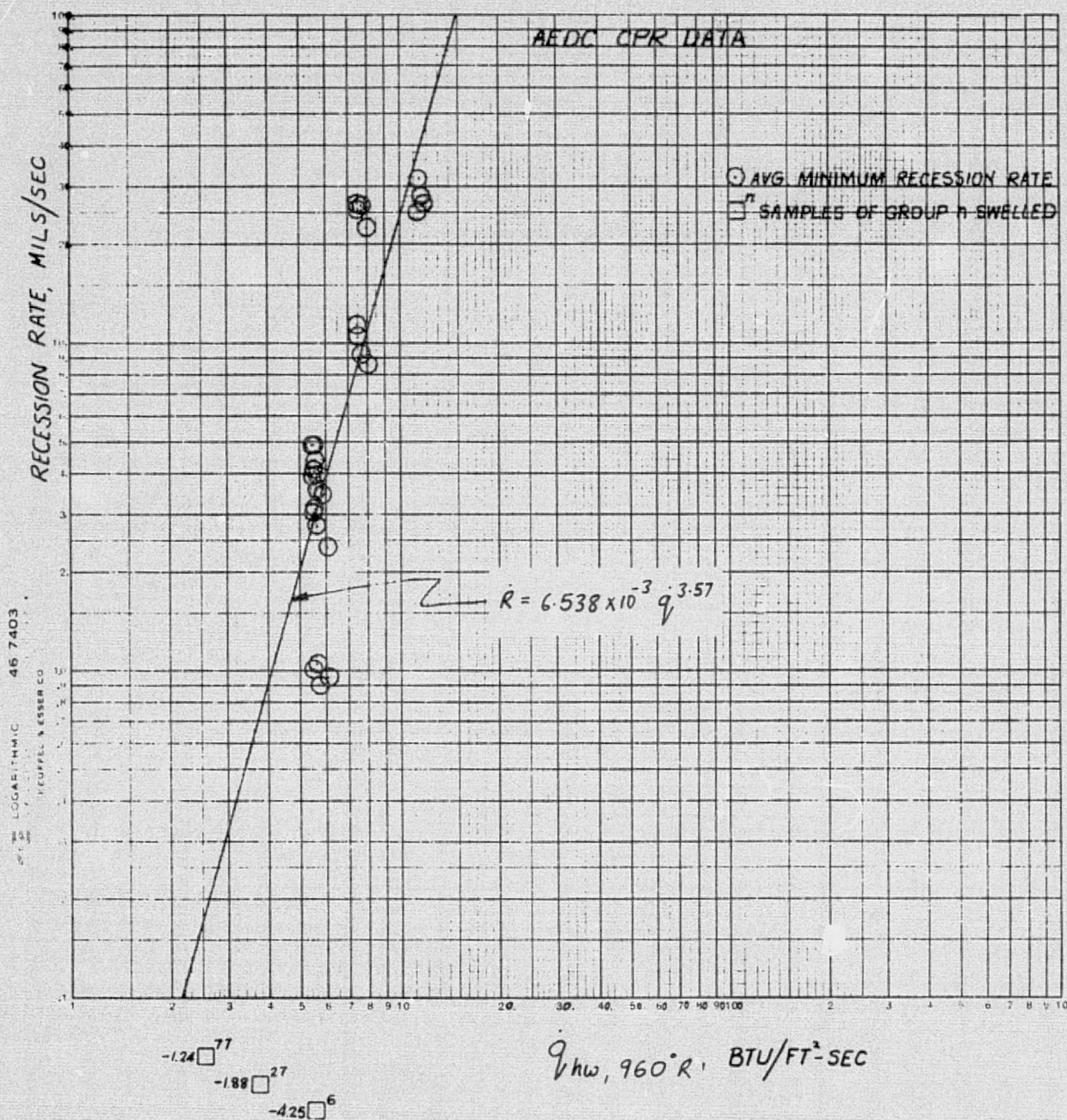


Fig. 70 - Average Minimum Recession Rate vs Cold Wall Heating Rate



REPRODUCIBILITY OF THE
ORIGINAL PAGE IS POOR

Fig. 71 - Average Minimum Recession Rate vs Hot Wall Heating Rate

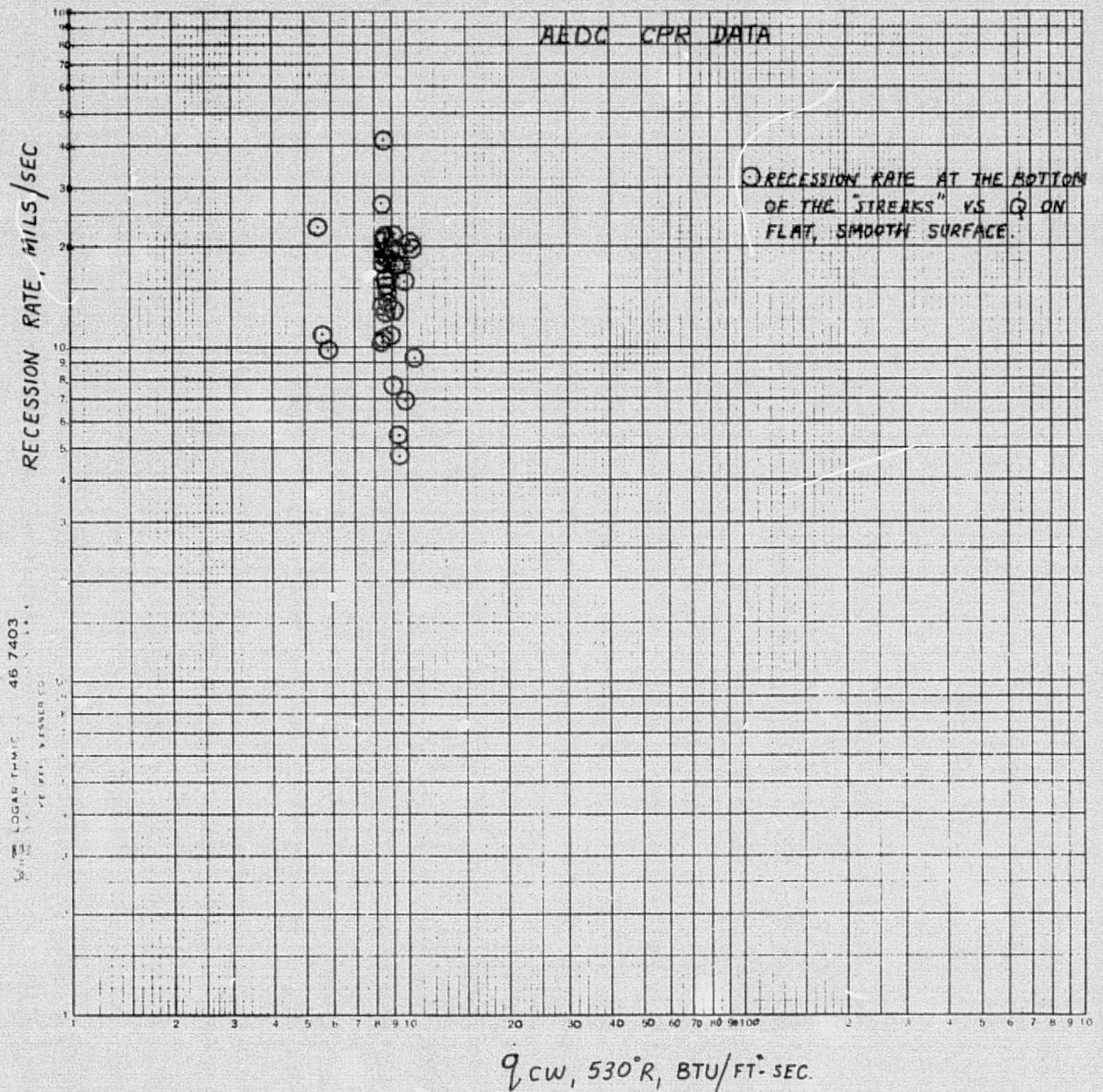


Fig. 72 - Recession Rate at the Bottom of the Streaks vs Cold Wall Heating Rate

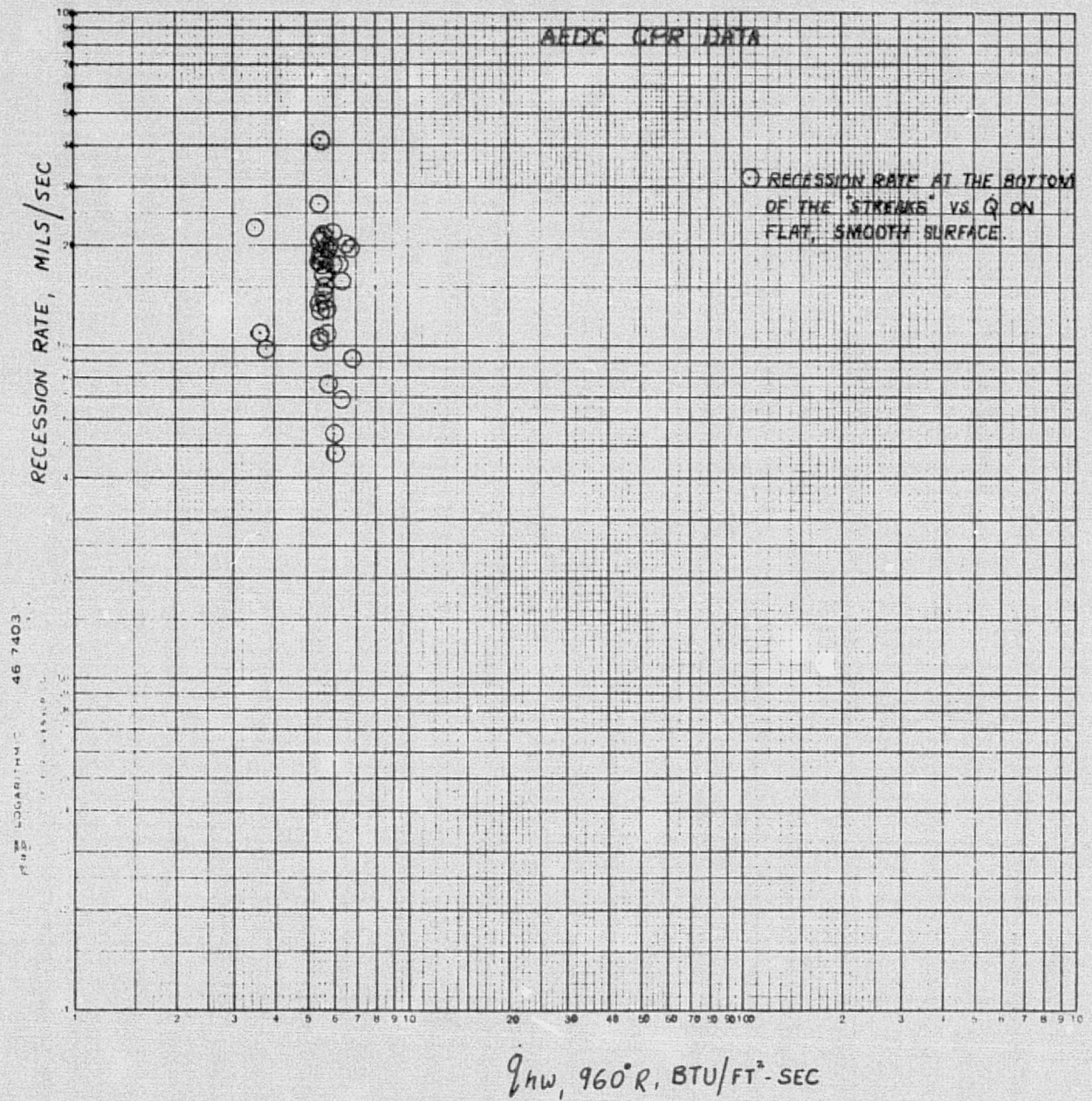
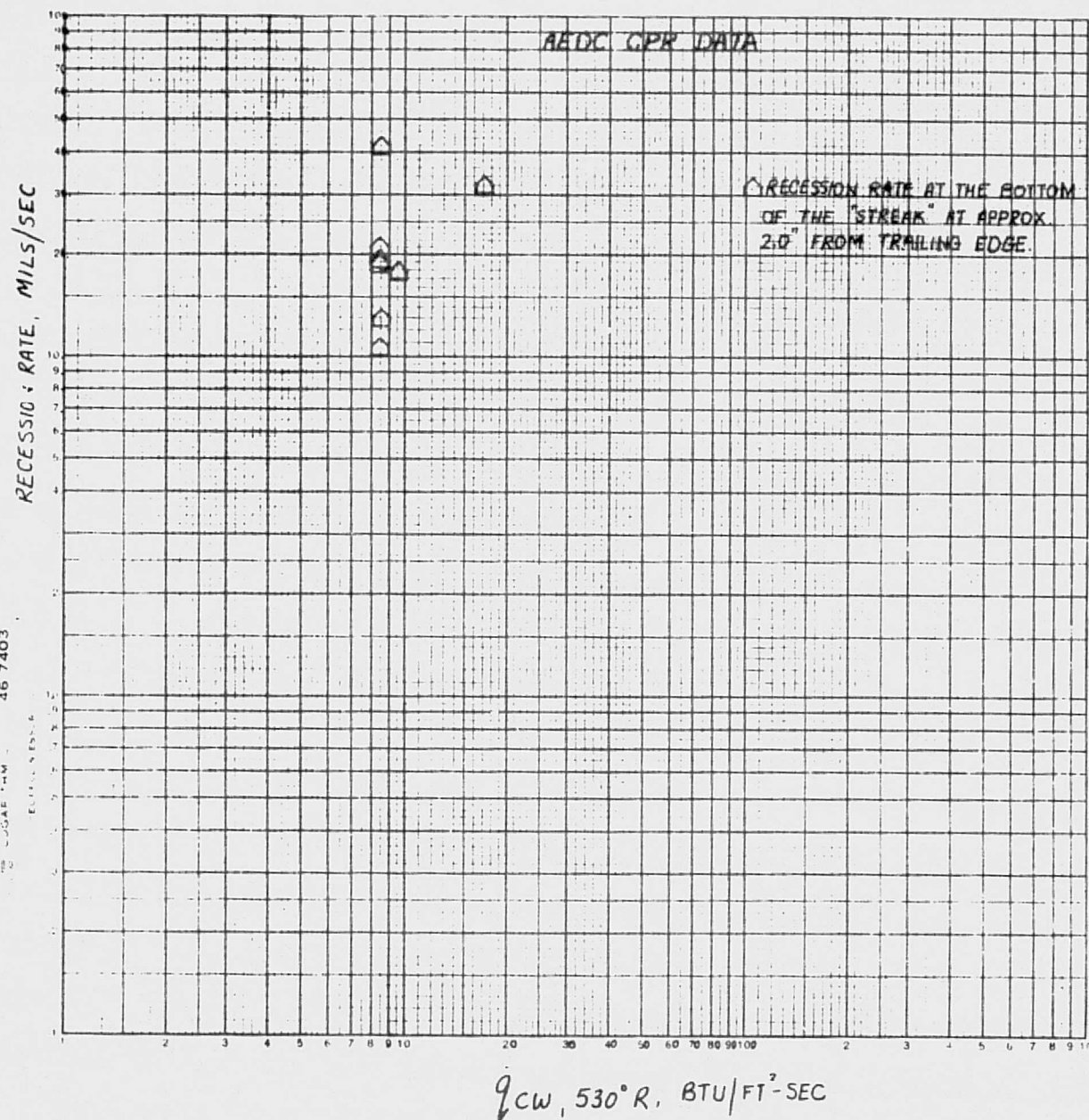


Fig. 73 - Recession Rate at the Bottom of the Streaks vs Hot Wall Heating Rate



REPRODUCIBILITY OF THE
ORIGINAL PAGE IS POOR

Fig. 74 - Recession Rate at the Bottom of the Streaks at 2 in. from the Trailing Edge vs Cold Wall Heating Rate

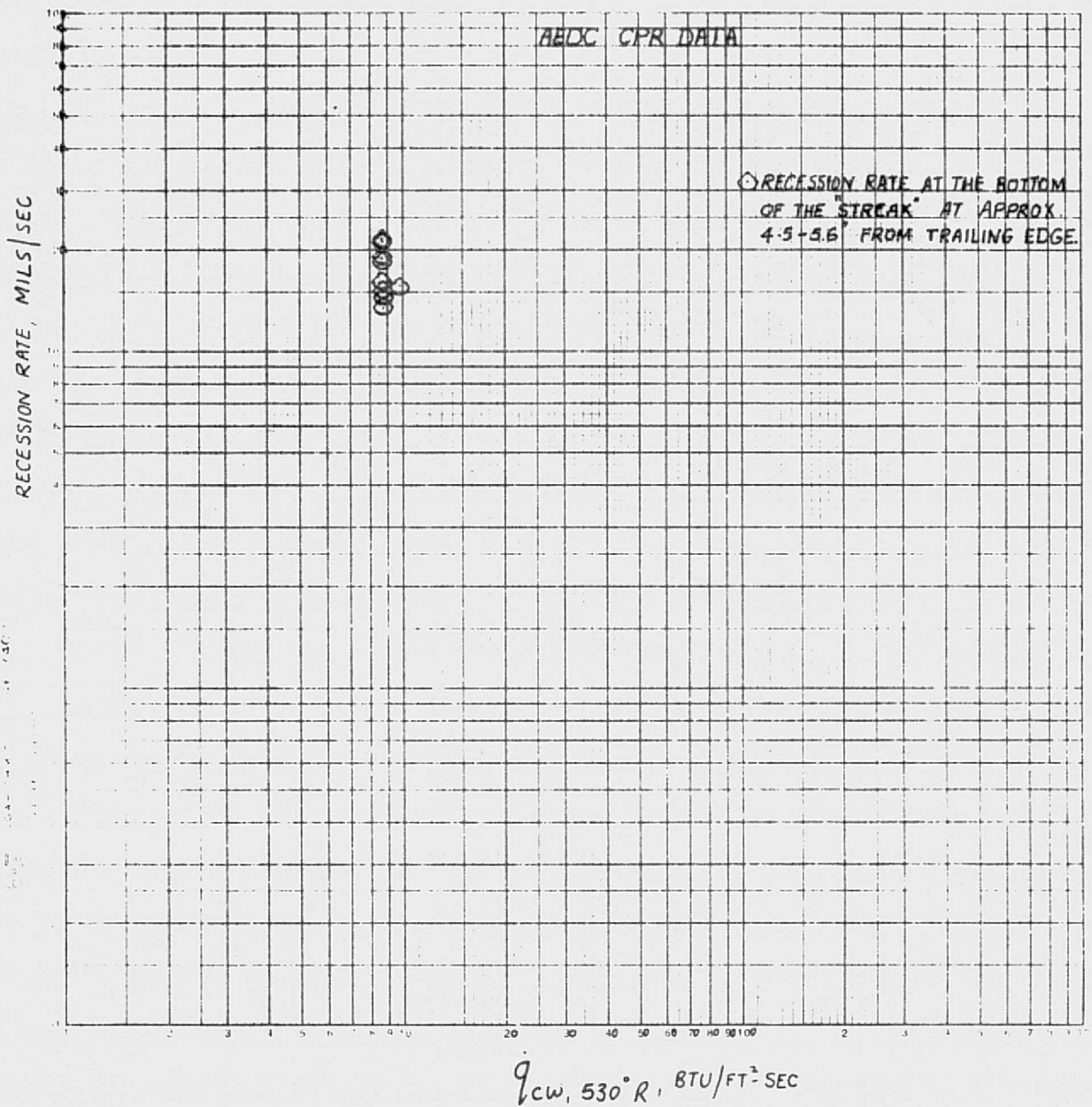


Fig. 75 - Recession Rate at the Bottom of the Streaks at About 5 in. from the Trailing Edge vs Cold Wall Heating Rate

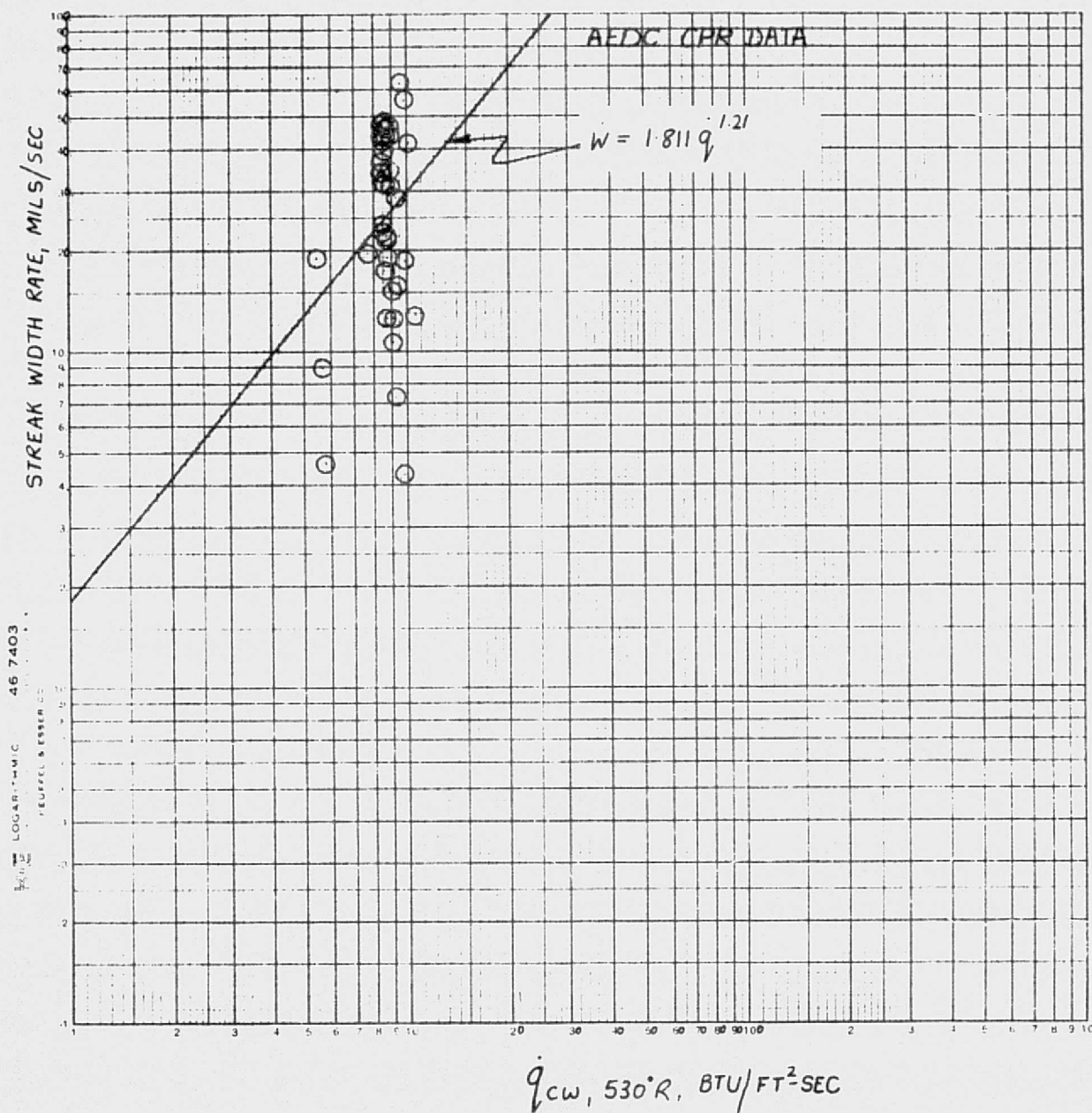


Fig. 76 - Streak Width Rate vs Cold Wall Heating Rate

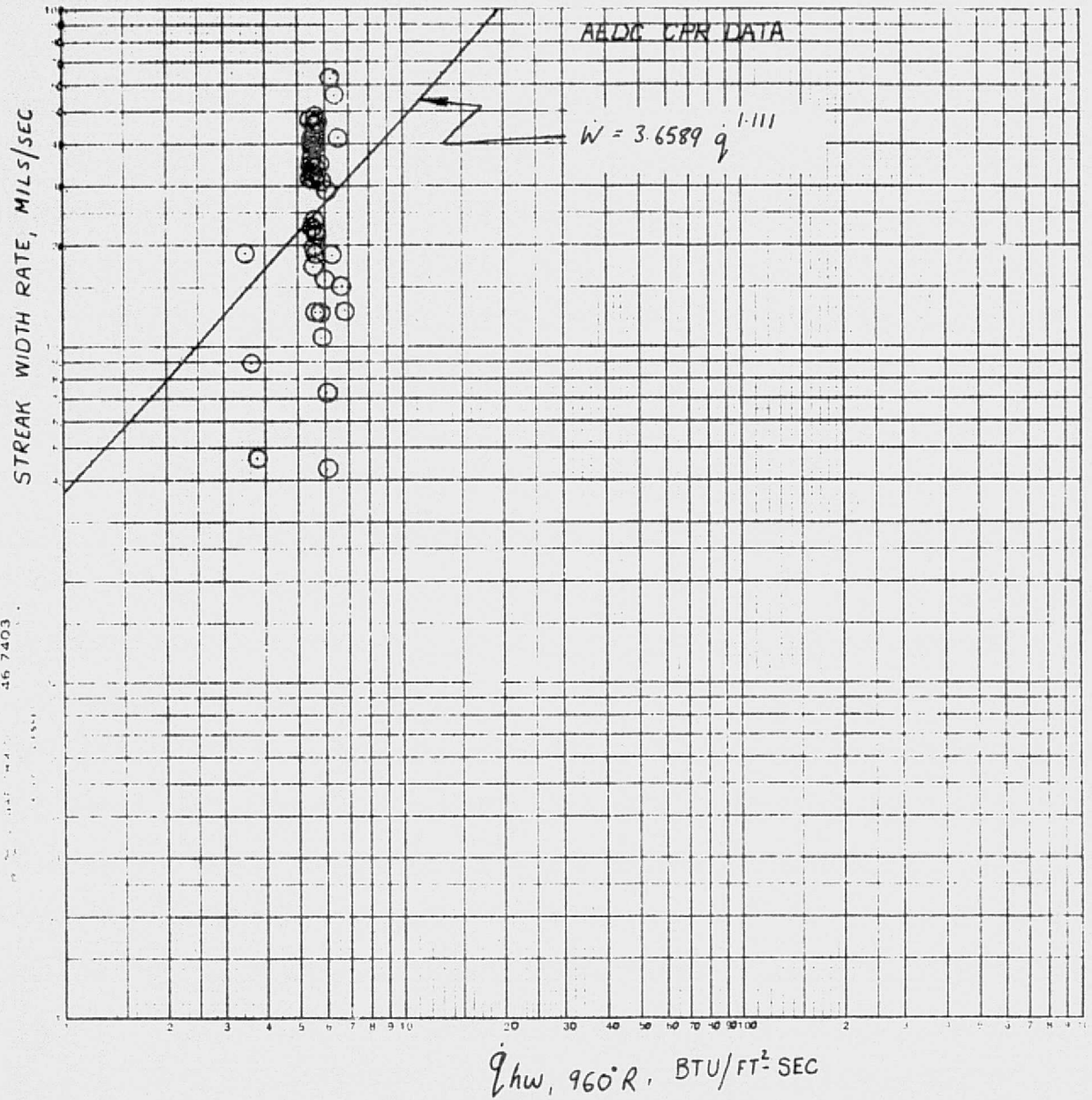
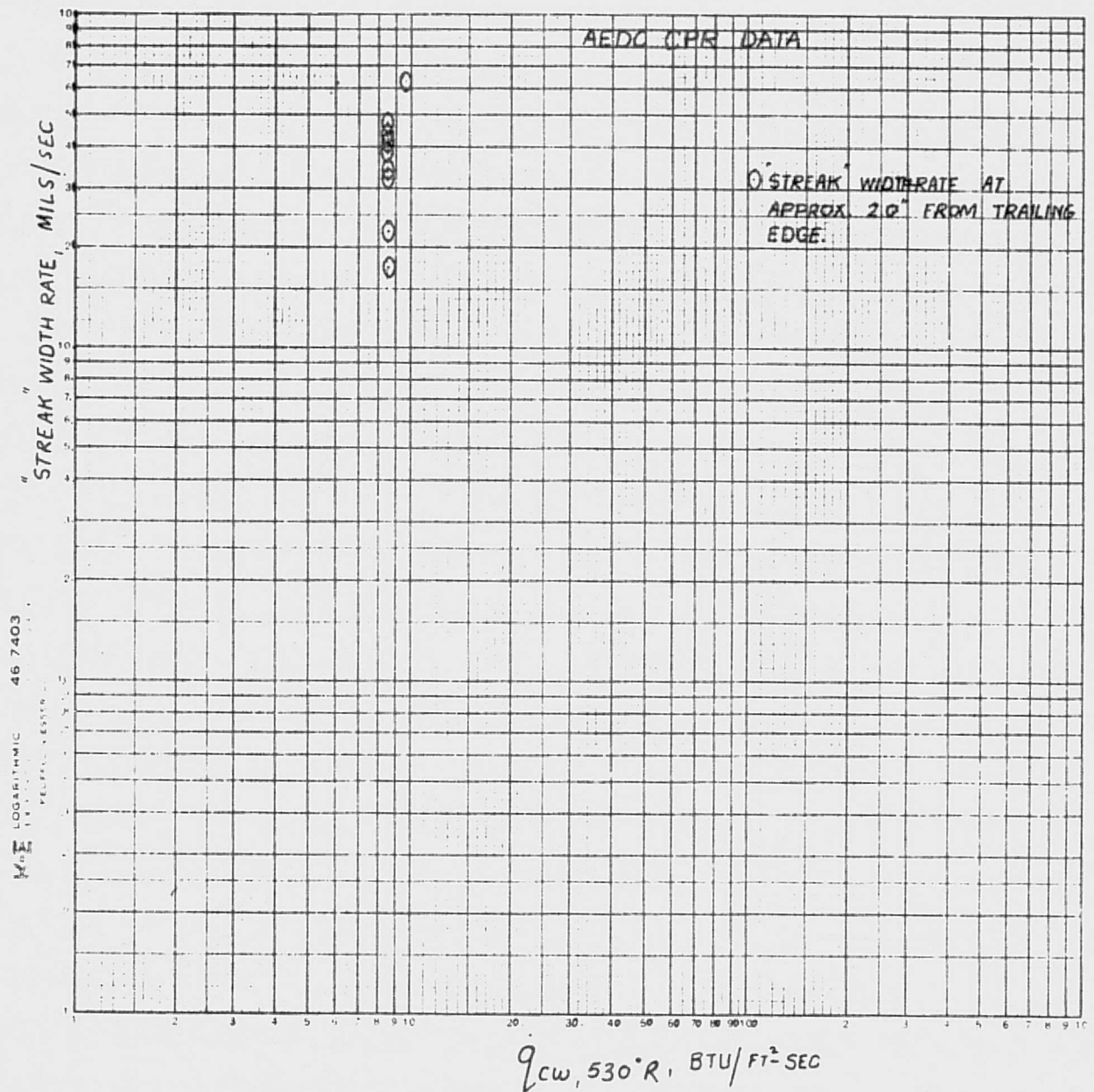


Fig. 77 - Streak Width Rate vs Hot Wall Heating Rate



REPRODUCIBILITY OF THE
ORIGINAL PAGE IS POOR

Fig. 78 - Streak Width Rate vs Cold Wall Heating Rate at 2.0 in. from Trailing Edge

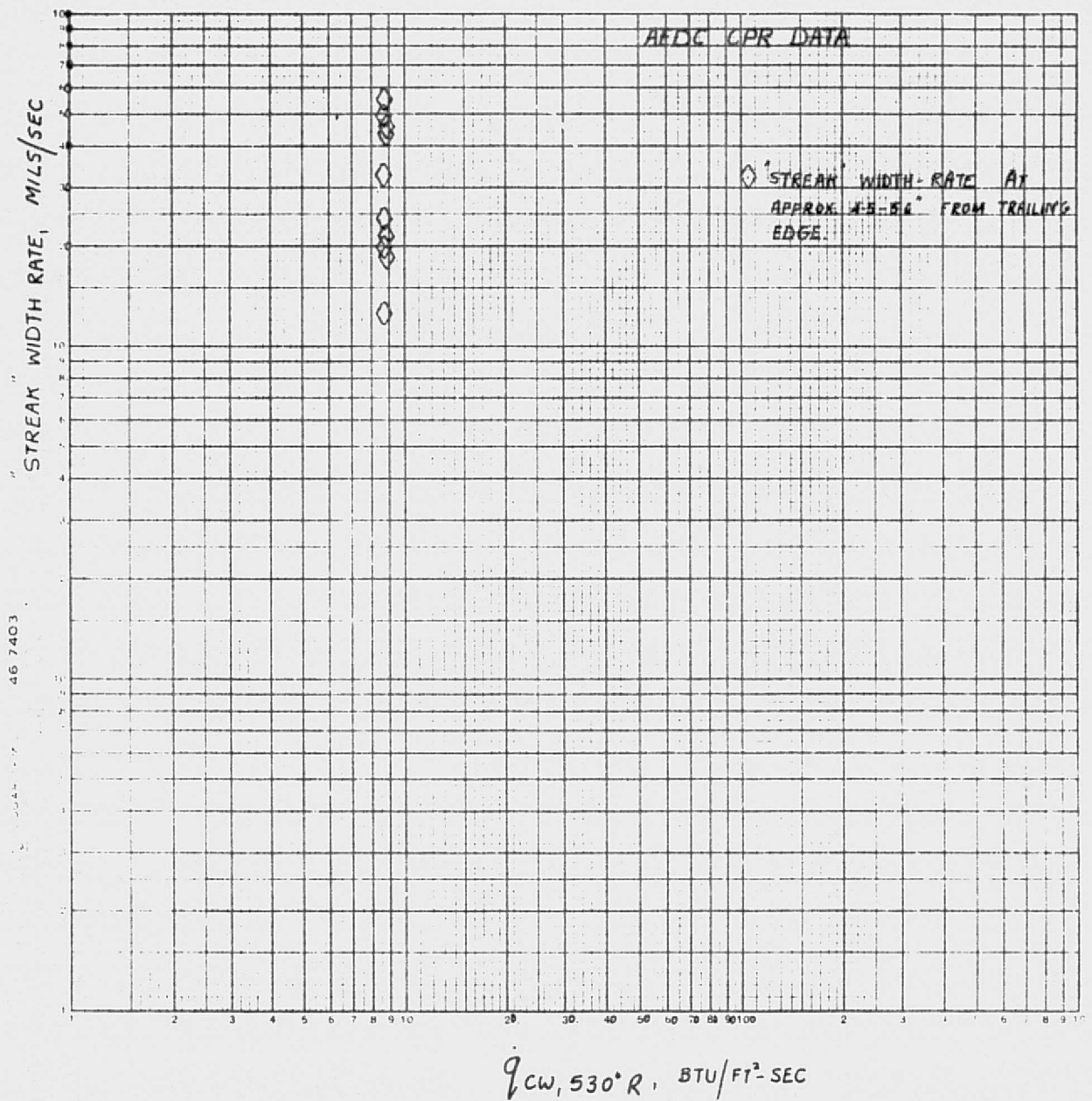


Fig. 79 - Streak Width Rate vs Cold Wall Heating Rate at About 5 in. from Trailing Edge

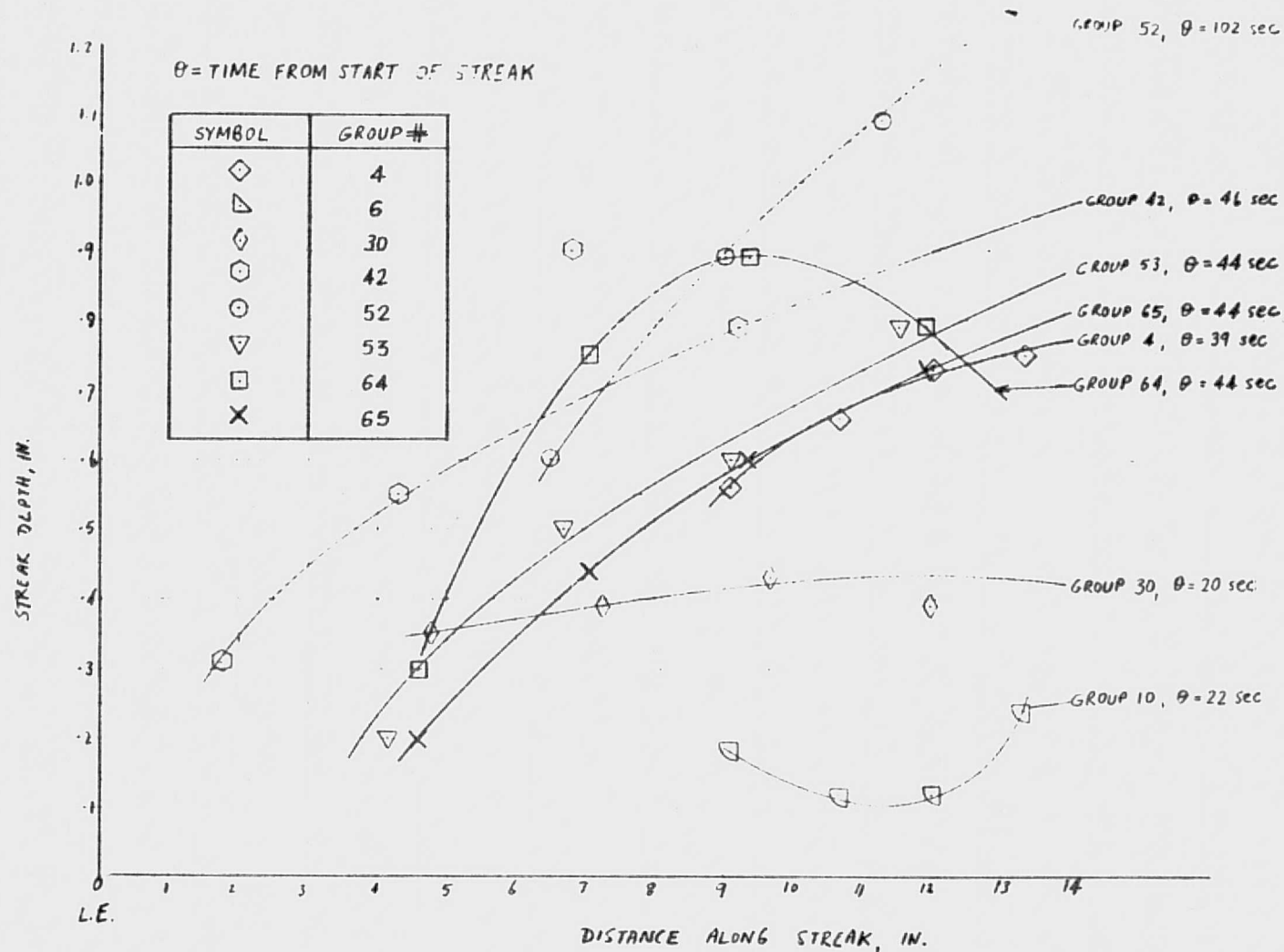


Fig. 80 - Streak Depth vs Distance Along the Streak for a Wedge Angle of 18 deg

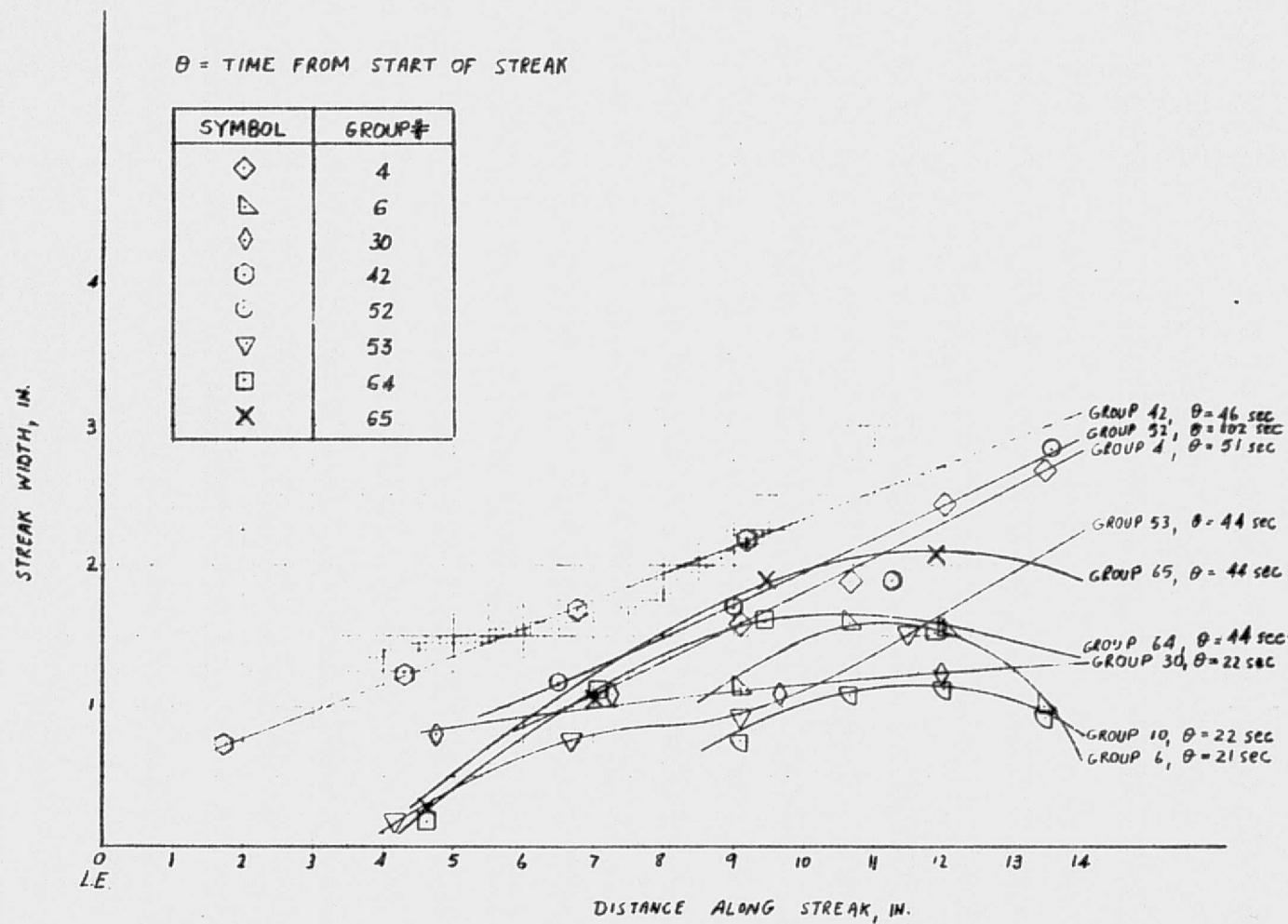


Fig. 81 - Streak Width vs Distance Along Streak for a Wedge Angle of 18 deg

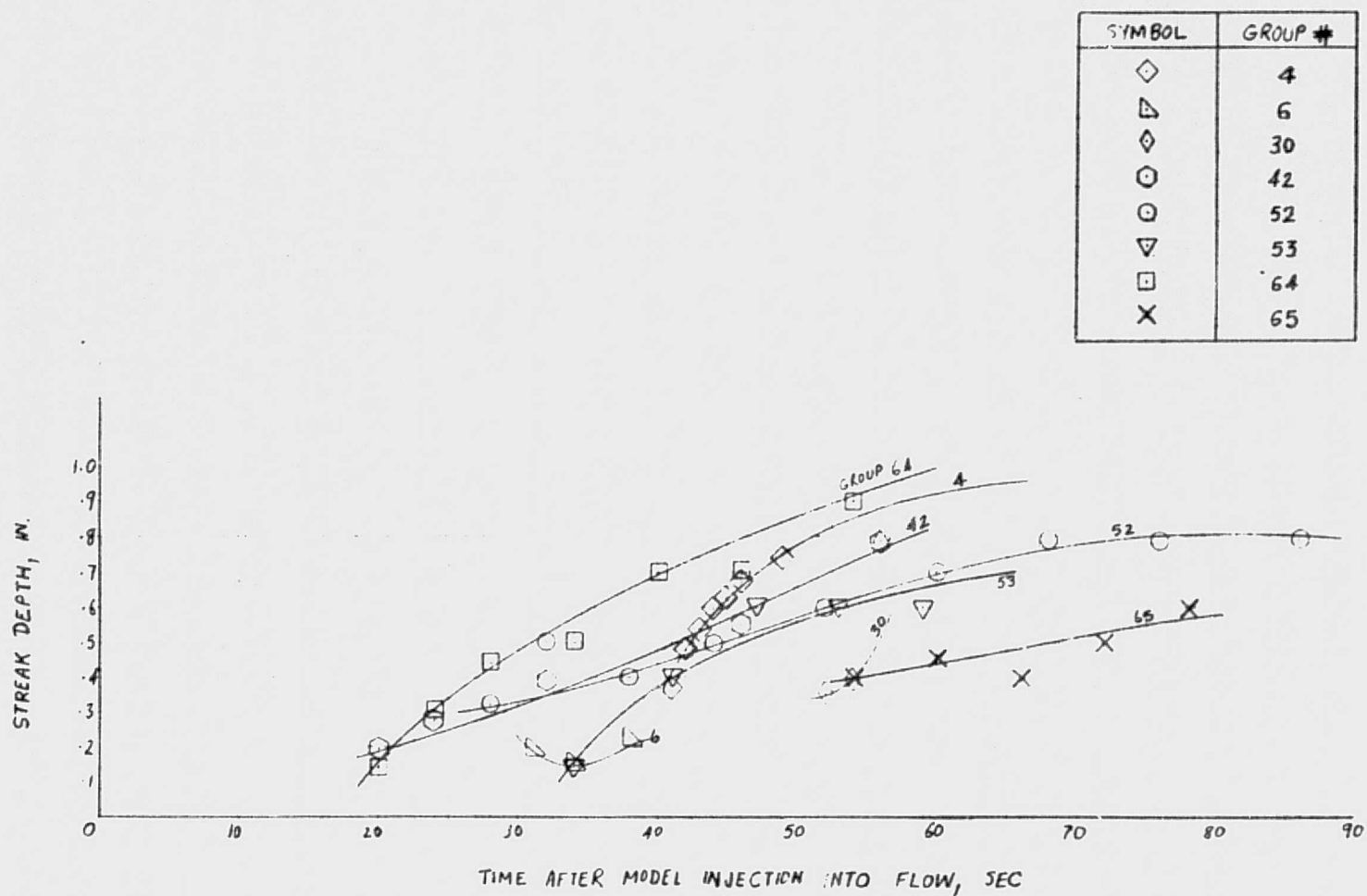


Fig. 82 - Streak Depth vs Time After Injection at Approximately 2 in. from Trailing Edge for Wedge Angle of 18 deg

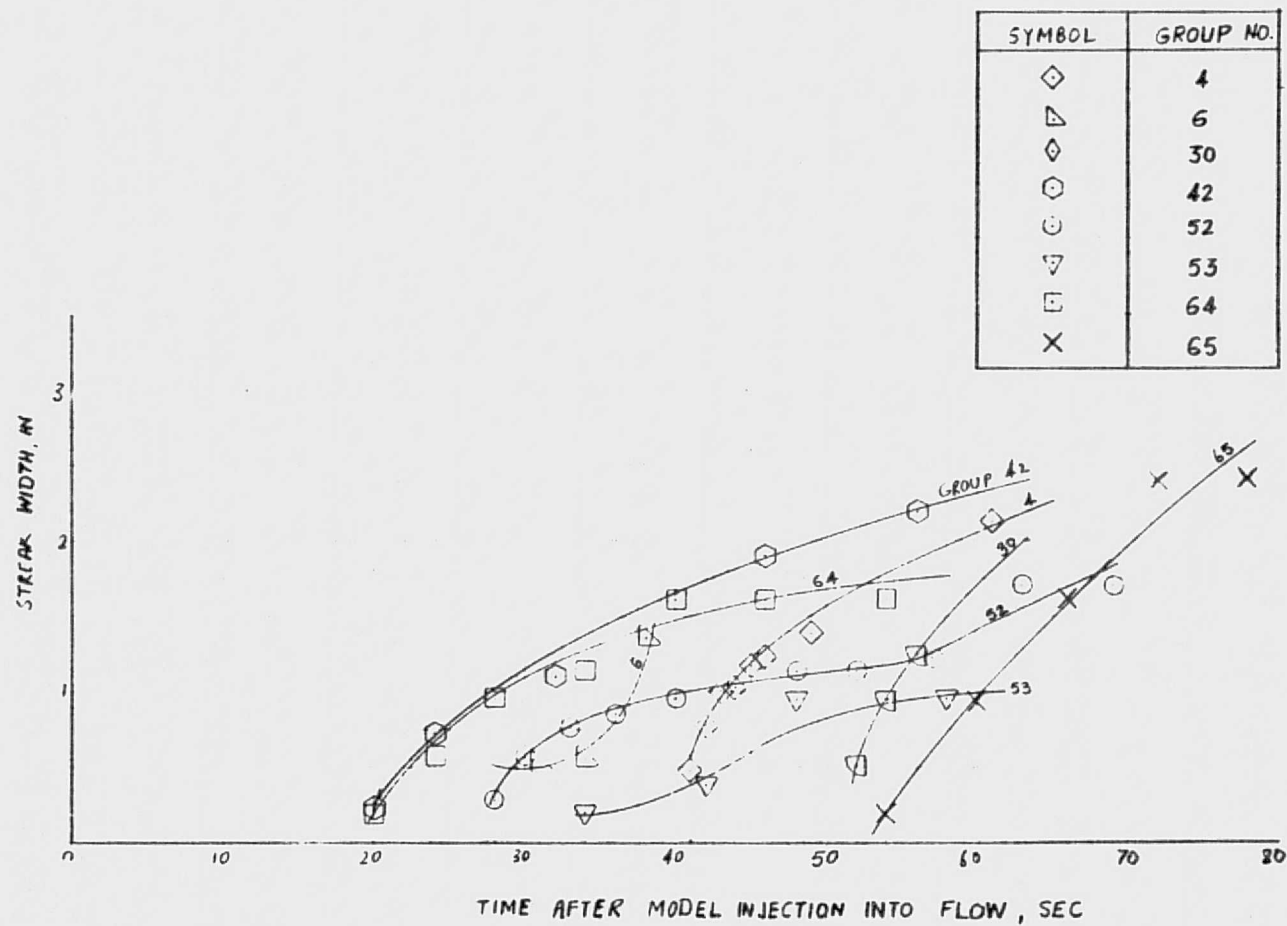


Fig.83 - Streak Width vs Time from Injection at Approximately 2 in. from Trailing Edge for Wedge Angle of 18 deg

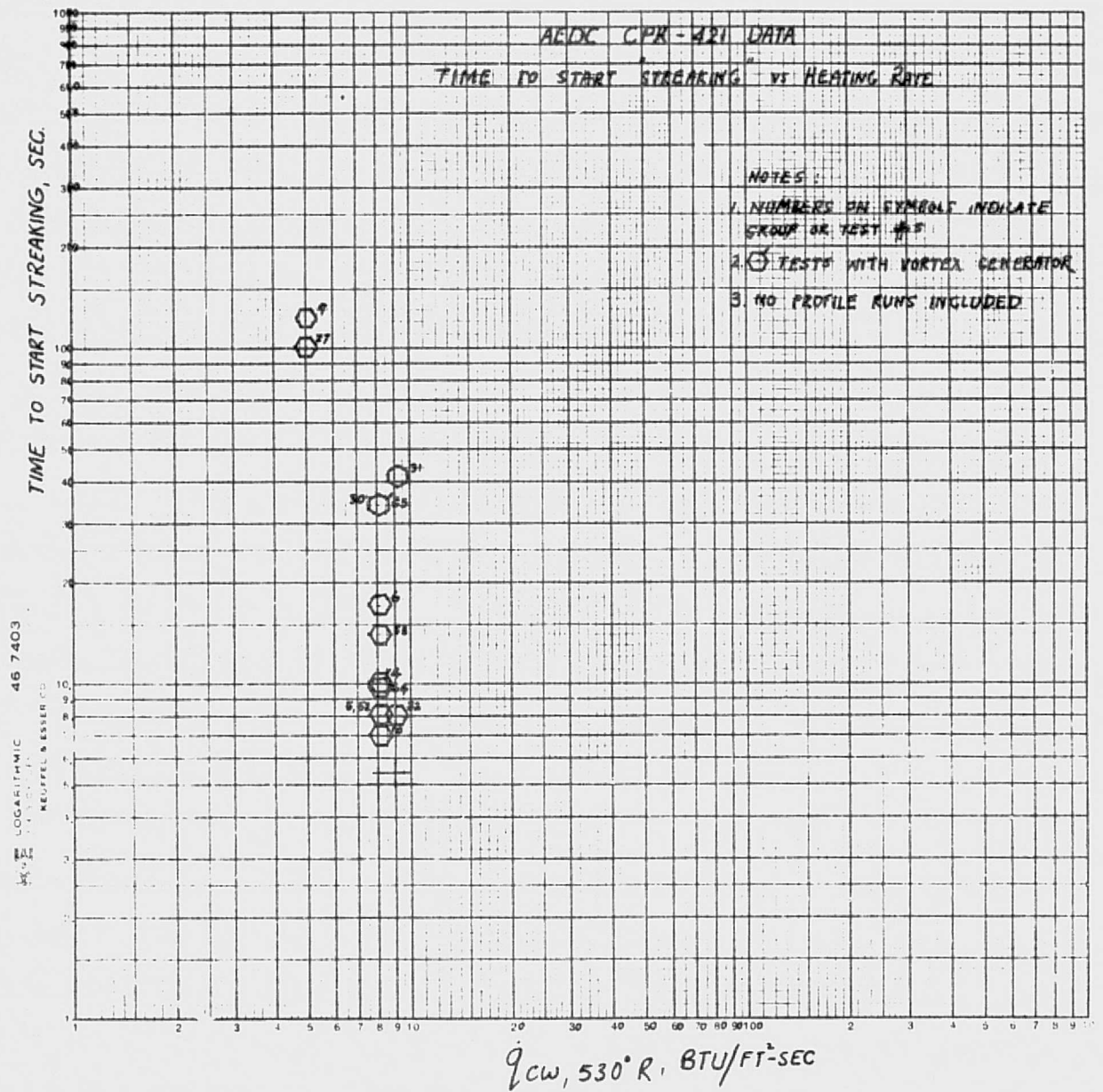


Fig. 84 - Time to Start Streaking vs Cold Wall Heating Rate

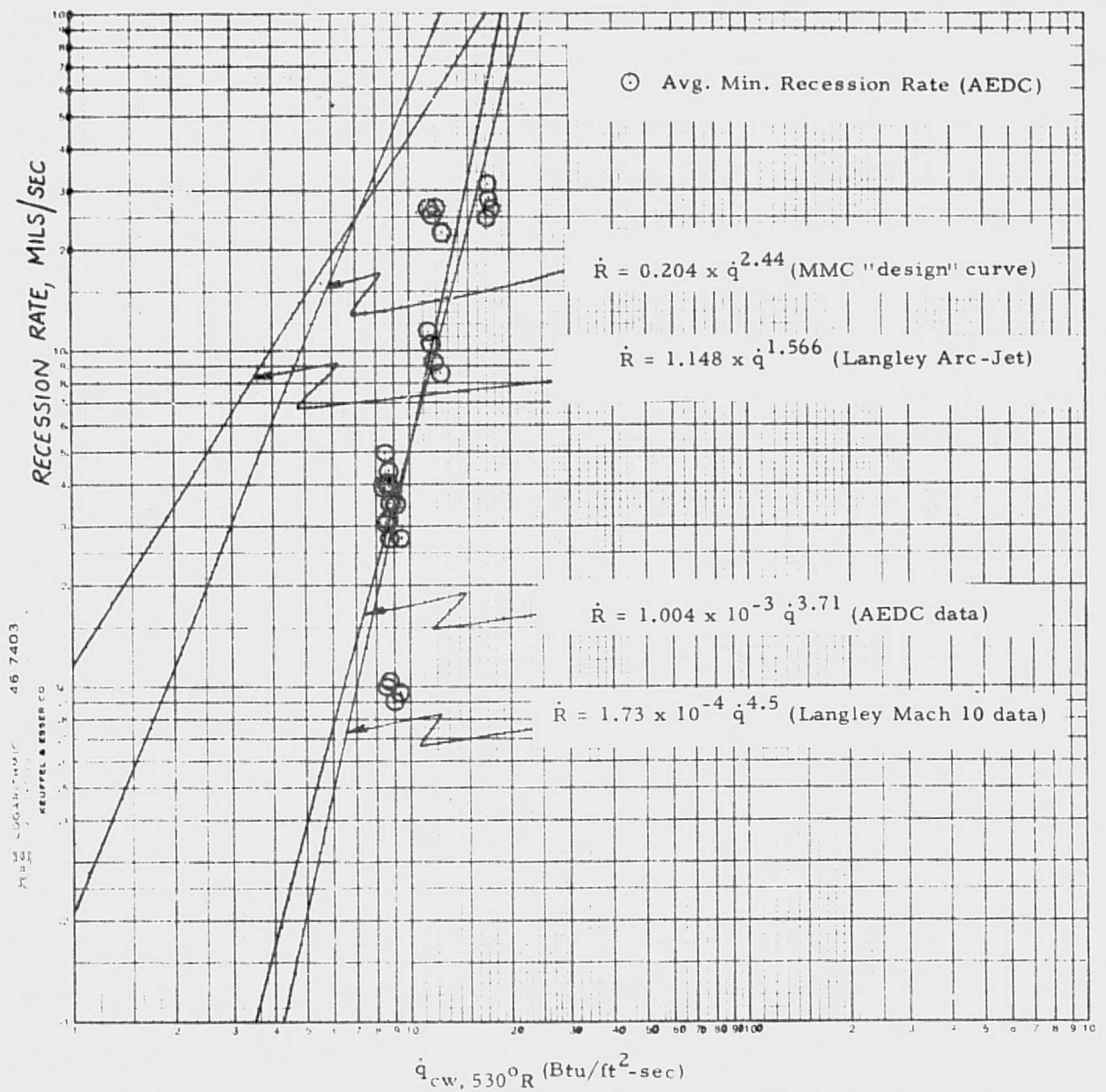


Fig. 85 - Comparison of AEDC Data with MMC "Design" Curve and Langley Arc Jet and Langley Mach 10 Data Curve Fits (Average minimum recession curve)

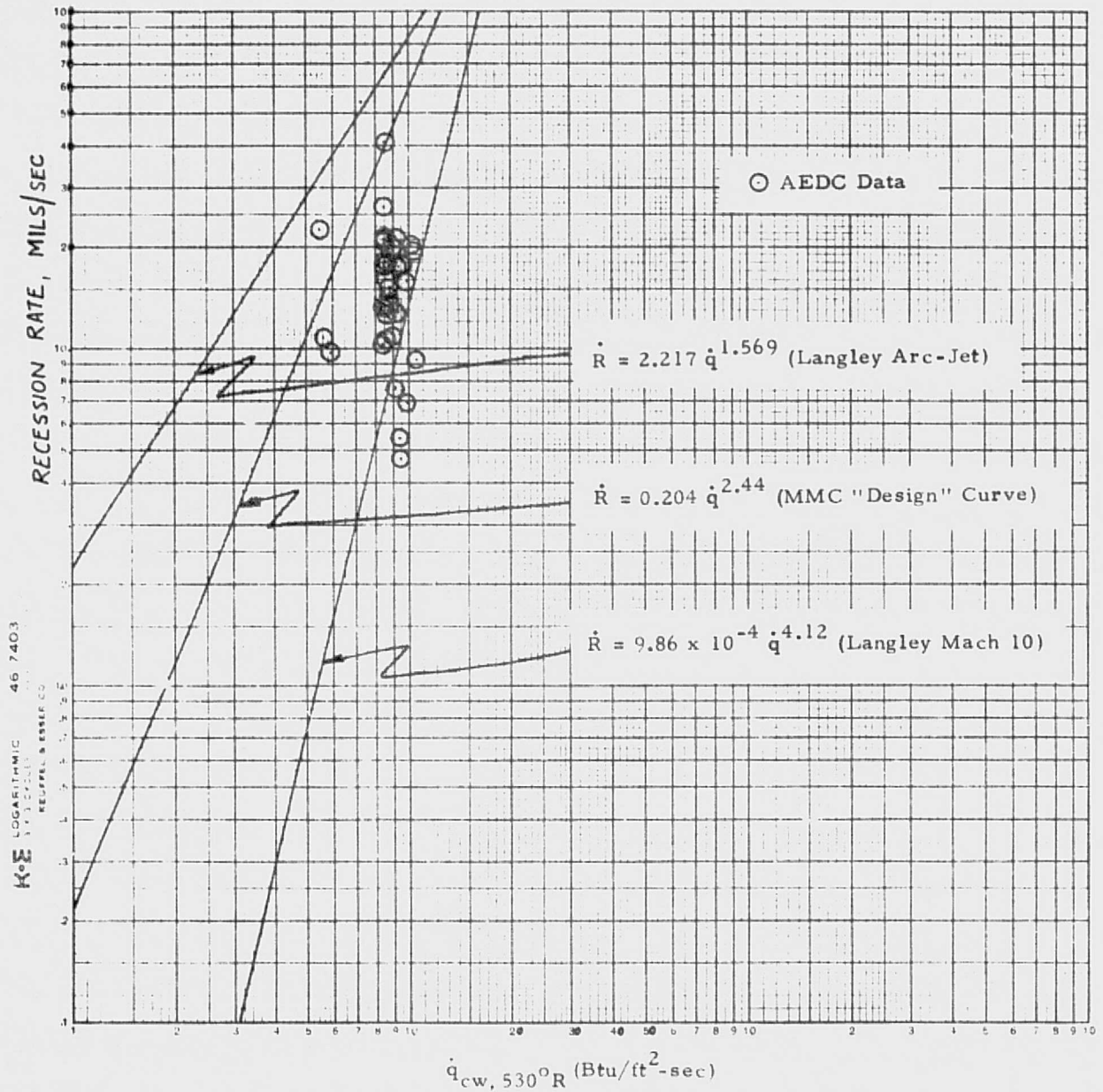
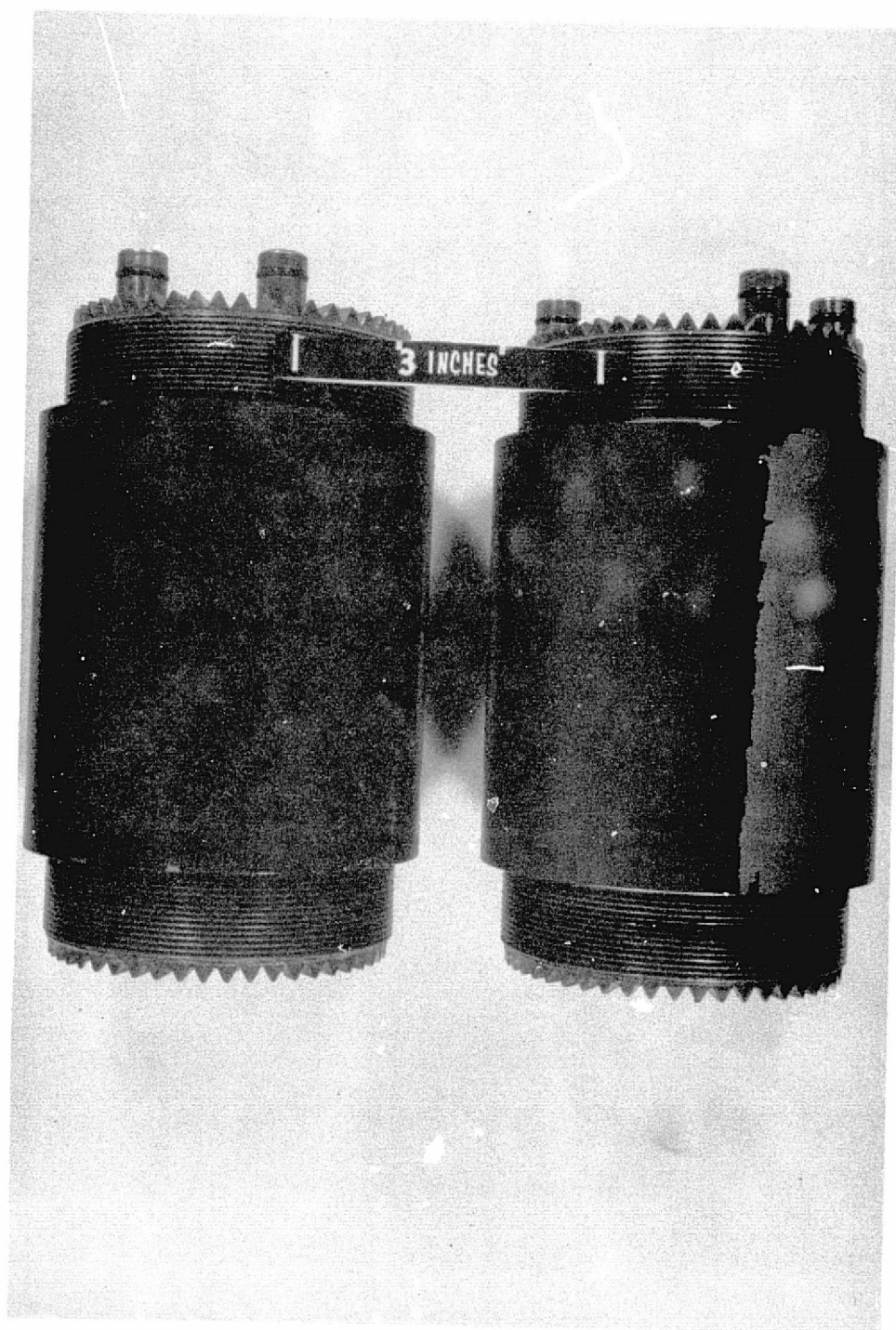


Fig. 86 - Comparison of AEDC Data with MMC "Design" Curve and Langley Arc Jet and Mach 10 Data Curve Fits (Recession rate at the bottom of the streaks)



REPRODUCIBILITY OF THE
ORIGINAL PAGE IS POOR

Fig. 87 - Tunnel 'C' Sting Adaptor Sections Showing Contamination from Foam 'Ablation' Products (Note right side of section on right where contaminants have been scraped off.)

Appendix I

McCutcheon, W. A., "Stress Analysis of Gas Generator Combustion Chamber Body and Throat," LMSC-HREC TN D390948, Lockheed Missiles & Space Company, Huntsville, Ala., 10 September 1975.

LOCKHEED

Huntsville Research & Engineering Center

Contract NAS8-25569

Date 9-25-75

Doc. LMSC-HREC TN D390948

Title: STRESS ANALYSIS OF THE GAS GENERATOR COMBUSTION CHAMBER
BODY AND THROAT

A finite element stress analysis was performed on the subject structure using the LMSC SAP-IV structural analysis program. The purpose of this study was to determine if slippage or yielding will occur at the interface of the steel and copper sections of the chamber.

Page one of the attachment is a general view of the structure analyzed.

Thermal loads were applied to the structure as shown on page two of the attachment.

Page three of the attachment presents the modeled structure and the locations of the connecting bolts which tie the steel and copper sections together. Compressive forces were applied to the structure at each bolt location based upon a 350 in-lb torque value for each bolt.

The structure was idealized using "brick" elements. Stress values at the centroid of each element were obtained as well as the stress values at the interface plane.

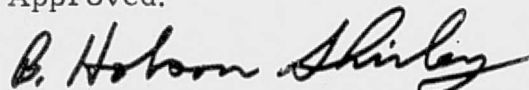
The highest stresses found in the structure indicate a margin of safety greater than 10 for the steel section, and greater than 7 for the copper section.

Also, no slippage should occur at the interface. The normal forces incurred by the torqued bolts are sufficient to overcome the shear forces due to temperature loading.

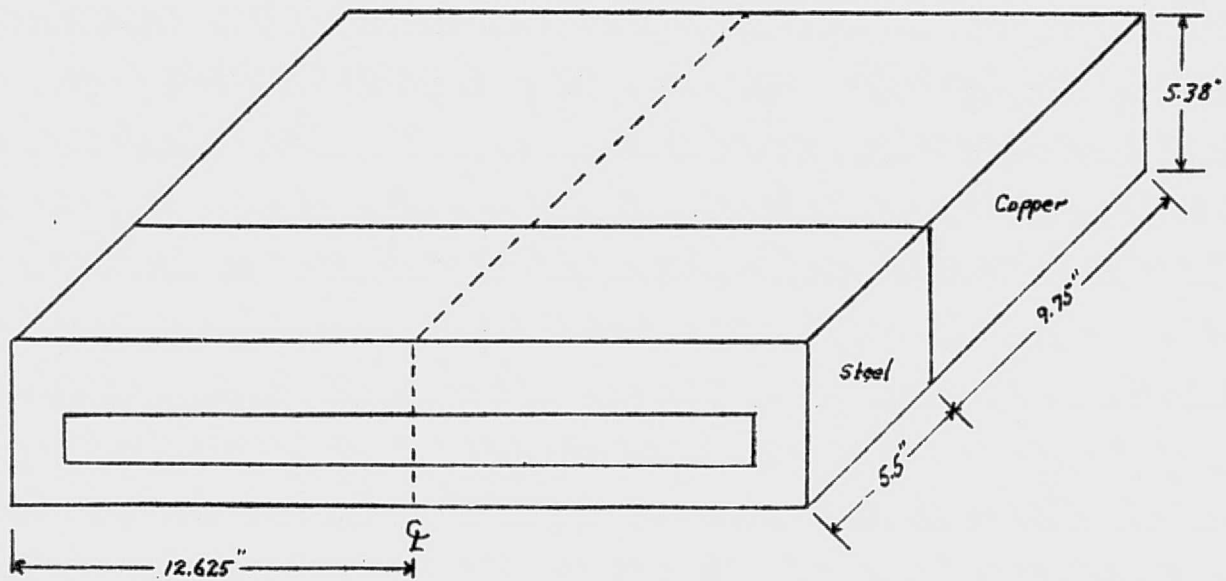

E. L. Bernstein


W. A. McCutcheon

Approved:

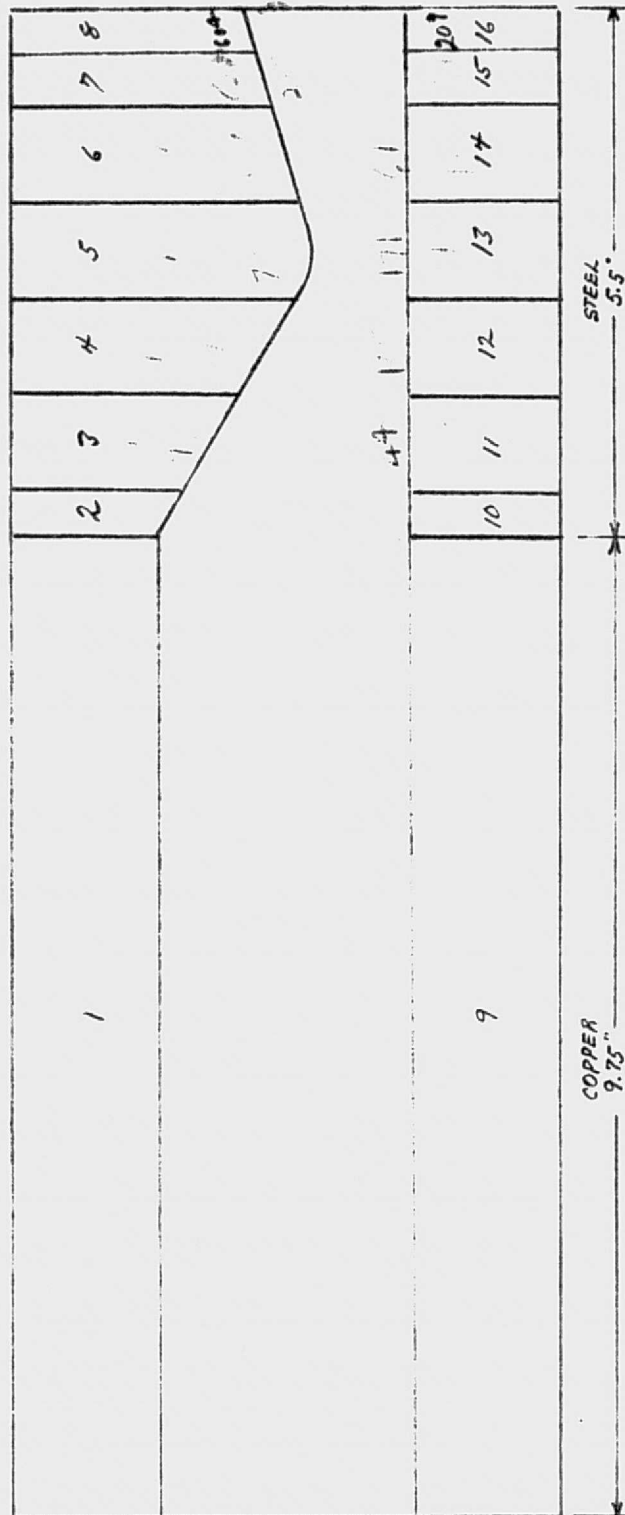
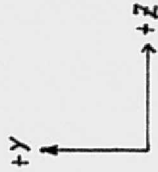

B. Hobson Shirley, Supervisor
Engineering Sciences Section

Attach: pp. 2 and 3.



2

STRUCTURAL ZONE	TEMP (F°)	STRUCTURAL ZONE	TEMP (F°)
1	100	9	100
2	465	10	465
3	758	11	802
4	811	12	946
5	973	13	944
6	674	14	735
7	624	15	339
8	604	16	209



Appendix J

McCutcheon, W. A., "Revised Stress Analysis of the Gas Generator Combustion Chamber," LMSC-HREC TN D390949, Lockheed Missiles & Space Company, Huntsville, Ala., 25 September 1975.

TECHNICAL NOTE

Appendix J

LOCKHEED

Huntsville Research & Engineering Center

Contract NAS8-25569

Date 9-25-76


Doc. LMSC-HREC TN D390949

Title: REVISED STRESS ANALYSIS OF THE GAS GENERATOR COMBUSTION CHAMBER

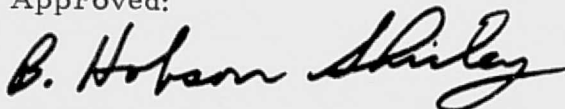
The subject analysis was accomplished using the revised torque loads (200 in-lb) on the connecting bolts.

Page one of the attachment shows the relative deformations which occur using the temperature loads of the previous analysis.

Page two shows the copper/steel interface plane, and the values of shear/normal stress along the plane. Based upon a friction coefficient of 0.36, the graph shows slippage will occur between the copper and steel faces.

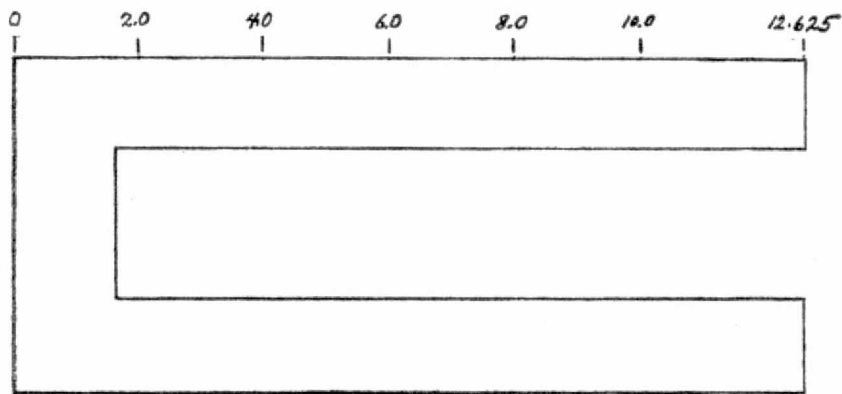
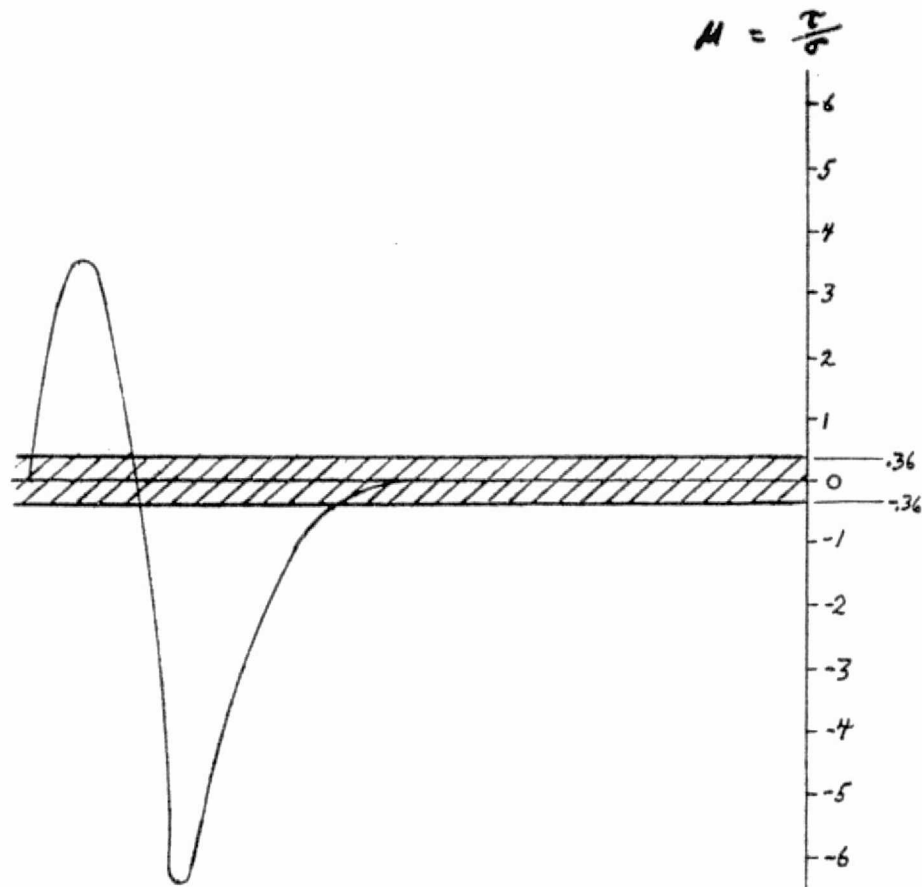

W. A. McCutcheon

Approved:



B. Hobson Shirley, Supervisor
Engineering Sciences Section

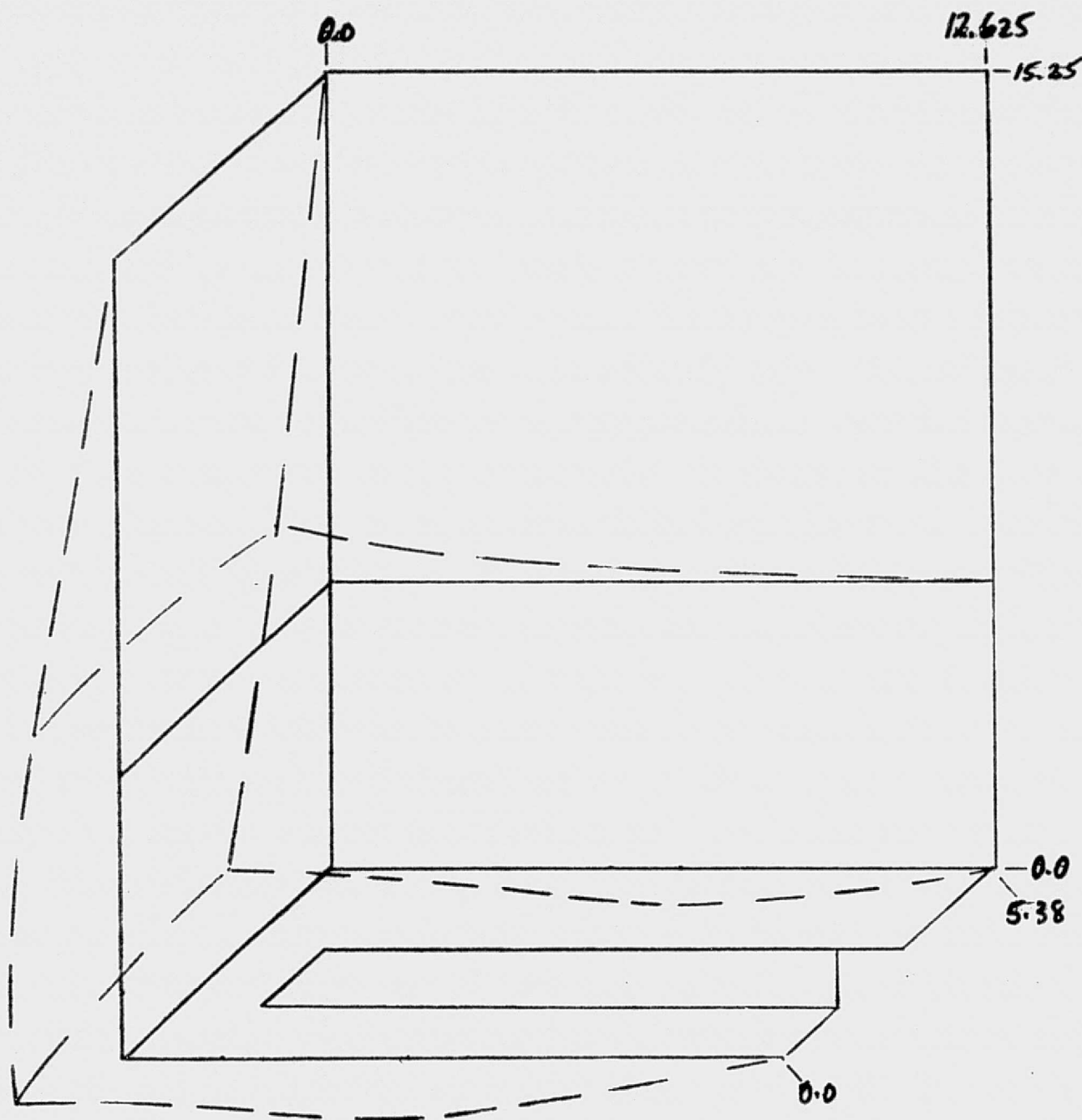
Attach: pp. 1 and 2



Cu/St Interface Plane

⊥

Deformation Scale = 10%



REPRODUCIBILITY OF THE
ORIGINAL PAGE IS POOR

Appendix K

Ratliff, A. W., "Analysis of Low Enthalpy Hot Gas Facility (LEHGF) Ignition Sequence," LMSC-HREC TN D496575, Lockheed Missiles & Space Company, Huntsville, Ala., October 1975.

TECHNICAL NOTE

Appendix K

LOCKHEED

Huntsville Research & Engineering Center

Contract NAS8-25569 Date October 1975 Doc. LMSC-HREC TN D496575

Title: ANALYSIS OF LOW ENTHALPY HOT GAS FACILITY (LEHGF) IGNITION SEQUENCE

Analysis of the Low Enthalpy Hot Gas Facility (LEHGF) ignition sequence was recently conducted utilizing the mixing finite rate reaction capability of the LAMP code.* The kinetic mechanism includes both ignition and quenching reactions (Table 1) since the main concern was whether or not the ignition could be sustained in the presence of large air flow rates.

Table 1
REACTION MECHANISM

Reaction Considered					Constants Used in Rate Constant Equation**		
					(A)	(N)	(B)
OH	+H	+M1 [†]	=H ₂ O	+M1	6.1 -26	2.0	
O	+H	+M1	=OH	+M1	2.0 -32		
O	+O	+M1	=O ₂	+M1	3.8 -30	1.0	-340.
H	+H	+M2	=H ₂	+M2	2.8 -30	1.0	
OH	+H		=H ₂	+O	1.4 -14	1.0	-7000.
OH	+O		=H	+O ₂	4.0 -11		
OH	+H ₂		=H ₂ O	+H	1.0 -17	-2.0	-2900.
OH	+OH		=H ₂ O	+O	1.0 -11		-1100.
H	+O ₂	+M14	=HO ₂	+M14	6.7 -33		580.
HO ₂	+H		=H ₂	+O ₂	4.2 -11		-700.
HO ₂	+H		=OH	+OH	4.2 -10		-1900.
HO ₂	+O		=OH	+O ₂	8.0 -11		-1000.
HO ₂	+OH		=H ₂ O	+O ₂	8.3 -11		-1000.
HO ₂	+H ₂		=H ₂ O	+OH	1.2 -12		-18700.
H ₂	+O ₂		=OH	+OH	2.8 -11		-48200.

* Thoenes, J., A. J. McDanal, A. W. Ratliff and S. D. Smith, "Laser and Mixing Program (LAMP) Theory and User's Guide," Lockheed Missiles & Space Company, Huntsville, Ala., June 1974.

** Arrhenius form of rate constant, $k = AT^{-N} \exp(B/RT)$

[†] The Ms represent the catalytic or nonreacting species.

REPRODUCIBILITY OF THE
ORIGINAL PAGE IS POOR

The analysis was carried out in a steady state mode using the nominal run conditions as follows:

$$P_c = 100 \text{ psia}$$

$$O/F \approx 150$$

$$\Delta P_{air} = 35 \text{ psia}$$

$$\Delta P_{GH_2} = 10 \text{ psia}$$

$$\dot{m}_{air} = 29.6 \text{ lb/sec}$$

$$\dot{m}_{GH_2} = 0.195 \text{ lb/sec}$$

The problem was formulated based on Fig. 1 which presents the general LEHGF configuration. An ignition source (J-2 igniter) was simulated by assuming the localized combustion products and properties about the source to be in equilibrium. The finite rate-mixing analysis was initialized and the combustion was then controlled by the relative effects of mixing rates and the kinetic mechanism. The mixing rates were defined by the turbulent kinetic energy model (TKE) which is based upon experimental measurements.

The results of this analysis indicate that with the continuous* ignition source providing an initialization of the finite rate calculation, the LEHGF system does indeed ignite and burn successfully utilizing the nominal operating conditions listed above. As shown on Fig. 1, the flame starts on the sides where the igniters are located and proceeds to the combustor centerline approximately six inches downstream of the injector face. These results are somewhat conservative since the flame front will likely propagate even more rapidly than indicated by this analysis.



Alan W. Ratliff

Advanced Technology Systems Section

Approved:



John W. Benefield, Supervisor
Advanced Technology Systems Section

Attach: Fig. 1

*If the igniters are not operated continuously, the flame is quickly extinguished due to the quenching reactions.

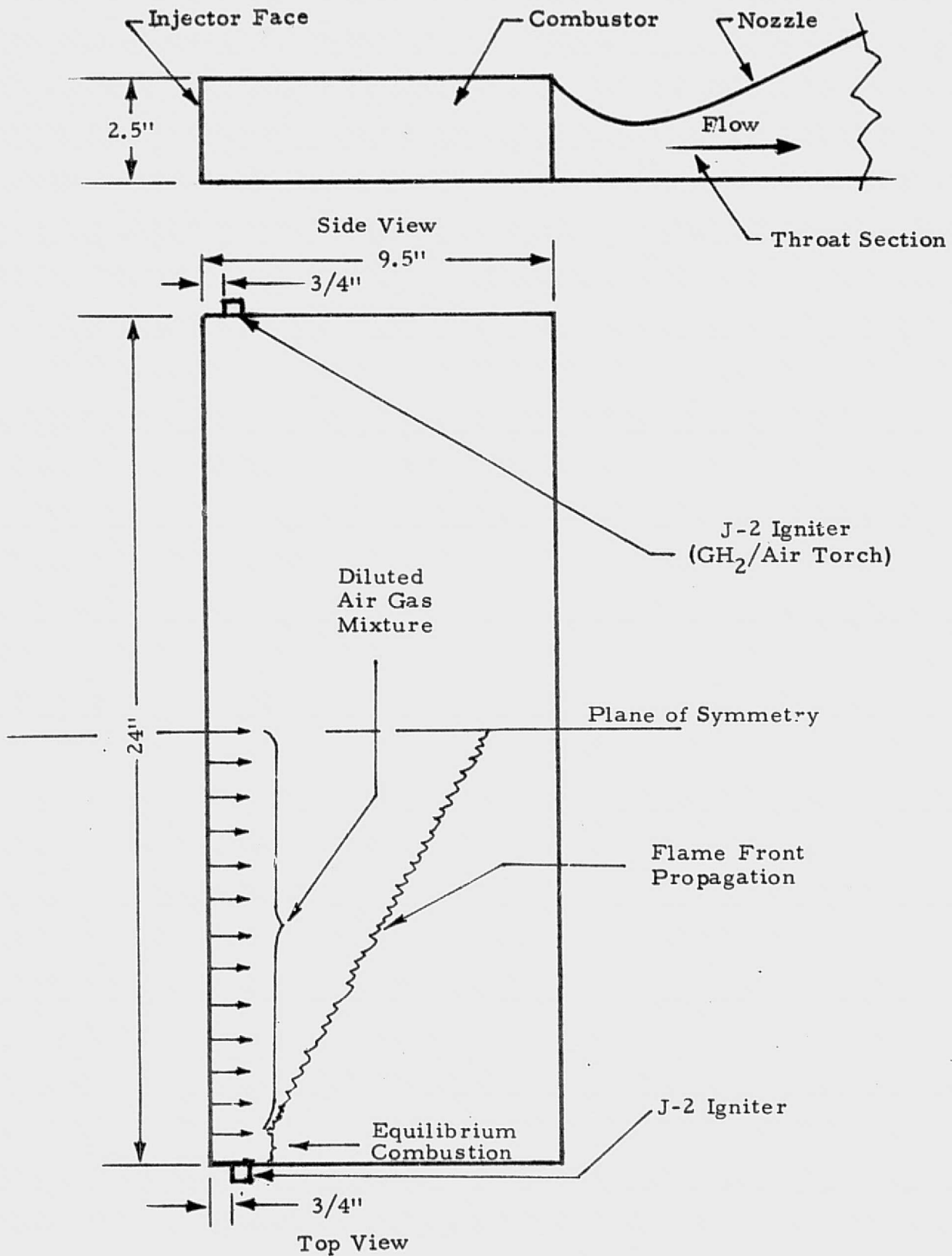


Fig. 1 - LEHGF Injector/Combustor Configuration

Appendix L

McCutcheon, W. A., "Stress Analysis of Gas Generator Throat with Revised Temperature Grid and Internal Pressure Loads," Lockheed Missiles & Space Company, Huntsville, Ala., 17 November 1975.

TECHNICAL NOTE

Appendix L

LOCKHEED

Huntsville Research & Engineering Center

Contract NAS8-25569

Date 11-17-75

Doc. LMSC-HREC TN D496707

Title: STRESS ANALYSIS OF GAS GENERATOR THROAT WITH REVISED
TEMPERATURE GRID AND INTERNAL PRESSURE LOADS

The gas generator throat stress analysis was accomplished using the SAP-IV structural analysis program. Results indicate that stresses will not exceed the yield values of the materials.

At the interface of the steel and copper structural components, particular attention was given to assessing the possibility of "slippage" occurring due to the different material properties and temperature disparities present. Reduction of stress data at the interface indicates "slippage" should not occur during the hot phase, but after cooling the structure should be examined and the connective bolts retorqued if required.

Internal structural deformations were examined as a possible source of flow distortion in the throat section. Cross sectional areas were calculated for the deformed structure at three planes as indicated on the attached figure, and compared with the unstressed structures' cross sectional areas.

The area of the plane bounded by:

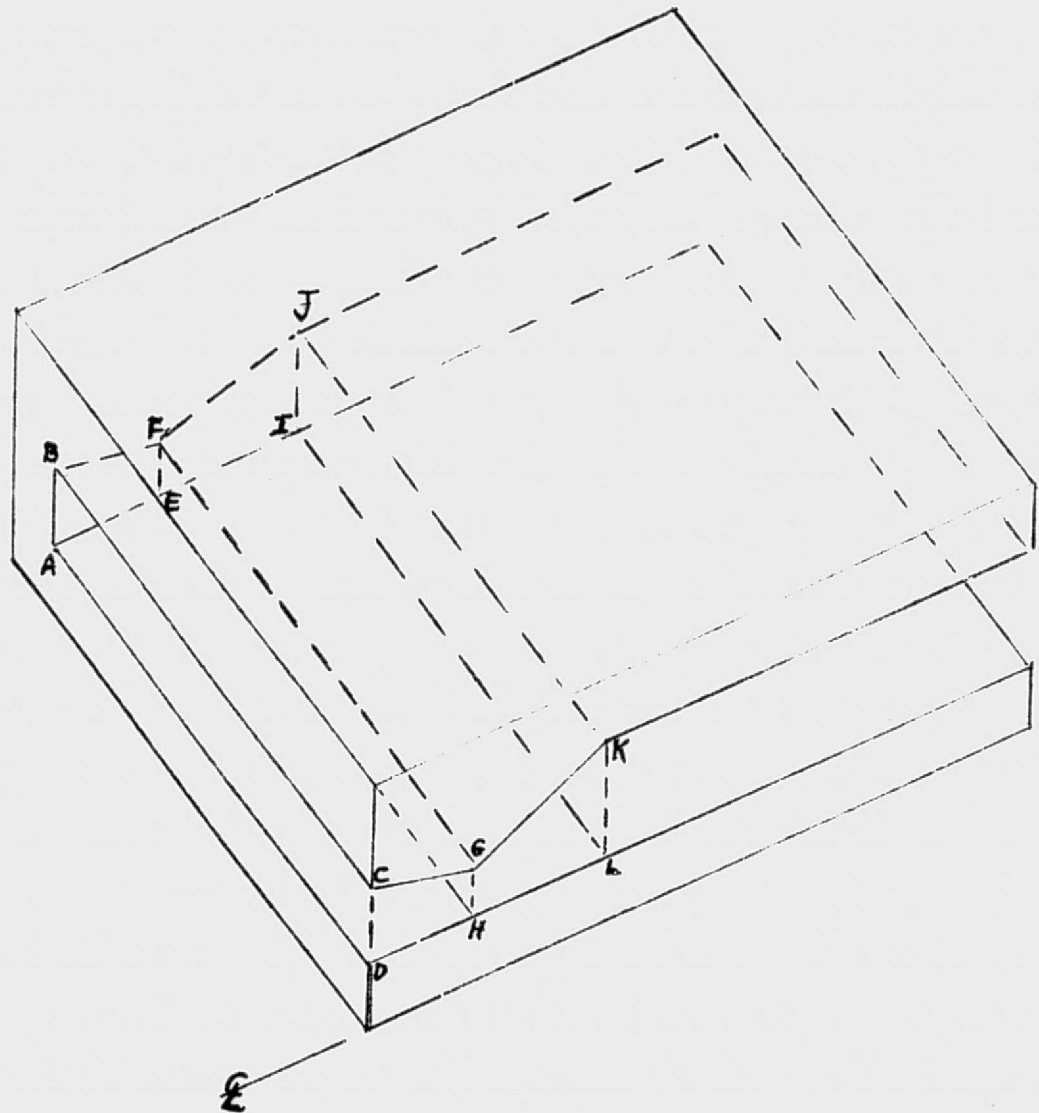
ABCD	Increases	0.7%
EFGH	Decreases	0.5%
IJKL	Increases	0.6%.

W. A. McCutcheon
W. A. McCutcheon

Approved:

B. Hobson Shirley
B. Hobson Shirley, Supervisor
Engineering Sciences Section

Attach: p. 2



Appendix M

Dean, W. G., "Quality Assurance and Inspection of Work Accomplished in the Design/Fabrication of the Modification of the NASA-MSFC Hot Gas Test Facility," LMSC-HREC TM D496686, Lockheed Missiles & Space Company, Huntsville, Ala., January 1976.

LOCKHEED

Huntsville Research & Engineering Center

Contract NAS8-25569 **Date** 14 January 1976 **Doc.** LMSC-HREC TN D496686

Title: QUALITY ASSURANCE AND INSPECTION OF WORK ACCOMPLISHED IN THE DESIGN/FABRICATION OF THE MODIFICATION OF THE NASA-MSFC HOT GAS TEST FACILITY

SUMMARY

This report documents the quality assurance and inspection efforts performed under Contract NAS8-25569 "Design and Develop the Modifications of the MSFC Hot Gas Test Chamber" by Lockheed-Huntsville for NASA-MSFC. The NASA CORs for this Contract were Dr. K.E. McCoy, S&E, EP 44, and Mr. R.N. Stone, S&E, ET 18.

The method used to document these efforts is generally to present copies of the various original documents executed during the contract for quality assurance and inspection, receiving, shipping, etc., purposes. This method was suggested by NASA-MSFC quality assurance personnel responsible for monitoring these efforts by Lockheed as being sufficient documentation for their requirements.

These copies are attached as separate sections as follows:

Section 1: Welding/Fabrication Subcontracted Efforts

- Subcontractor's "Quality Sensitive Hardware Capability Survey" statement for NASA-MSFC on Form DD-1232.
- Subcontractor's packaging/shipping form, showing inspection, welder, welding filler rod, certifications, and drawing number references which call out NASA-MSFC Welding Spec MSFC-135, and Lockheed receiving/acceptance signature.
- Subcontractor's material certification copies (for nozzle, test section, and support stand materials).

Section 2: LMSC Minimum Quality Control Specification

Section 3: Cryopanel Subcontractor's Efforts

- Cover letter
- ASME Form U-1A, (pressure vessel test report)
- Shop inspection/certification form
- ASME compliance/certification form
- Shop bill of materials
- Raw material certification

Section 4: Throat Section Material Certification

Section 5: Silicone O-Ring Material Certification

Section 6: Dummy Calibration Panel Materials Certification

Section 7: Air Manifold/Tubes Material Certification

Section 8: Subcontracted Manifold Welding Certification

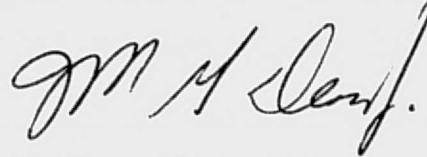
Section 9: Lockheed Project Engineer's Statement of Compliance with Drawings

Section 10: Calibration Panel Material Certification

Section 11: NASA-MSFC Acceptance Form, with Return of Government Supplied Hardware

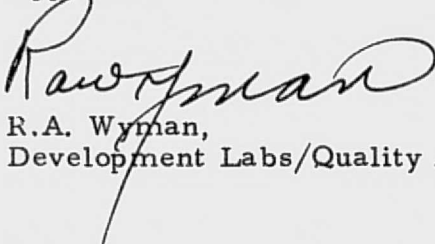
Section 12: Lockheed Shipping Notice/Loaning Windows to NASA

Proof Tests: All proof tests and their results are documented in the following report: Dean, W.G., "Modification/Fabrication of the NASA-MSFC Low Enthalpy Hot Gas Test Facility," LMSC-HREC TM D496690, January 1976.



W.G. Dean, Project Engineer,
Hot Gas Facility Modification Project

Approved



R.A. Wyman,
Development Labs/Quality Assurance



B.H. Shirley, Supervisor
Engineering Sciences Section

Attach: (1) Statement of Compliance
(2) pp. 5 through 30

QUALITY ASSURANCE REPRESENTATIVE'S CORRESPONDENCE

11

Mr. Robert Riener
MSFC-PG-22
Marshall Space Flight Center, AL 35812

2. FROM: (Name, address and ZIP Code of QAR)

Mr. Jesse P. King
DCASO Huntsville
2109 W. Clinton Ave.
Huntsville, AL 35805

3. CONTRACT, P. O., OR O. I. NUMBER

N/A

9. ITEM

N/A

5 FIRM* COMYNACTON NAME, ADDRESS AND ZIP CODE

Pedigo Welding & Fabrication Co. Inc.,
P.O. Box 40
Lacey's Spring, AL 35754

18. PLANT NAME, ADDRESS AND ZIP CODEX

SUBJECT: Quality Sensitive Hardware Capability Survey.

This survey was performed Aug 26 1975 with the assistance of Mr. Robert Riemer, and Mr. John Hofues both of MSFC Quality Lab. To assure that this supplier has the capability of performing work on Quality Sensitive Hardware, they were surveyed using these check lists. Check list #1, General Quality Requirements, Check list #7. Category 3, Check list #8, Category 4, Check list #15, Category 6, Category 5 deals with special processes, with the specified requirements being Category 5(a), Painting and Category 5(e), Welding. These two categories were reviewed and found to be acceptable and the supplier capable of performing work on Quality Sensitive Hardware in the areas.

It must be noted that during the required survey it was determined that Pedigo Welding also has the capability to perform the heat treat process. Their capability has a heat range up to 2000° and can take items up to 24"x18"x30". Although they can perform heat treatment, the required hardness checks must be accomplished by an outside vendor. This procedure is acceptable as Pedigo would be responsible for the Quality of all work performed by outside vendors. During the survey, no areas were noted that Pedigo was not in compliance with their written procedures. With this in mind it is recommended that Pedigo Welding be placed on the Qualified Suppliers list for Categories 3,4,6 & 5(a), 5(c) and 5(d). The only area that Pedigo was not surveyed for was Category 2. This Category is Precision and Specialized Machining. At this time Pedigo does not have this capability. If in the future, this supplier, obtains this capability, they will be surveyed using Check list #6. Based on the findings, of this survey it is the opinion of this team that Pedigo Welding and Fabrication Co. be placed on the Qualified suppliers list.

6. **ANALYSIS OF VARIANCE**

Charles F. Jones 4

4

۵۲۷۲۷۵

PEDIGO

Welding & Fabrication Company, Inc.

P.O. BOX 40

LACEYS SPRING, ALABAMA

Phone - 881-6173

PARTIAL ☐☒ COMPLETE

Packing Slip

MR. 216400
10-20-75SHIPPED TO Lockheed Missiles & Space Co., Inc. SOLD TO SameHuntsville Research & Engineering CenterHuntsville, AL 35807

CUSTOMER ORDER NO.

WORK ORDER NO.

GOVT. CONTRACT NO.

ROUTING

ZAL718720Y

W602

WAG825060

Pedigo truck

QUANTITY

PART NUMBER *

DESCRIPTION

P. O. Item No.

1 ea.

W60108

Test Section

Item 1

1 ea.

W60107

Nozzle

Item 2

1 ea.

W60123

Chamber Support

Item 3

2 ea.

W60119

Test Section Support

Item 4

Returned All Hardware, Cockets and Window spacer

Welding By: W. T. Marnier

Material Certification Attached--Filled material with 1/2" riv

INSPECTOR H. L. WalkerCUSTOMER
INSPECTORSHIPPED BY H. L. WalkerDATE Oct. 17, 1975REC'D. BY 216400

INV. NO. _____

NO. BOXES _____

* Test section
 Nozzle
 Combustor Support
 Test Section Supports (2)

REPRODUCIBILITY OF THE
 ORIGINAL PAGE IS POOR

PEDIGO

Welding & Fabrication Company, Inc.

P.O. Box 40

LACEYS SPRING, ALABAMA

Phone - 881-6173

PARTIAL ☐

☐ COMPLETE

Packing Slip

SHIPPED TO Eastport Marine & Supply

Mobile, AL

RECEIVED BY: <u>J. B. Bost</u>	DATE <u>11/5/75</u>
REGISTER NO:	
SOLD TO BY: <u>34B</u>	
INSPECTED BY: <u>Rae</u>	
DELIVERED TO: <u>Rae</u>	
COMPLETE <input type="checkbox"/>	
DEPT. NO <u>52/40</u>	DATE <u>11/5/75</u>

CUSTOMER ORDER NO.

WORK ORDER NO.

GOVT. CONTRACT NO.

ROUTING

QUANTITY	PART NUMBER	DESCRIPTION	P. O. Item No.
	R80104 *		MR 174127
	R80110		MR 174127
	R80109		MR 174128

INSPECTOR H. L. Walker

CUSTOMER INSPECTOR

SHIPPED BY H. L. Walker

DATE 11-5-75

REC'D. BY

INS. NO.

* INTERIOR WELDING
CALIBRATION PANEL WELDING
DUMMY PANELS "

NO. BOXES

REPRODUCIBILITY OF THE
ORIGINAL PAGE IS POOR

Section 1 page 3

PEDIGO

Welding & Fabrication Company, Inc.

P.O. BOX 40

LACEYS SPRING, ALABAMA

Phone - 881-6173

PARTIAL ☐

☐ COMPLETE

Packing Slip

REC'D RECEIVING
 SHIPPED BY: J. St. B. Smith DATE 11/2/57
 REGISTER NO: V869-004
 SOLD TO: 34B
 INSPECTED BY: [Signature]
 DELIVERED TO: [Signature]
 COMPLETE ☒ DEPT. NO. 52/111 DATE 11/6/57

SHIPPED TO [Address]

CUSTOMER ORDER NO.	WORK ORDER NO.	GOVT. CONTRACT NO.	ROUTING
QUANTITY	PART NUMBER	DESCRIPTION	P. O. Item No.
	<u>P80125 *</u>		

MR-174127

INSPECTOR [Signature] CUSTOMER INSPECTOR [Signature]
 SHIPPED BY H. L. Walker DATE 11-6-57 REC'D. BY [Signature]
 INS. NO. [Blank] NO. BOXES [Blank]

* THRUST STRUCTURE ASSEMBLY

Section 1 Page 4

PEDIGO

Welding & Fabrication Company, Inc.

P.O. BOX 40

LACEYS SPRING, ALABAMA

Phone - 881-6173

PARTIAL ☐

☐ COMPLETE

Packing Slip

SHIPPED TO Southland Industrial & Service Co., Inc. SOLD TO ZAA 726870 X

CUSTOMER ORDER NO. X

WORK ORDER NO. 1728

GOVT. CONTRACT NO.

ROUTING

QUANTITY

PART NUMBER

DESCRIPTION

P. O. Item No.

RECEIVED BY: HREC RECEIVING

DATE 11/26/75

REGISTER NO. V883-004

INSPECTED BY:

DELIVERED TO: R. J. Walker

COMPLETE ☒ 5-2-10 11-26-75

PARTIAL ☐

CUSTOMER INSPECTOR DATE 11/26/75

REC'D BY: 11-26-75

NO. BOXES 11-26-75

INSPECTOR H. J. Walker

SHIPPED BY H. J. Walker

INS. NO.

* STAINLESS STEEL THROAT

Station / Page 1

UNITED STATES STEEL CORPORATION
PRODUCTION DEPARTMENT - METALLURGICAL

CLAIRTON

WORKS

FILE NO. R01303

Test Report of _____ CHANNELS

APRIL 8th 1971

Product Description/Specification STPL ASTM A-36-70A

Charged to ONEAL STEEL INC. BIRMINGHAM ALABAMA

**Load Tally
or Shipping Notice.**

Shipped to _____ SAME

Car Number.

[illegible]

STATE OF PENNSYLVANIA
COUNTY OF ALLEGHENY

35

Subscribed and sworn to before me this

8th day of APRIL A.D., 1975

8th day of APRIL A.D., 1975
Thomas H. Harrison Notary Public

My Commission expires:

FBI - NEW YORK
 TO DIRECTOR
 FROM NEW YORK (100-100000)
 JULY 21, 1973

RICHARD G. WEISS, being duly sworn according to law, deposes and says that the figures set forth above are correct, as contained in the records of the company.

Richard Chas.

ALBERT I. BROWN
JAN 1971

REPRODUCIBILITY OF THE
ORIGINAL PAGE IS POOR

BY

Steel Corporation

JUNCTION 140 & HIGHWAY 27 - P.O. BOX 237
HARRIMAN, TENNESSEE 37748
PHONE: (615) 882-5331

ARKANSAS DIVISION
HIGHWAY 67 & VAN DYKE RD. - P.O. BOX 310
NEWPORT, ARKANSAS 72112
PHONE: (501) 523-3693

FURNISHED TO O NEAL STEEL, INC.
CUSTOMER ORDER NO. 8-12240

PACKING SLIP NO.

8528

2 CCB

Section 1 Page 7

174 PART 4

**My Commission Expires
September 12, 1977**

Sworn to and subscribed before me this
day of 11/16/74 19 74

Daniel S. Lemons V
NOTARY PUBLIC

METALLURGIST

* DOES NOT APPLY TO ANGLE

Republicsteel

Section 1 page 8

AMEANVEAM
315 9/22/75
INVG

CUSTOMER ORDER NUMBER AND DATE

ALIGNMENT
LTR. NO.RENEGOT.
YEAR

SHIPPED FROM

INVOICE DATE

INVOICE NUMBER

B-10009 8/1/75

ALA CITY

704-16290

DATE SHIPPED

9/21/75

RECEIVED
BY
DATE

ROSS NEELY

REPUBLIC ORDER NO.
DIST. NUMBER
13-43935-704CUSTOMER ABBREVIATION
ONEAL STEELSALES CO.
DIV. TYPE
2001SP
133CONTROL CARD
56531STATE
001COUNTY
037DIST. NO.
3TAX
3000OFFICE
DIST. SUB
13160ACCOUNT
NUMBER
56755001DEST.
160MKT. CLASS
160ONEAL STEEL, INC.,
P.O. BOX 2623
BIRMINGHAM, AL 35202ONEAL STEEL, INC.,
745 NORTH 41ST STREET
BIRMINGHAM, AL 35222TE
MAIL
4
SALES PRODUCT
CLASS
119000000

30-1/2-10

Certificate of Tests

("SHIP TO" SAME AS "SOLD TO" UNLESS OTHERWISE INDICATED)

* "P" PARTIAL SHIPMENT "C" COMPLETE SHIPMENT

REPUBLIC PRODUCT DESCRIPTION

ASTM A-283-74 GRD D HR STEEL PLTS
CLASS III

1/1-4 X 84 CUT EDGE X 240 3 PCS

ASTM A-36-74 HR STEEL PLTS
CLASS IV1/2 X 48 CUT EDGE X 240 13 PCS
LOOSE
ACT PCE CT USED 16 PCS

SHPT QOVD BY INVS 704-16290-92-92

L
ITEM
NO.

UNITS SHIPPED

A 1C

21417#

B 4C

20332#

41749#

WH 98630
5344

I HEREBY CERTIFY THAT THE MATERIAL LISTED HEREIN HAS BEEN INSPECTED AND TESTED IN ACCORDANCE WITH THE METHODS PRESCRIBED IN THE GOVERNING SPECIFICATIONS AND BASED UPON THE RESULTS OF SUCH INSPECTION AND TESTING HAS BEEN APPROVED FOR CONFORMANCE TO THE SPECIFICATIONS.

A. D. Gordon, Chief Metallurgist

By K. S. Brothers

FRT. PPD 51800#

ITEM NO.	HEAT NO.	E.H.N.	CARBON	MANG.	PHOS.	SUL.	SIL.	COPPER	NICKEL	CHROME	MOLY.	VAN.
1	7473240		20	77	011	026						
4	7482867		22	45	010	024						

PHYSICALS	HEAT NO.		SIZE		LBS. PER SQ. IN.		TENSIL STRENGTH		% ELONG.		% RED. AREA		BRINELL ROCKWELL		BEND TEST		REMARKS	
					YIELD POINT													
	7473240		1-1/4"		34680		66120		29.0						OK			
	7482867		1/2"		41950		64600		27.0						OK			

P. O. Box 1178, ASHLAND, KENTUCKY 41101
PHONE: 928-6441 - AREA CODE 606

TESTS REPORT

SHIPPING POINT
COALTON, BOYD COUNTY, KY

S
O L D O T
O'Neal Steel, Inc.
P.O. Box 2623
745 North 41st Street
Birmingham, AL 35202

SHIPPED TO

February 14, 1975

INVOICE No. 13270 DATE 2-17-77

CUSTOMER'S ORDER No. B-12569

L&N 36568

[illegible]

14 DAY OF February 19 75

Fassell L. Tackett
NOTARY PUBLIC, BOYO COUNTY, KY.

MY COMMISSION EXPIRES 10-27-76

RE

THIS IS TO CERTIFY THAT THE ABOVE IS A TRUE
CORRECT COPY OF CERTIFIED REPORTS OF THE ABC

William J. Conn

NOTARY PUBLIC



United States Steel Corporation

TEST REPORT OF H. R. PLATES
WORKS FAIRFIELD U.S.S. ORDER NO. 0026425 LOAD TALLY OR INVOICE NO. 261004
CUSTOMER ORDER NO. B-13771
CAR OR TRUCK NO. BS5854 SHIPPER NO. & DATE 09/09/75

O NEAL STEEL INC.
P O BOX 2623
BIRMINGHAM ALABAMA 35202

O NEAL STEEL INC.
BIRMINGHAM ALABAMA

ASTM A 36-75

MILL SWORN T/R

WH 98630
5 344

STATE OF ALABAMA
COUNTY OF JEFFERSON

SWORN TO AND SUBSCRIBED BEFORE ME
THIS 10 DAY OF SEPTEMBER

NOTARY PUBLIC

BEING DULY SWORN ACCORDING
TO LAW, DEPOSES AND SAYS
THAT THE CHEMICAL ANALYSIS
AND/OR TESTS SHOWN ON THIS
REPORT ARE CORRECT AS CON-
TAINED IN THE RECORDS OF
THE COMPANY.

J. M. EDGE
SIGNATURE CHIEF METALLURGIST
DATE September 10, 1975/CW

ITEM NO.	HEAT NO.	TEST OR PIECE IDENTITY NO.	MATERIAL DESCRIPTION					YIELD ST. PSI.	TENSILE ST. PSI.	ELONGATION %		% RED OF AREA
			NO. PCS.	THICKNESS OR SECTION	WIDTH, DIA. OR FT. WT.	LENGTH	WEIGHT			IN 8"	IN 2"	
03	X02325	D5794	1	3/8	84	240 IN	2142	35800 *	63600	27.0		
04	U03402	D8419	2	3/8	96	240 IN	4896	36900	64700	30.5		

* Accepted by Customer

SPECIMEN SIZE TESTED ACCORDING TO COMPANY RECORDS CONFORMS TO THE REQUIREMENTS OF THE SPECIFICATION LISTED ABOVE

* B OR H INDICATE COMPLIANCE OF BEND OR HOMO TESTS, RESPECTIVELY

HEAT NO.	TYPE	C	Al	P	S	Si	Cu	Ni	Cr	Mo	Sn	Al	N	V	B	Ti	Cb	Co
X02325	L	22	51	013	024													
U03402	L	22	47	024	015													

11/26/1991

SHIPPED TO

O'Neal Steel, Inc.
P.O. Box 2623
745 North 41st Street
Birmingham, AL 35202

February 14, 1964

INVOICE No. 13211 DATE 2-17-

CUSTOMER'S ORDER No. B-12568

L&N 36568

SUBSCRIBED AND SWORN TO BEFORE ME THIS

14 DAY OF February 19 75

DAY OF _____ 19____
Fassell R. Tackett
 NOTARY PUBLIC, BOYD COUNTY, KY.

MY COMMISSION EXPIRES 10-27-76

RM

THIS IS TO CERTIFY THAT THE ABOVE IS A TRUE
CORRECT COPY OF CERTIFIED REPORTS OF THE

William J. Ross

10/10/10

Section 2, Page 2

QUALITY ASSURANCE REQUIREMENTS
FOR ENGINEERING RESEARCH & DEVELOPMENT PROGRAMS

LMSC MINIMUM QUALITY CONTROL SPECIFICATION

1. SCOPE

1.1 This specification is the minimum quality control requirement for all hardware produced by LMSC, except shop, laboratory, or test aids produced under research and developmental programs which have no direct effect on program results or customer requirements.

1.2 Since practically all end-item and some non-end-item hardware production is governed by specifications contractually imposed by the customer, this specification is designed primarily to cover limited production, research and development, and Company-sponsored hardware programs.

2. APPLICABILITY

2.1 This specification is applicable to program hardware produced under these conditions:

- a. When no other quality control specification is invoked by a contract.
- b. When customer or contract requirements are less stringent than the LMSC Minimum Quality Control Specification.
- c. On Lockheed-funded programs where there is no contract with a customer.

3. OBJECTIVE

3.1 Quality and reliability shall be major considerations in the fabrication of all LMSC hardware. The objective of this specification is to establish a discipline for quality and reliability, consistent with the stage of hardware development, which will:

- a. Assure meeting contract requirements and the objectives of LMSC programs.
- b. Facilitate orderly and economical transition to the next phase of hardware development or production.
- c. Provide the freedom of action necessary for the timely prosecution of research and development effort and timely and economical fabrication of hardware.

4. GUIDELINES FOR USE

4.1 This specification covers a broad spectrum of hardware production and its provisions shall be applied and interpreted judiciously, with due consideration to the state of hardware development and intended use of the hardware itself.

Section 2, Page 3

QUALITY ASSURANCE REQUIREMENTS
FOR ENGINEERING RESEARCH & DEVELOPMENT PROGRAMS

LMSC MINIMUM QUALITY CONTROL SPECIFICATION

4.1 (cont'd)

Adequate consideration should be given to the possibility that development hardware may be used for purposes beyond the original intent. For example, development units may become prototype units and prototype units may become qualification test units.

5. REQUIREMENTS

5.1 Documentation

- a. Drawings, sketches, specifications, test procedures, and/or planning documents used to establish acceptance criteria, fabricate, and to test shall be controlled to the degree necessary to permit the item to be reproduced.
- b. Documents may be marked up and altered during fabrication or testing, as authorized by the program manager or responsible engineering authority but must be sufficiently clear and legible that hardware can be reproduced from the altered documentation.
- c. Program managers shall establish a permanent program record which will contain or facilitate location of hardware fabrication, test and inspection documentation sufficient for fulfillment of the Company objectives.
- d. A record of significant events affecting the quality of program hardware will be kept in enough detail so that at program completion a summary of the program can be made.
- e. Test results will be recorded in a permanent type notebook or similar document which can be identified to the hardware tested and retained as part of the permanent program records established by the program manager. Date of test and pertinent conditions influencing test results will be recorded.
- f. Inspection results and inspection discrepancies will be recorded as established by the Program Quality Plan and retained in the same manner as test results.

5.2 General Workmanship

- a. Quality of general workmanship shall be of a caliber that will neither jeopardize the usefulness of the hardware nor compromise the LMSC reputation for quality hardware.

Section: Page 3

QUALITY ASSURANCE REQUIREMENTS
FOR ENGINEERING RESEARCH & DEVELOPMENT PROGRAMS

LMSC MINIMUM QUALITY CONTROL SPECIFICATION

5.2 General Workmanship (continued)

- b. The organization assigned inspection responsibility by the program quality plan shall determine the inspection methodology and perform inspection and test functions as necessary to ensure compliance with the requirements of 5.2, a. above.

5.3 Receiving Inspection

All subcontracted or purchased material shall be inspected upon receipt for count, identification, and damage, and in addition shall be subjected to inspection and test as required for verification of compliance with other acceptance criteria as defined by the subcontract or purchase order.

5.4 Equipment for Hardware Inspection and Test


Inspection and test equipment employed to determine pertinent hardware characteristics should be calibrated as frequently as necessary to assure required accuracy. The calibration should be against measurement standards traceable to the National Bureau of Standards, except where the state-of-the-art precludes compliance.

5.5 Non-Conforming Material

Subject to contractual limitations and the cognizant Division's procedures, the program manager or his designee may waive or alter requirements as necessary to accomplish program objectives. Physical and functional characteristics of the completed hardware which do not meet the requirements of the documentation shall be recorded and dispositioned in accordance with Divisional procedures.

6. FINAL BUY-OFF AND DELIVERY

6.1 After all inspection and tests are completed, the appropriate manager(s) or designee(s), in accordance with Divisional procedures, shall be the final authority as to whether the hardware meets the design requirements and objectives of the program and is ready for delivery to the customer.


M. McGilvray, Chairman
LMSC Product Assurance Advisory Board

Section 3, page 1

Panelcoil®

DEAN PRODUCTS, INC.,
985 Dean Street,
Brooklyn, N.Y. 11238
Phone: (212) 789-4444
Telex: 126669
Cable: Deanpancol

12/2/75

MR-174026
Noted
11-14-75

Lockheed Missiles & Space Co.
4800 Bradford Drive
Huntsville, ALA 35807

Attention: Mr. Don Crutcher

Reference: Your P.O. No. ZAA 71884 GA
Dean F.O. No. 7921

Subject: ASME Certification

Gentlemen:

We are enclosing ASME Form U-1A, Nos. 6631 through and including - for your record and file.

We appreciate this opportunity to be of service to you.

Yours truly,

DEAN PRODUCTS, INC.

W. Kenny

W. Kenny
Order Service Dept.

WK:j
cc: SEE

FORM U-1A MANUFACTURERS' DATA REPORT FOR PRESSURE VESSELS
 (Alternate Form for Single Chamber, Completely Shop-Fabricated Vessels Only)
 As Required by the Provisions of the ASME Code Rules, Section VIII, Division 1

F.O. 7921

1. Manufactured by DEAN PRODUCTS, INC. 985 DEAN STREET, BROOKLYN, NEW YORK
(Name and address of manufacturer)
2. Manufactured for LOCKHEED MISSILES & SPACE CO. INC.
(Name and address of purchaser)
3. Location of Installation _____
(Name and address)
4. Type NA Vessel No. 6631
(Horiz., or vert. tank) (Mfr's Serial No.) (CRN) (Drawing No.)
 Year Built 1975
(Nat'l Bld No.)
5. The chemical and physical properties of all parts meet the requirements of material specifications of the ASME BOILER AND PRESSURE VESSEL CODE. The design, construction, and workmanship conform to ASME Rules, Section VIII, Division 1 _____ and Addenda to _____ and Code Case no. _____
(Year) (Date)
 Special Service per UG-120(d) _____
- Manufacturers' Partial Data Reports properly identified and signed by Commissioned Inspectors have been furnished for the following items of the report: _____

(Name of part, item number, mfr's name and identifying stamp)

6. Shell: Material SA-240 Nominal Thickness 0.078 in. Corrosion Allowance _____ in.
(Spec. No., Grade)
 Diam. 22 ft _____ in. Length 119 ft _____ in.
7. Seams: Longitudinal ELECTRIC RES. WELD R.T. _____ Efficiency _____ %
(Welded, Dbl., Sngl. Lap, Butt) (Spot or Full)
 H.T. Temp _____ F Time _____ Girth _____
(Welded, Dbl, Sngl, Lap, Butt)
 R.T. _____ No. of Courses _____
(Spot, Partial, or Full)

CERTIFICATE OF COMPLIANCE

We certify that the statements made in this report are correct and that all details of design, material, construction, and workmanship of this vessel conform to the ASME Code for Pressure Vessels, Section VIII, Division 1.

Date 11/10/75 Signed DEAN PRODUCTS, INC. by Charles Sherman
(Manufacturer) (Representative)
 "U" Certificate of Authorization No. 5023 expires FEBRUARY 28, 1978

CERTIFICATE OF SHOP INSPECTION

Vessel made by DEAN PRODUCTS, INC. at 985 DEAN STREET, BKLYN, N.Y. 11238
 I, the undersigned, holding a valid commission issued by the National Board of Boiler and Pressure Vessel Inspectors and/or the State or Province of NEW YORK and employed by ALLENDALE MUT. INS. CO. have inspected the pressure vessel described in this Manufacturers' Data Report on _____ 19 _____, and state that, to the best of my knowledge and belief, the Manufacturer has constructed this pressure vessel in accordance with ASME Code, Section VIII, Division 1.

By signing this certificate neither the Inspector nor his employer makes any warranty, expressed or implied, concerning the pressure vessel described in the Manufacturers' Data Report. Furthermore, neither the Inspector nor his employer shall be liable in any manner for any personal injury or property damage or a loss of any kind arising from or connected with this inspection.

Date 11/6/75
 Signed W.M. Campbell Commissions 2682
(Inspector) (Nat'l Board, State, Province and No.)

FORM U-1A (BACK)

8. Heads: (a) Material NONE (Spec. No., Grade) (b) Material _____ (Spec. No., Grade)

Location (Top, Bottom, Ends)	Minimum Thickness	Corrosion Allowance	Crown Radius	Knuckle Radius	Elliptical Ratio
(a) _____	_____	_____	_____	_____	_____
(b) _____	_____	_____	_____	_____	_____
Conical Apex Angle	Hemispherical Radius	Flat Diameter	Side to Pressure (Convex or Concave)		
(a) _____	_____	_____	_____		
(b) _____	_____	_____	_____		

If removable, bolts used (describe other fastenings) _____ (Material, Spec. No., Gr., Size, No.)
 Constructed for max. allowable working pressure 135 psi at max. temp. 358 F. Min. temp. (when less than -20 F) _____ F. Hydrostatic, pneumatic, or combination test pressure 212 psi.

9. Safety Valve Outlets: Number _____ Size _____ Location _____

10. Nozzles:

Purpose (Inlet, Outlet, Dra'n)	Number	Diam. or Size	Type	Material	Nominal Thickness	Reinforcement Material	How Attached
<u>INLET</u>	<u>(1)</u>	<u>1/2"</u>	<u>MALE</u>	<u>SS-304-L</u>	<u>SCH 40</u>		<u>WELDED</u>
<u>OUTLET</u>	<u>(1)</u>	<u>1"</u>	<u>MALE</u>	<u>SS-304-L</u>	<u>SCH 40</u>		<u>WELDED</u>

11. Inspection Openings:

Manholes No. _____ Size _____ Location _____
 Handholes No. _____ Size _____ Location _____
 Threaded No. _____ Size _____ Location _____

12. Supports: Skirt (Yes or no) _____ Lugs (No.) _____ Legs (No.) _____ Other _____ (Describe)
 Attached _____ (Where and how)

13. Remarks: PANEL HEAT EXCHANGER PAT. 301 TYPE "P" IS DESIGNED AND CONSTRUCTED
IN ACCORDANCE WITH ASME CODE AND CASE NO. 1292-9.

HEAT # 8650675

REPRODUCIBILITY OF THE
ORIGINAL PAGE IS POOR



Section 3 Page 4
OCT 1 1972

DEAN PRODUCTS, INC. Bill of Material for Shop

DEAN F.O. No.

DEANJ

CUSTOMER: {

CUST. P.O. No.

DEAN DWG.No.

PATTERN No.	TYPE	MATERIAL	GAGE	CUTTING SIZE	PIECES REQUIRED	REMARKS
301	P	304L	14	22 1/2" x 12 1/2"	1 ✓	Stamp
		"	14	22 1/2" x 12 1/2"	1 ✓	Plumb
		12-H		On 12-H	30%	HT 8650675
		12-H		24"		
				ASME JOB		
				(H-P-1000)	40%	

ACCESSORIES PER STANDARD DRAWINGS

	MATERIAL	GAGE or SCH. No.	TYPE	SIZE	PIECES REQD.	SHOP DWG. No.	REMARKS
PIPE AND FITTINGS	3/4" 40	40	PIPE	1/2" x 3/4"	1	T.D.C.	T.D.C.
	1" 40	40	PIPE	1" x 3/4"	1	T.D.C.	T.D.C.
ANGLES AND TABS							
HANDLES AND JACKETS	3/4" 40	40	PIPE	1/2" x 3/4"	2		
					23		

BY

DATE _____

CHKD BY

PG. OF

CUSTOMER ORDER NUMBER AND DATE

10735 7/7/72

ALLOY

PENALTY

SHIPPED FROM

SI MASS END 1

Section 3, Page 45
INVOICE DATE

INVOICE NUMBER

304-10485

DATE SHIPPED

7/7/72 WILSON FRT

CUSTOMER ABBREVIATION

SALES CO

SP

CONTROL CARD

STATE

COUNTRY

TAX

OFF

CE

DIST

SLS

ACCOUNT

NUMBER

MAY

CLASS

7-54299-304 KRS NET SPLY 1121791-11367 20310415950000714-40504003160-

KRS METAL SUPPLY INC
48-18 NORTHERN BLVD
LONG ISLAND CITY NY 11101

71 3

30-1/2-10

SALES PRODUCT
CLASS SIZE
359000000

Dean order #0-6183

Certificate of Tests

("SHIP TO" SAME AS "SOLD TO" UNLESS OTHERWISE INDICATED)

"P" PARTIAL SHIPMENT "C" COMPLETE SHIPMENT

REPUBLIC PRODUCT DESCRIPTION

ITEM NO.

UNITS SHIPPED

ASTM A240-71 EX ROCK ENDURO 18-8-S-L
TYPE 304L NBR 1 FIN STEEL SHTS.078 X 24 X CLS
1 CL

30

5266#

1 SKID TARE 4# TARPED
SKROUDED
SHIP COVD BY INV 304-10485 TO 83 INCLREPRODUCIBILITY OF THE
ORIGINAL PAGE IS POOR

I HEREBY CERTIFY THAT THE MATERIAL LISTED HEREIN HAS BEEN INSPECTED AND TESTED IN ACCORDANCE WITH THE METHODS PRESCRIBED IN THE GOVERNING SPECIFICATIONS AND BASED UPON THE RESULTS OF SUCH INSPECTION AND TESTING HAS BEEN APPROVED FOR CONFORMANCE TO THE SPECIFICATIONS.

A. MARCANTONIO - GENERAL SUPERINTENDENT
METALLURGICAL SERVICESBy: *A. Marcantonio*

FRT. COL 426764

ITEM NO.	HEAT NO.	C	W	N	CARBON	MANG.	PHOS	SUL	SIL	COPPER	NICKEL	CHROME	MOLY.	VAN
3650675					.018	1.73	.034	.015	.51		10.30	18.73		

HEAT NO.	SIZE	WELD POINT	TENSILE STRENGTH	ELONG.	RED. AREA	BRINELL ROCKWELL	BEND TEST	REMARKS
8650675	.078	39000	82000	57		B 75		

INDUSTRIAL METALS DEPARTMENT

BIRMINGHAM, ALABAMA

P. O. BOX 2072

REYNOLDS ALUMINUM SUPPLY COMPANY

00-5-766

SPECIFICATIONS:

THIS WILL CERTIFY THAT THE ABOVE DESCRIBED MATERIAL IS PRODUCED IN ACCORDANCE WITH

CERTIFICATION

7304 55 PLATE
3" THK 5 1/8" X 22 1/4"
MR. 2/16/43
11-5-75

MATERIAL

TO LOCKED MISSILE
#800 BARDECO DE
BIRMINGHAM, ALA
ATTN: MR. JOE BOOTH
DATE 11-4
#2A-718440-2
SO# 34218

REYNOLDS ALUMINUM SUPPLY COMPANY

Section 4, page 1

MR-216434 Section 4, Page #2

REYNOLDS ALUMINUM SUPPLY COMPANY

TO LOCKED MISSILE DATE 10-6-75
4800 BRADFORD DR. N.W. YOUR PO# 200-28430-7
HOUSTON, ALA OUR SO# 32562
ATTN: MR. DONALD CRUTCHER

MATERIAL

T304 L SS PLATE 1PC 3/16 3"X24"
" " " 1PC 1/2 6"X24"
" " " 1PC 1 3/4 6"X12"
T304 SS ANGLE 1PC 2X2X1/4 60"

CERTIFICATION

THIS WILL CERTIFY THAT THE ABOVE DESCRIBED MATERIAL IS PRODUCED IN ACCORDANCE WITH
SPECIFICATIONS:

ABOVE

REYNOLDS ALUMINUM SUPPLY COMPANY
P. O. BOX 2072
BIRMINGHAM, ALABAMA

[Signature]
INDUSTRIAL METALS DEPARTMENT

GO AIR

incorporated

SILICONE O-RINGS.



3562 elm street, hapeville, georgia 30054 phone (404) 767-7522

Date 11-5-75

CONFORMANCE CERTIFICATE FOR MATERIAL SHIPPED

GO-AIR Incorporated hereby certifies that all materials used in the manufacture of parts called for on purchase order no ZAA719380A received by us from Lockheed Aircraft conform to the material specifications indicated in drawings or specifications as called for on the said purchase order. Test reports are on file with us or with our suppliers for examination and indicate conformance with applicable specification requirements.

GO-AIR Incorporated also certifies that the parts listed below and shipped on 12247 are manufactured in accordance with the material specifications called for on said purchase order that are current on the date on which the order was accepted.

Item	Part Number	Specifications	Compound	Cure Date	C.B.I.	Qty.
1	MS906-835	AMS3304	5604-7	1975	10704	4

MR-29368

Ernest W. Bricker
NOTARY PUBLIC, GEORGIA STATE
at Large, My Commission Expires
May 22, 1977

GO-AIR Incorporated

by *J.R. McMillan*
Chief, Quality Control

REPRODUCIBILITY OF THE
ORIGINAL PAGE IS POOR

27

Section 5, Page 1

J. M. TULL METALS COMPANY

CERTIFICATION OF MATERIALS

Lockheed Missile & Space Co.

Date Sept. 19 19 75

P.O. Box 1103

Date Shipped _____

Huntsville Al 35805

Your Order No. 2AA718530X

Our Order No. 495417

MATERIAL

Item No. 1 Pc 1/2 x 48 x 120 Hot Rolled Steel Plate A-36 C F (19" x 30")

1 Pc 3/8 x 48 x 120 Hot Rolled Steel Plate A-36 CE (30" x 96")

CERTIFICATION

This will certify that, to the best of my knowledge and belief, the above described material was produced in accordance with the following specifications. HR Stl Plate A-36 CE

Signed and sworn to before me this

_____ day of _____ 19 _____

Notary Public

J. M. TULL METALS COMPANY

Signed

Kathy Camp

Tull warehouse location

Birmingham

City

Al

State

MR-216435
9-22-75
Not Has Fee.

Section 6, page 1

Section 7: pg 1

CERTIFICATE
OF TEST

TUBESALES.

175 TUBEWAY

FOREST PARK, GEORGIA 30050
(404) 361-5050

LOCKHEED MISSILES & SPACE

ZAA 7185 50 A

5-31930

09-12-75

CUSTOMER ORDER NO.

INVOICE NO.

DATE

1

10'0"

ITEM NUMBER

QUANTITY

SPECIFICATION

GRADE

2 X 095

SMLS 304

SIZE

PT

HEAT NO.

M8329

MANUFACTURER

MELTER

GRAIN SIZE

6

CHEMICAL ANALYSIS

C	MN	P	S	SI	TI	CB/TA	MO	NI	CR	CU	CU		
0048	1620	0 023	0 020	0440			0 140	10 540	18680	0 120			
ULTIMATE STRENGTH P.S.I.		YIELD POINT P.S.I.		% ELONGATION IN 2"	ROCKWELL B HARDNESS		BRINELL		HARDENABILITY			FREQ.	SEVER
82550		41860		70	77-78								

THE FOLLOWING TESTS HAVE BEEN PERFORMED SATISFACTORILY:

6 9 11 12

Test Legend:

- | | | | | | | | |
|-----------------|--------------|-----------------|---------------|--------------------|----------------|-------------|--------------------|
| 1 Dye Penetrant | 3 Ultrasonic | 5 X-Ray | 7 Microscopic | 9 Flattening | 11 Flaring | 13 Crushing | 15 Macro Etch |
| 2 Eddy Current | 4 Corrosion | 6 Embrittlement | 8 Bending | 10 Decarburization | 12 Hydrostatic | 14 Flanging | 16 Reverse Bending |

I CERTIFY THE ABOVE TEST INFORMATION TO BE CORRECT
AS CONTAINED IN THE RECORDS OF THE COMPANY

TUBESALES.

BY

AUTHORIZED TEST DEPARTMENT CLERK

PEDIGO

Welding & Fabrication Company, Inc.

P.O. BOX 40

LACEYS SPRING, ALABAMA

Phone - 881-6173

PARTIAL ☐

☐ COMPLETE

Packing Slip

SHIPPED TO Lockheed

Pinckville, Alabama

RECEIVED BY: J. H. Brill

HREC RECEIVING

DATE 11-1-75

REGISTER NO: V867-004

SOLD TO JHB

DELIVERED TO: Rawman

COMPLETE ☒

PARTIAL ☐

DEPT. NO. 52/40

DATE 11/1/75

CUSTOMER ORDER NO.

WORK ORDER NO.

GOVT. CONTRACT NO.

ROUTING

QUANTITY	PART NUMBER	DESCRIPTION	P. O. Item No.
	<u>101-174130</u>	<u>Attachment "A" (welded)</u>	
		<u>Welding by: J. H. Brill</u>	
		<u>Welder Material 2:1 Aluminum H</u>	
		<u>Material furnished on Lockheed Order 57292</u>	

INSPECTOR H. L. Walker

CUSTOMER
INSPECTOR

SHIPPED BY H. L. Walker

DATE 11-5-75

REC'D. BY

NO. BOXES

Section 8, Page 1

STATEMENT OF COMPLIANCE

All parts and components of the NASA-MSFC Hot Gas Facility as delivered on 17 December 1975 were inspected and found to comply with their applicable drawings. These drawings are as follows:

No. R80104 ✓	Modification to HGF Injector
No. R80105	Injector Face Plate
No. R80106 ✓	Throat Section
No. R80107 ✓	Nozzle
No. R80108 ✓	Test Section
No. R80109 ✓	Calibration Panel
No. R80110 ✓	Calibration Panel (Dummy)
No. R80111	Combustion Chamber Water-In Manifold
No. R80112	Combustion Chamber Water-Out Manifold
No. R80116	Glass Window Spacer
No. R80117	Test Panel Spacer
No. R80119 ✓	Test Section Support
No. R80120	Bottom Support Plate
No. R80121	Side Plate Thrust Structure
No. R80122	Side U-Plate Thrust Structure
No. R80123 ✓	Combustion Chamber Support
No. R80125 ✓	Thrust Structure Assembly


W.G. Dean,
Lockheed Project Engineer

REYNOLDS ALUMINUM SUPPLY COMPANY

TO LOCKED MISSILE DATE 10-6-75
NR00 BROWNEED DR N.W. YOUR PO# 200-7184612
SHININGVILLE, ALA 35401 OUR SO# 32561
ATTN: MR. THOMAS CRUTCHER

MATERIAL

T304 L SS PLATE 1/8 3/8 36X36

MR 216432
10-3-75

CERTIFICATION

THIS WILL CERTIFY THAT THE ABOVE DESCRIBED MATERIAL IS PRODUCED IN ACCORDANCE WITH
SPECIFICATIONS:

T304 L

REYNOLDS ALUMINUM SUPPLY COMPANY
P. O. BOX 2072
BIRMINGHAM, ALABAMA

Robert L. L...
INDUSTRIAL METALS DEPARTMENT

REPRODUCIBILITY OF THE
ORIGINAL PAGE IS POOR

**MATERIAL INSPECTION
AND
RECEIVING REPORT**

1-6-ET-02777 (IF)

NAS8-25569 S/A19

DATE 16Dec75

7. PAGE 1 OF 1
8. ACCEPTANCE POINT "D"

2. SHIPMENT P.O. RC-0001	3. DATE SHIPPED 16Dec75	4. B/L TCN HREC/752	5. DISCOUNT TERMS Net 30
9. PRIME CONTRACTOR Lockheed Missiles & Space Co., Inc. Huntsville Research & Engineering Center P. O. Box 1102, West Station Huntsville, Alabama 35807		10. ADMINISTERED BY DCASO-Huntsville 2109 West Clinton Avenue Huntsville, Alabama 35805	

Section 11, page 1

11. SHIPPED FROM (If other than 9) Same as Block "9"	12. PAYMENT WILL BE MADE BY Financial Management Office George C. Marshall Space Flight Center Huntsville, Alabama 35805
---	---

13. SHIPPED TO National Aeronautics & Space Administration George C. Marshall Space Flight Center, Marshall Space Flight Center, Alabama 35812	14. MARKED FOR Accountable Property Officer THRU: Bldg. 4471 TO: R. N. Stone, S&E ET18 Bldg. 4561 453-0098
---	--

15. ITEM NO. 1	16. STOCK PART NO. (Indicate number of shipping containers - type of container - container number.) Hot Gas Test Chamber Modification Hardware designed and built under S/A 19 to NAS8-25569. (See NOTE in Section 23 below)	17. QUANTITY SHIP/REC'D 1	18. UNIT Ea	19. UNIT PRICE NA	20. AMOUNT NA
-------------------	---	---------------------------------	----------------	----------------------	------------------

21. PROCUREMENT QUALITY ASSURANCE	22. RECEIVER'S USE
-----------------------------------	--------------------

A. ORIGIN <input type="checkbox"/> POA <input type="checkbox"/> ACCEPTANCE of listed items has been made by me or under my supervision and they conform to contract, except as noted herein or on supporting documents.	B. DESTINATION <input type="checkbox"/> POA <input type="checkbox"/> ACCEPTANCE of listed items has been made by me or under my supervision and they conform to contract, except as noted herein or on supporting documents.
--	---

DATE RECEIVED 12-17-75	SIGNATURE OF AUTH GOVT REP <i>L. B. Boulton</i>
---------------------------	--

TYPED NAME AND OFFICE John W. Boulton ET 18	TYPED NAME AND TITLE L. B. Boulton
---	---------------------------------------

23. CONTRACTOR USE ONLY	* If quantity received by the Government is the same as quantity shipped, indicate by 1 or 1 mark, if different, enter actual quantity received below - quantity shipped and encircle.
-------------------------	--

NOTE: Hot Gas Generator Combustion Chamber and Injector Assembly FSN 1800-BLO0001, furnished by the Government on 9/8/75 (DCN 2-6-04-60075) for integration into the Hot Gas Test Chamber is being returned as part of Item #1 listed above.

57574

ORIGINATOR'S CONFIRMATION

Appendix N

Dean, W. G., "Modification/Fabrication of the NASA-MSFC Low Enthalpy Hot Gas Test Facility," LMSC-HREC TM D496690, Lockheed Missiles & Space Company, Huntsville, Ala., January 1976.

Lockheed

Missiles & Space Company, Inc.

Appendix N

HUNTSVILLE RESEARCH & ENGINEERING CENTER

Cummings Research Park
4800 Bradford Drive,
Huntsville, Alabama

**MODIFICATION/FABRICATION
OF THE NASA-MSFC LOW
ENTHALPY HOT GAS
TEST FACILITY**

January 1976

Contract NAS8-25569

Prepared for National Aeronautics and Space Administration
Marshall Space Flight Center, Alabama 35812

by

W.G. Dean

APPROVED:

B. Hobson Shirley
B. Hobson Shirley, Supervisor
Engineering Sciences Section

J. S. Farrior
J. S. Farrior
Resident Director

FOREWORD

This report presents a review and summary of the work conducted by Lockheed-Huntsville for NASA-Marshall Space Flight Center under Contract NAS8-25569, "Design and Develop the Modification of the Hot Gas Test Chamber." This work was begun on 19 September 1975, and the hardware was delivered on 17 December 1975.

The NASA-MSFC Contracting Officer's Representatives for this contract were Dr. K. E. McCoy, S&E-EP44 and Mr. R. N. Stone, S&E-ET18.

CONTENTS

Section		Page
	FOREWORD	ii
1	INTRODUCTION	1
2	GENERAL DESCRIPTION OF THE FACILITY AND COMPONENT HARDWARE	7
	2.1 Injector Body	7
	2.2 Water-Cooled Copper Combustor	9
	2.3 Throat Section	9
	2.4 Nozzle Section	9
	2.5 Test Section/Duct	9
	2.6 Thrust Structure and Support Stands	10
	2.7 Water Manifolds	10
	2.8 Calibration and Dummy Calibration Panels	10
	2.9 Cryopanel	11
3	SUPPORTING ANALYSES	12
4	PROOF TESTS PERFORMED	13
	4.1 Vacuum Test of Test Section/Nozzle	13
	4.2 Pressure Test of the Water Manifolds	13
	4.3 Pressure Tests of the Injector, Copper Combustor, Throat Section Unit	14
	4.4 Helium Pressure Test of the Hydrogen Manifolds, Feed Pipes, and Burner Tubes	16
	4.5 Weld Joint Tests with Dye Penetrant	16
5	INSPECTION/QUALITY ASSURANCE	17
6	INSTRUMENTATION	18
7	APPLICABLE DOCUMENTS	19

Section	Page
8 LOAN OF WINDOWS	20
9 DELIVERY OF HARDWARE	21
10 OPERATIONAL CONSIDERATIONS	22
10.1 Calibration Panel Loading	22
10.2 Mating Gap Consideration	22
10.3 Facility Calibration	23
10.4 Foam Panel Design	23
10.5 Facility Disassembly/Reassembly Notes	24
11 FACILITY OVERALL DIMENSIONS	26
REFERENCES	28

Section 1 INTRODUCTION

On 17 September 1975 Lockheed-Huntsville received a contract from NASA-MSFC to modify and fabricate a low-enthalpy hot gas test facility for testing large thermal protection system (TPS) panels in support of the External Tank (ET) and Solid Rocket Booster (SRB) TPS development programs. A preliminary design of this facility had already been completed under a separately funded study.

Throughout the design, every effort was made to: (1) minimize cost; (2) meet the requirements of simulating the flight environment as closely as possible; (3) use as much existing hardware as possible from a set of backup hardware previously fabricated for the high enthalpy version of the MSFC Hot Gas Test Facility; and, (4) test large (22 x 113 inch) panels.

The design requirements and capabilities of this "modified" facility are:

- Will run on hydrogen/air, as opposed to hydrogen/air or hydrogen/oxygen for the present configuration
- Will run without the steam ejector system, i.e., it will exhaust to atmospheric pressure. This will greatly reduce operating cost and complexity
- Will run large panels (over 113 inches long and 22 inches wide)
- Will require no wall cooling water except for the existing water-cooled copper combustor section, i.e., none of the new parts will be water-cooled
- Will simulate the effect of varying \dot{q} on streaks, i.e.: Do they stop when they proceed into a low \dot{q} region?
- Will simulate local pressure, heating rate, shear and enthalpy near body point 7065. (Figures 1, 2 and 3 present plots of these parameters for a comparison with flight vehicle values as listed in Table 1.) The heating rates will be turbulent without using trip spheres.

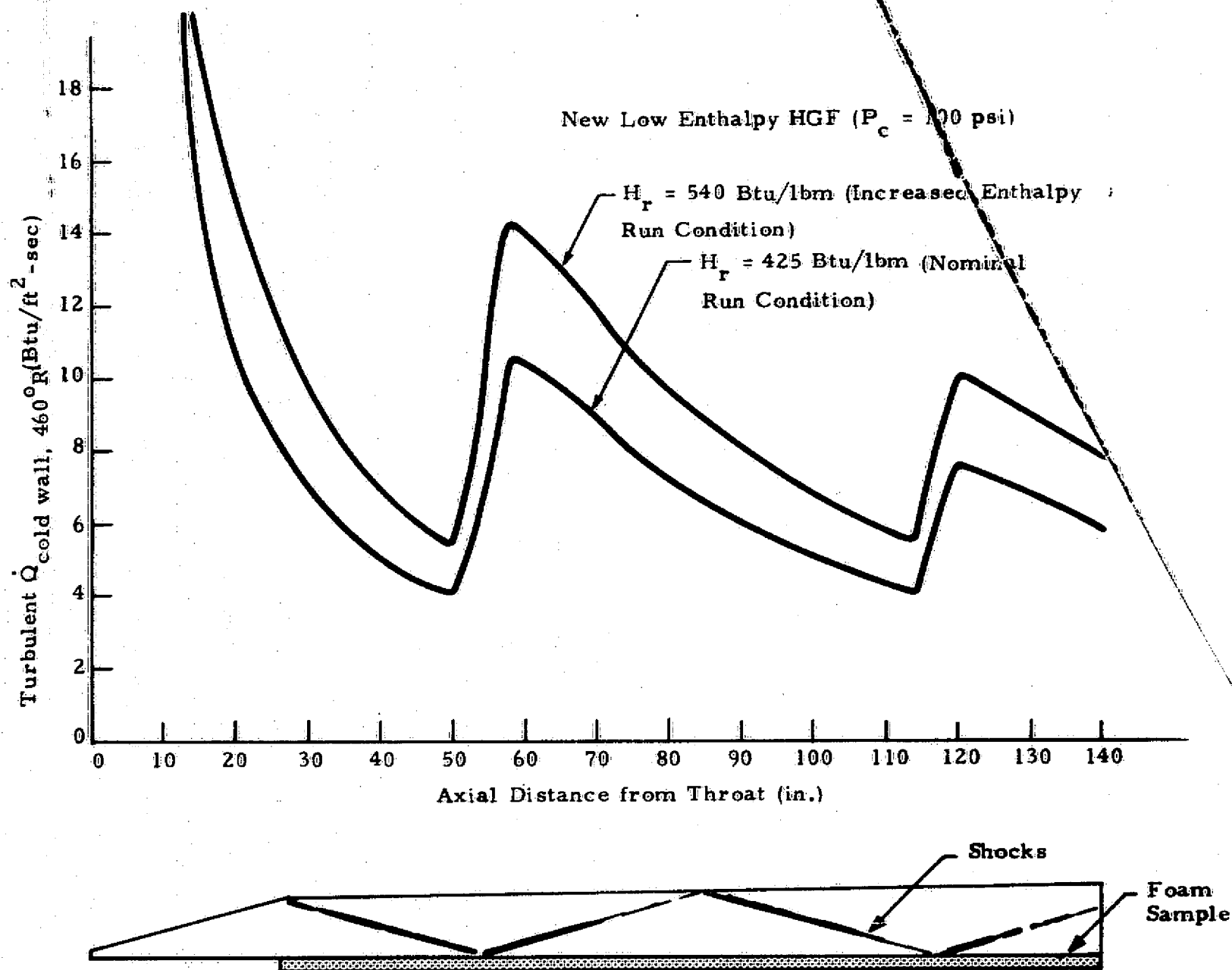


Fig. 1 - Heating Rate vs Distance for Modified Hot Gas Chamber for Two Run Conditions

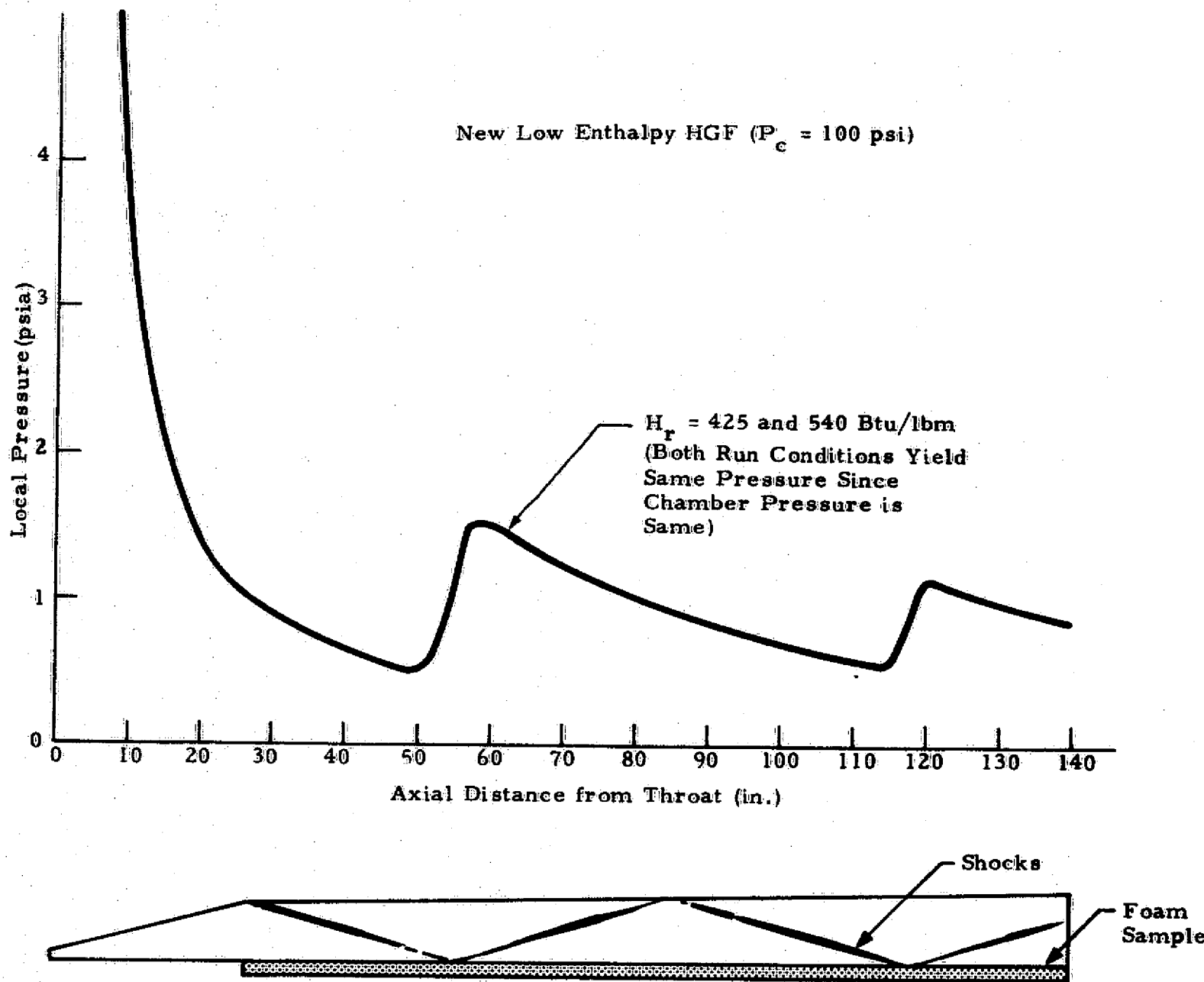


Fig. 2 - Pressure vs Distance for Modified Hot Gas Chamber for Two Run Conditions

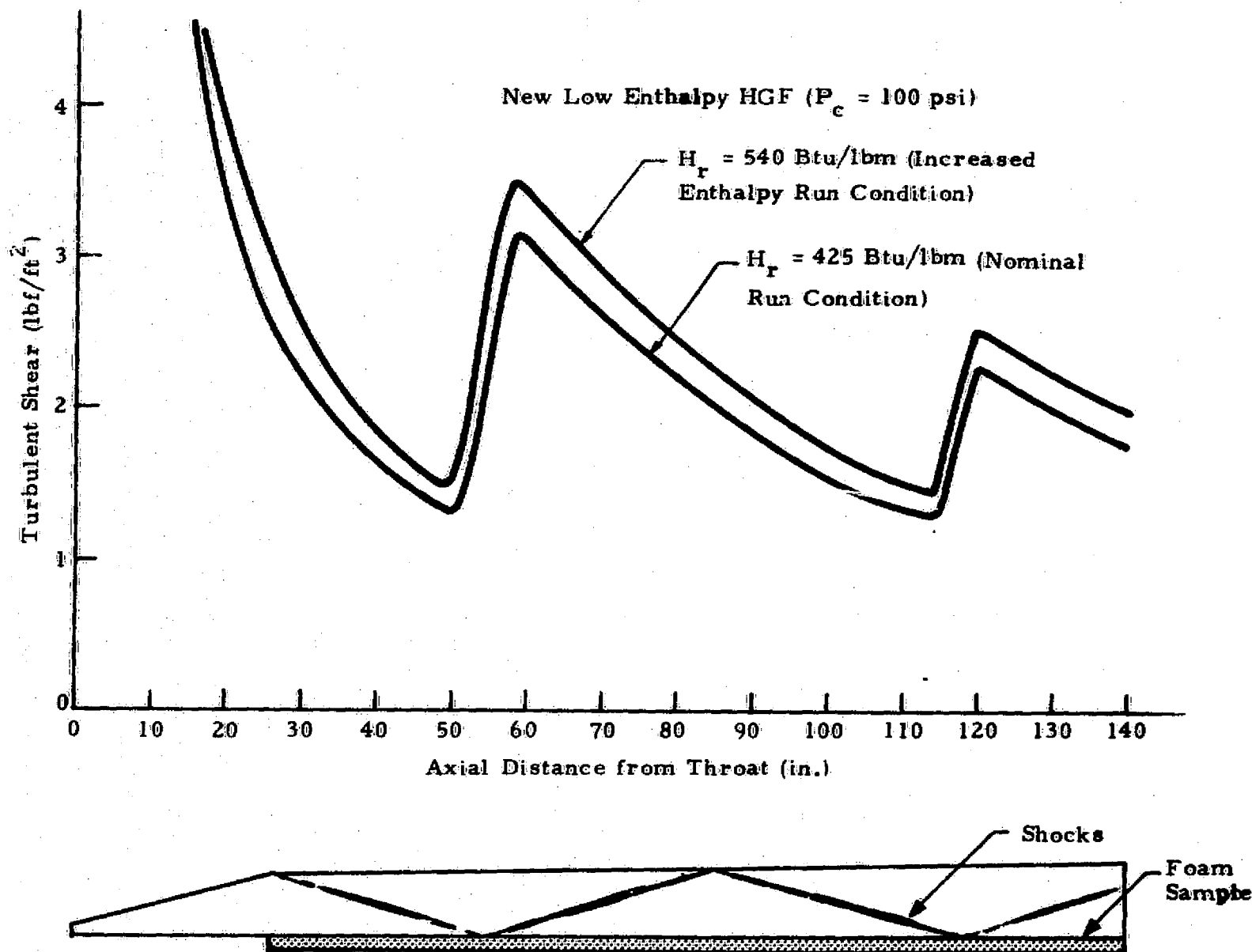


Fig. 3 - Shear vs Distance for Modified Hot Gas Chamber for Two Run Conditions

Table 1

FLIGHT VEHICLE VALUES (REF. 1)
(55 N. MI. AOA TRAJECTORY AT TIME OF MAX. HEATING - 110 SEC)

External Tank Body Point	\dot{q}_{cw} (Btu/ft ² -sec)	P_L (psia)	Shear (lbf/ft ²)
Max. Heating Point on LOX Tank (BP No. 7065)	10.2	2.5	3.2
SRB Shock Impingement Point (BP No. 7325)	12.4	3.9	4.0
Orbiter Shock Impingement Point (BP No. 7430)	11.9	3.7	4.1

- Will simulate shock impingement effects on ET/TPS (Orbiter/ET and SRB/ET shock impingement areas)
- Will simulate cryogenic backface temperature using a cryopanel.
- The flowfield chemistry will closely simulate that of the vehicle in flight (air): The combustion products for the design operating point are:

<u>Constituent</u>	<u>Mass Fraction(%)</u>
H ₂ O	5.8
N ₂	74.9
O ₂	17.8
Ar	1.5

- The recovery enthalpy for this modified chamber is 425 Btu/lb as compared to 424 Btu/lb for the flight vehicle at a trajectory time of 110 seconds (near the time of maximum heating) for the 55 n.mi., AOA design trajectory.

Section 2

GENERAL DESCRIPTION OF THE FACILITY AND COMPONENT HARDWARE

Figure 4 shows an artist's sketch of the modified facility. This sketch was taken from the proposal (Ref. 1), and several design changes were made since then. However, the basic facility/components are the same. (No photographs are yet available of the completed facility.) The facility consists of: (1) an injector body; (2) water-cooled copper combustor; (3) stainless steel throat section; (4) nozzle section; (5) test section or duct; (6) thrust structure; (7) two support stands; (8) camera mounts and light brackets; (9) camera/light purge boxes; (10) one "live" calibration panel; (11) three "dummy" calibration panels; (12) four cooling-water manifolds; (13) a stainless steel cryopanel to provide a cold ET tank wall panel substructure simulation; (14) two angular seals inside the bottom of the duct where the foam panels mate with the side-walls; and, (15) two "tailgate" seals.

Each of these components is described in the following sections. Final drawings of all components have been delivered to NASA with the hardware. The injector body and combustor are modified existing hardware. All other components are new.

2.1 INJECTOR BODY

The injector was modified as follows:

The "Rigimesh" injector face was removed and a new face of 304 stainless was made with the same burning hole locations but with additional rows of air "bleed" holes to allow a large increase in the air flow rate. Also new air manifolds and manifold feedline pipes were made and welded in place of the old ones. Also the feed holes from the manifolds through the injector body side walls were greatly enlarged to accommodate the larger air flow rate. No changes were made to the hydrogen manifolds, lead-in pipes, or injection tubes. The injector face was sealed in place with RTV

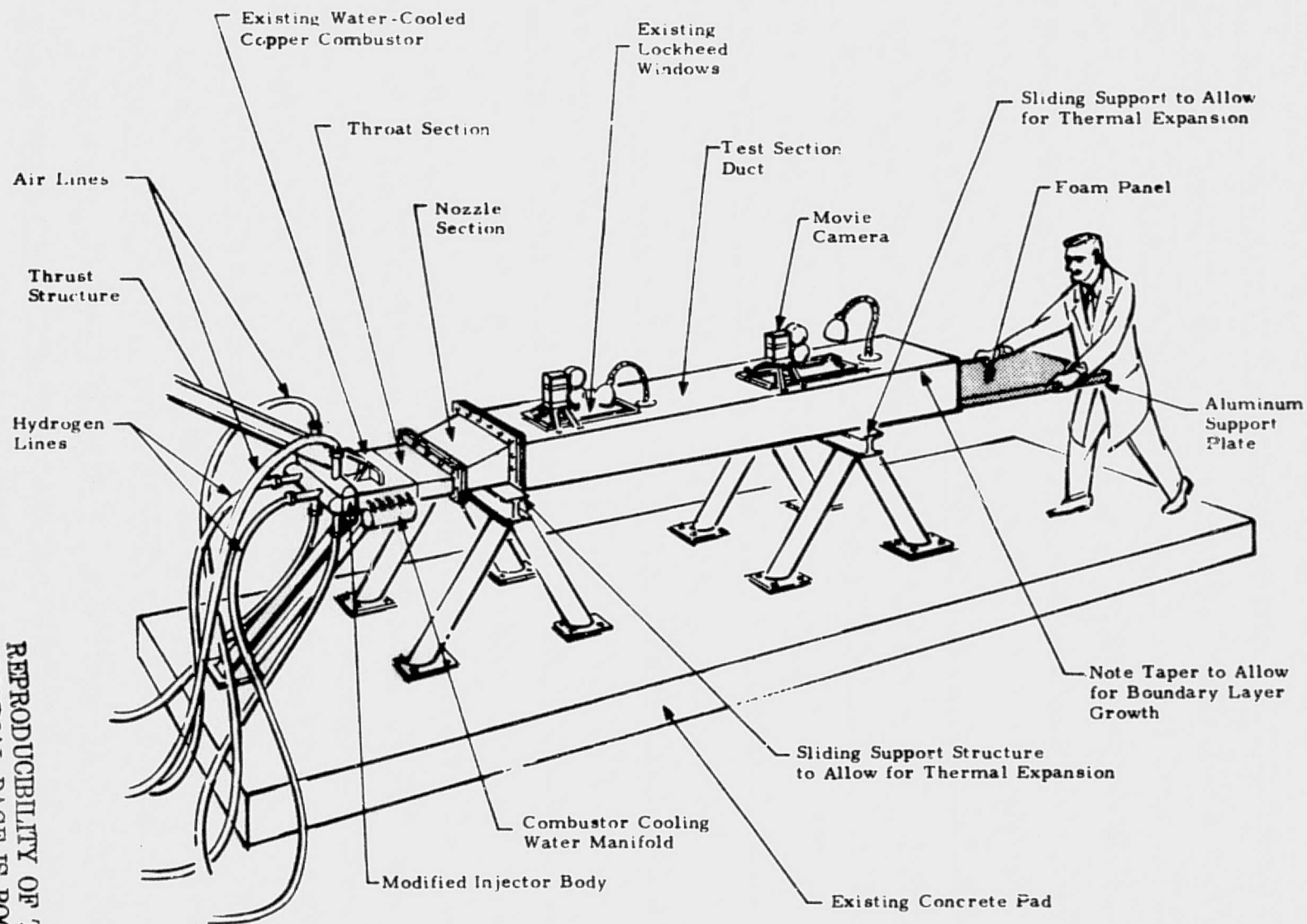


Fig. 4 - Sketch of Modified Chamber

LMSC-HREC TM D496690

rather than being welded in place so it can be removed if any additional modifications are required.

2.2 WATER-COOLED COPPER COMBUSTOR

The combustor was obtained from the NASA warehouse, separated from the copper throat section and used "as is" except for drilling and tapping one hole for the chamber temperature measurement thermocouple assembly. This hole is on the top side about one inch upstream of the combustor/throat interface.

The copper throat section was returned to NASA "as is" and will not be used in this facility.

2.3 THROAT SECTION

A completely new throat section was made. It is 304 stainless steel and has an inside throat height of one inch rather than the approximately 0.31 inch height of the old copper throat. It is made of four parts: top and bottom, and two side plates welded together at the sides. The throat section has no water cooling.

2.4 NOZZLE SECTION

The nozzle is made of mild steel. It is essentially a two-dimensional expansion nozzle. The entrance height is approximately 1.5 inches and its exit height is approximately 8 inches. It is a "half-cone" or "half nozzle" design, all the expansion being on the top side with the bottom flat. The expansion angle is 15 degrees, and the exit Mach number is about 3.6. The nozzle has a 0.35 inch lateral expansion to allow for boundary layer growth along the side walls (0.175 inch on either side).

2.5 TEST SECTION/DUCT

The test section is made of mild steel. It has two rectangular view ports or windows on top for taking movies during the tests. Light and camera mounting

brackets are also provided, as well as purge boxes for safety purposes since CH_2 is involved. The camera brackets allow for moving the cameras up and down and for aiming at various angles. The duct is essentially rectangular except for the approximately 1 inch taper on each side wall and 2 inch taper on the top wall to allow for boundary layer growth. The bottom is flat. The foam test panels are mounted in the bottom of the test duct resting on the cryo-panel and bolted in place from the bottom. The maximum panel size is 2 x 22.25 x 113.3 inches. Two angles are used as seals along the sides of the panel where they mate with the sides of the duct.

2.6 THRUST STRUCTURE AND SUPPORT STANDS

The thrust structure was changed from that shown in Fig. 4. It is now an over/under design and sits on a "sawhorse" stand similar to those shown in Fig. 4. Four height alignment bolts are provided for aligning the duct to the nozzle, and rollers are provided under the duct for longitudinal movement of the duct away from the nozzle.

2.7 WATER MANIFOLDS

These manifolds provide cooling water to the copper combustor. A water pressure drop of about 40 to 50 psi is predicted to supply a sufficient cooling water flow rate.

2.8 CALIBRATION AND DUMMY CALIBRATION PANELS

One "live" calibration panel is provided to measure pressures and heating rates along the bottom of the duct where the foam panels will be tested. This panel is approximately 22 inches wide and 28 inches long. It is to be placed at various positions along the duct during each of several calibration runs to determine the environment. Three dummy panels are provided to alternate with the calibration panel as spacers as the "live" panel is moved to each position.

Twenty-two pressures and 22 adjacent heating rate measurement locations are provided in a cross pattern to get distributions both along and across the duct length and width. These locations are numbered and etched on the top of the panel for reference/data reduction purposes. Pressure tubes and thermocouple leads approximately 12 feet long are provided and numbered with corresponding numbers.

Heating rates are to be measured using the standard "thin-skin/thermocouple" method using chromel-alumel thermocouples. Data reduction curves have already been made for obtaining heating rates from the temperature versus time traces.

It is expected that the time required for the pressures to stabilize will be about 5 to 10 seconds which will also be sufficient time to obtain heating rates.

2.9 CRYOPANEL

An "off the shelf" cryopanel was bought and installed inside the duct. It is made of 304-L stainless and certified for a 135 psia pressure capability. It is mounted on a 1 in. thick layer of rigid ceramic (Glassrock) foam insulation. The insulation was used to reduce heat loss from the cryogen (LN_2) to the heavy steel bottom wall of the test section during chill-down, etc.

"Tailgate" pieces were also provided at the exit end of the duct to seal around the top of the cryopanel and also to seal around the pressure tubes and thermocouple leads.

Section 3

SUPPORTING ANALYSES

Most of the supporting analyses were completed during the preliminary design phase. However, several additional stress analyses were conducted during this modification/fabrication phase. These included stress analyses of:

1. Bolts connecting thrust structure to its support stand. Result: large margin of safety.
2. Problem of having the hot (uncooled) stainless steel throat section bolted to the water-cooled copper combustor (Refs. 2, 3 and 4). Results showed that there will be some slippage between these parts, but no stress problem.
3. Rod bolts connecting injector, combustor, throat and nozzle flange. (allowable dry torque 200 in-lb).
4. Effect of three sides of test section being heated while bottom is cold due to its being protected by the foam panel. Results: large positive margin of safety, maximum deflection of 0.172 inch in middle of duct upper wall.
5. Nozzle section pressure and thermal loading. Result: a 1-3/4 inch support angle was added to the original design across the top of the nozzle.

In addition to these stress analyses, an ignition/burning/mixing analysis of the combustor "flow field" was performed (Ref. 5). This was a two dimensional finite-rate analysis where the ignition was started on the side of the combustor (simulating the flame igniters) and allowed to propagate across the width of the combustor toward the centerline. The flame front reached the centerline about two-thirds of the way down the combustor. This means that the large air flow will not "flame out" the flame front. It is felt that this analysis was conservative and that the propagation will actually be faster than predicted. However, it is assumed that the igniters are burning continuously, which is the planned operational mode. If the igniters are turned off the flame is quickly extinguished due to the quenching reactions.

Section 4

PROOF TESTS PERFORMED

Five proof tests were conducted as follows:

4.1 VACUUM TEST OF TEST SECTION/NOZZLE

Since the pressures inside the nozzle and test section are less than atmospheric during facility operation (Fig. 2) a vacuum leak test was performed. The test section was bolted to the nozzle and both ends blanked off. The windows were mounted in place and a vacuum pump used to bring the inside pressure down. The pressure did not reach the planned test point of 1.0 psia. However, it stabilized at about 1.3 psia due to the combination of small leaks around the blank-off plates at the ends, and the small pumping capacity of the pump at this pressure level. At this point the pump was shut down and the valve closed. A pressure-rise rate and internal volume was used to calculate the leak rate. The value turned out to be 0.13 in-Hg/min, as compared to an allowable value of 2.36 in-Hg/min. This was therefore declared to be an acceptable leak-rate proof test.

This allowable leak rate was established as follows; a criterion of 1% of the mass flow rate in a 1 in. wide strip of boundary layer was established as a value to assure no flow disturbance. This yielded a mass leak rate of 0.003 lbm/sec which converts, with the proper volume, to 1.164 psia/min or 2.36 in-Hg/min.

4.2 PRESSURE TEST OF THE WATER MANIFOLDS

The design water pressure for the water manifolds is 50 psia. A proof pressure of 60 psi was selected for leak checks. The four manifolds were connected to the copper combustor, and the two circuits were filled with water and the air bled out. They were pressurized to 60 psia using an argon pressure bottle. Some small leaks were found in the braze joints and in the copper combustor end plugs. These were stopped and the system retested until no leaks were seen.

4.3 PRESSURE TESTS OF THE INJECTOR, COPPER COMBUSTOR, THROAT SECTION UNIT

The design chamber pressure during operation is 100 psia, therefore a 300 psia value was selected to give a "safety factor" of 3. The purpose of this test was to check the weld joints in the air and hydrogen manifolds, and the O-ring joints between the throat/combustor and the injector/combustor.

The unit was assembled with a blank plate used on the downstream end of the throat section and B-nuts/plugs in each of the manifold feed lines. It was originally proposed that this 300 psia pressure check be performed using helium gas. However, this was "outlawed" by Lockheed safety personnel and a hydrostatic test was substituted. That is, the unit was filled with water and the air bled out and then it was pressurized using an argon pressure bottle with regulator.

Three tries were required before the full 300 psi pressure was obtained. On the first two tries leaks were observed at the O-ring and at the seal between the throat and blank plate. These were stopped by using an "oversized" (fatter) O-ring and by using a thicker blank plate plus bolting the nozzle in place to let the flange serve to stiffen the blank plate so it didn't bulge out and cause a leak.

On the third try a pressure of approximately 300 psi was reached at which time the O-rings started leaking. During disassembly of the unit after this last test it was discovered that both the copper combustor and the throat section lower wall had taken on a permanent deformation. Figure 5 shows the extent of this deformation of the copper. In the middle the deformation was measured to be about 0.2 in. The steel section was deformed about .050 in. This also caused some "egging" of the rod-bolt holes.

This problem was immediately brought to the attention of the Technical COR of the contract. It was decided that we should try to straighten these parts back to their original position on a hydraulic press. This was

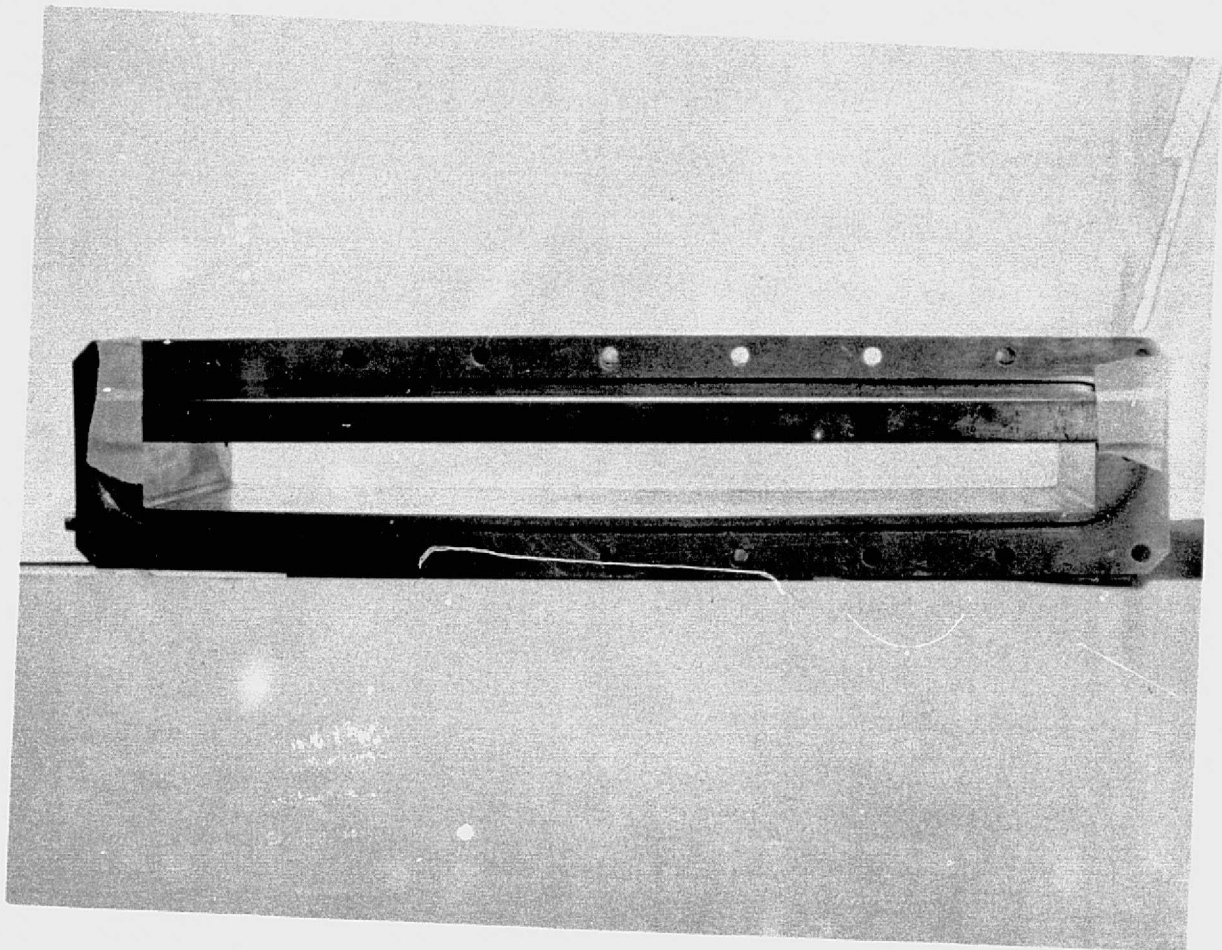


Fig. 5 - Post Test Photo of Copper Combustor Showing
Approximate 0.2 in. Permanent Deformation

REPRODUCIBILITY OF THE
ORIGINAL PAGE IS POOR

accomplished without a great deal of extra effort and the straightened parts were re-inspected by NASA representatives. The steel throat section went back into place to within about 0.007 inch of its original size, and the copper was straight enough so that the rod bolts "fell through" without effort.

Since no leak was observed on the welds at 300 psia and the O-rings did not leak until approximately this value, it was decided that the test objectives had been met and therefore no further tests were performed.

An "after-the-fact" cursory stress analysis showed that some permanent deformation of the copper should have been expected. This was an oversight on our part and should have been caught before we conducted the test.

A dye-penetrant test was made of the copper combustor after it was pressed back into shape and no cracks were found.

4.4 HELIUM PRESSURE TEST OF THE HYDROGEN MANIFOLDS, FEED PIPES, AND BURNER TUBES

The 92 GH_2 burner tubes were blanked off using "shrink" tubing and taken to the NASA-MSFC test lab shops for a helium leak detector test. The unit was purged and then pumped up to 30 psia and "sniffed" thoroughly. No leaks were found.

4.5 WELD JOINT TESTS WITH DYE PENETRANT

All weld joints were checked using a "Zyglo" dye-penetrant test kit. No problems were found.

Section 5 INSPECTION/QUALITY ASSURANCE

All parts were inspected before delivery and found to meet requirements as specified on the applicable drawings (see Section 7, Applicable Documents, for drawing numbers and titles).

A separate document (Ref. 6) has been written to cover quality assurance of this project. Included in this document are: material certifications, LMSC Minimum Quality Assurance Statement, subcontracted work inspection form, welder certification, welding rod certification/specification references, NASA acceptance form DD-250, etc.

Section 6 INSTRUMENTATION

In addition to the 22 pressure and heating rate measurements provided with the "live" calibration panel as discussed earlier the following "facility" instrumentation is provided:

- Combustion chamber pressure tap
- Combustion chamber temperature thermocouple assembly. (Omega brand, chromel-alumel, 1/16 inch diameter, with inconel sheath, ungrounded junction, max temp capability = 2100°F, approximately 2-11/16 inches long, extends to centerline of combustor, located about 1 inch upstream of throat/combustor interface.)
- Nozzles upper wall temperature: Chromel-alumel thermocouple, located about 2 inches downstream of throat/nozzle interface.
- Test section/duct upper-wall temperatures: Two chromel-alumel thermocouples are provided: one about 2 inches downstream of the nozzle/test section interface and one about 3 inches upstream of test section exit plane.
- Test section upper wall pressures. Seven pressure tap locations are provided on the test section upper wall. These are more or less equally distributed along the duct length.

In addition to this instrumentation, consideration is now being given to the addition of acoustic instrumentation. The purpose of this is to determine how well this facility simulates the flight acoustics environment. This has been discussed with NASA-MSFC acoustics personnel and their estimated acoustics level is 140 to 165 dB. They have also made a recommendation as to the type of instrumentation to install. If it is decided to add these transducers, they can be installed in one of the "dummy" calibration panels.

Section 7 APPLICABLE DOCUMENTS

The documents applicable to this facility are covered in the Reference section.

Also the following drawings are applicable:

No. R80104	Modification to HGF Injector
No. R80105	Injector Face Plate
No. R80106	Throat Section
No. R80107	Nozzle
No. R80108	Test Section
No. R80109	Calibration Panel
No. R80110	Calibration Panel (Dummy)
No. R80111	Combustion Chamber Water-In Manifold
No. R80112	Combustion Chamber Water-Out Manifold
No. R80116	Glass Window Spacer
No. R80117	Test Panel Spacer
No. R80119	Test Section Support
No. R80120	Bottom Support Plate
No. R80121	Side Plate Thrust Structure
No. R80122	Side U-Plate Thrust Structure
No. R80123	Combustion Chamber Support
No. R80125	Thrust Structure Assembly
No. R80156	Long Foam Panel
No. R80157	Hole Pattern Template - HGF Panel

Final copies of these drawings were delivered to the NASA-MSFC Technical COR at the end of the contract period.

Section 8
LOAN OF WINDOWS

The two quartz windows and frames used on the top of the test section for camera viewing ports are on loan (without charge) from Lockheed to NASA. The present loan period is one year. It is expected that this loan period can be extended at the end of one year if needed. These windows are from a surplus wind tunnel owned by Lockheed. Under the terms of the loan agreement, if Lockheed should need these windows before the end of the loan period, a three-month notice will be given so that replacement windows may be made or purchased. However, this need is not expected to occur.

Section 9
DELIVERY OF HARDWARE

Delivery of all applicable hardware was made by Lockheed-Huntsville to NASA-MSFC on 17 December 1975. It was accepted and received under form DD-250. Government furnished parts (copper combustor and throat sections) were also returned or accepted under this same form.

Section 10 OPERATIONAL CONSIDERATIONS

10.1 CALIBRATION PANEL LOADING

The calibration panel has a front and rear edge, obviously located by the direction the pressure leads run. The "dummy" calibration panels have dowel alignment pins for mating to the front of the duct, to each other, and to the "live" calibration panel. These dummy panels also have front and rear edges. These are stamped on the lateral edges, "FR and RR." The "FR" edge goes nearest the combustion chamber end of the test section. These dummy panels also have position numbers 1, 2, 3. Panel No. 1 goes nearest the combustion chamber, etc.

10.2 MATING GAP CONSIDERATION

When the calibration panels are loaded they must be sealed at their gaps on the sides and front. This is required to prevent redistribution of the pressure along the test section which would foul the flow field. This will be done using 2-component RTV as they are loaded into the test section from its downstream end. On the sides two angle "seals" are provided. RTV gaskets are attached to these rails already. However, some additional wet RTV will be required to obtain a proper seal. This RTV can be removed without a great deal of effort from these surfaces if they are not primed. (This has been tried and it works!)

Also the two tailgate pieces must be sealed with RTV to prevent air from being drawn into the cavity under the cryopanel and calibration panels during facility firing.

10.3 FACILITY CALIBRATION

Lockheed personnel will be available for helping monitor and coordinate facility checkout/calibrating and data reduction/analyses.

Temperature time histories have been predicted for each of the calibration panel heating rate areas. Heating rate and pressure predictions are shown on Figs. 1 and 2, respectively. Upper wall pressures have also been predicted.

The time required to get pressure and heating rates is estimated at 5 to 10 seconds. The acoustics instrumentation will also obtain sufficient data in this time period.

At least four runs will be required for calibration - one for each of the live calibration parallel positions.

10.4 FOAM PANEL DESIGN

A preliminary design drawing of the foam panel has been made - Drawing No. R80156.

There are two basic ways these panels could be made. The simpler, and less expensive from a manufacturing standpoint, is recommended as shown on the drawing. This is simply a flat plate 1/8 inch thick aluminum backup structure with drilled and tapped holes for mounting from the bottom. The gap or joint between the foam sides of this panel and the test section walls would be sealed with the two angle seals coated with RTV. The disadvantages of this design is that if the RTV gaskets now on the angle seals do not completely seal against the foam, then "wet" RTV will have to be used during panel loading to ensure a seal. This means the angles may stick to the foam and have to be cut loose after each test.

The second approach would be to have the panel manufacturer furnish a substructure which extends up the walls of the duct far enough to be bolted

in place at the holes which presently hold the angles in place. This would give a "breadpan" for the foam to be sprayed into and it would then be "stuck" to the sides and no seal would be required at the foam/metal interface.

As stated earlier, the first (simpler) approach is recommended at least for the first batch of panels. An alternative, which is probably advisable, is to have MSFC spray some "trial" panels of the simple design to see how they will actually work.

10.5 FACILITY DISASSEMBLY/REASSEMBLY NOTES

The facility consists of two basic units: the parts upstream of the nozzle/duct interface and then the duct itself.

The first assembly is held together with 18 rod bolts 3/8 inch in diameter. Silicone O-rings are provided between the injector body/copper combustor and between the copper combustor and steel throat. These O-rings are quoted to be good up to 700°F for short periods of time. However, they are not predicted to get this hot and therefore no disassembly or replacement of these between runs is required. However, periodic inspection of these is recommended. If there is a leak at these joints during operation it should be obvious from "burn marks" on the outside. If the temperature capability turns out to be a problem, then "Vitron" O-rings are available which are good to higher temperatures.

Specifications for these O-rings are Parker Ref. No. 2-385, size 15.955 inch i.d., and 0.210 inch cross-sectional diameter.

Dowel pins are provided for alignment at the throat/nozzle interface and nozzle/duct interface. No alignment pins are provided between the copper combustor and steel throat because of the differential expansion problem during operation because the throat is not water cooled. The alignment between the injector body/copper combustor is provided by a "boss" that fits into the copper.

Alignment between the nozzle/test section is controlled by four threaded studs, two in each of the test section support stands. These allow lateral and horizontal adjustment of the test section to match up with the nozzle dowel pins. Longitudinal movement of the test section is provided by rollers on top of these two stands.

When assembling the facility the mating surfaces should be aligned to obtain the best match of joints at their lower surfaces. This is because flow disturbances are critical on the lower wall where the foam is to be tested.

An RTV "mold-in-place" gasket is provided between the nozzle/test section. If damaged it is easily patched or replaced.

Recommended torque on the rod bolt nuts is 200 in.-lb-dry. Recommended tightening pattern is: alternate top and bottom; start in middle working outward. Go over pattern three times.

Recommended torque on nozzle/test section mating flange connecting bolts is 35 in.-lb-dry. Tightening patterns are the same as for the rod bolts.

Section 11
FACILITY OVERALL DIMENSIONS

Figure 6 shows a sketch of the assembled facility with overall dimensions, etc.

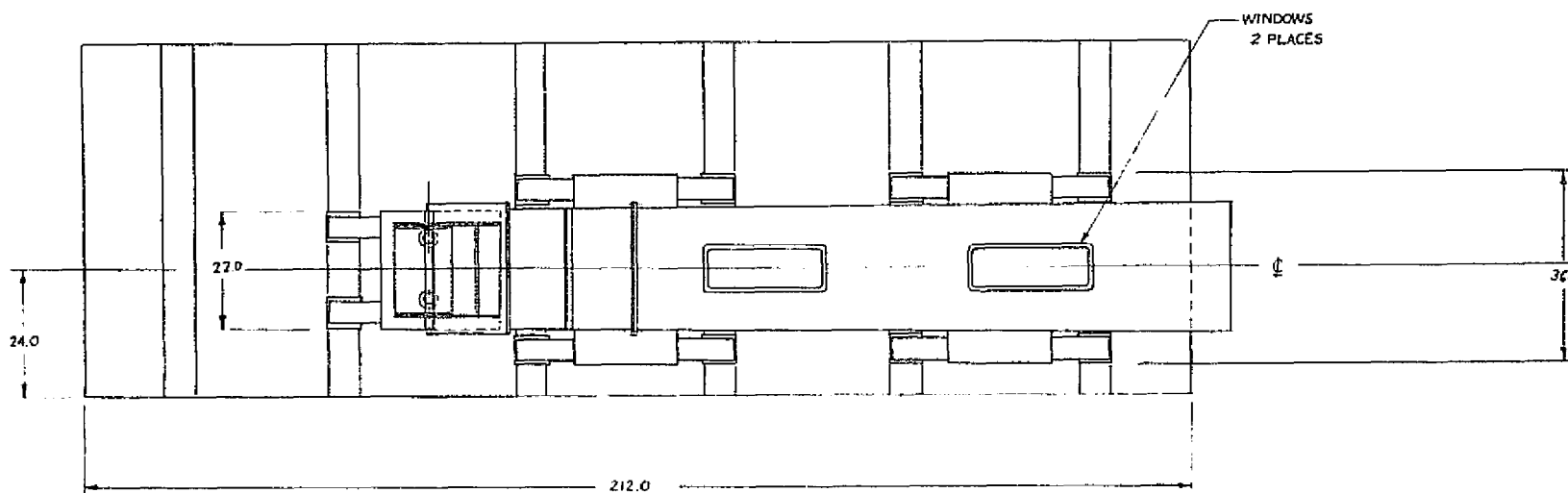
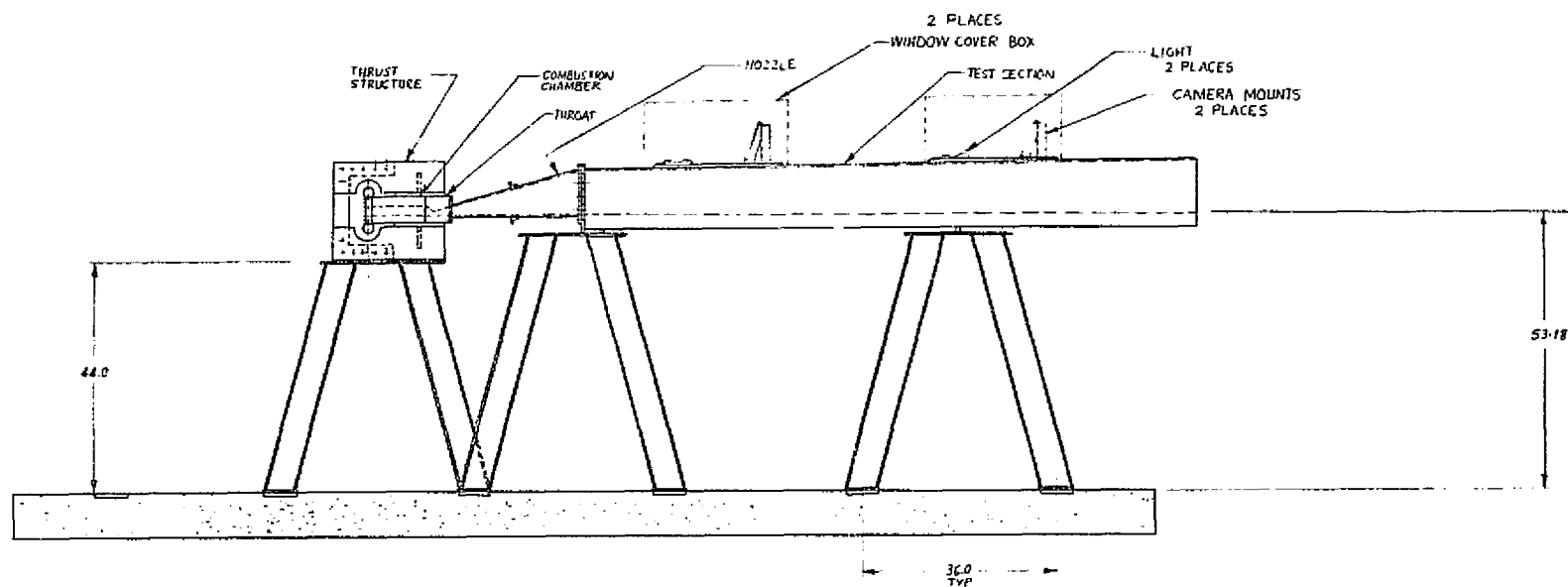


Fig. 6 - Overall Sketch of NASA-MSFC Hot Gas Test Facility

LMSC-HREC TM D496690

REFERENCES

1. Lockheed-Huntsville Technical Proposal, "Design and Develop the Modifications of the MSFC Hot Gas Test Chamber," LMSC-HREC D390940-231, Lockheed Missiles & Space Company, Huntsville, Ala., 15 August 1975.
2. "Stress Analysis of Gas Generator Combustion Chamber Body and Throat," IDC from W.A. McCutcheon to W.G. Dean and Z.S. Karu, Lockheed Missiles & Space Company, Huntsville, Ala., 10 September 1975.
3. "Revised Stress Analysis of the Gas Generator Combustion Chamber," IDC from W.A. McCutcheon to W.G. Dean and Z.S. Karu, Lockheed Missiles & Space Company, Huntsville, Ala., 25 September 1975.
4. "Stress Analysis of Gas Generator Throat with Revised Temperature Grid and Internal Pressure Loads," IDC from W.A. McCutcheon to W.G. Dean and Z.A. Karu, Lockheed Missiles & Space Company, Huntsville, Ala., 17 November 1975.
5. Ratliff, A. W., "Analysis of Low Enthalpy Hot Gas Facility (LEHGF) Ignition Sequence," LMSC-HREC TN D496575, Lockheed Missiles & Space Company, Huntsville, Ala., October 1975.
6. Dean, W.G., "Quality Assurance and Inspection of Work Accomplished in the Design/Fabrication of the Modification of the NASA-MSFC Hot Gas Test Facility," LMSC-HREC TM D496686, Lockheed Missiles & Space Company, Huntsville, Ala., January 1976.

Section 12 FACILITY DATA SUMMARY

The following information is presented in summary form for quick reference in the future use by the reader.

• Nominal Run Conditions

$$P_c = 100 \text{ psia}$$

$$T_T = T_c = 1773^\circ\text{R} = 1313^\circ\text{F}$$

$$T_R = 1620^\circ\text{R} = 1120^\circ\text{F}$$

$$H_T = 472 \text{ Btu/lb}$$

$$H_R = 425 \text{ Btu/lb, (R. F. = 0.9)}$$

$$C^* = 2630 \text{ ft/sec}$$

Theoretical values
using 100% burning
efficiency

Maximum predicted run time: 120 seconds.

Limiting factor on run time: temperatures of
nozzle and duct.

• Propellant Flow Rates

$$\text{Air} = 29.1 \text{ lb/sec}$$

$$\text{GH}_2 = 0.1914 \text{ lb/sec}$$

$$\text{O/F} = 152$$

Assuming
 $\eta_{C^*} = 92\%$

• Propellants Pressure Drop Across Injector Face

$$\text{Air} \sim 35 \text{ psi}$$

$$\text{GH}_2 \sim 10 \text{ psi}$$

- Cryopanel

Material 304-L

Nominal Size: 22-1/8 x 119 in.

Proof Test Pressure: 135 psia

Predicted Pressure Drop: 70 psi

Predicted LN₂ Flow Rate: 36 gpm

Connections:

Inlet: 0.5 in. M. F. Pipe Thread

Outlet: 1.0 in. M. F. Pipe Thread.

- Foam Panel

Nominal Size: 22.25 x 113.30 x 2.0 in.

- Water Manifold

Inlet Pressure: 50 psi

Flow Rate: 56 gpm

- O-Rings

Quantity: 2

Material: Silicone Rubber

Size: 15.955 in. i.d., x 0.210 in. Cross-Sectional
diameter

Specification No: Parker No. 2-385

- Calibration Panel

Pressures: 22

Heating Rates: 22

Thermocouples: Type K (Chromel Alumel)

Material: 304-L Stainless Steel

Nominal: Thin-Skin/T. C.

Location Thickness: 0.030 in. \pm .01

Plate Thickness: $3/8$ in.
Size: 22.25 x 28.44 x 2.00 in.

• Dummy Panels

Sizes:

Panels 1 and 2
22.25 x 28.44 x 2.00 in.

Panel 3
22.25 x 27.81 x 2.00 in.

Material: Mild Steel
Plate Thickness: $3/8$ in.

• Bolt Torque:

Injector/Combustor/Throat/Nozzle
Rod Bolts: 200 in-lb (dry)
Nozzle/Duct Bolts: 35 in-lb (dry)

• Window Size:

Glass: $4-1/2$ x 20 in.
Inside Frame: $7-1/2$ x 22 in.
Outside Frame: $10-5/8$ x 24 in.